Physics Reports 1017 (2023) 1–96

Contents lists available at ScienceDirect

Physics Reports

journal homepage: www.elsevier.com/locate/physrep

Signal propagation in complex networks

Peng Ji [a,b,c,*], Jiachen Ye [a,d,*], Yu Mu [e], Wei Lin [f,g,h], Yang Tian [i,j], Chittaranjan Hens [k], Matjaž Perc [l,m,n,o,p], Yang Tang [q,g], Jie Sun [r], Jürgen Kurths [s,t,f]

[a] Institute of Science and Technology for Brain-Inspired Intelligence, Fudan University, Shanghai 200433, China
[b] Key Laboratory of Computational Neuroscience and Brain-Inspired Intelligence, Ministry of Education, Shanghai 200433, China
[c] MOE Frontiers Center for Brain Science, Fudan University, Shanghai 200433, China
[d] CMA-FDU Joint Laboratory of Marine Meteorology, Institute of Atmospheric Sciences, Fudan University, Shanghai 200433, China
[e] Institute of Neuroscience, State Key Laboratory of Neuroscience, Center for Excellence in Brain Science and Intelligence Technology, Chinese Academy of Sciences, 320 Yue-Yang Road, Shanghai 200031, China
[f] Research Institute of Intelligent Complex Systems and MOE Frontiers Center for Brain Science, Fudan University, Shanghai 200433, China
[g] Shanghai Artificial Intelligence Laboratory, Shanghai 200232, China
[h] School of Mathematical Sciences, SCMS, and CCSB, Fudan University, Shanghai 200433, China
[i] Department of Psychology & Tsinghua Laboratory of Brain and Intelligence, Tsinghua University, Beijing 100084, China
[j] Laboratory of Advanced Computing and Storage, Central Research Institute, 2012 Laboratories, Huawei Technologies Co. Ltd., Beijing 100084, China
[k] Center for Computational Natural Sciences and Bioinformatics, International Institute of Information Technology, Gachibowli, Hyderabad 500032, India
[l] Faculty of Natural Sciences and Mathematics, University of Maribor, Korošška cesta 160, 2000 Maribor, Slovenia
[m] Department of Medical Research, China Medical University Hospital, China Medical University, Taichung 404332, Taiwan
[n] Alma Mater Europaea, Slovenska ulica 17, 2000 Maribor, Slovenia
[o] Complexity Science Hub Vienna, Josefstädterstraße 39, 1080 Vienna, Austria
[p] Department of Physics, Kyung Hee University, 26 Kyungheedae-ro, Dongdaemun-gu, Seoul, Republic of Korea
[q] Key Laboratory of Smart Manufacturing in Energy Chemical Process, Ministry of Education, East China University of Science and Technology, Shanghai 200237, China
[r] Theory Lab, Central Research Institute, 2012 Labs, Huawei Technologies Co., Ltd., Sha Tin, 999077, Hong Kong Special Administrative Region of China
[s] Potsdam Institute for Climate Impact Research (PIK), 14473 Potsdam, Germany
[t] Department of Physics, Humboldt University, 12489 Berlin, Germany

ARTICLE INFO

Article history:
Received 28 March 2023
Accepted 29 March 2023
Available online xxxx

Keywords:
Signal propagation
Complex networks
Nonlinear dynamics

ABSTRACT

Signal propagation in complex networks drives epidemics, is responsible for information going viral, promotes trust and facilitates moral behavior in social groups, enables the development of misinformation detection algorithms, and it is the main pillar supporting the fascinating cognitive abilities of the brain, to name just some examples. The geometry of signal propagation is determined as much by the network topology as it is by the diverse forms of nonlinear interactions that may take place between the nodes. Advances are therefore often system dependent and have limited translational potential across domains. Given over two decades worth of research on the subject, the time is thus certainly ripe, indeed the need is urgent, for a comprehensive review of signal propagation in complex networks. We here first survey different models that determine the nature of interactions between the nodes, including epidemic models, Kuramoto models, diffusion models, cascading failure models, and models describing neuronal dynamics. Secondly, we cover different types of complex networks and their topologies, including temporal networks, multilayer networks, and neural networks. Next, we cover

* Corresponding author at: Institute of Science and Technology for Brain-Inspired Intelligence, Fudan University, Shanghai 200433, China.
E-mail addresses: pengji@fudan.edu.cn (P. Ji), jcye19@fudan.edu.cn (J. Ye).

https://doi.org/10.1016/j.physrep.2023.03.005

network time series analysis techniques that make use of signal propagation, including network correlation analysis, information transfer and nonlinear correlation tools, network reconstruction, source localization and link prediction, as well as approaches based on artificial intelligence. Lastly, we review applications in epidemiology, social dynamics, neuroscience, engineering, and robotics. Taken together, we thus provide the reader with an up-to-date review of the complexities associated with the network's role in propagating signals in the hope of better harnessing this to devise innovative applications across engineering, the social and natural sciences as well as to inspire future research.

Contents

1. Introduction and motivation ... 3
2. Basic model systems ... 6
2.1. Epidemic models ... 6
2.1.1. Metapopulation models ... 7
2.1.2. Agent-based models ... 11
2.2. Kuramoto model ... 12
2.2.1. Traveling wave state ... 13
2.2.2. Perturbation propagation ... 15
2.3. Diffusion models ... 16
2.3.1. Random walks ... 16
2.3.2. Reaction–diffusion process ... 20
2.3.3. Percolation process ... 22
2.4. Cascading failures ... 23
2.4.1. Load-capacity model ... 24
2.4.2. Fraction threshold model ... 25
2.5. Neuroscience dynamics ... 26
2.5.1. Neural networks as dynamical systems ... 26
2.5.2. Synergies between neural dynamics and data analysis ... 27
3. Complex networks ... 28
3.1. Temporal networks ... 28
3.1.1. Diffusion speed ... 30
3.1.2. Epidemic spreading ... 31
3.2. Spatiotemporal signal propagation ... 33
3.3. Multilayer networks ... 34
3.3.1. Epidemic spreading ... 34
3.3.2. Cascading failures ... 36
3.4. Control on networks ... 38
3.4.1. Static topology ... 39
3.4.2. Dynamic topology ... 39
3.5. Graph neural networks ... 41
4. Network time series analysis techniques ... 41
4.1. Information transfer and nonlinear correlation tools ... 41
4.2. Network reconstruction ... 45
4.3. Source localization and link prediction ... 52
4.3.1. Link prediction ... 53
4.3.2. Source localization ... 55
4.4. AI driven time series analysis ... 56
4.4.1. Time series processing ... 56
4.4.2. Time series forecasting ... 57
5. Applications ... 59
5.1. Epidemic ... 59
5.1.1. Agent-based models ... 59
5.1.2. Metapopulation models ... 60
5.2. Social dynamics ... 61
5.2.1. Opinion formation ... 61
5.2.2. Human cooperation ... 62
5.2.3. Other models ... 63
5.3. Neuroscience ... 63
5.3.1. Circuit neuroscience ... 63
5.3.2. Propagation directions: Bottom-up, top-down ... 64

5.3.3. Propagation in time: Sequential activation ... 65
5.4. Power grids ... 66
5.4.1. Dynamical perturbations ... 66
5.4.2. Structural perturbation ... 69
5.5. Robot swarms ... 69
5.5.1. Collective behaviors in robot swarms ... 69
5.5.2. Swarm attack ... 72
6. Conclusion ... 74
Declaration of competing interest ... 76
Acknowledgments ... 76
References ... 76

1. Introduction and motivation

Collective behavior is the hallmark of complex systems, and as such, it has attracted much attention during the past two decades [1–9]. It is an emergent phenomenon that is due to the interactions between many units that make up complex systems, be it neurons in the brain or ants in an anthill, as well as due to external disturbances that often act upon them. Most importantly, collective behavior is often universal in nature, such that models describing very different complex systems share qualitatively identical spatiotemporal dynamics and phase transitions leading up to it [10–13]. Consequently, as physicists, we can reach a deeper understanding and appreciation of complex systems through the lens of collective behavior.

For the study of collective behavior, signal propagation is a commonly used metric to discern the processes that are involved and their impact across time and space. In fact, the propagation of signals is the very lifeline of collective behavior, since it enables the proper functioning of complex systems in nature, social systems, and engineering. With the advent of complex systems science, or complexity science, we have witnessed significant advances in this field, both from an experimental and a theoretical point of view. For example, the propagation of neuronal activity in a healthy brain across multiple spatio-temporal scales empowers fascinating cognitive abilities, while failures or changes in this propagation can be utilized to diagnose disease [10,13]. Similarly, in social systems, modeling opinion dynamics across social networks entails a cognitive process that determines how a group of agents shapes their opinion, and in man-made systems, the cascading failures in power grids can lead to rolling or even total large-scale monster blackouts [14–16]. Even in swarm robotics, which relies strongly on collective behavior, errors or attacks could easily give rise to damage or disrupt formation control and cooperative manipulation [17]. Finally, also in the brain system of the zebrafish, bottom-up and top-down signal propagation, starting from presynaptic neurons to downstream postsynaptic neurons, might be the key for the emergence of elementary functions at behavioral and cognitive level [18].

From a theoretical point of view, there are two different approaches we can use to study signal propagation complex networks. One is modeling-driven, based on the interplay between structure and dynamics, to generate various patterns of propagation. The other is data-driven, as an inverse problem to reveal hidden patterns from empirical data.

(i) Let us firstly consider modeling-driven methods. Fundamentally, the effective and often highly efficient realization of signal propagation is achieved by means of a complex interplay between the structure and dynamics of the underlying system [12]. Various dynamical models determine the nature of interactions between nodes. For example, the dynamics of hosts or pathogens characterizes how a disease spreads over contact networks, and agent-based models address the stochastic properties of the spreading process [19]. The Kuramoto model with positive and negative coupling allows for the emergence of traveling waves, pattern formation, and even Chimera states [20,21]. Load-capacity models reveal the mechanism behind cascading failures, where a failure of one part could trigger further failures of other parts and finally endanger the whole system [14,16]. Neuronal modeling is aimed at describing macroscopic activity patterns that arise from the interactions between excitatory and inhibitory neurons. For example, synaptic and external excitatory inputs interact and helps us understand the neuronal pathway from single-neuron physiology to behavior in Larval zebrafish [22]. The topological connections between nodes provide the underlying platform for signal propagation, and various types of networks have been studied frequently and in much detail. Temporal networks, for example, could speed-up or slow-down the spreading process depending on the nature of the waiting time distribution, and they could also allow the system to become controllable, even if the corresponding static network is uncontrollable [23–25]. The interplay between the internal dynamics and the network degrees jointly determines the response time of spatiotemporal propagation, and the self-consistent linear response theory can determine the separate contribution of topology and the dynamics towards the observed spatiotemporal propagation patterns [10,13]. Namely, both the topological and the dynamical properties are crucial for inducing distinctive patterns of propagation, such as traveling waves, spiral waves, chaos, sources, and sinks.

(ii) Besides modeling-driven methods, the quantification of propagating features from empirical data, as an inverse problem, can reveal typically or at least often hidden underlying topological-dynamical relations [26]. A fundamental question in the data-driven analysis of complex systems is to address, to what extent, two components are related given observational data. Various theoretical and computational methods have been developed to serve as tools to infer

Nomenclature

List of Abbreviations

ABM	Agent-based model
ABR	Rate of actual human biting
ADN	Activity-driven network
AES	Advanced Encryption Standard
ASTGCN	Attention-based spatiotemporal graph convolutional network
BSG	Balanced sequence generator
BT	Bluetooth
CCG	Cross-correlograms
CNN	Convolutional neural network
COVID	Corona virus disease
CR	Contact rate
CRLI	Cluster representation learning
CT	Continuous time
DM	Dorsal medial area
DMD	Dynamic mode decomposition
DRM	Distributed robust maximization
DT	Discrete time
EOE	End of the epidemic
ER	Erdos–Renyi
EWS	Early-warning signals
GAEs	Graph auto-encoders
GAN	Generative adversarial network
GCN	Graph convolutional network
GE	Graph embedding
GLEaM	Global epidemic and mobility model
GRNs	Gene regulatory networks
HETS	Hybrid event-triggered strategy
HMF	Heterogeneous mean-field
IATA	International Air Transport Association
IT	Inferior temporal cortex
KM	Kumamoto model
LBS	Location-based services
LIF	Leaky-integrate and fire
LSTM	Long short-term memory
MAS	Multi-agent simulation
MFPT	Mean first passage time
MMCA	Microscopic Markov chain approach
MMS	Multimedia messaging system
MPC	Mobile phone-call
MT	Medial temporal area
N-BEATS	Neural basis expansion analysis for interpretable time series
NE	Neighbor exchange
NIMFA	N-intertwined mean-field analysis
NPI	Non-pharmaceutical interventions
OAG	Official Aviation Guide
RA	Robust nucleus of the arcopallium
RD	Reaction-diffusion

RGC	Retina ganglion cells
RNN	Recurrent neural network
RW	Random walks
RWC	Random walk centrality
SARS-CoV-2	Severe acute respiratory syndrome coronavirus 2
SEIR	Susceptible–exposed–infected–recovered
SF	Scale-free
SIR	Susceptible–infected–recovered
SIS	Susceptible–infected–susceptible
SMNs	Social media networks
SSE	Superspreading events
STCN	Self-supervised time series clustering network
STDP	Spike timing-dependent plasticity
StemGNN	Spectral temporal graph neural network
STSGCN	Spatiotemporal synchronous graph convolutional network
SW	Small-world
TB	Tuberculosis
TDOA	Time difference of arrival
TI	Turing instability
tnGAN	Three network- based form of generative adversarial network
TOA	Time of arrival
TW	Traveling wave
USL	Unsupervised saliency subsequence learning
W-MSR	Weighted mean subsequence reduction
ZIKV	ZIKA virus

List of Symbols

a	Activity
$\boldsymbol{A}$	Adjacency matrix
$\mathcal{BS}$	Basin stability
$c(\cdot)$	Concentration
C	Capacity
E	Number of exposed agents
$E(\cdot)$	Energy function
$G_0(\cdot)$	Generating function
GC	Granger causality
H	Entropy
I	Number of infected agents
$I(\cdot,\cdot)$	Mutual Information
L	Laplacian matrix/Load
K	Coupling strength
M	Inertia coefficient
N	Network size
$P(\cdot)$	Probability
S	Number of susceptible agents
t	Time
T	Length of time
TE	Transfer Entropy
$\mathcal{X}$	Indicator function
Y	Reduced admittance
α	Tolerance parameter

β	Infection rate
γ	Euler constant
δ_{ij}	Kronecker symbol
$\delta(\cdot)$	Dirac delta function
ϵ	Perturbation strength
ζ	Characteristic length
θ	Phase
$\Theta(\cdot)$	Heaviside function
λ	Eigenvalue
μ	Recovery probability/Average
ν	Frequency
ξ	Noise
π	Ratio of circumference to diameter
$\rho(\cdot,\cdot)$	Correlation coefficient
σ	Standard deviation
τ	Time delay
ϕ	Perturbation frequency
ω	Natural frequency
Ω	Locking frequency
$\langle\cdot\rangle$	Ensemble average

the causality between components, ranging from basic linear correlation measures to more sophisticated information-theoretical quantities, thereby forming the cornerstone of extracting the structural backbone of complex networked dynamics [27]. Inferring the topology of connectivity and extracting important variables at different scales has a great potential for exploring biophysically plausible circuit arrangements for neuronal signal propagation [28]. In addition to inferring methods, link prediction and source localization methods have also been developed and applied frequently, for example to find the source of wireless sensor networks, or the source of disease or information dissemination based on incomplete information and network structure [29–31].

In the light of the wealth of modeling-driven and data-driven methods, and even though remarkable surveys and perspective works have been published on related subjects, a comprehensive contemporary review of signal propagation in complex networks has ample potential to guide as well as to motivate future research in this very vibrant field.

This review is organized as follows. We begin by discussing the multiscale modeling of disease spreading, the Kuramoto model, random walks, reaction–diffusion and percolation processes, and models for cascading failures, in Section 2. All these models, at least to some extent, allow for the emergence of signal propagation. In Section 3, we review the topological factors that significantly influence signal propagation, including temporal and multilayer networks. There, we also present a general theoretical framework for the interplay between dynamics and topology, and the recent research dedicated to the control of various types of networks. In Section 4, we review recent techniques that reveal signal propagation from measured data, including information transfer and artificial intelligence techniques. In Section 5, we summarize relevant applications concerning epidemics, social dynamics, neuroscience, power grids, and robotics. Finally, we conclude with a summary and a discussion of promising directions for future research.

2. Basic model systems

2.1. Epidemic models

The dynamics of hosts or pathogens on top of contact networks can characterize how a disease spreads. However, the network's high-dimensionality feature makes the analytical calculation more challenging. There are various approaches to modeling disease spread in intricate networks. Modeling through a metapopulation network is one of them which can capture the mobility of the populations from one patch to another. Thus a metapopulation is typically defined as a collection of subpopulations that are related because the agents or hosts are mobile. In ecological systems where recolonization, maintaining variety, and extinction equilibrium of specific species are explored, metapopulation models are well-studied [32–38]. Due to the rapid development of transportation systems, it is necessary to study how an epidemic spreads by taking into account human movement (diffusion) at different scales [39–45], where hosts or people interact, spread the disease, and then either recover from it or get rid of it. On the other hand, agent-based models (ABM) or individual-based stochastic models are developed based on "bottom-up" setup similar to Cellular Automata [44–52]. These models represent how individuals (or agents) interact with one another and with their surroundings, while being trained to act in certain ways. These methods address the stochastic character of the epidemic process, which may help them

getting beyond the limits of the traditional deterministic method. Here the agents observe their environment and adapt their behavior accordingly. Such agent-based, disaggregate models have been researched for the past 20 years to examine the disease spread across social networks [48,53,54].

2.1.1. Metapopulation models

For recent epidemics such as the SARS outbreak in 2003 [55], H1N1 disease in 2009 [56], and COVID-19 [57,58], where the normal time scale to disseminate the disease from one country to another is within few months, mobility or dispersal becomes a crucial component. It is possible to ignore the movement of the diseased people from one patch to another in a well-mixed, homogeneous population, but this is not always the case. One is motivated to take into account the reaction–diffusion dynamics [59], in which the particles/hosts/humans interact ("react") within a community and "diffuse" (mobility) within shorter time scales. Thus, a metapopulation model is captured by the numbers of patches (N), links representing the movement of the agents/humans, and the interaction mechanism in a patch governed by disease dynamics.

Reaction–diffusion models: mean-field approach. Analogous to the chemical rate equations, one can express disease dynamics as follows [59] $B \to A$, and $B + A \to 2B$. Here B acts as an infected agent and converts the susceptibles agent A into B with the infection rate β and the infected agents become susceptible (A) with a recovery probability μ. The networks are considered heterogeneous, in which each node contains the agents A and B. The diffusion from one node to another depends on the inverse degree of the source node. Two types of reactions can be considered: either (I) In the same nodes, agent A will react with the rate β to all the B agents, or (II) Each agent will have a finite number of contacts, i.e the reactions rate is rescaled concerning the population size. In the heterogeneous mean-field approach (HMF) the nodes with the same degree are considered statistically equivalent. In this backdrop, if x_i is the number of A agents confined in a node having degree d and y_i is the number of B agents confined in a node having degree d, one can write $\rho_{A,d} = \frac{1}{N_d}\sum_i x_i$, and $\rho_{B,d} = \frac{1}{N_d}\sum_i y_i$, where the sum runs over all nodes having degree d which is N_d. Thus, $\rho_d = \rho_{A,d} + \rho_{B,d}$. In this setup, the HMF for the degree class d can be written as (say for agents B)

$$\partial_t \rho_{B,d} = -\rho_{B,d} + d\sum_{d'} P(d'|d)\frac{1}{d'}\left[(1-\mu)\rho_{B,d'} + \beta\Gamma_{d'}\right], \tag{1}$$

where the first term represents the diffusion process, and the second term is coming due to the contribution of the neighbors. Here $P(d'|d)$ is the probability that vertices d and d' are connected. Here Γ_d is the reaction term for generating new agents. Similarly, one can design the dynamical rate equations for particles A in any given degree class. The non-zero infection exists if the total density of particles crosses the value $\frac{\langle d\rangle^2}{\langle d^2\rangle}\frac{\mu}{\beta}$. Thus, firm heterogeneity of networks suppresses the phase transition in the thermodynamic limit as $\rho_c \to 0$. For the type (I) process, the transmissibility is independent of the population size, whereas it is inversely proportional for the type (II) process. On the other hand, the invasion threshold has been studied in the presence of a heterogeneous coupling pattern [60]. Here the basic reaction–diffusion model is derived, in presence of traffic-dependent as well as population-dependent mobility. It is also shown that temporal infection in the same degree block (statistically equivalent degree nodes) is independent of the arrangement of the initial infection. On the other hand, in a deterministic setup, multipatch SEIR dynamics (Susceptible–Exposed–Infective–Removed) can be captured by [44,61] $\dot{S}_i = \mu(1-S_i) - S_i\sum_{j=1}^{N}\beta_{ij}I_j$, $\dot{E}_i = S_i\sum_{j=1}^{N}\beta_{ij}I_j - (\mu+\alpha)E_i$, $\dot{I}_i = \alpha I_i - (\mu+\gamma)I_i$, and $R_i = 1 - S_i - E_i - I_i$. Note that, here the diffusive flux is not considered assuming the movement from one patch to another is short lasting. Here β_{ij} is the per capita infection rate when an individual of the i th patch is infected by the individual of the j th patch. The eigenvalue of the matrix encoding the interaction pattern determines the synchronous homogeneous solution. A more mechanistic approach, based on individual movement patterns has also been established in which the dynamics of an individual who stays in a patch is currently in the same patch or migrating to another one is considered [32,33]. For two patch systems, the equivalence of the parameters of standard phenomenological models of coupling, and mechanistic models are analytically studied in these works.

To capture the propagation pattern, particularly, the arrival time t_1 of infection, a more realistic metapopulation network is developed in which the SIS dynamics is applied on top of the network [62,63]. If the cause of the first infection and the connectivity pattern is known a priori, it is possible to statistically determine when epidemics will strike a city. Assume a disease propagates from city A (population N_A) to city B (population N_B) and at time $t = 0$, city A has $I_0 = 1$ infection. If the passenger flux is w, then the probability of the arrival time (t_1) of epidemics in the city B is $P_b(t_1) = [1-(1-p)^{I_0(t_1)}]\prod_{i=1}^{n-1}(1-p)^{I_0(i\Delta t)}$, where $t_1 = n\Delta t$, $p = \frac{w}{N_A}\Delta t$ is the jump probability, and Δt is the discrete step [62]. Assuming the initial infection is small, and the infection at A is large enough (at $t = t_1$) one can reach a Gumbel distribution $P(t)dt = \frac{w}{N_A}\exp\left(\beta t - \frac{w}{N_A\beta}e^{\beta t}\right)\Theta(t)dt$, where $\Theta(t)$ is the Heaviside function and β is the spreading rate. The average arrival time can be calculated as $\langle t_1\rangle = \frac{1}{\beta}[\ln(\frac{N_A\beta}{w}) - \gamma]$, where γ is the Euler constant. For a one-dimensional (1-D) chain, where the flux (w_i) is drawn from a random distribution, the average arrival time can be written as $\chi(n) \equiv \ln\left[\prod_{i=0}^{n-1}\frac{N_i\beta e^{-\gamma}}{w_i}\right]$, where N_i is the size of the population of the i th city. For a general transportation

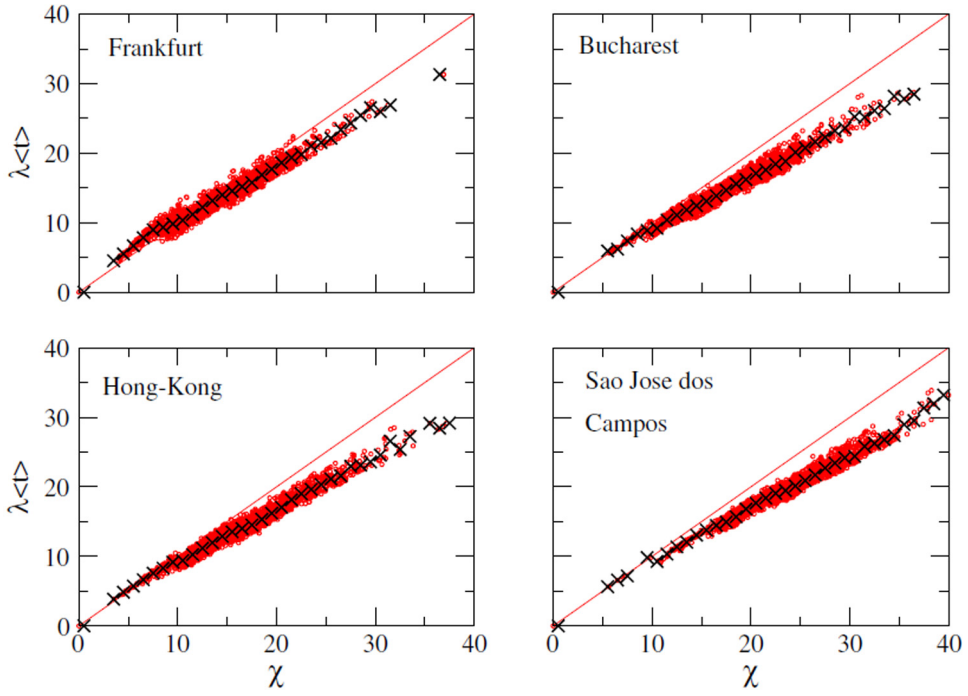

Fig. 1. The average arrival time of infection is plotted as a function of χ (analytically calculated average infection time). Each red circle corresponds to a city. Crosses are an average over cities with the same χ. The name of the city which is initially infected is also written in each of the graphs [62,63]. The ansatz successfully determines the propagation of infection.
Source: Adapted from [62].

network, the arrival time for a target city t from the source s can be captured by $\chi(s,t) = \min_{P_{st}} \sum_{(a,b)\in P_{st}} \left[\ln\left(\frac{N_a\beta}{w_{ab}}\right) - \gamma\right]$. Here P_{st} is the set of all possible shortest paths between s and t, and (a, b) is one of the links on the path $s - t$. The w_{ab} along the shortest path provides the most accurate result. This approach has been successfully tested in air traffic networks across the globe (Fig. 1). It differentiates between two cities in the arrival time if both are at the same topological distance from the source of infection.

Structured metapopulation stochastic dynamics can also be developed on a multiscale network to predict the propagation of influenza pandemics or vector-borne diseases. The multiscale network is designed by incorporating short-range as well as long-range connections to describe the propagation. This is called a global epidemic and mobility model (GLEaM).

Global mobility is a very complex multiscale network that varies by several orders of magnitude from short-range commuting networks on a local scale to long-range air-traffic networks [40,56]. This type of model successfully predicts the propagation of influenza-like epidemics. The multiscale networks are incorporated into the GLEaM model which encodes the characteristics of structured metapopulation stochastic dynamics. The community network for local short-range connections follows a gravity law: $w_{ij} \propto \frac{N_i^\alpha N_j^\gamma}{f(d_{ij})}$, where $f(d_{ij})$ is a distance-dependent function and α, γ are calculated from the census data. Considering the intra- and inter-specific (mobility) transmission dynamics on local and non-local scales, it has been shown that the global epidemic behavior is determined by the air traffic network connectivity pattern, whereas the local level of the commuting network determines the flow from hubs to the other subpopulations.

Effective Distance in metapopulation networks. Another method of predicting the propagation of contagious phenomena in a metapopulation network is to employ a probabilistically motivated shortest path, for example, if the epidemic spreads over a network of air traffic, as proposed by Brockmann et al. [64]. The underlying structure of the network is constructed through the air-traffic data. The impact of local-scale mobility is discarded here. The usage of "effective distance" translates the spatiotemporal complex patterns of epidemic propagation into regular patterns. Here the connectivity pattern is encoded in the normalized matrix **p**. The element of this matrix such as p_{ji} quantifies the passenger flux from i to j. The effective distance is calculated from the structure of the passenger flux matrix as $d_{ji} = (1 - \log\ p_{ji}) \geq 1$. The logarithm comes because the effective distance is considered additive, whereas the probabilities of transition for a distance greater than 1 are multiplicative. Finally one can calculate the directed path length $\lambda(\Gamma)$ for all possible shortest paths as $D_{ji} = \min_\Gamma \lambda(\Gamma)$ where Γ is the set of all possible effective lengths along all possible shortest paths between i and j. Thus by calculating D_{ji} one can easily determine the time required to spread the disease from the location i to the

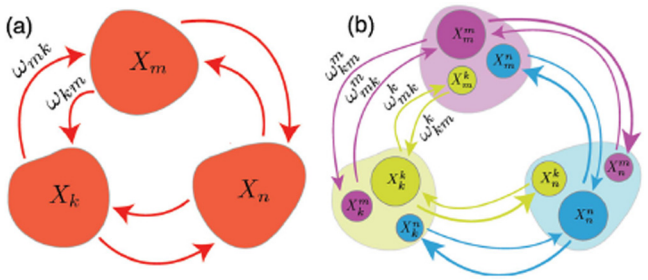

Fig. 2. Mobility diagram of individuals. Populations are marked by patches and people's movements by arrows. (a) Here the transition rate from m to k is denoted by w_{km}. The travel movement of the indistinguishable populations is marked by random Diffusive dispersal. (b) The bidirectional mobility incorporates the movement of individuals from their base location k to the connected locations m and back is denoted by w^k_{mk}, and w^k_{km} [68]. *Source:* Adapted from [68].

long-distance location j. A random walk-based computationally efficient approach (hitting time for a Markov chain) is recently developed to calculate the effective distance [65]. The previously developed logarithmic-based shortest path [64] is included as a particular case of this method. This method can easily be extended to a directed weighted graph.

Another version of a metapopulation network is proposed recently. Earlier, the commuters are considered as random walkers [62,63], which is not always true. Particularly, human mobility follows a recurrent pattern [66,67] i.e., movements of individuals are not random. Instead, they frequently move between a few places, say from home to working-class and somewhere between. Against this backdrop, an alternative framework is also proposed where the assumption about the statistical equivalence of the same degree class is relaxed [68]. Instead, the authors develop a model for the individuals who belong to the base location i and are currently located at n as follows:

$$\partial_t S^i_n = -\frac{\beta}{N_n} S^i_n \sum_m I^m_n + \sum_m (w^i_{nm} S^i_m - w^i_{mn} S^i_n), \tag{2}$$

$$\partial_t I^i_n = \frac{\beta}{N_n} S^i_n \sum_m I^m_n - \mu I^i_n + \sum_m (w^i_{nm} I^i_m - w^i_{mn} I^i_n). \tag{3}$$

Here the dispersal dynamics follows a Markov process as $X^i_n \rightleftharpoons X^i_m$ where i is the base location and $X : S, I, R$ represents the states of individuals (Fig. 2). w^i_{nm} denotes mobility rate between the location n and m. So ordinary migration is replaced by individual mobility. For ordinary diffusion, the speed of the traveling waves is scaled with the square root of the diffusion rate, and it monotonically increases.

For constant return rate $w^i_{mi} = \omega$ (rate is larger than the infection or recovery rate) the wave velocity follows the relation as $c = \dfrac{2\sqrt{6D}\beta\omega}{(\alpha + 3\omega)}$ (Fig. 3). Here $D = \dfrac{l^2}{2}$, where l^2 is the size of the lattice. In contrast to the reaction–diffusion process, here c saturates for $\omega \to \infty$. Therefore, constrained mobility in a bidirectional setup can restrict the high-frequency travel events in certain locations attached to the base locations.

Microscopic Markov Chain Approach (MMCA). A discrete-time approach can also be considered. The model is composed of three activities: Movement, Interaction, and Return [69–71]. An individual's choice of movement depends on the origin–destination matrix (OD) which encodes the weights of the links connecting patches. The decision of the population to move in the morning is controlled by the parameter p. The interaction part encodes the reaction phase in school, as well as in workplace. A mean-field assumption is made i.e. there is a homogeneous mixing between individuals at the same locations. The final step is to incorporate the recurrent model where individuals return to their residential patches. For SIR dynamics one can write

$$\rho_i(t+1) = (1-\mu)\rho_i(t) + [1 - \rho_i(t) - r_i(t)]\Pi_i(t), \tag{4}$$

$$r_i(t+1) = r_i(t) + \mu\rho_i(t), \tag{5}$$

where $\rho_i(t)$ is the fraction of infected individuals at the patch i at time t and r_i is the fraction of recovered individuals at the patch i. The probability that a susceptible node is infected living in the patch i is captured by $\Pi_i(t) = (1-p)\xi_i(t) + p\sum_{j=1}^{N} R_{ij}\xi_j(t)$. Here $\xi_i(t)$ is the probability to be infected by a healthy individual irrespective of his/her residential patch, and R_{ij} is the element of the OD matrix. The critical invasion threshold is captured by $\lambda_c = \dfrac{\mu}{\Lambda_{\max}(\mathcal{R})}$, where the elements of $\mathcal{R}$ depend on p, R and the effective infected and total population after the movement stage at time t (Fig. 4).

Recently, a deterministic metapopulation network is designed to study the spatiotemporal propagation of the spreading and recovery process in a square lattice [72]. If the disease starts from the core, the migration supports a faster spread, whereas if the initial infection is randomly spread in the lattice, the spreading can be stopped with a slower migration rate.

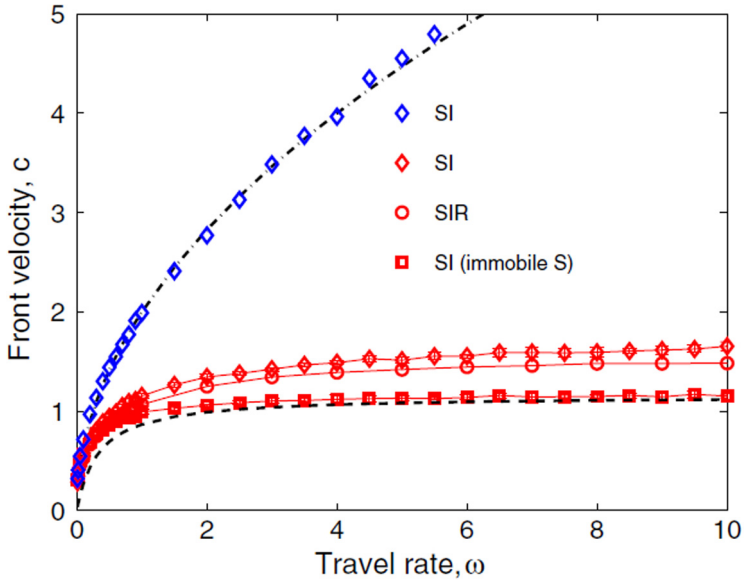

Fig. 3. Front velocity ($c(\omega)$) as a function of the travel rate ω in comparison to ordinary reaction–diffusion dynamics (blue symbols). Mean velocities are indicated by red (bidirectional mobility) and blue (reaction–diffusion) symbols. For large ω, the front velocity saturates due to the restriction of high-frequency travel events.The dashed and dash-dotted lines, are the theoretical lines [68].
Source: Adapted from [68].

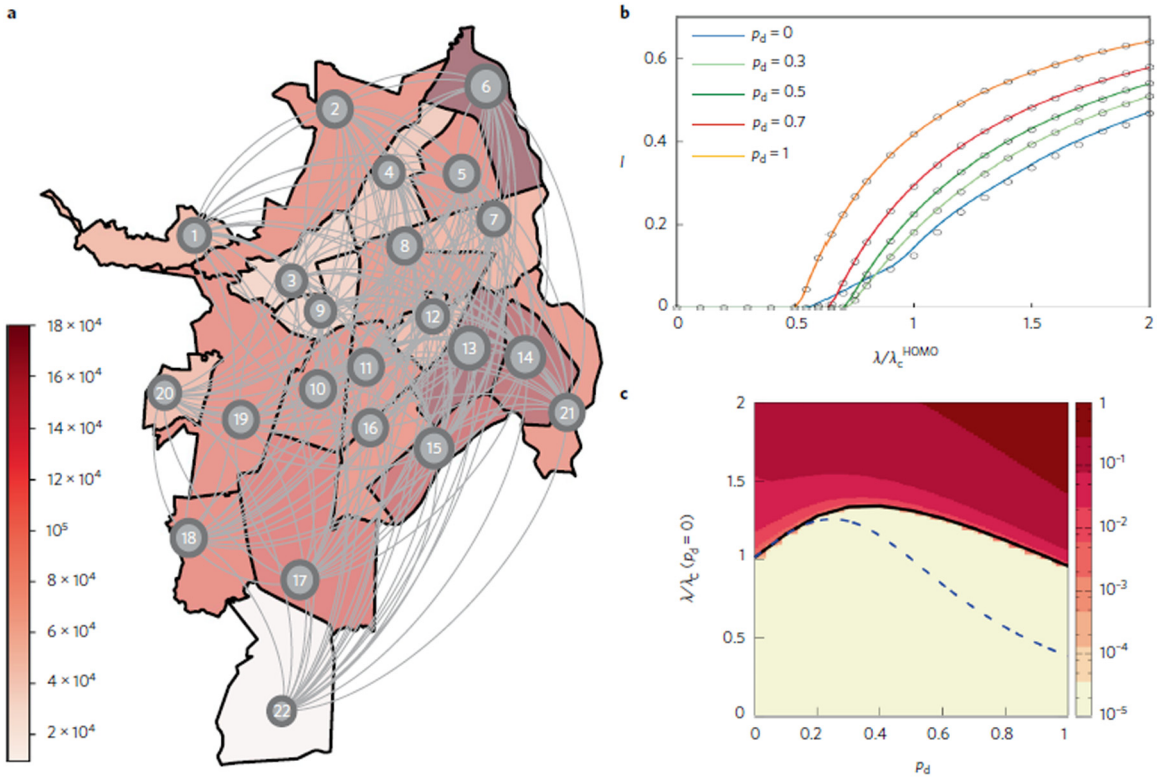

Fig. 4. (a) The metapopulation network of the city of Cali (Colombia). Here the city is subdivided into 22 parts (districts). The gray links signify the movement of the people. (b) The strength of infection as a function of infection probability. A repeated MC simulation is performed for different probabilities of moving: p_d. (c) Two-dimensional phase diagram of incidence as a function of infection probability and movement probability. The color bar in (a) represents the population strength. Solid and dashed lines are theoretical lines [69–71].
Source: Adapted from [71].

2.1.2. Agent-based models

The agent-based modeling (ABM) tracks every detail (micro rules. i.e. endogenous representation of individuals) of how infection transmits from one to another as well as its movement pattern from one place (say home) to the other place (school or office) [73–76]. Even physical networks like roads, geographic environments, or social network-based interactions can also be considered in this approach.

The likelihood of transmission when an agent comes into touch with an infected agent, contaminated food, water, or an affected species is estimated using a probability distribution. A few factors that could affect the transmission [77] are transmission dynamics, public interaction networks, the environment, and public behaviors. Earlier, a square-shaped cell of size L is used to study the infection spread for SIS dynamics [78] for moving agents. Here the interaction between agents is constructed from the Lennard–Jones potential. The agents' movement and infection states are updated based on molecular dynamics simulation. The epidemic threshold is calculated when the infection times are drawn from a power-law distribution. In a more general setup, Hufnagel et al. used the daily data on domestic and international air travel [41] as a transition matrix to describe stochastic transport in a worldwide network. At the local scale, probabilistic infection dynamics are applied. By incorporating local and global data, such stochastic models can accurately depict the trend of severe acute respiratory syndrome outbreaks in certain regions. The network's significant heterogeneity compromises high predictability. An excitable mobile agent system is also developed in which the physical contact between susceptible and infectious agents is maintained for a finite time [79]. The dynamics of each agent is captured by $\dot{\mathbf{x}}_i = \frac{\mathbf{F}_i}{\xi} + \frac{1}{\xi}\sum_{i\neq j}\nabla U(\mathbf{x}_i(t)\mathbf{x}_j(t))$, where $\frac{\mathbf{F}_i}{\xi}$ is the active velocity and ξ is the friction coefficient. The active direction of motion is drawn from Poisson process. For the agent–agent interaction, a "soft-core two body" potential is used to make it a slow process, and it is captured by $U(\mathbf{x},\mathbf{x}') = \gamma[|\mathbf{x}-\mathbf{x}'|^{\lambda} - (2r)^{-\lambda}]$. The potential will be active when $|\mathbf{x}-\mathbf{x}'| < 2r$. Here λ is constant, γ depends on the constant active speed, and r is the radius of the agents. If the characteristic time for infection to recovery and conversion time from recovery to susceptible (τ_I, τ_R respectively) all are modeled by Poisson processes; the basic reproduction number can be captured by $R_0 = (1 - e^{-\frac{w}{\tau_T}})v\sigma_0\rho\tau_I = \beta\langle k\rangle$, where σ_0 is the scattering cross section, w is the mean duration of collision event (exposition time), ρ is the population density, β, and $\langle k\rangle$ denote the per person infection rate and the average contact rate (CR) respectively. The authors have also calculated minimum speed v_m from the transcendental equation : $e^{[-w(v_m)/\tau_T]} = 1 - 1/(v_m\sigma_0\rho\tau_I)$. It has been analytically shown that the exposition time and contact rates are crucial for understanding the disease spreading in systems of mobile agents. Epidemic spreading in communities with different densities of mobile agents is also studied. Depending on the jumping efficiency, a community whose contagion rate is less than the critical value may sustain the disease [80]. Eubank et al. considered dynamic bipartite graphs to simulate the patterns of physical interaction brought about by people moving between different sites [48]. Here an agent-based simulation (EpiSims) tool is developed based on land use and census data. The mobility pattern is extracted from the Transportation Analysis and Simulation System (TRANSIMS) developed at the Los Alamos National Laboratory. As a case study, they considered data from Portland, Oregon, USA (1.6 million vertices) and identified the structure of the networks. It has been shown that the degree distribution of people vertices is different from the locations graph. It was observed as scale-free, whereas the contact network among people follows a small-world-like structure. The authors have put up several smallpox spread mitigation ideas using large-scale simulation. The disease can be controlled with a well-tailored immunization plan and early detection. A scalable parallel algorithm called EpiSimdemics is also designed for large contact networks (∼100 million individuals) [53]. Here the probability of infection (at a given location) is captured by $p_i = 1 - \exp(\tau\sum_{r\in R} N_r \ln(1 - rs_i\beta))$. N_r is the number of infected individuals with infectivity strength r, τ is the exposure time, β is the transmissibility, and s_i is the susceptibility of i. To study the pandemic event in any country, a similar type of stochastic spatially-structured individual-based approach can also be considered, where the agents are human individuals and the model acquires the spatial data explicitly [74,75,81]. Municipalities are assumed to be the primary spatial structures considered in the model. A gravity model which captures the commuting probability from municipality to municipality is derived as follows: $w_{ij} \propto \frac{N_i^{\alpha}N_j^{\gamma}}{f(d_{ij})}$, where $f(d_{ij})$ is a distance-dependent function and α, γ are calculated from census data and travel data to work or school. This distance dependence functional form which can be chosen as exponential or power-law, encodes all the hierarchical levels ranging from the transmission on a national level to the local scale such as municipality or district. Any susceptible individual i becomes infected at time t with a probability $p_i = 1 - e^{-\lambda_i\Delta t}$. Here λ_i is the instantaneous risk of infection and Δt is the simulation time step. These risk factors are the combined effect of the contacts within households, contacts within the workplace/schools, and random contacts in the general population. Note that the GLEaM model and ABM both can predict disease propagation with a high level of accuracy. The pattern of such propagation is simulated for Italy for 127 days, 148 days, and 176 days after the first importation of infected individuals in Italy (Fig. 5).

ABM can also be used for modeling the transmission of Tuberculosis (TB) [82] for homogeneous as well as for heterogeneous mixing. Also, the age-dependent transmissibility of TB is encoded in the model. For homogeneous mixing, the risk of infection is captured by $\lambda_i = \sum_{k=1,\ldots,N}\beta_R\frac{I_k s_k}{N}$, where N is the total population at a given time, $I_k = 1$ if the individual k is already infected, β_R is the transmission rate per year, and s_k is the relative infectiousness of individual k. For preferential transmission, contacts from different levels are included. Contacts within a household, attending the same

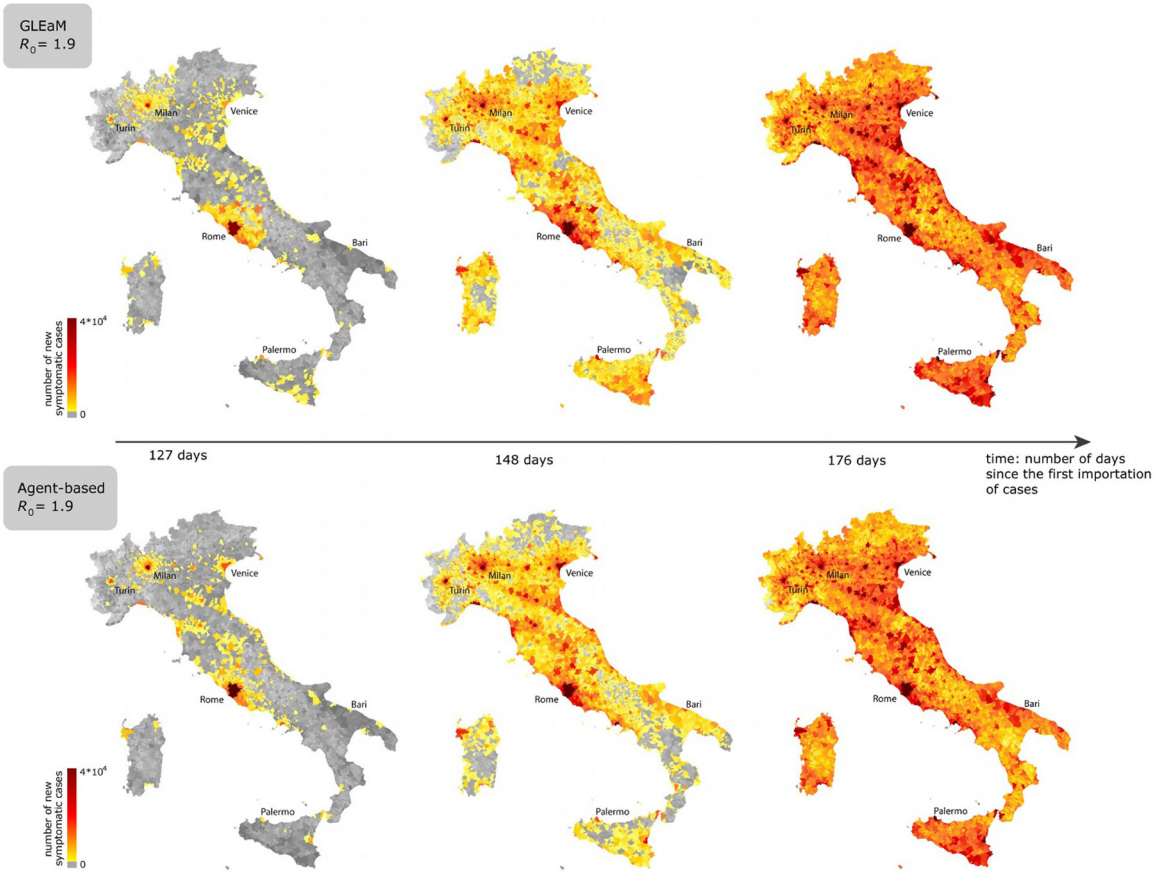

Fig. 5. GLobal Epidemic and Mobility mode (GLEaM) vs Agent-based model. In GLEaM (upper panel), the world surface is subdivided grid-wise, integrating the detailed population database. The demographic layer comprises two mobility layers: the short-range commuting layer and the long-range air travel layer. The agent-based model (lower panel) is stochastic, where agents represent individuals. Spatio-temporal epidemic propagation in Italy is compared for both models. The simulation is performed by fixing the reproduction number at $R_0 = 1.9$. The propagation looks similar for both models [40,56].
Source: Adapted from [40].

school or workplace, or random contacts in the populations are all sources of infections encoded in the risk of infection parameter. The re-infection from the exposed compartments is also considered a typical TB scenario. ABM is also held accountable for accurately forecasting the spread of malaria. The basic notion for the modeling of malaria spread follows a hypothetical "decision tree", where the agents (mosquitos) will assess their situations at each time step t and choose their next action(s) i with a chance of success p_i [83,84].

2.2. Kuramoto model

The Kuramoto model (KM) was initially proposed from chemical and biological systems by Yoshiki Kuramoto [85,86], and has been applied to various typical systems, including but not limited to brain dynamics, power grids, epidemic spreading and so on [87–89]. It has become a classical model for the study of the emergence of collective behaviors among coupled oscillators. The KM contains N oscillators with the following governing equations:

$$\frac{d\theta_i}{dt} = \omega_i + \frac{K_i}{N}\sum_{j=1}^{N}\sin(\theta_j - \theta_i), \quad i = 1, 2, \ldots, N, \tag{6}$$

with the coupling strength K_i. $\theta_i \in [0, 2\pi)$ and ω_i are the phase and natural frequency of the ith oscillator, respectively. Each oscillator i rotates at certain natural frequency ω_i and couples with its adjacent neighbors through the phase difference.

The signal propagates among oscillators through the adjacent coupling, and the propagation could be local or global, depending on the interplay between the system dynamics, the underlying networks and the nature of the signal. Here, we consider two processes of signal propagation: (1) Traveling wave (TW) state [20] in the KM with both positive and negative

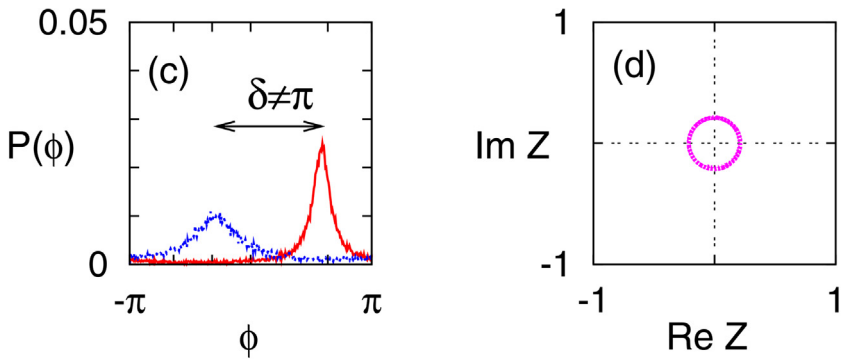

Fig. 6. Traveling wave state. (a) Phase distribution of TW state with red and blue lines corresponds to the conformist and contrarian oscillators, respectively. The mean-phase difference between the distributions is smaller than π. (b) The order parameter of TW state in the complex plane. The circle trajectory indicates a nonzero mean phase velocity.
Source: Adapted from [20].

couplings. Distinct from normal states such as incoherent state or partially-synchronized state in the KM, the phase distribution of the TW state spontaneously travels at a constant speed along the phase axis and signals transmit steadily within each oscillator group. (2) External perturbation spreading across the system through connections between units. The system could transmit from one state to another with even relatively small perturbation or fall into desynchronization if the perturbation is strong enough. The key point of this process lies in how to uncover the topological roles for the system dynamics, from both qualitative and quantitative perspectives.

2.2.1. Traveling wave state

In the simplest case of the KM (6), the coupling strength is usually assumed to be uniform with equal connections to adjacent oscillators, and is assumed to be positive with an attractive interaction. While, in the models of spin glasses [90] and neural networks with excitatory and inhibitory couplings [91], the interactions need to be asymmetric and could be positive or negative. For such cases, adjusted model turns out to be necessary [20], where the coupling strength is K_i, outside of the sum of the phase difference of Eq. (6). Such adjustment splits oscillators into two categories: those with $K_i > 0$ are 'conformists', who are attracted by the emerged giant population and tend to synchronize with it; whereas those with $K_i < 0$ are 'contrarians', who are repelled from the giant population and prefer opposed phases. For simplicity, binary values of coupling strength are considered, i.e., $K_i = K_1 > 0$ for conformist and $K_i = K_2 < 0$ for contrarian [20]. Considering that a random oscillator is a conformist by the probability p, the distribution of coupling strength K_i can be written in the form of a double-δ distribution: $\Gamma(K) = p\delta(K - K_1) + (1 - p)\delta(K - K_2)$. The TW state does not occur in the original KM ($p = 1$) or in the model with purely repulsive interactions ($p = 0$), an extreme case studied in [92]. It emerges only from the asymmetry in couplings, indicating that both types of oscillators contribute to the special phenomenon [20]. In this emergent state, the conformist oscillators converge to an instantaneous partially synchronized state and travel at a constant speed $\Omega = \sum_i \dot{\theta}_i/N \neq 0$, as do the contrarian oscillators. Moreover, the peaks of distributions are always separated by an angle smaller than π, as shown in Fig. 6(a).

For the quantification of the overall synchrony of the population, reflecting the characteristic of the TW state, the order parameter Z is generally applied [85–87], as follows,

$$Z = Re^{i\Phi(t)} = \frac{1}{N}\sum_{j=1}^{N} e^{i\theta_j(t)}. \tag{7}$$

Z represents the centroid of points $\{e^{i\theta_j}\}_{j=1}^{N}$ on the unit circle in the complex plane. When the phases are evenly distributed in $[0, 2\pi]$, the synchrony is entirely absent and $R \approx 0$; when all the phases gather around the same value Φ, complete synchrony is achieved and $R \approx 1$. For the case of TW state, one may find that the trajectory of the order parameter $Re^{i\Phi(t)}$ in the complex plane traces a circle, corresponding to the constant traveling speed of phase distribution, as shown in Fig. 6(b).

The discovery of the novel TW state has attracted great attention but its mechanisms need further exploration from the aspects of the distribution of natural frequencies, the underlying networks and others [93,94]. From the aspect of natural-frequencies distribution, there are various considerations, including homogeneous natural frequencies with coupling strengths in more complicated forms and heterogeneous natural frequencies with the correlation to coupling strengths.

Homogeneous Natural Frequencies: Even with the homogeneous natural frequencies, $\omega_i \equiv \omega$, TW state can emerge in the KM [95]. This motivates researchers further for the investigation of its emergence conditions, especially of the parameter space. Additional to the term K_i determining the in-coupling strength of the ith oscillator from the others, the

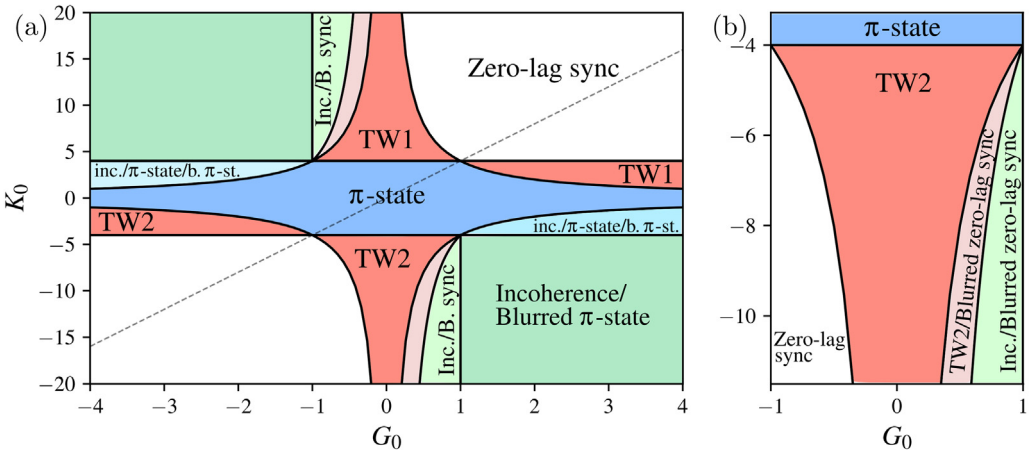

Fig. 7. Bifurcation diagram of the system (8) under $\Delta K = 8$ and $\Delta G = 2$. Panel (b) shows zoom-in regions of panel (a). *Source:* Adapted from [21].

out-coupling term G_i was also introduced, indicating the contribution from i to others [21,96]. The governing equations without noise [21,96] become then

$$\frac{d\theta_i}{dt} = \omega + \frac{K_i}{N}\sum_{j=1}^{N} G_j \sin(\theta_j - \theta_i), \quad i = 1, 2, \ldots, N. \tag{8}$$

Constant value of the out-coupling term $G_i \equiv 1$ leads to the original model [95]. Additionally, consider the parameters for couplings $K_{1,2} = K_0 \pm \frac{\Delta K}{2}$ of two groups, $G_{1,2} = G_0 \pm \frac{\Delta G}{2}$, where K_0 (G_0) is the average in-coupling (out-coupling) strength and $\Delta K > 0$ ($\Delta G > 0$) is the mismatch. When $|K_0| < |\Delta K|/2$ or $|G_0| < |\Delta G|/2$, both positive and negative couplings co-exist. TW state appears if one and only one of these two conditions is satisfied. More specifically, there are at least two types of TW states, indicated by the local order parameter of groups of oscillators: one for $R_1 = 1$ and $R_2 < 1$ (denoted by TW1) and the other for $R_1 < 1$ and $R_2 = 1$ (denoted by TW2), where R_k ($k = 1,2$) is the magnitude of the order parameter of group k. By using the dimensional reduction method of the Ott–Antonsen theory [97,98], the existence of traveling wave and π-states was also identified. Fig. 7 shows the bifurcation diagram of the system with respect to different values of average couplings.

With the inclusion of Gaussian white noise and with nonuniform and mixed attractive–repulsive interactions in Eq. (8), the two groups can partially oscillate in-phase or with a constant phase difference to each other. In this case, the bifurcation diagrams can be achieved on the basis of the Gaussian approximation, and TW state emerges where the whole population oscillates with a frequency different to that of the individual units [96]. Although these investigations provide a nice theoretical analysis of the existence and stability of TW state, each oscillator is coupled to all others. The interplay between the topology and the transient network dynamics is a central question but remains open. By considering the arbitrary adjacent connections, three major synchronization phenomena, consisting of phase synchronization, chimera states and traveling waves, have been revealed analytically. The analytical approach suggests that these three phenomena correspond to the contribution of different eigenmodes of networks, e.g., synchronized state and traveling waves as localizations in higher eigenmodes [94].

Heterogeneous Natural Frequencies: In spite of the ideal setting of the homogeneous natural frequencies, in most applications each oscillator oscillates differently and this arises from its intrinsic frequency. Considering a Lorentzian distribution of the natural frequencies and the relative strengths and proportions of the positive and negative interactions, the π state and the TW state do not appear [99]. This is in contrast to the previous finding [20]. Additionally, these results are based on the independence of the natural frequency of each oscillator and its coupling strength. Further investigation show that, if both terms are correlated, asymmetrical correlations can trigger the emergence of coherent traveling waves with the complex order parameter rotating with a constant frequency different from the mean natural frequency [93].

A general theoretical framework for the analysis of the KM with an arbitrary joint-probability density $g(\omega, K)$ of natural frequency and in-coupling for TW state is feasible in the continuum limit, $N \to \infty$ [100]. In this case, the probability density function (PDF) $f(\theta, \omega, K, t)$ denotes the probability of oscillators with phase θ, natural frequency ω, in-coupling strength K at time t. By using the Ott–Antonsen ansatz, the PDF could be expressed as $f(\theta, \omega, K, t) = \frac{g(\omega,K)}{2\pi}\left(1 + 2\mathrm{Re}\frac{\alpha e^{i\theta}}{1-\alpha e^{i\theta}}\right)$, with $\alpha = \alpha(\omega, K, t)$ satisfying $\frac{\partial \alpha}{\partial t} + i\omega\alpha + \frac{KR}{2}(\alpha^2 e^{i\Phi} - e^{-i\Phi}) = 0$. The TW state is in a stationary with a nonzero frame frequency $\Omega \neq 0$ and a time-independent PDF: $\partial f/\partial t = 0$. The latter condition is equivalent to

$\partial\alpha/\partial t = 0$, leading to

$$\alpha_s(\omega, K) = \frac{e^{-i\Phi}}{KR} \begin{cases} \sqrt{K^2R^2 - \omega^2} - i\omega, & \text{for } |\omega| \leqslant |KR|, \\ -i\left[\omega - \text{sgn}(\omega)\sqrt{\omega^2 - K^2R^2}\right], & \text{for } |\omega| > |KR|, \end{cases} \tag{9}$$

which could further induce the parameters of possible TW states and approximate stability [100]. Actually, for symmetric and unimodal $g(\omega, K)$, TW state exists only if K takes both signs and is in pairs, while for asymmetric distributions, the broken symmetry implies individual TW state. The asymmetric setting is more natural than symmetric, and the influence of distribution asymmetry on traveling waves has also been analyzed numerically and analytically [101].

Additionally, considering the dependence between each oscillator's natural frequency and the corresponding coupling, a series of exact solutions has been extracted to describe the critical points for emerging stationary collective phenomena, including chimera, π and TW states, and has been analyzed by means of a linear stability analysis and mean–field theory [102]. Thanks to the dependence, a non-stationary state, named the Bellerophon state, has been identified different from other phenomena. Some particular forms of distribution motivated by practical significance are capable of inducing multi-types of TW states [102–104]. The abrupt transition from the incoherent state to the TW state experiences a long-lasting metastable state with large fluctuations, a signature of a hybrid phase transition [105]. The transition is dominated by varying the density of the interactions [105]. Besides, TW state has also been found in various versions of the KM, e.g., with phase lag [106] (also known as Sakaguchi–Kuramoto model [107]), with bi-harmonic interaction term [108], with a pinning force [109] and with inertia [104].

2.2.2. Perturbation propagation

For the emergence of signal propagation, the interplay between dynamics and network structure is a crucial but hard question. Different aspects of the propagation process have been intensively investigated, including nodal perturbation and the important role of topology factors, along with multi-target and global perturbation.

The nodal-harmonic perturbation targeting to oscillator i takes the form $F_i(t) = \epsilon\delta_{ik}e^{i\phi t}$ with the strength ϵ and the perturbation frequency ϕ [110]. The function $F_i(t)$ is the time-varying perturbation and δ_{ij} is the Kronecker symbol. On regularly and sparsely connected networks, the pattern of response to such perturbation depends on the perturbation frequency ϕ and the distance [111]. At low frequency, the entire system dynamically responds homogeneously, i.e., all oscillators respond essentially and identically, and this resonant effect reaches its maximum when ϕ coincides with the natural frequency of the oscillators; On the other hand, at high frequency, the influence of perturbation becomes localized. Despite a constant propagation speed, the amplitude of the perturbation decreases exponentially with the distance [111].

The nodal harmonic perturbation can also be applied on the networked second-order KM, with a theoretical framework to uncover the underlying mechanisms of systematical response to the nodal harmonic perturbation [11]. Oscillators in the second-order KM are governed by

$$M_i\frac{d^2\theta_i}{dt^2} + D_i\frac{d\theta_i}{dt} = \omega_i + K\sum_{j=1}^{N} A_{ij}\sin(\theta_j - \theta_i), \tag{10}$$

where the inertial parameter M_i and the damping term D_i represent, respectively, the relative influence of change rates of phase velocities and phase angles [112]. By applying the perturbation $F_i(t) = \epsilon\delta_{ik}e^{i\phi t+\varphi}$ and considering homogeneous parameters $M_i \equiv M$ and $D_i \equiv D$, the relative response strength $a_i^{(k)}$ for oscillator i approaches ND as $\phi \to 0$ and $a_i^{(k)} \sim \phi^{-2d-1}$ as $\phi \to \infty$ where $d = d(i, k)$ is the topological distance between the driving oscillator k and responding one i. This indicates that, at low driving frequency, the responses of all oscillators share the same amplitude of an intrinsic parameter of the model and without any information of network topology, resulting in a homogeneous response of the whole system; at high driving frequency, the strength decays exponentially with the distance and the influence is then localized around the driving oscillator. These analytical results exhibit the universality with the independence of specific network structures, and the theoretical framework could also be applied on arbitrary topology for the generalization of previous works [110,111]. Fig. 8 shows the response patterns on a theoretical random tree and on the topology of an artificial British power grid-maybe coarsened.

Considering the arrival time, multiple approaches have been proposed to reveal universal features through the topological and dynamics effects of signal propagation on networks [12]. By defining the arrival time as the time that the response phase of a target exceeds a given threshold ϵ_{th}, the estimation is given by

$$t_{i,\text{est}}^{(k)} = |(\mathcal{L}^d)_{ki}|^{-1/(2d+2)} \cdot \left|\frac{\epsilon_{\text{th}}(2d+2)!}{\epsilon\cos(\varphi)}\right|^{1/(2d+2)}, \tag{11}$$

where $\mathcal{L}$ is the weighted Laplacian matrix with $\mathcal{L}_{ij} = -kA_{ij}\cos(\theta_j^* - \theta_i^*)$ for $j \neq i$ and $\mathcal{L}_{ii} = -\sum_{j\neq i}\mathcal{L}_{ij}$, and θ_i^* is the stable state of oscillator i without an external perturbation [12]. The estimation Eq. (11) isolates the topological factor (first term of the right side of Eq. (11)) clearly, encoding all information of the initial system including network structure, coupling strength and steady state of phases. On the other hand, the term $|\epsilon_{\text{th}}/\epsilon\cos(\varphi)|$ in the second part of the right side of Eq. (11) quantifies the relative level of response. Therefore, the arrival-time estimation helps to understand the

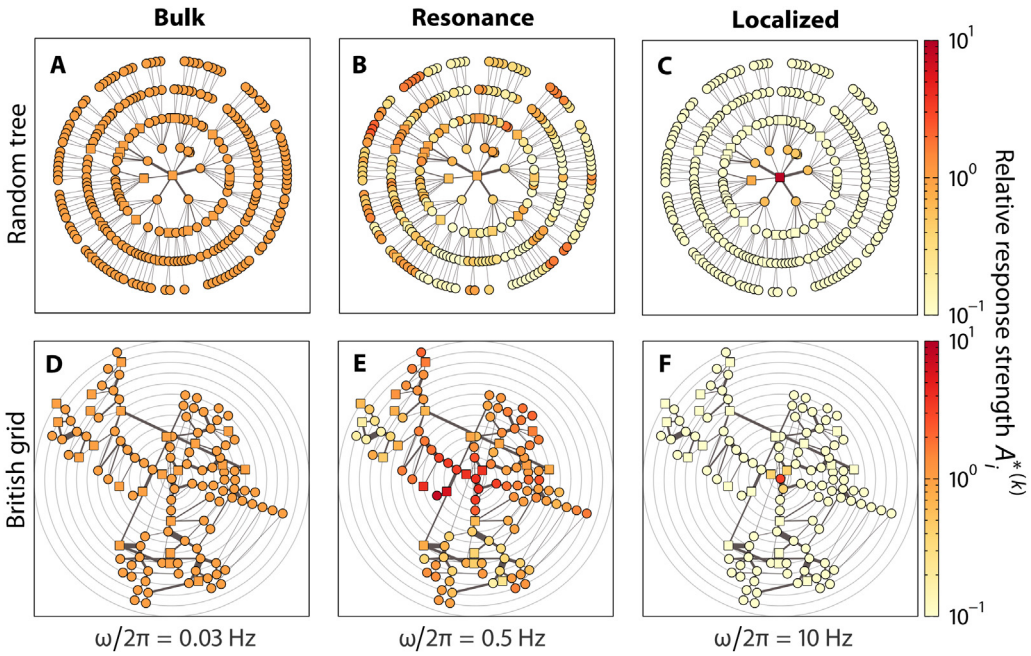

Fig. 8. Response patterns on two example networks with different driving frequency. (a) to (c) A random tree with $N = 264$. (d) to (f) Topology of the British power grid with $N = 120$. Color depth represents the relative response strength. The driven oscillator is placed at the center and all others are distributed on the concentric circle (gray lines) with radius proportional to topological distance.
Source: Adapted from [11].

hidden impact of network topology on the diffusive dynamics of a nodal harmonic perturbation. Although the prediction of the perturbation arrival time deviates from the actual arrival times with the increase of the topological distance d, due to the neglection of higher-order terms in the estimation, one can improve the prediction through the combination of a master function and an ensemble of network topologies [12].

Compared to nodal perturbations, the diffusive dynamics with multi targets and global perturbation becomes much more complicated. For example, perturbation in the form of non-Gaussian noise motivated by real systems controls the desynchronization rates around bifurcation points, either speeding up or slowing down the process depending on the network topology [113]. For the difficulty of tracing specific propagation routes, much efforts has been addressed to enhancing the system stability against perturbation through various ways. By suppressing targeted fluctuations at specific and desirable fixed points, network isolators allow us to control multistability not only for the linear flow dynamics but also for the nonlinear coupled KM [114]. When the natural frequency is tangent to the dominant eigenvector of the Laplacian matrix, the alignment function, as a combination of the Laplacian matrix and the natural frequency, has been found to approach optimization, by using the Gershgorin disk theorem [115].

2.3. Diffusion models

It is common practice to simulate a diffusion process by keeping track of nodes (people, blogs, users, etc.) as they gather, use or transfer information, particularly when they become infected, or when they buy anything [116–123]. Understanding the diffusion process in contact and social networks may be a useful tool for research into how information (such as blogs, memes, an epidemics, and the transmission of illness) travels among users and how frequently it must pass from source(s) to targets. This is because while contagious people can be identified, we are not always aware of how our neighbors or the next-door neighbors can infect us. Similarly, it is not always easy to pinpoint the source nodes that are pressuring a client to make a purchase or sign up for a service (directly or indirectly). In physical system, the diffusion process is exemplified by the Brownian motion, in which particle mixing is a process that results from random collisions between particles or with other particles [124]. Here we explore the diffusion dynamics in social, biological, and technological systems, where the agents are used to transfer or spread the piece of information i.e disease, or any ideas, memes, etc. To study the diffusion dynamics in networks, we explore a stochastic random walk-based approach and classical reaction–diffusion dynamics.

2.3.1. Random walks

Random walks process examine how information, such as diseases, ideas, or memes is transferred or propagated in social, biological, and technological systems via various agents. Agents may actively adopt a particular behavior or idea

and then spread it out of motivation [120], or they may be passive but still experience the diffusion process because of close contact (such as disease spreading and diffusion through biological pathogens). We investigate the diffusion process as random walks in a media, particularly in complex networks.

Discrete-time and continuous time random walks. Random walks (RW) are related to a stochastic process used to study the neuronal firing of the brain, or functional brain networks [125–128], movement and food hunt strategy of animals or humans [129–136], and technological systems such as a swarm of robots [137–141]. Depending on the structure of waiting time for hopping from one point to another, RW can be categorized as discrete-time (DT) RW or continuous time (CT) RW. In DTRW (on one dimension infinite line), if the probability density ($p(x;n)$) defines that a random walker is at the position x after n steps, one can write $p(x;n)=\int_{-\infty}^{+\infty} f(x-x')p(x';n-1)dx'$. Here if the particle is at x and it moves to $[x+r, x+r+\Delta r]$ in one step, then the probability of moving on that interval is captured by $f(r)\Delta r$. It can be shown that the solution of $p(x;n)$ converges to a Gaussian profile [118]. For the CTRW process, there will be a waiting time (τ) between two moves. This τ will be extracted from some probability density function. If the waiting times are drawn from an exponential distribution, the probability density $p(n,t)$, which is the walker covering n steps at physical time t will obey a Poisson distribution. Here we target to explore RWs in complex networks and their signal propagation properties. In a general setup, a diffusion of biased random walkers can be captured by the master equations as follows: let $P_v(t)$ denote the probability that the walker visits node v at time t. Then the master equation is given by $P_v(t+1)=\sum_{u=1}^{N} A_{uv}W_{uv}P_u(t)$, where the matrix A is the adjacency matrix having N nodes and L links. Here W_{uv} is the probability for a walker on node u to move to node v in a single time step. It can be written as $W_{uv}=\dfrac{A_{uv}(d_v)^{\alpha}}{\sum_{l=1}^{N}A_{ul}(d_l)^{\alpha}}$, where d_v is the degree of node v, and α is the bias parameter [60,142–148]. The simple RW corresponds to $\alpha=0$. Note that, for preferential navigation, one can write the transition probability more generally: $W_{uv}=\dfrac{A_{uv}(q_v)^{\alpha}}{\sum_{l=1}^{N}A_{ul}(q_l)^{\alpha}}$. Here q_v is a degree, the clustering coefficient, or the betweenness centrality [149]. If q_v is the eigenvector centrality, it is termed as maximal entropy random walks, in which the stationary distribution of random walks in a particular node is scaled with the square of the corresponding eigenvector element [150], and it can maximize the entropy rate production [150,151].

Signals Propagation. For an unbiased network of size N, the mean first passage time (average reaching time to the target from the source for the first time (MFPT): $\langle T_{uv}\rangle$) is written with the expression [145] $\langle T_{uv}\rangle=\dfrac{N}{d_u}$ for $u=v$, and $\langle T_{uv}\rangle=\dfrac{N}{d_v}[R_{vv}^{(0)}-R_{uv}^{(0)}]$ for $u\neq v$. Here the n th moment $R_{uv}^{(n)}=\sum_{t=0}^{\infty}t^n[P_{uv}(t)-P_v^{\infty}]$. Further, it has been shown that for general heterogeneous networks where, due to the presence of directionality, the MFPT between two nodes may differ, i.e.: $\langle T_{uv}\rangle-\langle T_{vu}\rangle=C_v^{-1}-C_u^{-1}$, where C_u is the random walk centrality (RWC), the ratio between the coordination number and the relaxation time of the node u. The strength of RWC determines the ability of a node to receive a signal faster (slower) compared to its counter-node. Thus, in heterogeneous networks, the information diffusion does not occur uniformly, rather the nodes with higher values of C have advantages in gaining information compared to the others. For a biased random walk, the MFPT can be captured by $\langle T_{uv}\rangle\sim\dfrac{N\langle d^{\alpha+1}\rangle}{d_v^{\alpha+1}}+\dfrac{N\langle d\rangle^2}{\langle d^2\rangle}\dfrac{1}{d_v}-2$, [142] i.e. the MFPT depends on the degree d of the target node. For $\alpha=-1$, the degree has no strong role in MFPT; rather it is highly affected by the size of the graph. Note that it has been numerically tested (for unbiased random networks) that a self-avoiding random walk can be an efficient way of exploring the network [152]. Recently, a local biased random walk model (α values are non-identical) is proposed, in which a simulated annealing algorithm is used to obtain the optimal exploration time of the entire graph [153]. For a review of random walks on local and non-local (un) biased random walks, one may check the recent review article [148].

A traffic model in a communication network is proposed where local topological structure (in a biased random walk) determines how the packets are routed in the network [147]. It has been shown that the average number of packets at node i follows a power law: $n(d)\sim d^{\alpha+1}$, which signifies that the systems' capacity (navigation efficiency) is highly enhanced at $\alpha=-1$ when each node can forward a constant number of data packets. The rate of change of the number of packets in the network follows a universal rule and does not depend on the bias parameter α. Based on the knowledge of the nodes' queue lengths, a global dynamic routing technique for network systems [154] is established. For a review of traffic dynamics on complex networks, one may check [155].

The coverage time, defined as the average fraction of nodes visited at least once by the random walker within or equal to the time t, is analytically derived for interdependent networks [156]. For a multiplex network having α number of layers, $\mathcal{P}_{ii}^{\alpha\alpha}$ denotes the probability of staying in the same vertex i and the same layer α. In the same way, one can construct different transition rules (within the same layer or between different layers): $\mathcal{P}_{ii}^{\alpha\beta}$, $\mathcal{P}_{ij}^{\alpha\alpha}$, and $\mathcal{P}_{ij}^{\alpha\beta}$. In this backdrop, the master equation for the probability of finding one walker in vertex j, and layer β at time $t+\Delta t$ is captured by

$$p_{j,\beta}(t+\Delta t)=\mathcal{P}_{jj}^{\beta\beta}p_{j,\beta}(t)+\sum_{\alpha=1,\alpha\neq\beta}^{L}\mathcal{P}_{jj}^{\alpha\beta}p_{j,\alpha}(t)+\sum_{i=1,i\neq j}^{N}\mathcal{P}_{ij}^{\beta\beta}p_{i,\beta}(t)+\sum_{\alpha=1,\alpha\neq\beta}^{L}\sum_{i=1,i\neq j}^{N}\mathcal{P}_{ij}^{\alpha\beta}p_{i,\alpha}(t), \tag{12}$$

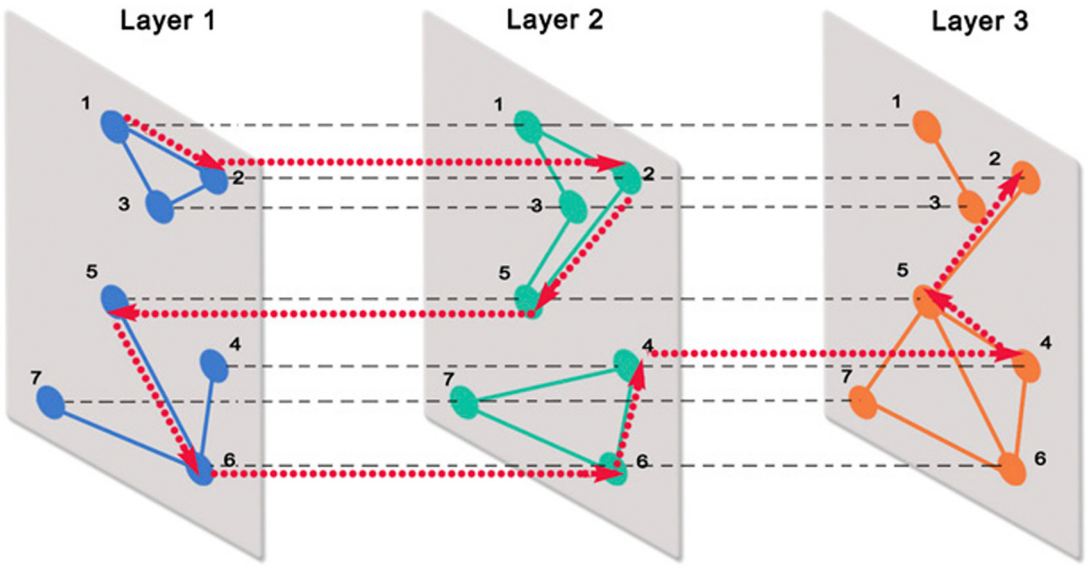

Fig. 9. Navigability of random walker in interconnected networks. The dotted red line is the path of the random walker to trace the way to jump between disconnected components. Here the navigability is calculated from the master equation of the random walkers by using the supra-Laplacian matrix, and the transition matrix of movement from layer to layer or within the layer [156].
Source: Adapted from [156].

where N is the number of nodes in each layer. In a compact form, it can be written as $\dot{\mathbf{P}}(\mathbf{t}) = -\mathbf{P}(\mathbf{t})\mathcal{L}$, where $\mathcal{L}$ is the supra-Laplacian matrix. Solving the master equation, one can obtain the coverage time as

$$\rho(t) = 1 - \frac{1}{N^2}\sum_{i,j=1}^{N}\delta_{i,j}(0)\exp[\mathbf{P}_j(0)\chi\mathbf{E_i}^{\dagger}], \tag{13}$$

where $\mathbf{E_i}^{\dagger}$ is the supracanonical vector, χ is the matrix encoded by the probability to reach other vertices of any pathlengths (Fig. 9). This analytical approach is successfully tested for the public transport of London to detect the navigability resilience under random failures, i.e the work provides a path for the "dynamical reachability" of vertices.

Epidemic propagation and time course. Random walks in graphs are a commonly used process to understand the epidemic spreading [157]. The hosts hop from one node to another by following an independent random walk. The infection can only spread from an infected person to a susceptible person if they appear in the same nodes [158]. If λ is the infection rate, $1-\exp(-\lambda\tau)$ is the probability of the virus being active for the time interval of length τ. In [158], they consider a single infected and a single healthy individual and attempt to determine the likelihood that the susceptible individual will become infected by time t. For an Erdős–Rényi model, the coincidence time is inversely proportional to the network size, and for a heterogeneous network, it has been proved that the coincidence time depends on the average, the maximum degree, and the exponent of the underlying power law ($p(d) \sim d^{-\gamma}$). For $\gamma < 3$, the walkers spend more time at high-degree nodes, and the epidemics propagate faster compared to regular or homogeneous graphs [159]. For multiple agents, the upper bound for all the particles to be infected is also derived [158,160], as well as the Laplace transform of the meeting time is derived in a closed form [161]. Recently, a study examined [162] the time required for the end of the epidemic (EOE) for two mobile agents in SIS setup, in which it has been shown that the Laplace transforms of EoE is a function of the meeting time which depends on the network structure only. The analysis unveils that depending on the network structure, the duration of a pandemic can be very short or very long.

Recently, a point process model (with motion) has been designed. Here the waiting time before the next jump in the plain is drawn from an exponential distribution. The fraction of infected individuals is calculated from a polynomial derived from the conservation equations of moment measures [164]. The upper bound of reproduction numbers ($\mathcal{R}_0$) is derived for discrete-time random walker hopping from one node to another in a finite ergodic graph [165]. The spreading pattern of disease (in which one agent is infected initially) in a 2-D network is examined, and it depends on the infection probability, mean particle velocity, characteristics time of infectivity, and the duration of immunity. Hallatschek [163] investigated evolutionary spreading dynamics, which include long-distance jumps of walkers (mutants) that result in the seeding of new clusters of mutants. If jump-distributions follow the power law tail $J(r) \sim \frac{1}{r^{d+\mu}}$, where d is the dimension of the space and $\mu > 0$. The spatiotemporal propagation pattern changes concerning the parameters μ and d: the zone of the mutant population may grow at a constant speed, revealing a circular wave, or the propagation growth becomes

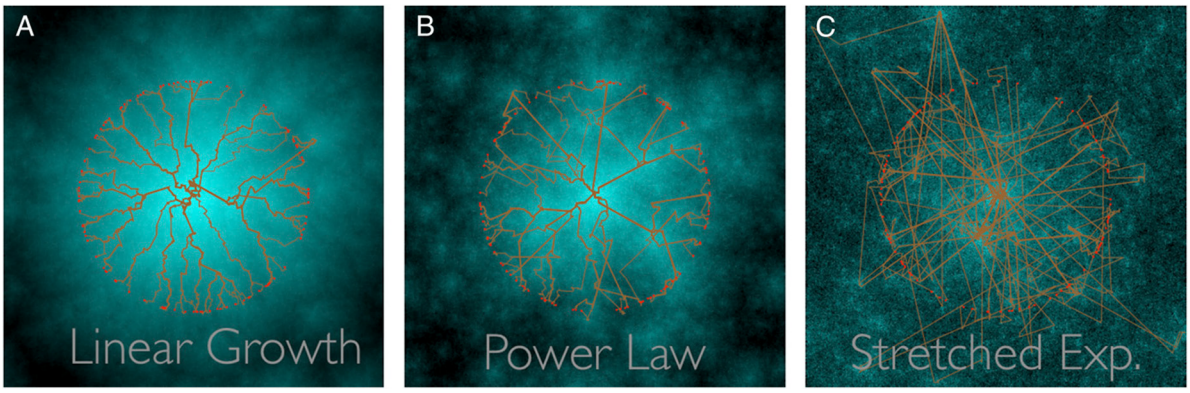

Fig. 10. Infection trees in epidemiology, generated by a power-law dispersal. Depending on the parameter μ, the propagation growth becomes linear ($\mu = 3.5$) (A), superlinear ($\mu = 2.5$) (B), or exponential ($\mu = 1.5$) (C).
Source: Adapted from [163].

a superlinear power law of time if $0 < \mu - d < 1$. For the condition $-d < \mu - d < 0$, the spreading dynamics exhibits stretched exponential growth (Fig. 10).

Note that the dynamical network model of random agents (robots) for long-range connections is also used to control the robots [166] and further used to study the infection pattern of the agents [167]. If the agents are chaotic, and the agents' motion in a shorter time scale compared to its dynamical evaluation, it can be shown that the synchronization behavior depends on the agent density, and global behavior can be captured by the all-to-all Laplacian matrix [168]. The opposite effect, close to the continuum percolation transition point, reflects that more time is required for synchronization [169]. Note that, under repulsive interaction of mobile dynamical agents, even extreme events may appear [170,171] and the authors have also investigated the evolutionary game dynamics in interdependent networks [172]. A heterogeneous interaction radius is considered for studying epidemic spreading in random walkers. The variance of the radius distribution determines the epidemic threshold [173]. Recently, a random walk simulation in 2-D space has been used to investigate the spread of infection based on proximity [174]. The parameter $\langle r \rangle$ is defined as the average separation between individuals, and the step length l of a random walker is assumed to be a multiple of $\langle r \rangle$. For smaller step sizes ($l \leq \langle r \rangle/2$), the epidemic growth is quadratic, and for $l = \langle r \rangle$, the growth follows a power law, similar to China's initial infection trend [175]. This simulation is further extended for predicting secondary and tertiary waves of infections with reasonable accuracy. The infection parameter in the 2-D Monte Carlo simulation is chosen as time-dependent [176]. Recently, another approach has been considered where an infected random walker can take τ steps and in each step, it can infect the visited site with some probability p. The spatiotemporal outbreak propagation is studied as a function and p and τ [177].

The application of random walks in complex networks has diverse directions. Community detection [178,178,179] is one of them. Rosvall et al. partitioned the network into modules by compressing a description of the probability flow of random walkers, which is used as a stand-in for information flows in the actual system [179]. Based on these tools for detecting communities in networks, recently neuroscientists are trying to make a bridge between the structural and functional network of the brains [180,181].

The career trajectories of individual artists concerning a network of galleries and institutions using an extensive record of exhibition and auction data [182] are studied in detail. If $p[i_{\tau+1}|i_\tau]$ reflects the probability of an artist's exhibition at the Institute i_τ, then $i_{\tau+1}$ will be their next exhibition. The model shows that the artist's next exhibition venue will be determined by the artist's previous exhibition history. Thus the probability of transition from i_τ to $i_{\tau+1}$, can be written as $p[i_{\tau+1}|i_\tau, \ldots, i_1] = K \times \frac{p[\pi_{i_{\tau+1}}|m_\tau]}{p[\pi_{i_{\tau+1}}]} \times p[i_{\tau+1}|i_\tau]$, where $\pi_{i_{\tau+1}}$ is the prestige at time $\tau + 1$, m_τ is the average reputation of the artist calculated from the past exhibition history, and K is the normalization factor. Early enrollment in elite universities has been proven to benefit students over the long run, whereas a substantial percentage of people who begin their careers in non-elite institutions drop out in the future. A second-order Markov dynamics (higher-order memory) has been developed for community detection and to understand the information spreading. Mainly it has been used to capture the actual travel pattern in air traffic networks [183]. For a review and latest updates on higher-order RWs, one may check [184–191]. Another application of the RWs-based approach is used to identify the Bluetooth (BT) contagion and a multimedia messaging system (MMS) virus by simultaneously tracking the location, mobility, and communication networks of mobile phone users [192]. A short-range nonlocal diffusion of virus spreading occurs for BT connections, whereas long-range non-local connections are allowed for MMS-based virus spread. In contrast to this non-local interaction, a classical two-dimensional diffusion process is considered as a null model where the virus can only diffuse to its nearest virus neighbor towers service areas. Due to slow progress, the virus diffusion for BT cannot act on

a large scale. Similarly, a phase transition on the underlying call graph restricts the outbreak of MMS viruses. Here the dynamics of infection are captured by $\frac{dI}{dt} = \beta SI/N$, where S is the susceptible users and $\beta \sim \langle k \rangle = NA/A_{\text{tower}}$ in which A is the BT communication area and N/A_{tower} represents the population density of that particular tower service area. The virus can diffuse to the new location when the user moves to another location.

2.3.2. Reaction–diffusion process

Microorganisms, cells, chemicals, and animals frequently move at random, causing a scattered and irregular motion of the entire population. However, a complex spatiotemporal pattern may be generated due to the formation of cell clusters under chemical signaling or mechanical forces [193–198]. The pattern formation is the central theme of embryology [199] and these models are called morphogenetic models. There are two approaches developed for pattern generation. One of them was developed by Alan Turing in his seminal paper "The chemical basis of morphogenesis" [200] in which, the two simple chemical ingredients can generate an instability in a homogeneous medium causing a complex pattern. The chemical compounds i.e. the morphogens locally *react* and transform into each other and disperse (*diffuse*) across the surface in space through tissue. The spatial heterogeneous pattern emerges under certain conditions (particularly if the diffusion coefficients are not identical): called the reaction–diffusion theory of morphogenesis and the patterns are called Turing patterns [194,200]. Here, pattern formation comes first and morphogenesis takes place later. On the other hand, a mechanochemical approach developed by G.F. Oster and J.D. Murray and their colleagues [199,201,202] in which pattern formation and morphogenesis are viewed as occurring simultaneously and models are described by quantifiable parameters like cell densities, deformation of tissues, etc.

In an ecological context, If $c(\mathbf{x}, t)$ is assumed to be the concentration of the species i.e density of the species, $\mathbf{J}$ be the flux of the species, and f represents the birth–death process, one can write the conservation equation [194]

$$\frac{\partial}{\partial t}\int_V c(\mathbf{x}, t)dv = -\int_S \mathbf{J}.\mathbf{dS} + \int_V f dv, \tag{14}$$

where S is an arbitrary surface enclosing volume V. Using the divergence theorem of surface integral, one can write (assuming that $c(\mathbf{x}, t)$ is continuous) $\frac{\partial c}{\partial t} + \nabla.\mathbf{J} = f(c, \mathbf{x}, t)$. For classical diffusion, $\mathbf{J} = -D\nabla c$ leading to the conservation equation $\frac{\partial c}{\partial t} = f + \nabla.(D\nabla c)$. If $f = rc(1 - \frac{c}{K})$, where K is the carrying capacity and r be the birth rate. Note that D is the diffusion constant, and may also depend on the spatial variables. Finally, one can obtain the generalized *Fisher–Kolmogorov equation* [203] for several interacting species ($u_i(\mathbf{x}, t)$) as $\frac{\partial \mathbf{u}}{\partial t} = r\mathbf{u}(1 - \frac{\mathbf{u}}{K}) + \nabla.(D\nabla\mathbf{u})$ for constant r and K. Here D is a matrix encoding the strength of diffusivities. The classic simplest case in 1-D space can be captured by $\frac{\partial u}{\partial t} = ku(1-u) + D\frac{\partial^2 u}{\partial x^2}$. $u = 0$ will be the stable solution if it is spatially homogeneous. To obtain the traveling wave solution, one may consider a solution $u(x, t) = U(z) = U(x - ct)$, where c is the speed of the wave. After rescaling the equation with $t^* = kt, x^* = x(k/D)^{1/2}$, one can write $U'' + cU' + U(1 - U) = 0$ where the system has two fixed points : $(0, 0)$ and $(1, 0)$. The origin becomes a stable spiral if $c^2 < 4$, and a stable node if $c^2 > 4$. It can be shown that the range of wave speed satisfies $c \geq 2(kD)^{1/2}$. If $u_{1,2}$ are the two fixed points of the logistic growth function, and $f'(u_1) > 0; f'(u_2) < 0$, using the singular perturbation technique, one gets the asymptotic solutions and show that, for a suitable initial condition, the wavefront moves from u_1 to u_2 with wave speeds $c \geq c_{\min} = 2[f'(u_1)]1/2$ [194]. One can construct a two-component system i.e for two interacting chemicals. In that case, patterns are generated due to the diffusion-dependent symmetry-breaking instability in a homogeneous medium [200]. The reaction–diffusion systems of two chemicals can be captured by

$$\frac{\partial u}{\partial t} = f(u, v) + D_u\nabla^2 u, \tag{15}$$

$$\frac{\partial v}{\partial t} = g(u, v) + D_v\nabla^2 v, \tag{16}$$

where the functions f, and g describe the reaction between two chemicals, and D_u, D_v are the respective diffusion rates. To generate Turing instability (TI) one has to maintain the following conditions [193,200,204] : $f_u + g_v < 0, f_u g_v - f_v g_u > 0$, and $D_u g_v + D_v f_u > 2\sqrt{D_u D_v}\sqrt{f_u g_v - f_v g_u} > 0$, where the subscripts of f and g represent the partial derivative. Gierer and Meinhardt developed phenomenological models [205] to determine the pattern formation of the tissue based on auto- and cross-catalysis, particularly considering short-range activation, and long-range inhibition, where the concentrations of activators and inhibitors change rapidly and the source density changes in a slow time scale. Here, the autocatalytic activation and self-inhibition are captured by $f(u, v) = a_1 + b_1\frac{u^r}{v^s} - \mu u$, and $g(u, v) = c_2\frac{u^p}{v^\chi} - \nu v$ respectively. All the parameters (a_1, b_1, μ, ν are the deterministic reaction rates) are taken as constants and a pattern exists if the condition $0 < \frac{r-1}{s} < \frac{p}{\chi+1}$ holds. Diverse patterns appear for identical or non-identical choices of s, and χ. For a detailed review and mathematical description of models ranging from chemical kinetics to neuronal dynamics, one may look into the following articles [193,196,204,206–209]. These types of the framework can be used to mimic the pigmentation

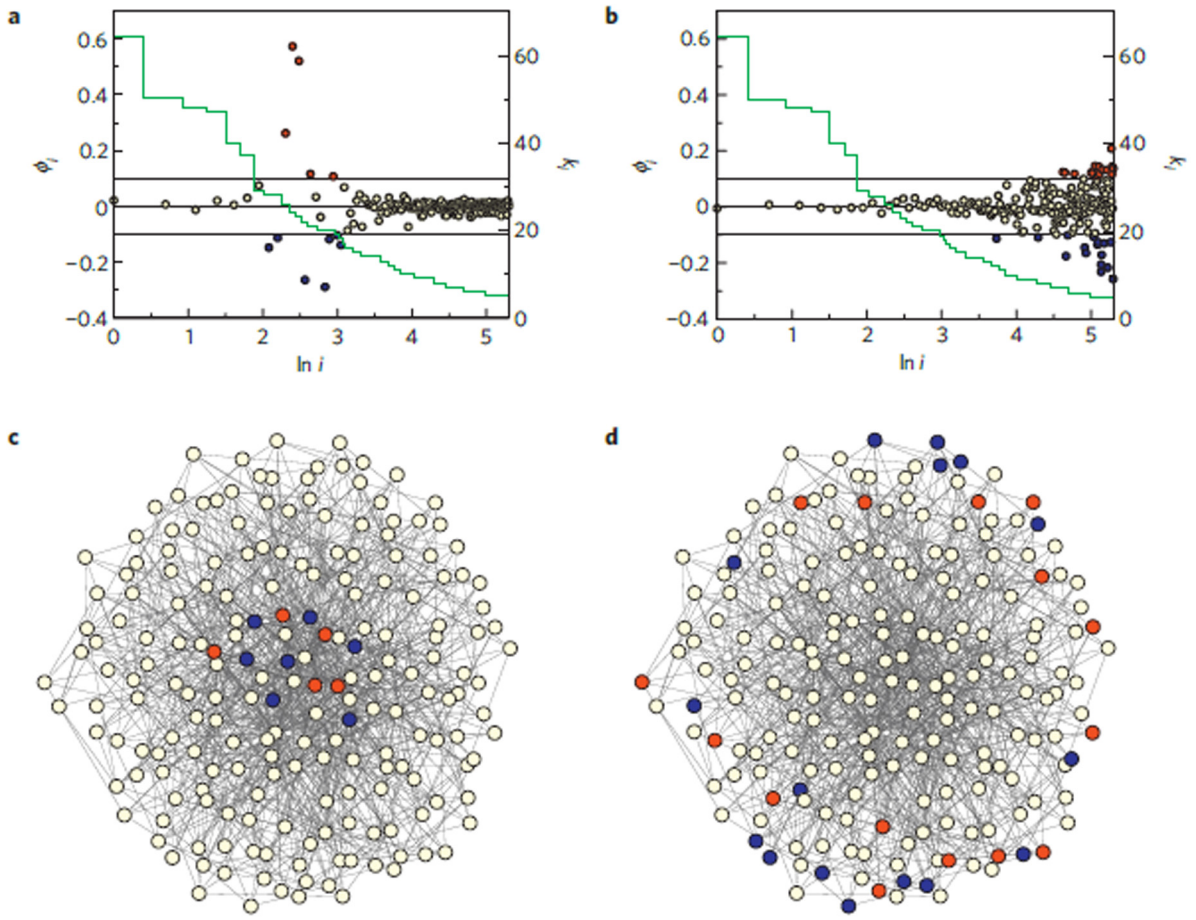

Fig. 11. Turing modes of a scale-free network with the size $N = 200$ with average degree 10. (a) (b) Critical eigenvectors are plotted against node indices. The degrees are shown with green lines. (c–d) The modes are either localized or spread to the periphery. The degree and index of red and blue nodes are reported in (a) and (b).
Source: Adapted from [215].

patterning in fish, the patterning in Hydra etc. [204,206]. Note that, in evolutionary ecology, spatial patterns like entangled spirals may emerge due to the mobility i.e diffusion in cyclic Lotka–Volterra model i.e in the rock–paper–scissors game (particularly in a periodic lattice) [210–214].

TI in complex networks. Turing instability may also occur at large random networks [215,216]. The network-organized activator–inhibitor model is described by: $\frac{du_i(t)}{dt} = f(u_i, v_i) + \epsilon \sum_{j=1}^{N} L_{ij} u_j$, and $\frac{dv_i(t)}{dt} = g(u_i, v_i) + \sigma\epsilon \sum_{j=1}^{N} L_{ij} v_j$. Here ϵ is the diffusion strength and σ represents the ratio between the diffusion strength of the activator and inhibitor species. The Laplacian matrix of the network is written as $L_{ij} = A_{ij} - d_i\delta_{ij}$, in which d_i is the degree. To calculate the emergence of TI, a small perturbation around the uniform state is applied, and the perturbations are expanded over a set of eigenvectors (ϕ^{α}). The TI occurs when one of the modes grows i.e the real part of the eigenvalue of the characteristic equation is positive. The ultimate stable patterns in a large random graph, which were analytically confirmed, vary from their critical mode, and TI occurs in some localized nodes (Fig. 11) with near degrees and depends on diffusional mobility (ϵ). This work is further extended for directed graphs [217]. Analytical results have demonstrated that "topology-driven" TI is also feasible in asymmetric networks, even when the system under study is unable to demonstrate TI in a regular lattice. A multiplex setup has been designed in which species diffuse through intra-layer connections and react from layer to layer [218]. In the presence of identical mobility, the multiplex system can generate the TI in the activator–inhibitor system. Different strategies are developed to control the TI pattern in directed networks [219,220]. Delay-induced TI in complex networks has also been investigated in Leslie–Gower Holling-type III predator–prey model [221]. Recently, the TI condition is derived for the cross-diffusive SI epidemic model. For specific initial infections, the arrival times of the first peak and final outbreak size are derived [222]. This formalism is further used in a SIR model [223], SIRS with delay [224], and to control the TI pattern in infectious disease [225]. Recent developments of TI in networked and regular lattices are

reported in [226]. RD process using stochastic formalism for epidemics has been discussed in the section metapopulation model in more detail.

Note that the behavior of the eigenvalues of the Laplacian matrix can be used to characterize a variety of dynamical processes, including synchronization transition and synchronization time [9,227,228], and diffusive processes provide a suitable approximation for these processes. A heat diffusion in a network can be captured by $\mu\frac{dx}{dt} = Lx$ [24], where μ is the time scale of the intrinsic dynamics and L is the Laplacian of the network. After a suitable transformation of the variables, this diffusion dynamics can represent the synchronization transition of identical systems or it can capture the consensus problems of multiagent systems [229].

2.3.3. Percolation process

Percolation initially refers to the diffusive process of fluids filtering through porous materials in the field of physics, chemistry and material science. The thriving development of network science breathes new vitality into the percolation theory, leading to a broader scope of applications including epidemiology, biology, sociology, engineering, and so on [230]. The key issue of percolation on networks lies in revealing the formation of the giant cluster, as one of the most fundamental topological features, after removing a fraction of nodes. Understanding the percolation is fundamental to a series of problems, such as prediction of diffusion scale, system robustness against attack and identification of critical components. In this subsection, we focus on two processes related to the topic of signal propagation on networks, i.e., k-core and bootstrap percolation.

As the generalization of classical percolation on lattices, k-core percolation is one of the most basic and typical models on networks [231–233]. The k-core percolation can be obtained through a recursive pruning process, where nodes with degree less than k are removed at each time step, after a fraction $1-p$ of nodes initially removed, and the iterative process continues until no more nodes in the remaining network satisfy the condition. As the result, one gets a giant cluster in which nodes have at least degree k, the so-called k-core. This pruning process may remove all nodes even if there are no initially attacked nodes, implying the intrinsic absence of k-core in certain network structures. This process may correspond to a continuous or discontinuous phase transition for the emergence of a giant cluster [234–236]. The phase transition of k-core percolation occurs at the critical point $p = p_c$, above which a k-core with finite size S_k scaled by the network size N emerges. There are two novel transitions, which complement classic percolation (equivalent to the degenerative case $k = 1$), emerging in k-core percolation depending on the value of k: the continuous transition in 2-core percolation, whose critical phenomena belong to the same type of biconnecting percolation [234]. This corresponds to bicomponents, of which real-world networks appear to be robust [237]; the discontinuous one for $k \geqslant 3$, termed as hybrid transition, with a jump of the order parameter [235,236]. The size of the k-core for a local tree structure is given by

$$S_k = p\sum_{d=k}^{\infty} p_d \sum_{n=k}^{d} \binom{d}{n} R_k^{d-n}(1-R_k)^n, \tag{17}$$

with R_k satisfying the self-consistent equation $R_k = 1-p+p\sum_{n=0}^{k-2}\left[\sum_{d=n+1}^{\infty}\frac{dp_d}{\langle d\rangle}\binom{d-1}{n}R_k^{d-1-n}(1-R_k)^n\right]$, where p_d is the probability of chosen nodes with degree d [235,236]. For general structures, there is an approximate relationship between S_k and the critical point through the exponent β, which was initially discovered in a Bethe lattice [238] and was later confirmed in other networks. For example, in ER networks, the parameter takes the value of $1/2$ for $k \geqslant 3$[239]. In scale-free networks, the ratio $\beta_{k=2}/\beta_{k=1}$ is solely determined by the exponent of the degree distribution [240]. For BA networks, the construction rules have a larger impact than the degree distribution on determining the component size of biconnected components [241]. This is associated with the susceptibility of the structure under intentional attacks [242]. For multiplex networks, the transition of k-core percolation shows rich comprehensive characteristics [243–246]. For instance, multiplex networks exhibit a discontinuous phase transition, different to single networks [245]. On modular networks with network communities, the 2-core percolation undergoes a continuous phase transition with changes of the network density, while the 3-core displays a first order transition [247]. The nature of phase transition has also been analyzed in high-order dependent networks [248].

Different thresholds for different nodes in k-core percolation lead to the so-called heterogeneous k-core percolation [249]. Generally, under $\mathbf{k} = (k_1, k_2, \ldots, k_M)$, a randomly chosen node of the network has a pruning threshold k_m with probability f_m satisfying $\sum_{m=1}^{M} f_m = 1$. The binary mixture of thresholds $\mathbf{k} = (k_1, k_2)$ has been extensively studied for its simplicity and representatives. However, even for this simple case, the transition nature of heterogeneous k-core percolation varies given different values of $\{k_m\}$ as well as the corresponding probabilities. One typical example is the difference of phase transition between $(1, 3)$ and $(2, 3)$-core percolation, despite the similarity shared by 1 and 2-core percolation. For (2,3)-core percolation, the discontinuous and hybrid phase transition is linked, i.e., for fixed p_c and f, only one type of phase transition exists [250]. While, for (1,3)-core percolation, there is a parameter region where both percolation transitions co-exist, with the first appearance of a continuous transition followed by that of a hybrid transition [249]. It was later pointed out that the tricritical point connecting two types of phase transition is quite rare in heterogeneous k-core percolation [251]. In fact, these phenomena could never emerge for $(1, k)$-percolation and only occur for $(2, k)$-percolation when $k = 3$. Glass-transition singularities are characterized by the coalescence of two critical points

in heterogeneous k-core percolation with ternary mixture [252]. For the generalized heterogeneous k-core percolation, the nature of transition is captured by the series of continuous and hybrid transitions of different order-parameter exponents β, as well as three kinds of multiple transitions [253].

Bootstrap percolation can be taken as an inverse process of k-core percolation and it describes the state switch of each node depending on the states of its adjacent neighbors [254]. The general rule of the bootstrap percolation with a fixed threshold $k \geqslant 2$ is as follows: Initially, a fraction $1-p$ of nodes are randomly chosen to be inactive, while the rest are active. Each inactive node switches its state to become active if it has at least k active neighbors. It will keep active once it adopts the state. The process continues until the system reaches the stable configuration without nodes having k more active neighbors. Like other percolation process, one of the key questions in bootstrap percolation is the existence of a giant active cluster of size $\mathcal{O}(N)$ with various critical phenomena.

Bootstrap percolation model shares many similarities including, e.g., mechanism and application with the threshold model [255], many aspects of which have been conducted intensively. The model was initially studied on lattices, such as finite size behavior [256–258] and existence of sharp metastability threshold [259–262], followed by behavior exhibited in infinite trees [263] and regular networks [264,265]. The process on random networks suggests an important role of the underlying structure for the switching dynamics. For power-law random networks with the scaling exponent between 2 and 3, a certain critical sublinear number of initially activated nodes is, in most cases, capable of inducing the giant cluster of finite size [266]. This observation is in contrast to that on ER random networks [267,268]. Theoretical investigations for the active component size of bootstrap percolation have also been investigated intensively [267,269,270]. Theoretical results can match well with simulation models and can also predict well e.g., the hysteresis loop [270].

Between k-core and bootstrap percolation, much efforts have also been devoted to establishing a theoretical relationship. A precise statement of the relationship was obtained for random regular networks [271]. For more generalized structures, by mapping bootstrap percolation with threshold k and the heterogeneous $(1, k)$-core percolation with nodes of threshold 1 and k corresponding to activated and inactivated state respectively, the transition observed in $(1, k)$-core percolation is similar to that in the bootstrap one [249]. However, such simple mapping has intrinsic defects, since all activated nodes at the end of bootstrap percolation are the subordinate branches of source nodes. While for heterogeneous $(1, k)$-core percolation, nodes survive from the pruning process just because they are part of the k-core, independent of their neighbors' states. An alternative idea is to take the Watts threshold model as the intermediary [255,272]. By interpreting the k-core and bootstrap percolation as special cases of the Watts threshold model, a complementary relation between heterogeneous k-core percolation and heterogeneous bootstrap percolation with different thresholds for activation process has been revealed, with degree d satisfying

$$k^b + k^c = d + 1, \tag{18}$$

where k^b and k^c are the thresholds of bootstrap and k-core percolation, respectively [272]. This relation indicates that, in non-regular structure, the homogeneous bootstrap percolation complements heterogeneous k-core percolation and homogeneous k-core percolation does likewise. Fig. 12 shows an example of this complementary relationship based on the same network structure. This relation was further generalized to the situation of arbitrary degree and threshold distributions [269] satisfying:

$$P(k^b \leqslant d - j|d) + P(k^c \leqslant j|d) = 1, \tag{19}$$

where $P(k^b \leqslant j|d)$ ($P(k^c \leqslant j|d)$) is the probability that a node with degree d has a threshold k^b (k^c) lower than or equal to j in bootstrap (k-core) percolation.

2.4. Cascading failures

Cascading failures refer to the process where a failure of one part could trigger further failures of other parts and finally endangers the whole system, resulting in system dysfunction or even catastrophic collapse. Such process could occur in both artificial and natural systems, such as power grids, transportation, internet, organisms and ecosystems. Taking South Australian blackout in September of 2016 as an example, the cascading failures triggered by the damage of 23 pylons on electric transmission lines due to a severe storm cut off the supply of the entire state, affecting 850,000 customers [273]. To this extent, one may interpret the successive failures as one typical kind of signal propagation on networks.

Concerning cascading failures, a great deal of attention has been devoted to preventing the negative influence of the process, including enhancement of system robustness, identification of critical parts for possible catastrophe, and recovery strategies driving system back to normal function. Here, focusing on signal propagation, we review two physical models to decode the underlying mechanism of cascading failures: one is the load-capacity model interpreting the failure as the result of overload [274] and (2) the other one is the fraction threshold model where the failure of one unit is caused by failures of its neighbors [255]. Despite their simplicity, these two models are capable of capturing key features of cascading failures.

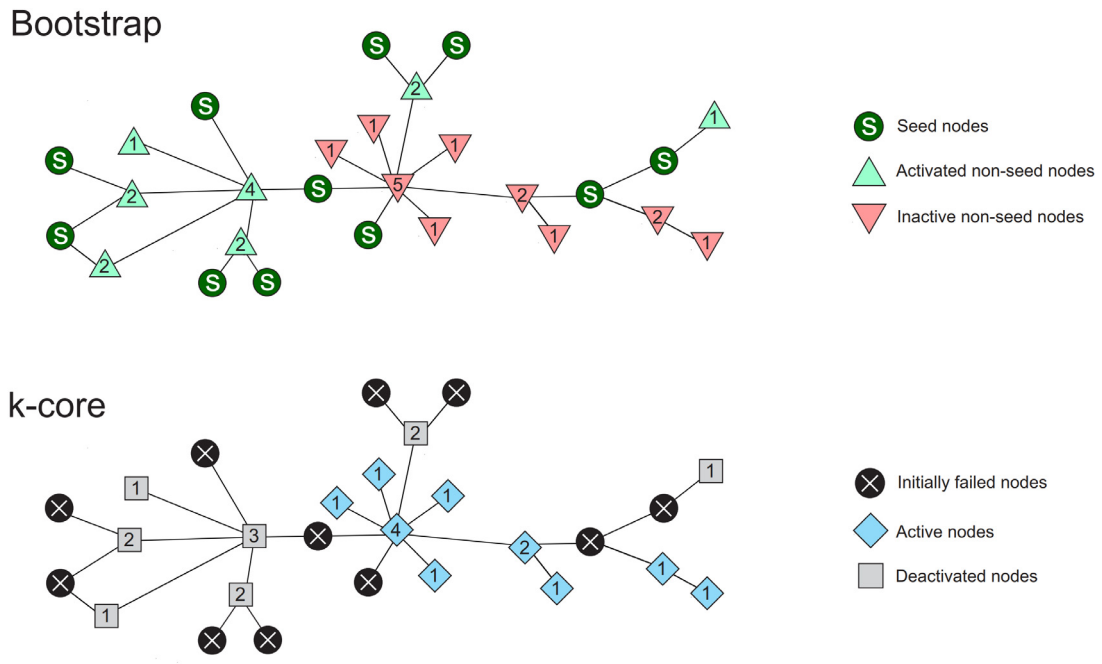

Fig. 12. Evolution of bootstrap and k-core percolation on the same network structure. The threshold of a node with degree d is $k^b = \lfloor d \rfloor + 1$ in bootstrap percolation and $k^b = d - \lfloor d \rfloor$ in k-core percolation. Since the condition Eq. (18) is satisfied, the two processes are thus complementary. All activated (inactive) non-seed nodes in bootstrap percolation are the same as those pruned (surviving) in k-core percolation.
Source: Adapted from [272].

2.4.1. Load-capacity model

The load-capacity model is inspired by the real systems with flows of physical quantities. Examples include power station dealing with a load of energy in power grids and routers transmitting large amounts of information in the internet. A salient feature of such systems lies in the phenomena of overload, i.e., the current load exceeds the maximum amount that a unit could afford, giving rise to unit malfunction. After load redistribution, this process will repeat until a new stationary state is achieved. Here, we introduce firstly the original load-capacity model proposed in [274] and focus on the analysis of cascade size as well as mitigation and control strategies.

In the load-capacity model, each node has two attributes, i.e., a time-varying load representing the relevant quantity of the specific system and a fixed capacity indicating the maximum load which the node could handle. The load $L_i(t)$ of node i is defined as the number of shortest paths that pass through it, depending on the current network structure, and the capacity C_i is assumed to be proportional to its initial load,

$$C_i = (1 + \alpha)L_i(0), \tag{20}$$

where $\alpha \geqslant 0$ is the global tolerance parameter ensuring that there is no overload at the beginning. The failure occurs to a node only if its current load exceeds the capacity, modeled as the removal of itself and its adjacent links. Although an extremely high tolerance parameter makes the failure impossible, the investment cost in reality severely limits the practical capacity. After the initial attack (removal of a set of nodes or links), the load redistributes across the system, leading to the further failure of a batch of nodes. This results further load redistribution and induces subsequent failures. The step-by-step process will continue until no more nodes fail due to overload. One could also construct the cascading-failures rule for edges, by defining the load and capacity of edges, since there are some arguments that the failure of edges is more realistic than that of nodes.

The cascade size, the number of survived nodes after the stop of cascading failures, is of great concern. Numerical simulations indicate that the breakdown of even a single node is sufficient to cause large-scale cascading failures if the distribution of networks is heterogeneous enough [274]. Since the distribution of loads is in line with the distribution of links, this result points out the fragility of heterogeneous networks, like scale-free networks, when facing cascading failures [275]. A similar result was also found in a variant model in which each edge is assigned a weight representing communication efficiency, underlining the destructive effect of removing a single node [276]. When the failure is modeled as the removal of a fraction $(1-p)$ of nodes rather than a single one, the fraction of surviving nodes exhibits a first-order phase-transition at the critical point p_c, which is associated with the tolerance parameter α. Most nodes survive and the giant component remains ensuring the relative integrity of the network when $p > p_c$, while the giant component disappears for $p < p_c$ [277]. Compared to random networks, real-world networks exhibit special characteristics,

e.g., spatial–temporal features, and this requires a concrete analysis. For example, cascading failures on spatially embedded networks propagate in a radial way with the center of initial failure, quantified as the average Euclidean distance of the failures from the center, the increase at a constant speed and finally reach its maximum proportional to the network size [278]. A statistical framework based on the concept of cosusceptibility allows the prediction of cascade size possible for arbitrary network structures. A cosusceptible group refers to a set of nodes tending to fail together, the partition of which corresponds to the cascade size distribution [279].

According to mitigation strategies, several methods have been proposed to enhance the system's robustness against cascading failures:

From the aspect of network design, the nonlocal effect could be strongly suppressed in networks with high clustering and short characteristic path length, as in small-world networks [5,280]. Apart from these two characteristics, the role of modularity, serving as isolators of failure, was also emphasized [281]. Setting edge weights with respect to topological properties of adjacent nodes reduces the risk of the occurrences of catastrophic dynamics, such as the product of degree under a generalized load-redistribution rule according to the number of weighted shortest paths, and the product of betweenness centrality or harmonic closeness under a local flow redistribution rule [282–285]. Adaptive weights dependent on the current load turn a heterogeneous load distribution into a relatively homogeneous one, and this induces the increase of network robustness, which is quite crucial for critical infrastructures like communication and transportation networks [286].

From the aspect of dynamics parameters, adjusting factors including tolerance parameter and capacity, is an alternative method. Heterogeneous tolerance parameter, dependent on the initial load or the one following Weibull distribution, allows more nodes to survive under an attack than the homogeneous one [287,288]. By freeing the capacity from the constraints of linear relationship with the initial load, the redistribution of extra capacity maximizes the robustness and minimizes the cost at the same time [289,290]. Hence, one can adjust mitigation strategies to enhance the load redistribution rule of overload nodes [291]. Additionally, to avoid large-scale destruction, it is necessary to perform an action in time during the propagation of cascading failures. Early research suggested that intentional removal of nodes with small load and edges with large excess of load right after the initial failure could effectively suppress the propagation of successive failures and dramatically reduce the cascade size [292]. Controllability for system under different attacking types and based on different network structure has also been discussed in [293].

2.4.2. Fraction threshold model

The fraction threshold model is motivated by the phenomenon that decision makers tend to take the action in line with the majority when they have to decide between two alternative ones, known as binary decisions [294]. The phenomenon is quite common in social and economic systems, and the decision-making process exhibits a strong threshold nature, i.e., the individual will not change his/her decision unless his/her personal fraction threshold of neighbors holding a contrary opinion is reached. In this subsection, we introduce the fraction threshold model [255] and review theoretical analysis of the model as well as several factors which may influence the propagation process of cascading failures.

In the fraction threshold model, each node is either in a functional state (denoted by 0) or in a failed state (denoted by 1) at any step t. At the beginning, all nodes function normally and adopt state 0. The transition from state 0 to state 1 of a node occurs only if a threshold fraction β of its d neighbors are in state 1, while the reverse transition is forbidden. To model the dynamics of cascading failures, the initial attack turns the state of a small set of nodes (called seeds) from 0 to 1 and the system evolves according to the transition rule until no transition takes place anymore. To mimic the complexity of cascading failures, both degree d and individual threshold β can be taken as heterogeneous. Specifically, p_d denotes the probability of nodes with degree d, $\sum_d p_d = 1$, and β is chosen from a distribution with cumulative distribution function $F(\beta)$ denoting the probability that a node has a threshold less than β. The influence of such heterogeneity on the cascading propagation could be taken from two aspects: increase in threshold heterogeneity promotes the process, while increase in network heterogeneity prevents it, which is contrary to the fragility of heterogeneous networks in load-capacity model.

The key question of the model is then when the global cascade occurs. Considering an attack in a sparse network, it is reasonable to assume that no nodes are connected to more than one seed. This assumption indicates that the failure could further propagate only if at least one neighbor of the seed has the degree $d \leqslant 1/\beta$. Nodes satisfying this condition are called vulnerable ones, and the probability u_d of vulnerable nodes with degree d is given by

$$u_d = \begin{cases} 1, & d = 0, \\ F\left(\dfrac{1}{d}\right), & d > 0. \end{cases} \tag{21}$$

The global cascade is possible if the vulnerable nodes percolate through the whole system. By constructing the generating function of vulnerable nodes' degree $G_0(x) = \sum_d p_d u_d x^d$, the global cascade condition, according to the percolation theory, could be expressed as $G_0''(1) = \sum_d d(d-1)p_d u_d = \langle d \rangle$, where $\langle d \rangle = \sum_d d p_d$ is the average degree. For $G_0''(1) < \langle d \rangle$, vulnerable clusters are too small to reach each other, making the cascades localized, while, for $G_0''(1) > \langle d \rangle$, the percolating vulnerable cluster with infinite average size is capable of facilitating the appearance of global cascade. Moreover, the monotonically increment of the term $d(d-1)$ and the monotonically decrease of u_d with d imply two phase transitions with different critical points. In fact, below the smaller critical point, the propagation is limited by segregated clusters due to the sparse connection, while above the larger critical point, the dense connection leads to local stability, which is

strong enough to prevent further propagation. The global cascade is thus only expected when the network density lies between these two critical points.

With the generalization of the assumption of scarce seeds in [255], the influence of the seed size has also been studied further [295] and the cascade condition turns to

$$\sum_d d(d-1)p_d\left[F\left(\frac{1}{d}\right)-F(0)\right]=\frac{\langle d\rangle}{1-\rho_0}, \tag{22}$$

where ρ_0 is the scaled-seed size. In this case, the previous cascade condition [255] is a special case of $\rho_0 \to 0$ with $F(1/d) = u_d$ and $F(0) = 0$. Moreover, explicit expression of scaled-seed size ρ linked to ρ_0 is given by $\rho = \rho_0 + (1-\rho_0)\sum_{d=1}^{\infty} p_d \sum_{m=0}^{d}\binom{d}{m} q_\infty^m (1-q_\infty^m)^{d-m} F\left(\frac{m}{d}\right)$, where q_∞ is the fixed point of the recursion relation $q_{n+1} = \rho_0 + (1-\rho_0)\sum_{d=1}^{\infty}\frac{dp_d}{\langle d\rangle}\sum_{m=0}^{d-1}\binom{d-1}{m} q_n^m (1-q_n^m)^{d-1-m} F\left(\frac{m}{d}\right)$. For cascades triggered by scarce seeds, the phase transition is considered to be continuous at the smaller critical point and discontinuous at the larger critical point [255], while numerical simulations suggest that the transition at small critical points can also be discontinuous in certain parameter regimes [295]. When cascades are associated with a local dependence on random networks without interdependent links, there is a crossover between these two types of transitions, indicating the complexity of transition dynamics of cascading failures in the fraction threshold model [296].

Network characteristics are crucial for the propagation of cascading failures. From a local perspective, modularity tends to limit the process within each module, where nodes exhibit similar characteristics and close connections, preventing the failure propagating from one to another [297–299]. Considering the degree–degree correlation, the cascade size decreases for positive correlation values in assortative networks, while it increases for negative values in disassortative networks [299], with detailed derivation for the fractional size of the giant vulnerable cluster as the function of degree–degree distribution [300]. Clustering [301] reduces the cascade size for small or large average degree, while increases it when the network has a medium value of an average degree [302].

As for different types of network structure, it turns out that random links could either promote the propagation of cascading failures in small-world networks compared to regular lattices, or inhibit the process if thresholds approach critical values [303]. In multiplex networks, the interaction between layers facilitates the system vulnerability to cascading failures, compared to networks of each single layer [304]. Without sufficient knowledge about the multi-layer structure of the system, this induces the difficulty of the prediction of cascading failures, but also provides a practicable way for controlling the propagation process through introduction or removal of layers. For the model applied on temporal networks, the bursty activity patterns could either facilitate or slow down the cascading-failures propagation, depending on the setup of state transition rules [305–307].

2.5. Neuroscience dynamics

2.5.1. Neural networks as dynamical systems

Biologically, spiking neurons are the elementary processing units in the central nervous system, and information propagates within neurons as electrical signals but between them mainly as chemical signals. At the molecular and cellular level, biological research has accumulated an enormous amount of detailed knowledge about the structure and function of neurons and synapses, as well as the properties of action potentials. At the network level, however, signal propagations among the intricately-connected neurons still need to be characterized [308,309]. A coherent understanding of the brain from local to global is necessary for understanding the signal propagation in nervous systems [18,310–312].

Due to the highly variable nature of neural responses and inherent nonlinearities in the dynamics of neurons, it is essential to apply complex network analysis tools to assess the interaction patterns and functional organization of the brain [309,313,314]. The differential equations of neural dynamics can create qualitative models of responses [315–317] and contribute to inferring the topology of connectivity and extracting the important variables and internal drive at different scales [318–320].

Larval zebrafish is a genetically accessible vertebrate model animal with a transparent brain, which allows a large-scale neural dynamic analysis [321]. With the development of genetics and optical imaging techniques, larval zebrafish becomes the only vertebrate animal whose whole-brain dynamics can be captured at the single-cell resolution [322–324]. Thus, this system offers an outstanding potential for exploring biophysically plausible circuit arrangements for neural signal propagation.

A whole-brain scaled model can be built from existing tools at the single-neuron level. For example, the leaky-integrate and fire (LIF) model [309,325,326] and the stochastic binary neuron model [327] are used for understanding how different components (excitatory and inhibitory neurons, synapses, and external excitatory inputs) and their interactions determine the global in-coming activity pattern. The LIF model is a classic model describing the membrane potential of neurons and well captures their nonlinearity (23). The LIF model depicts analog signals in single neurons, as

$$\frac{dv_i(t)}{dt}=a_i-v_i(t)+I_i^{syn}(t), \tag{23}$$

where $v_i(t)$ denotes the membrane potential of neuron i, a_i denotes the external input current, and $I_i^{syn}(t)$ denotes the synaptic current due to the incoming adjacent connections. In contrast, the stochastic binary neuron model captures digital

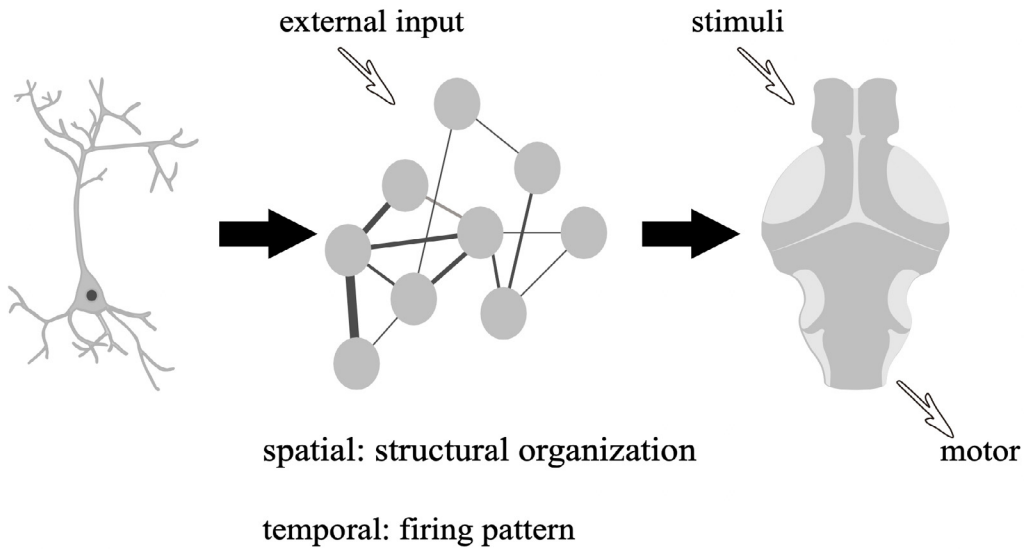

Fig. 13. Dynamical systems are found at all organizational levels in signal propagation of the neuronal system. At the single-cell level, communications are both digital and analog. At the neural mass level, information between different cells, such as excitable and inhibitory neurons, propagates through synapses. Here, macroscopically, structural organization and firing pattern are the predominant properties that affect signal propagation. At the individual level, the behavior evoked by visual motion offers a paradigm to digest brain-scale sensorimotor circuits underlying vertebrate behavior. Behavioral analysis reveals the basic algorithmic properties by which the brain integrates inputs to adjust the internal state and generates motor outputs [308].
Source: Adapted from [308].

signals by depicting the spike series of single neurons. In the stochastic binary neuron mode, the neuronal activation levels are history-and-external-information dependent and spontaneous.

Approaching from the network level also characterized propagation properties of the nervous system; non-random structure properties, such as power-law degree distribution [325] and a modular and hierarchical organization [327], were found in the zebrafish brain. Applied to brain-wide observation, tools of nonlinear dynamics have successfully reconstructed the organization and evolution of neural signals, and also improved the understanding of the influence of single-neuron physiology on behavior.

Assemblies of neurons are influenced by a series of components, including external input, intrinsic excitability, and connectivity strength. To process information effectively, patterns of these components are well-structured, i.e., groups of neurons tending to fire together in spontaneous activation as a Bayesian prior over possible stimuli [327], and the delicate balance between excitatory and inhibitory neurons near a phase transition for shaping near-critical dynamics [326]. With the methodology of neural dynamics, theoretical frameworks can incorporate different-scaled data and identify the functional modules and pathways. Integrating concepts from statistical physics, such as emergence [327], avalanches, and Hebbian plasticity rule, the neural dynamics is very appropriate to depict the highly structured patterns of neural activity. To test if the concepts from statistical physics are just idealized inferences, these theories have been applied to in vivo brain-wide observations from zebrafish to explain the neural activities and animal behaviors [326,327].

When dealing with the large scales of whole-brain observation, conceptual models provide tractability in modeling complex neural circuits. Studies use neural mass models [328], based on the simplification of synaptic connectivity and neural responses to describe a local population of interacting neurons (Fig. 13). Both stereotyped and variable signals exist during propagation, so the brain transits between different states and maintains stable firing patterns within each state, comparable to the concepts like criticality and attractor in dynamical systems. Phase analysis is naturally suitable for sensory-biased behaviors and has been applied to persistent activity [329] and orientation-selection [317,330]. These methods offer a straightforward evaluation of the robustness and susceptibility of a given dynamic system to both extra perturbations [329,330] and spontaneous changes [18,317]. State-dependent computation is also widely used when the neural dynamics can determine the temporal structure of internal states [331]. The resulting behavior is the interaction of a hierarchically organized background with input from any designated stimulus [332], thereby revealing critical hidden variables that shape the temporal structure of motivation and decision-making.

2.5.2. Synergies between neural dynamics and data analysis

The neural-dynamics-based tools have promoted investigating the mechanisms of neural computation. But their applications to study the functional interaction patterns of real biological systems are limited, primarily due to the lack of suitable calibration methods to confirm and test the models.

The brain is a dynamic system that simultaneously possesses neuronal activities, spontaneous regulatory networks, and networks of stimulation reactions. Its products, the motor outputs and behaviors, provide excellent measurements for evaluating models. Simple behavioral functions, such as orientation-selection and evidence-accumulation, are ideal and the increased availability of qualitative measures for behaviors supports the integration of model simulation and experimental data. Overall correlation score [317] and motion probability [330] are reported to estimate quantitative agreement between stimulation and behavioral observations. Furthermore, as quantified by the slow decay of turning, the orientational persistence mechanism reveals the robustness of a two-module model from a circuit called anterior rhombencephalic turning region [333] in zebrafish for orientation-selection in the absence of stimuli.

In more complex dynamical systems, e.g., a plethora of models distinguished by the relative strength of different components all have the same 'line attractor' but behave quite differently around it. Perturbation experiment attributes pose new constraints on the circuit connectivity of the system and provide new insights into the underlying mechanisms [317,329].

In 2013, the light-sheet microscopy imaging method was applied in zebrafish and obtained whole-brain functional dynamics at cellular resolution [322]. Later, advanced imaging analysis tools [323] and behavioral measurements were developed [334], so the dynamics of all neurons in the central nervous system can be extracted with single-cell resolution, in accompany with the sensory inputs and motor outputs, over long periods, as shown in Fig. 14(a). While improvements in microscopy allow us to probe whole-brain signal propagation in great detail, they require algorithmic techniques that can scale up to entire neural populations.

An optimization-theoretical approach can be applied to the model-fitting procedure by reducing the distance between the experimental and simulated features [309,326]. In single-neuron models, features, such as the cumulative sum of spike train, are usually functions of time, and it is reasonable to perform heuristic algorithms, such as the Nelder–Mead downhill simplex algorithm. Therefore within reasonable limits, the result is qualitatively independent of its value. To fit the functional circuit connectivity encompassing the constraints on anatomical patterns, tuning curve, and firing rate drift patterns, an algorithm with constraints is usually taken, like a constrained linear regression procedure and grid search across an explicit range. In practical terms, the cost function should be set as a regularized mean squared error term to ensure that each neuron can fit separately from the others.

Despite establishing the algorithm principal, the fitting procedure should be determined by how the network can be quantified, which relates to the imaging or recording processing complexity and the final visualization form of dynamical models. Some commonly used features and insights into neural signal propagation are: (i) edge density, the density of effective connections between neurons, representing the network topology; (ii) the distribution of edge weights between neurons, representing the network geometry, parallel to in-degree distributions in graph theory; (iii) intrinsic excitability, which stands for the excitability of individual neurons and can be depicted by the response curve. More generally, by counting the spike distribution of the whole neuron group in time windows, the spike train is calculated as a function of time or the distribution of firing rates. The synaptic connections and neuronal linearity are difficult-to-measure microscopic variables. Still, their distribution probabilistically estimates macroscale properties of the brain, which is an appealing approach from statistical physics. A popular method to study the exhibitory–inhibitory balance in the term of criticality is governed by scale-invariant avalanches, which are contiguous clusters of activity that propagate in space and time [326], as shown in Fig. 15.

In the calibration procedure, a recurrent network of excitatory leaky-integrate-and-fire (LIF) neurons generates models that well-fit three stages for the emergence of pathological state transitions. On the other hand, to compare each parameter's importance, models are tested when keeping a subset of parameters free for fitting, while constraining the others. The results indicate that different neuron dynamical stages have different emergence conditions, including network topology, network geometry, and intrinsic excitability.

For example, an increase in edge density of reorganization of network topology best explains the loss of criticality that emerges with the onset of generalized seizures [326]. These properties generally reflect an efficient design that ensures near-critical dynamics in spontaneous activity and information processing, as shown in Fig. 14(b). Moreover, the large-scale oscillations reflect in the distribution of currents indicating remarkable small-worldness, which is recovered by an inverse reconstruction scheme aimed at inferring the distributions of both firing rates and network connectivity from global activity fields [325]. The anatomical districts considered in the analysis can be divided into two groups according to the reconstructed probability distributions of both their excitatory connections and excitability. And the group results are associated with the functions of each brain region and the perturbations on the zebrafish.

Noteworthy, approaches combining multicellular Ca2+ imaging and graph-theoretical have also been conducted in the study of whisking behaviors [335] and seizure [336]. In all these studies, computational models are all united with data, based on a series of mathematical estimation schemes, thereby offering a framework for statistical inference, which would not be possible with conventional methodological tools.

3. Complex networks

3.1. Temporal networks

Temporal networks, compared to static ones, allow signal propagation along links only when they exist in time, and this leads to considerable influences on the propagation efficiency [337,338]. Traditional compartment model and

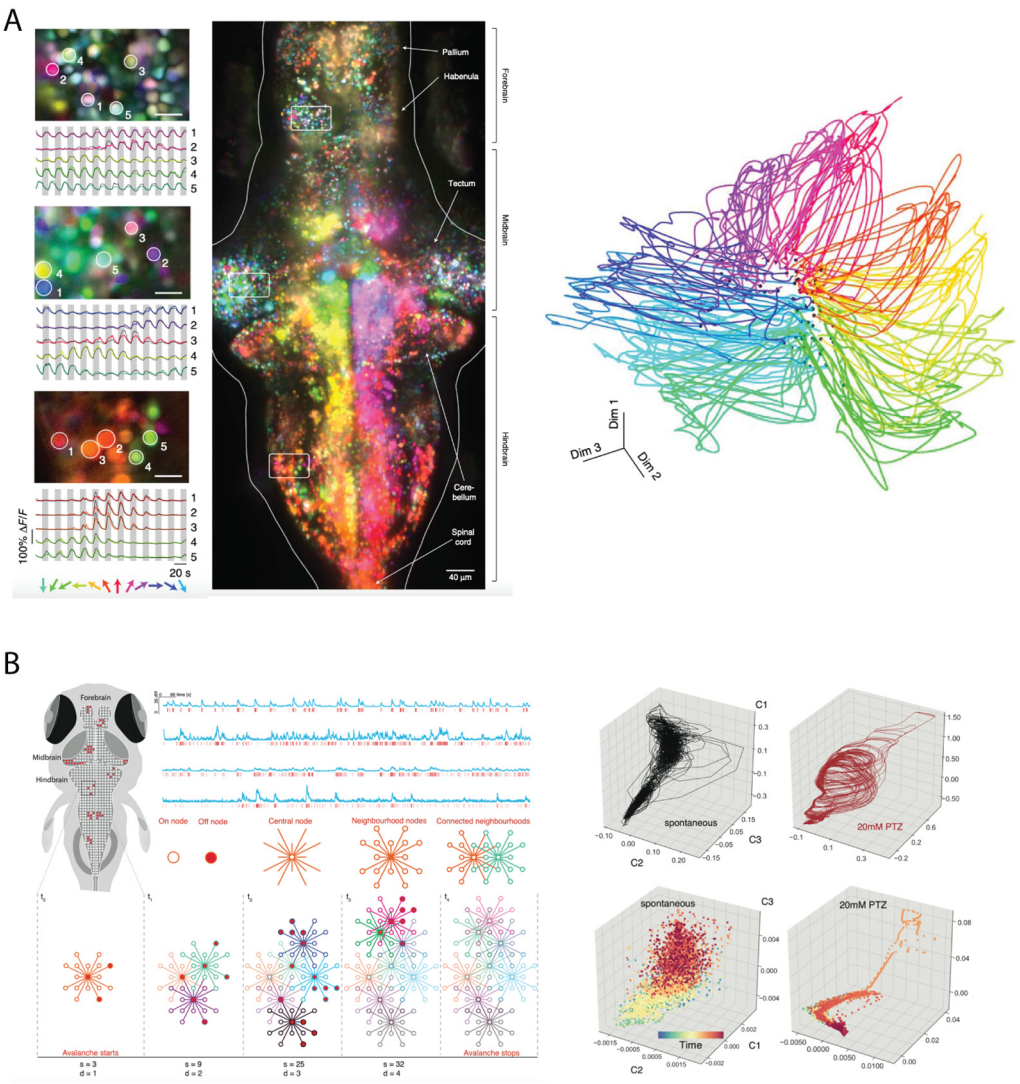

Fig. 14. Whole-brain imaging revealed neural dynamics of zebrafish. A. Visual cue-induced activity. Left, calcium response to moving grating stimuli in 12 different directions. Color, preferred direction.; saturation, tuning width, brightness, response strength. Right, whole-brain dynamics across time. Each line represents a single trial. B.Whole-brain dynamics during epileptic seizure. Left, avalanche estimation. Right, isomap 3d embedding of reconstructed attractors.
Source: Adapted from [323,326].

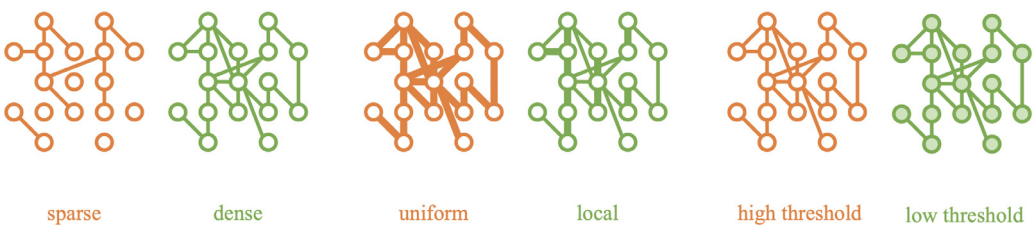

Fig. 15. Schematic overview of 3 parameters that could be altered by synaptic EI imbalance in a neuronal network.
Source: Adapted from [326].

static-networks based model assume in general that contact between individuals takes place uniformly in time and an appropriate reproduction number is capable of the transformation of the majority of individuals into infective state for epidemics [339,340]. But, in reality, this is not always the case. Based on the data-driven dynamic contact patterns between

individuals, the temporal-pattern of contacts typically can reduce the possibility of infection and slow down the disease spread [341]. Based on the human activity patterns on information diffusion, similar phenomena of slow diffusion on temporal networks were also found in information propagation and could be induced by the large heterogeneity in the response time [337,338]. While, depending on specific network construction and diffusion dynamics, temporal networks allow the acceleration of the propagation process. In this subsection, we review the impact of temporal network structure on the diffusion velocity, including empirical data of burst activity, activity driven network and the memory network.

3.1.1. Diffusion speed

The slowness effect of spreading processes on temporal networks originates from the large heterogeneity of the bursty feature of human communication dynamics [337,338]. Empirical data-driven analysis on contact sequences suggests that, rather than having a uniform or Poissonian statistics, the inter-event times are heavy-tailed and can be described by power-law distributions [342,343]. This feature is sufficient to induce a large deviation from expectations of the spreading dynamics, as previously studied [344]. By considering the email activity patterns from university and commercial data sets, based on the susceptible–infected (SI) model, it was found that the key difference between Poissonian and power-law distribution of inter-event times lies in the generation times, i.e., the length of time between individual receiving information and transmitting it to his/her neighbors. Longer average times to the next event for the long-tailed inter-event times distribution make the exponential decay of the number of new infections at later stage significantly slower, and this prediction is in line with the empirical data on real computer worms [344]. Furthermore, the power-law distribution of inter-event time induces a power-law decay in the number of new infections in the long-time limit, whose exponent is determined by the distribution of generation times [345]. The extension of the data-driven framework and the analysis of the emergence of heterogeneous ties in social networks show that strong ties may have a negative role in networked information spreading [346]. The comparison between the original model of a call network and null models, in which event sequences are shuffled, reveals the role of structural and temporal correlations slowing down the spreading [347].

However, temporal networks do not always slow down the diffusion process. For example, temporal order and correlations were found to speed up epidemic spreading based on the dataset of sexual contacts of internet-mediated prostitution, especially in the early phase of a superlinear growth [348,349]. In spite of slow-down effects in the asymptotic-time limit or global scale, heterogeneous activity patterns are capable of inducing faster diffusion in the short-time or local scale. The heterogeneous contacts of epidemics based on SI models spread faster in the early stage with a higher reproduction number R_0 than that for homogeneous patterns, and later these results were analytically supported [350,351]. In call networks based on SIR models, there are abundant short relay times, which refer to times between individual i participating a call with individual j and he/she participating a call with any other individual [352]. This phenomenon was taken as the signature of group conversation, i.e., calls could trigger further calls, making activity patterns of adjacent links correlated. Under realistic transmissibility, the group conversations lead to a more efficient local-information propagation [352]. Moreover, in the deterministic threshold model with the exposure of infected neighbors in the past, which is usually neglected in standard epidemics models like SI, SIR and SIER ones, the burst activity patterns accelerate contagion spreading [305].

The twofold impacts of temporal features have also been confirmed in RWs, the simplest diffusion model. There, a random walker arrives at a node, becomes isolated at the successive time step, and remains trapped until a new link connecting the node emerges, thus slowing down the diffusion process. For example, based on the dataset of time resolved patterns of a face-to-face co-presence of individuals, numerical simulations on temporal networks exhibit longer mean first-passage time and smaller coverage, compared to that of theoretical predictions on aggregated networks [353]. The mean first-passage time (MFPT) is defined as the average time taken by the random walker to arrive at a particular node for the first time from a random starting position, while coverage refers to the number of different nodes that have been visited by the walker at a given time point, quantifying the search efficiency. These two quantities imply slow diffusion in temporal networks.

Additional to empirical data-driven analysis of burst activity, the theoretical framework of RWs on an activity driven model has also been investigated intensively [354,355]. By considering a power-low form of the activity distribution $F(a) = \frac{1-\gamma}{1-\epsilon^{1-\gamma}} a^{-\gamma}$, where the activity $a_i \in [\epsilon, 1]$ representing the probability that node i becomes active and γ is the exponent, the probability $P(a, t)$, of which random walkers are at a node of activity a at time t, satisfies

$$\frac{dP(a,t)}{dt} = -aP(a,t) + F(a)\sum_{a'} a'P(a',t). \tag{24}$$

The steady state solution $P_\infty(a) = \lim_{t\to\infty} P(a,t)$ is given by $P_\infty(a) = \frac{F(a)}{a}\sum_{a'} a'P_\infty(a') = \frac{1}{\langle a^{-1}\rangle}\frac{F(a)}{a}$. The occupation probability $P(a, t_w)$ of nodes with activity a evolving for a time t_w, which reflects the time evolution of the process, was observed to exhibit a quite slow relaxation from a short-term state $P(a, t_w \to 0) \sim F(a)$ towards the steady state $P_\infty(a) \sim F(a)/a$. The speed of this relaxation is actually inversely proportional to ϵ, the smallest activity of nodes.

Considering other factors influencing the diffusion velocity, further research has pointed out that, even if the activity pattern is bursty, the question of whether temporal features slow down or speed up the propagation is comprehensive. The mixing time τ_{mix}, characterizing the worst-case relaxation time from any initial state to stationary, was jointly determined by the network structure and waiting-time distribution [24,356]. Specifically, the topology is captured by the second-largest eigenvalue λ_1 of the associated Laplacian matrix, satisfying $\lambda_0 = 0 \geqslant \lambda_1 \geqslant \lambda_2 \geqslant \cdots \geqslant \lambda_{N-1}$, while the waiting-time

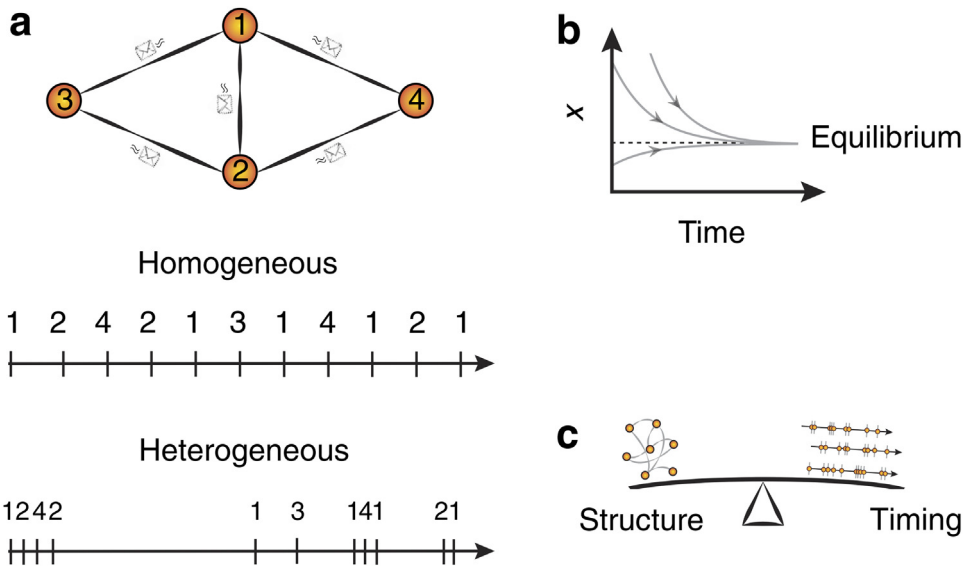

Fig. 16. Speed of diffusion on temporal networks. (a) A RW process illustrated by information propagation among four nodes through electronic or physical mails. The temporal patterns of waiting time between departure and arrival of mails could be homogeneous and heterogeneous. (b) Relaxation time describes the time that the random walker takes to reach the stationary state or equilibrium from any initial state. (c) The competition between structural factor and temporal patterns to determine the diffusion speed.
Source: Adapted from [24].

distribution is described by its exponential tail τ_{tail} and burstiness $\beta = (\sigma^2 - \mu^2)/(2\mu^2)$, where μ and σ are the average and standard deviation of the distribution. In this case, the mixing time is approximated as

$$\tau_{\text{mix}} \approx \max\left\{-\frac{\mu}{\lambda_1},\ \mu\beta,\ \tau_{\text{tail}}\right\}. \tag{25}$$

When the waiting times are distributed around the mean value with negative burstiness $\beta < 0$ such as Dirac and Erlang distributions, the structural factor dominates the diffusive dynamics and slightly accelerates mixing. On the other hand, high temporal heterogeneity significantly slows down the process [24]. Fig. 16 shows such competition between structure and time for determining the diffusion speed. Besides, the additional tendency or repulsion for random walkers to return to previously visited nodes may either slow down or accelerate the diffusion, depending on the number of steps leading to mixing [357].

Based on memory temporal networks with realistic non-Markovian characteristics taken into account, memory is confirmed to constitute an additional factor for the diffusion investigation. For RWs, the connectivity of causal topology either slows down or accelerates diffusion, which could be predicted through the spectrum of the transition matrices and had been validated on various empirical datasets [23,358]. For epidemic models, although lots of research showed that the memory slows down the contagion spreading [183,359,360], opposite result could also occur [361], where memory effects accelerate the dynamics while topological correlations induced by the community structure slow it down. The diffusion speed depends on the competition between memory and topological structures in a non-trivial way. Furthermore, the optimal memory length for the maximization of the spreading time depends on the combination of the strength of the memory and the density of links [362].

3.1.2. Epidemic spreading

Structural changes in a network may alter the spreading phenomena there [146,363–366]. Time ordering of link removal or reconstruction can determine the fate of the disease propagation. This feature cannot be visible on a static network. In temporal networks, the activation time of edges depends on a certain probability distribution [363]. The information flow via e-mail exchanges [367,368], rumor propagation in social media [365], epidemic spreading in contact networks [341,369,370], or patterns of functional networks generated from spiking or irregular activities of brain data [371–374], all are interesting examples where a time-varying structure of the underlying connectivity plays a determining role for propagation of complex signals. As we have discussed, a large class of literature is already been devoted to the understanding of the epidemic spreading in heterogeneous and static networks [340,375,376], particularly the critical epidemic threshold β_c has been determined as a function of the degree moments of the networks. Note that, a coarse-graining projection of temporal networks into a static one will not always capture the true notion of reality. Recently due to the increasing accessibility of a large number of contact and mobility data [363,377,378], the accurate

prediction of infection spreading becomes possible. However, it is more challenging for analytical calculations due to the presence of two-time scales: one from dynamics and the other comes from networks [24,379,380]. In contrast to static cases, for long-lasting outbreaks, as human mobility and contacts are time-varying, the disease spreads or locally confines due to transitory contacts i.e individual's contact changes with time [363,364,379,381,382].

Neighbor exchange (NE) model. It has been demonstrated that the *neighbor exchange* (NE) model [381] can describe time-varying complex human interaction patterns and their function in disease transmission. Here, the number of contacts per person is fixed, but the connections are transient, meaning that neighbors' identities are modified stochastically and dynamically. This is called random mixing: links $X-Y$ and $Y-Z$ are broken after a certain time and links $X-Y$ and $Y-Z$ are generated. If the rate of epidemic spreading is faster than the changes in contact rates, the static network approximation holds well [383,384]. Alternatively, if the random mixing occurs within a shorter time scale, then the network information is no longer required and a mass-action model can capture the outbreak. In the intermediate time scale, the NE model provides a suitable solution to epidemic spreading. If the recovery rate (μ), the probability of transmission from *ego* to *alter* during a contact period (τ), the constant disease transmission rate from an infectious node along each its edges (β), and the swapping rates (ρ) all are taken into account, one can write R^* ("expected number of secondary infections from an individual who is infected early in an epidemic") for arbitrary graphs as follows $R^* = \frac{\tau\rho}{\mu} + \tau\frac{\mu+\rho}{\mu} \times \frac{g''(1)}{g'(1)}$. Here $g(k)$ is the probability-generating function for the degree distribution and "$\prime$" provides the order of derivative. For Poisson networks (degree distribution: $p(k)\frac{\lambda^k e^{-\lambda}}{k!}$), $R^* = \frac{\rho\tau}{\mu} + \frac{\lambda\tau(\mu+\rho)}{\mu}$ and for power law graphs ($p(k) \sim k^{-\gamma}$), $R^* = \frac{\rho\tau}{\mu} + \left(\frac{\sum_{k>\kappa} k^{2-\gamma} - k^{1-\gamma})}{\sum_{k<\kappa} k^{1-\alpha}}\right)\frac{\tau(\mu+\rho)}{\mu}$. On the other hand, the critical mixing rate can be captured by

$$\rho* = \frac{\mu(\beta+\mu)g'(1) - \beta\mu g''(1)}{\beta g''(1) + g'(1)(\beta-\mu)}. \tag{26}$$

This critical condition suggests fast mixing does not always lead to epidemic spreading and low to medium mixing can be mimicked with static network approximation. In [381], they have successfully tested the NE model of the 1996 outbreak of syphilis among Atlanta adolescents and estimated the relevant parameters.

Activity driven networks. In the activity-driven network (ADN) model, the link structure of each node changes each time (Fig. 17). In particular, an "activity potential" parameter determines how it will be connected to other nodes [354]. Links are formed according to the following rules in a memoryless process: (i) At each step t the graph starts with N nodes with no links. (ii) Each vertex is allowed to be "active" with $a_i\delta t$ probability and generates m links to connect m "active" or "non-active" nodes. (iii) In the next step, all the edges are removed, and new m nodes are chosen randomly. Here, the activity rate a_i is the probability of interactions with other nodes and chosen (randomly or from empirical data) from a probability distribution and it is rescaled with a constant propensity factor η. The creation of hubs depends on the high strength of activity rate. Analytically, it can be shown that the spreading of the disease i.e. the critical threshold for the onset of the disease (in a discrete-time setup) depends on the activity rate as follows: $\frac{\beta}{\mu} > \frac{2\langle a\rangle}{\langle a\rangle + \sqrt{\langle a^2\rangle}}$. Here the critical threshold does not depend on the structural factor appearing from the time-aggregated networks, rather it depends on the moments of the considered "active" potential. Currently, this approach is further analytically derived in a continuous time domain [385], and the validity is checked from simple susceptible–infected–susceptible dynamics to more complex contagious phenomena. In realistic situations, the choices of active nodes are not purely random, rather choices of links are determined by some memory effect or non-Markovian process [386,387]. The preferential attachment of links in the backbone of a static network [388], or a mix of static network and ADN [389] have been proposed to accurately capture the infection trend. Further, strong and weak ties formation in intra, as well as inter-communities, are proposed in the ADN framework [388,390]. Also non-Markovian memory effects i.e emergence of heterogeneous ties are studied in [346] for the large-scale mobile phone-call (MPC) dataset, and it has been demonstrated that strong ties significantly impede information dispersion. Modular structures are also considered in ADN setup [391]. Tightly connected clusters can inhibit the propagation of disease in the SIR process but enhance the speed of the SIS process. Also, the time-independent nature of the activity parameter can be relaxed, and it was observed that the temporal feature of the activity parameter may suppress the disease [392]. It can also be used for the Leader–follower consensus problem [393]. Note that the ADN type dynamics is successfully tested [394] for the Ebola outbreak in Liberia. Also, the two-layer temporal network for Uganda is developed in which one layer is fixed encoding the static contacts among family levels and another layer represents the temporal network extracted from human mobility based on cattle trade, fish trade, etc. Here the simulation suggests that reduction of physical contact and increasing the strength of preventive measures can reduce the infection [395].

Other approaches. Recently, to calculate the epidemic threshold in an arbitrary time-varying network, a multilayer-based approach is provided in a discrete as well as in a continuous time epidemic spreading framework [396–400]. In this approach the spectral radius of a multilayered matrix that encodes the information of a time-varying structure network and disease dynamics provides the critical onset of disease. On the other hand, the dynamic message-based edge-centric approach [401,402] may capture the outbreak trend in Markovian susceptible–infected–recovered temporal networks [380]. The tools of temporal networks are used to predict disease propagation in livestock movement (sheep and cattle) in Scotland. The outbreak of a multi-species dynamic network significantly differs from its static and single

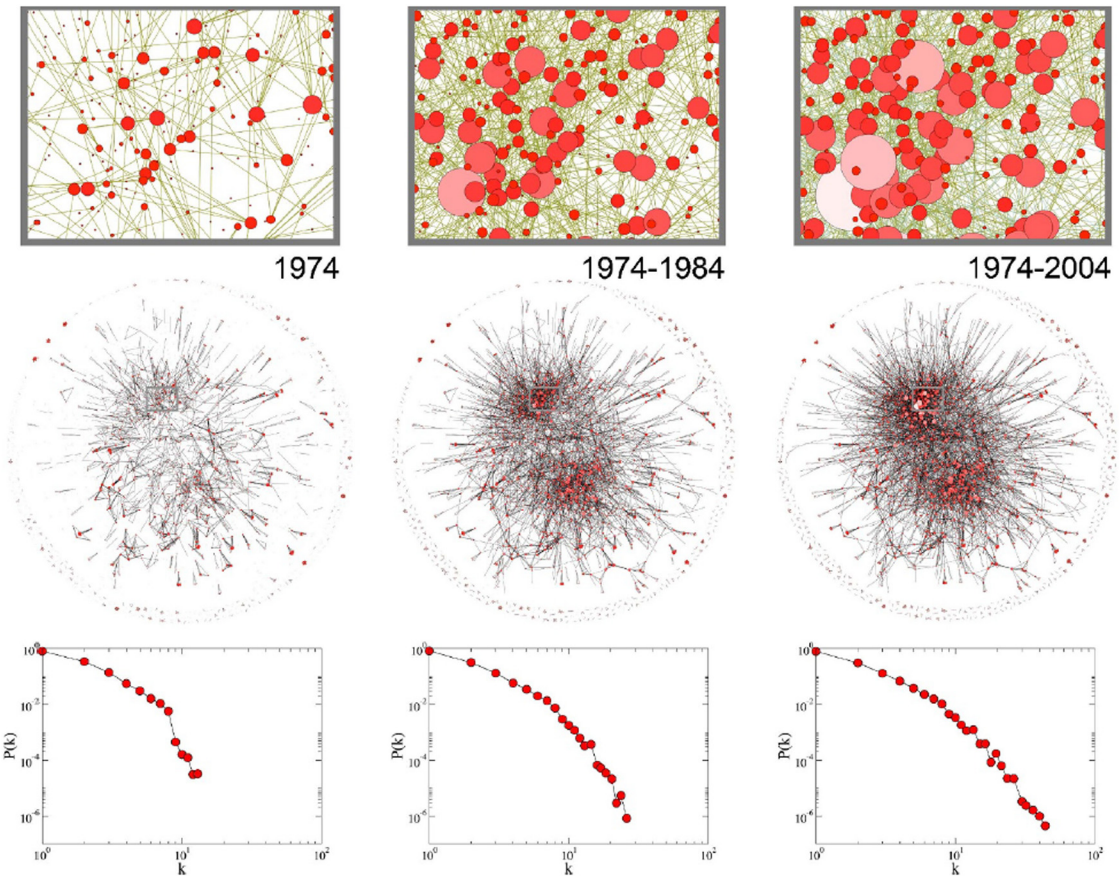

Fig. 17. Three collaboration networks from the PRL dataset are constructed for three different time windows: one year, 10 years, and a window of 30 years. The upper panel reflects the zoomed version of each of the particular networks. The density of the network increases when the time window is taken as broader (left to right in the central panel). In each visualization, the size and color of the nodes are proportional to their degree. A time-invariant activity potential function can be constructed that can encode the intrinsic temporal nature of the network dynamics.
Source: Adapted from [354].

species network [403]. Based on the contact chain measure of temporal networks, they can identify the key farms responsible for spreading. In sexually transmitted diseases particularly for the early growth of an epidemic, the concept of concurrency encodes the information of time-overlapping partnerships among individuals [404] might be useful. Note that, the timing between two successive occurrences may deviate from the Poissonian process rather than it may follow a heavy tail or a power law statistics, indicating that activity patterns are excessively diverse. For instance, the inter-event distribution for high-resolution email data follows a power law with an exponential cut-off rather than an exponential distribution [344]. This kind of heterogeneous inter-event time distribution, as opposed to an exponential distribution, may delay the transmission of viruses in computer networks [344,345,347].

3.2. Spatiotemporal signal propagation

A common way to understand the propagation pattern in spatial and temporal scales is to study the effect of local or non-local perturbation of the dynamical process. Barzel et al. have developed a self-consistent linear response theory and investigated a broad class of nonlinear perturbed systems. This approach systematically splits the contribution of topology and the considered dynamical process to predict the spatiotemporal pattern of the perturbed signals [10,405–407]. The nonlinear deterministic dynamical equation is captured by

$$\frac{dx_i}{dt} = M_0(x_i(t)) + \sum_{j=1}^{N} A_{ij} G(x_i, x_j). \tag{27}$$

This type of nonlinear model can encode epidemic processes, biochemical dynamics, or birth–death processes. Here the left side represents the temporal activity of the i the node. This activity depends on the inherent activity ($M_0(x_i)$) of the

i the node, and the interaction ($G(x_i, x_j) = M_1(x_i(t))M_2(x_j(t))$ is pairwise multiplicative nonlinear function. If a constant, permanent perturbation is applied as $x_i(t) = x_i + dx_i$ on the activity of node i, and if the subsequent changes of the qth node are described by dx_q, then one can write a correlation matrix (in the asymptotic limit) as $F_{qi} = \left| \frac{\frac{dx_q}{x_q}}{\frac{dx_i}{x_i}} \right|$. Barzel et al. have proved that the probability of F can be written as $P(F) \sim F^{-\nu}$ [405]. The distant dependent correlation function ($\Gamma(l) = \frac{1}{N}\sum_{i=1}^{N}\sum_{q\in K_i(l)} F_{qi}$, and $K_q(l)$ is the set of all nodes having the path length l from i and is also designed to track the propagation strength of the perturbation. For biochemical dynamics and birth–death processes, the decay rate of $\Gamma(l)$ is zero reflecting conservative propagation. For epidemic dynamics, this decay rate becomes non-zero, signifying that the penetration strength of the perturbation is reduced for long-distance nodes. Based on linear response theory, one can write (at steady state, using Laurent expansions), $M_1^{-1}(x) = \sum_{n=-\infty}^{\infty} a_n x^n$, and $M_2\left(M_1^{-1}(x)\right) = \sum_{m=-\infty}^{\infty} b_m x^m$. Here $M_1^{-1}(x)$ is the inverse function of $M_1(x)$. Using these, for nearest neighbor nodes (say q) of i, each element of the correlation matrix can be written as $F_{qi} = \frac{x_i M_1(x_q)}{d_q x_q}\left(\frac{dM_2}{dx_i}\right)\left(\frac{dM_1}{dx_q}\right)^{-1}$, where $x_q \sim M_1^{-1}(1/d_q)$. For a large degree ($d_q \gg 1$) node, the non-vanishing terms determine the decay rate of the distant dependent correlation function. The exponents are further calculated for experimental micro-array data collected for Saccharomyces cerevisiae, where the authors measure the impact of 55 perturbed genes on 6000 genes. Here it has been shown that the penetration of the perturbation is conservative.

Recently, Hens et al. have investigated [10] the spatiotemporal propagation pattern of perturbed signals, i.e how many times a neighbor node of i will take to respond if i is permanently perturbed? Based on the same theory described above, it has been shown that joint contributions of the interaction structure and local dynamics can be disentangled from three specific classes (called as degree driven, distance driven and composite) characterized by the interplay between network paths, degree distribution, and the interaction dynamics [10,408,409]. The individual response time τ_q, capture the transient response of the node q to direct incoming perturbations from its interacting neighbors. Particularly, it has been proved that the response time depends on the internal dynamics and the network degrees: $\tau_q \sim d_q^{\theta}$ with a scaling exponent θ that depends on the associated dynamics (it depends on M_0, M_1), see Fig. 18 for a propagation pattern between two communities. Here, the propagation time (T_{ij}) from the source of perturbation i to an arbitrary node, j can be captured by analyzing the cumulative strength of the minimum of the shortest paths. Here the strength of the path depends on the intrinsic response time τ of the intermediate nodes. Altogether, one can write a metric for predicting the response of any arbitrary node in the network as follows: $\mathcal{L}(i \to j) = \min_{\Pi(i\to j)}\left[\sum_{p\in\Pi(i\to j), p\neq i} d_p^{\theta}\right]$. Several key features in the response of local perturbation in complex networks such as who will be affected earlier, and how many nodes will be affected at a particular time are explained in [10]. This formalism is also applied to two real systems, capturing the spread of SIR dynamics through air-traffic networks, and applied to the propagation of a power cascade. Recently a modification is suggested by Ji et al. in which the inclusion of a suitable prefactor is necessary to maintain the expression for deriving the exponents [410]. However, the scaling exponents remain the same for both analyses [409–411]. An alternate framework is also created by observing the system's response as a probability distribution over time. The effective expectation values are used to describe the state trajectories under perturbation in order to roughly extract the peak times and amplitudes [409,412,413]. Most recently, another theoretical framework is developed based on the extension of [10] which is based on a network decomposition into independent edges and edges as part of motifs [13]. The developed framework of response dynamics conceptually links the small and large-scale topology of a network with the spatiotemporal spreading induced by a small constant perturbation. In particular, they identified and predicted the interplay of propagation paths, degree and motif distributions, and interaction dynamics on the response dynamics.

3.3. Multilayer networks

In the multilayered perspective of networks, the same node/individual can participate in different layers [3,4,414]. For instance, one individual who forms a physical network with his/her family, or friends in one layer can construct another layer of the network (online ties) with the new and existing nodes using some, even the links structure may vary from one layer to another one. This interconnected competition structure may lead to rich complex dynamical processes.

3.3.1. Epidemic spreading

Notably, in the perspective of the epidemic process, one layer which represents the physical contact relates to disease spreading, whereas, at the same time, the virtual network may work as a positive effect for the awareness to maintain distance rule [415,416] or for the strong vaccination program. Such intertwined layers can diminish the severity of the disease. Several approaches are provided to study epidemic processes in multiplex or multilayered networks.

Microscopic Markov Chain Approach (MMCA). A MMCA [417,418] is designed to spreading in multiplex structure [415]. The *virtual* contact layer consists of the population of aware (A) and unaware of the existence of the epidemics. Here aware

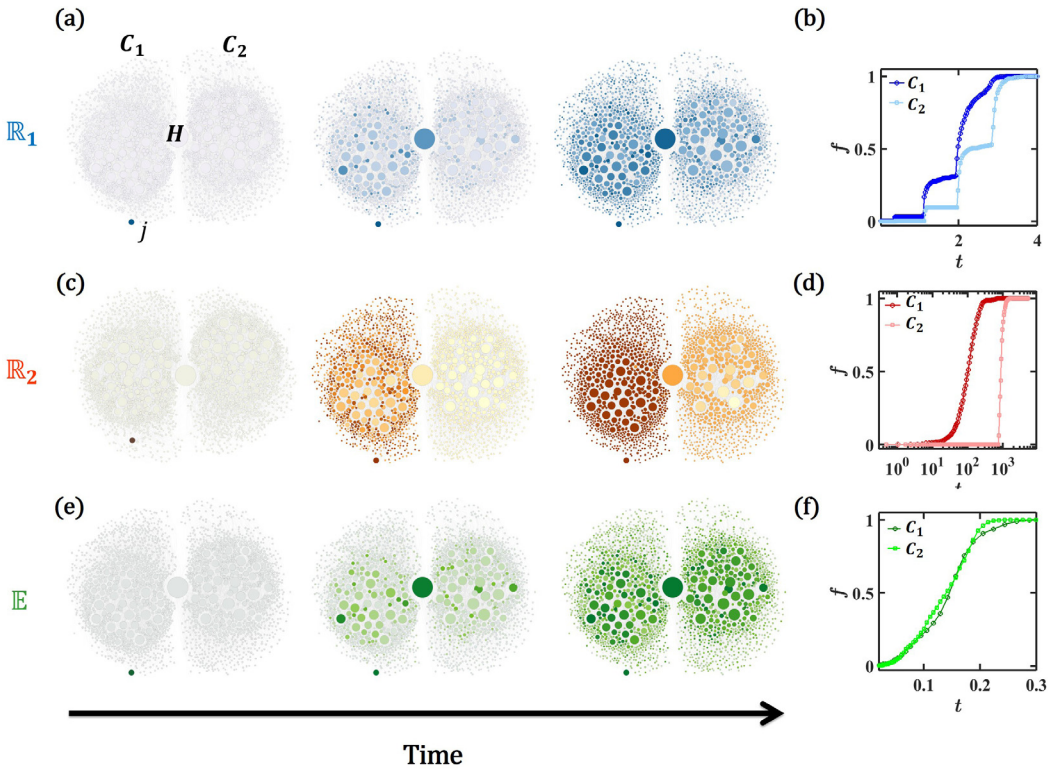

Fig. 18. A modular network is constructed with two SF communities C_1, and C_2. Three dynamical models ranging from gene regulation to SIS dynamics (**E**) are used here. A perturbation is introduced at one single node (blue/red/green node at bottom left) for each model. (a–b) Distance-driven propagation. Here C_1 starts to respond earlier and then C_2 starts to respond. The fraction of response nodes (f) increases stepwise. This is because the considered regulatory dynamics ($\mathbf{R}_1$) follows the distance-driven propagation. The central panel (c–d) relates to degree-driven propagation. As the intermediate node is a hub, the response time of the nodes of C_2 is much higher than C_1. (e–f) For this case, both communities responded almost at the same time [10].
Source: Adapted from [10].

individuals have information (due to self-infection or getting updates from the aware neighbors) on how to be uninfected with some personal restrictions and measures. Due to seasonality or other reasons the awareness may vanish from the aware individuals with some probability. The other layer consists of susceptible–infection–susceptible (SIS) dynamics. Note that one individual reduces their own infectivity if it is aware of the disease. They showed that the onset of infection (*meta-critical* point) depends on awareness dynamics. Particularly, the critical onset can be captured by $\beta_c^U = \dfrac{\mu}{\Lambda_{\max}(H)}$, where μ is the rate of recovery from the infection, and $H_{ij} = [1-(1-\gamma)p_i^A]b_{ji}$, the element of matrix H encodes the information of awareness dynamics, particularly the stationary states (p_i^A) of aware individuals. Here γ is the recovery rate and b_{ij} the interaction matrix of the physical layer. $\Lambda_{\max}$ is the largest eigenvalue of H. In a nutshell, a metacritical point emerges, where the diffusion of awareness controls the disease propagation. These two propositions that infection means awareness and total awareness implies total immunization are further relaxed in their later work [416]. The meta-critical point can vanish with the addition of the mass media effect (an external node connecting to all nodes). Further, epidemic propagation is checked in the setup of two-layered multiplex networks coupled with awareness diffusion and SIR-like epidemics [419]. The critical threshold depends on awareness diffusion and the epidemic networks. The mass media effect is also investigated in two-layered multiplex networks of SIR and UAU mode [420]. A contact-based framework is developed to study the contagion process in which the epidemic threshold is determined by the largest eigenvalue of the contact probability matrices of the layers [421] and the dynamics of the dominant layer determine the contagious process. In the two-layer step up, it has been shown that the equilibrium (disease-free and information-saturated equilibrium) is globally stable if the basic reproduction number of the physical layer is less than one and the reproduction number of the virtual layer is greater than 1 [422]. A local awareness-controlled contagion spreading is investigated, and depending on the strength of local awareness control [423] an abrupt jump of infection strength may emerge. The assumption of the identical effect of awareness is further relaxed by assigning a heterogeneous local awareness threshold, and the infection rate for each group of nodes [424]. The groups are marked here by k-core decomposition, or the degree of the individuals, and three models are prescribed depending on the correlation. In degree-based heterogeneity, the outbreaks occur more rapidly for the negative correlation mode. The heterogeneity is further decategorized into three types: two are coming

from two layers: virtual and individual, and the third one comes from the individual's response. The heterogeneity of the information layer affects the critical threshold of awareness and has two-stage effects on the epidemic threshold [425].

Already a decade ago, two-layered SIS dynamics between two competitive viruses were studied, and expressions for the extinction and coexistence of the viruses have been derived [426]. The interaction of two concurrent diseases is also studied in a two-layered setup [427]. A non-vanishing threshold for spreading on scale-free networks is analytically derived here. An explosive transition may also occur in the presence of interaction between the contagion-consensus process [428]. For a comprehensive review, one can check the currently published review [429] and a previous one [398]. Currently, a theoretical formalism is developed to analyze spreading processes in multiplex metapopulations, e.g recurrent mobility networks [70]. The epidemic threshold is calculated as $\lambda_c = \frac{\mu}{\Lambda_{\max}(\mathcal{M})}$, where μ is the recovery rate and the elements of the supramatrix $\mathcal{M}$ signify the contact probability of two agents associated with two different patches and with two different types. The approach is tested for a location in Colombia. The mobility patterns are categorized depending on the socioeconomic hierarchy of the agents.

Heterogeneous Mean-field analysis. A heterogeneous mean-field analysis is performed in two-layer inter-connected networks for the calculation of epidemic threshold [430]. Here the epidemics may not prevail in the isolated networks, however spreads globally in the presence of interconnection with some critical conditions. Further, the effect of the underlying structure is investigated rigorously to understand the SIS epidemic threshold in interconnected networks [431]. Using N-intertwined mean-field analysis (NIMFA), the critical threshold is captured by $\beta_c = \frac{1}{\Lambda_1(A+\alpha B)}$, where the denominator is the largest eigenvalue of the matrix $(A + \alpha B)$. A denotes the intraconnections within each layer and B reflects the interconnection between layers. The parameter α tunes the infection rates along with the interconnections. The denominator gets higher if the interconnecting nodes have a higher eigenvector component product. The diversity of multilayer networks, particularly evenness, i.e. connectivity pattern among layers, and difference: how layers are shared with overlaid edges have a vital role in the spreading process of collaborating viral agents [432]. A mean-field analysis is also provided to infer the epidemic threshold by analyzing the mean matrix of the considered branching processes. The critical thresholds are investigated in a two-layers disease set up, and it is observed that the percentage of vulnerable nodes and overlapping links have contrasting effects on the disease propagation [433]. Another approach is to use bond percolation to predict the epidemic threshold [434]. A tensorial representation is introduced to extract the upper and lower bounds for the disease incidence and the critical points for SIS and SIR dynamics [435]. An isolation parameter capturing the quarantined effect is also introduced for the multilayered social and physical networks, and the link percolation approach predicts that isolation increase the critical threshold [436].

Spatiotemporal Propagation in multilayer networks. From the perspective of multiplex networks, less work has been focused on studying epidemic spreading in a micro-scale. For instance, if the disease starts locally in a single layer, how does it spread to the other layers? Which nodes will get infected earlier? It has been demonstrated that for a two-layer combination (ER-SF) if the initial infection begins (in a SIR scenario) at the homogeneous network (ER), it stays contained on that network and later spreads to a SF network due to the localization impact of an ER network [70]. Here the final outbreak size for each node in an ER network is almost the same. However, it follows through the heterogeneous distribution in the SF layers (Fig. 19). The propagation pattern is checked in the realistic metapopulation network of the city of Medellin in Columbia. The strength of contagious dynamics becomes higher inside the same economic classes. This is obvious as less movement occurs between two layers if they have substantial economic disparity. In the multilayer perspective, the role of bridge nodes connecting the layers is investigated for disease propagation [437]. At the proximity of a critical number of bridge nodes, the arrival times follow a power law. An illustrative mesoscopic design reflects the impact of bridge nodes. However, spatiotemporal propagation in node levels is not explored here.

Application: Multilayer network. Recently, an adaptive multilayer network including different contact types between individuals (sporadic, social, and household connections) is proposed [438]. Each layer's probability is taken as different and two of the layers' contacts vary depending on the public health measure. This model is successfully implemented in Costarica to project the impact of Covid-19 variants, and it provides a suitable and efficient vaccination strategy [439]. To reduce the severity of the COVID-19 infection, an optimal segregation scheme in multiplex networks is proposed in which link removals are minimized [440]. If the links of the social layer are dynamic, the outbreak size increases. Recently, Aleta et al. [441] has considered three-layered multilayer networks and investigated the role of social distancing and robust level of testing and contact tracing. Such strict measures are crucial for the containment of the disease.

3.3.2. Cascading failures

Intensive research on cascading failures in multilayer networks were motivated by the fragility of interdependent infrastructures [442,443]. The underlying interdependence makes the propagation of failure among various infrastructures possible, triggering a disruptive avalanche of a system of systems. For example, the localized malfunction of power grids may strongly affect the operation of communication as well as transportation networks, and failures in these networks accelerate the collapse of electrical system afterwards [443,444]. The infrastructures interdependence can be represented as multi-layer networks, and the investigation of the propagation of cascading failures in such networks does not only deepen the understanding of the chain reaction in real systems but also promotes resilient infrastructures. In this subsection, we focus on cascading failures in multi-layer networks, in particular on structural factors influencing the process as well as mitigation and recovery strategies.

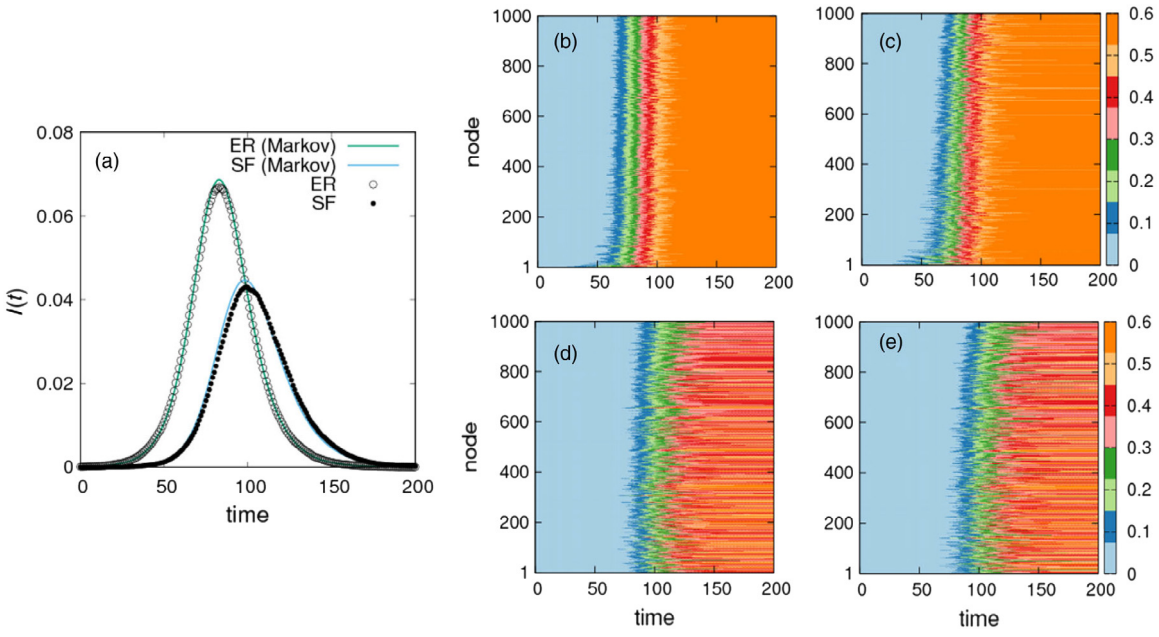

Fig. 19. Propagation of epidemics in multiplex networks composed of an ER and an SF layer. Here metapopulation network of the SIR model has been used. In (a), infection in each layer is plotted as a function of time. The infection starts at the ER layer. (b–c) The fraction of recovered individuals in each patch of an ER network is plotted as a function of time. (d–e) Spreading pattern in the SF layer. Initially, the disease is contained in the ER layer and then transmits to the other layer (SF). Interestingly, due to the heterogeneity in the SF layer, the final outbreak size of each patch is not identical.
Source: Adapted from [70].

The model of cascading failures in multilayer networks can be taken as the mutual percolation one [443]. Consider two networks having the same number of nodes with one-to-one correspondence between networks but different structures within each one. There are two types of links: (1) intraconnectivity links within the same network, representing the interaction between units of same type and (2) interdependency links between networks, standing for indispensable relation. The failure of each node could be triggered according to internal (within the same layer) and external (between different layers) rules. Once a node fails, all the corresponding connectivity and dependency links will also be removed. For example, the propagation of cascading failures is triggered by the removal of several nodes in one network. The initial failure introduces that some nodes break away from the giant component and hence fail. These failures propagate to the other network through dependency links and cause further failures, which subsequently propagate back to the initially perturbed network and so on. This process is iterated until a stationary stated is reached. Figs. 20(a–b) illustrates cascading-failures propagation on multi-layer networks.

For the quantification of cascading failures, percolation theory provides a deeper insight by approaching the final fraction of nodes in the giant component P_∞. Considering the initial failure by the removal of a fraction of $1-p$ nodes, there exists a critical threshold $p=p_c$ through the percolation phase transition: the giant mutually connected component remains when $p>p_c$, while it disappears when $p<p_c$ [443]. From the perspective of the value of P_∞, it jumps to zero as p approaches p_c from above in the first-order transition. Further investigation shows that around the critical point p_c, the time evolution of P_∞ exhibits a second-order percolation transition [445], characterized by a plateau stage where the size of a giant component nearly stays invariant. Moreover, the value of p_c is significantly larger than that of a single network, theoretically suggesting the fragility of interdependent networks. Nodes with high degree have a high probability to belong to the giant component and serve as anchors, but they may also fail easily for low-degree adjacent nodes of the other network [446]. Mean-field generating functions in the large-system limit are utilized to derivate the expressions of giant-components size S^A and S^B [447,448]. Let $H\in\{A,B\}$ represents one of the two networks. Denoting the probability that a randomly chosen node in network H has the degree d by p_d^H satisfying $\sum_d p_d^H=1$, the generating functions of the degree distribution and the underlying branching process are given by $G_0^H(x)=\sum_d p_d^H x^d$, $G_1^H(x)=\frac{1}{\langle d\rangle^H}\sum_d p_d^H d x^{d-1}$, where $\langle d\rangle^H$ is the average degree of network H. Based on these, the probability that a randomly chosen node belongs to the final survival giant component, equivalent to the giant-components size, could be concisely expressed [449].

These results shown above are obtained based on ideally-constructed interdependent networks, while real networks exhibit abundant features, which have rich impacts on the cascading failures propagation and need a concrete analysis for each specific system. For local structure, clustering is capable of region transitions [451–453] while communities tend to disconnect with each other and collapse separately [454,455]. The effects of various topological features have also

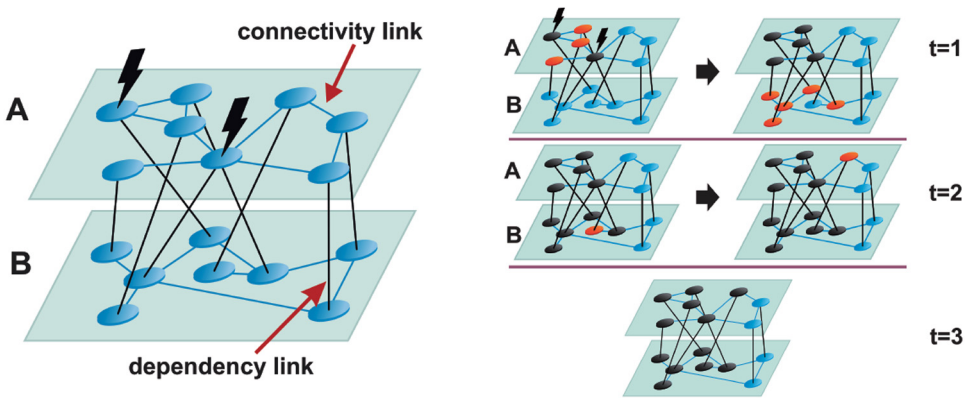

Fig. 20. Cascading failures in multilayer network. (a) Illustration of interdependent networks A and B with connectivity and dependency links highlighted by blue and black, respectively. The lightning marks indicate nodes that initial failure takes place. (b) Propagation of cascading failures on networks described in (a). Blue nodes stand for functional ones while red and black nodes are failed ones at current and past steps, respectively. *Source:* Adapted from [450].

been investigated, including degree–degree correlation [456–459], link overlap [460–463] and directed links [464,465], as well as situations of nodes supported by multiple dependencies [466–468] and autonomous ones independent of the other network [469–472], breaking the limitation of one-to-one correspondence. Much efforts have also been devoted to the generalization of global structure of the system, with more than two interdependent layers [473–479]. Additionally, spatial networks, where nodes have physical locations and link length is limited by geometrical distance, exhibit more realistic characteristics compared to random ones [480]. When link length of dependency ones is constrained by a certain distance threshold r [481–485] or that of connectivity ones drawn from an exponential distribution $P(\ell) \propto \exp(-\ell/\zeta)$ with characteristic length ζ, the cascades process exhibits a phase transition determined by the critical points $r = r_c$ and $\zeta = \zeta_c$ [486,487]. Combined with a variation of the average degree, the link length parameters of r and ζ are capable of the introduction of three phases, i.e., unstable, stable and meta-stable states, with a surprising similar phase diagram.

To avoid large-scale cascading, various mitigation and recovery strategies have also been proposed. A structural modification is usually taken to enhance the systems' robustness against targeted attacks, such as priority of low-degree nodes to choose their dependency partners [488] as well as various connectivity and dependency link-addition strategies [489–492]. During the propagation process, the inclusion of links between the nearest neighbors of failed nodes [493,494] and selectively saving finite connected components before they fail [495] can effectively prevent the further spread of failures. As for the recovery process, the question of how to spend minimization of resources to bring the entire system back to the functional state attracts great attention. Examples include the minimum Manhattan distance in the phase diagram [496] and repairing a fraction of failed nodes with recovery probability [497], as well as certain clusters formed by ineffective nodes and links [498]. A systemic spontaneous recovery process was discussed in [499]. Additionally, the mutual percolation model provides a basic framework for the extension of other cascading models on a single network to multilayer ones [443]. This could be achieved by replacing the internal rule with a corresponding one, such as k-core percolation [244–246,467], overload effect [500–502], finite functional components [503,504] and more complicated dynamics [505,506]. Similarly, the external rule is also adjustable. For example, the failure of node in one network may not definitely lead to the failure of its counterpart but with a probability q [449].

3.4. Control on networks

The ultimate understanding of complex networks, including natural and technological systems, can be reflected in our ability to control them [507]. Consider a network consisting of N nodes governed by the equation below [508]:

$$\dot{x}_i(t) = f_i(x_i(t)) - c_i \sum_{j=1}^{N} l_{ij} h_{ij}(x_i(t), x_j(t)), \ \ i = 1, 2, \ldots, N, \tag{28}$$

where $x_i(t) \in \mathbb{R}^n$ denotes the state vector of the ith node, and $f_i(x_i(t))$ is the corresponding vector function describing the evolution without coupling $c_i = 0$; $h_{ij}(x_i(t), x_j(t))$ represents the generic output function describing the coupling relationship between node i and node j. In a way, a control of networks is to achieve the desirable behavior by a specific regulation, i.e., reaching the desired target of $x_i(t)$, $\forall i = 1, 2, \ldots, N$, observed in the form of climate, power grid, social community, etc. Considering the large scale property of complex networks such that it is impractical to control each node, and inspired by the research advances where a part of nodes always can play a leading role in a whole network [509–511], a natural idea to realize control of complex networks is deploying a small number of controlled nodes, which is exactly

consistent with the key idea of pinning control [512]. The pioneering work in [507] proposes an efficient method to select a fraction of driver nodes to guarantee controllability of a complex network, beginning with the canonical linear, time-invariant dynamics:

$$\dot{\mathbf{x}}(t) = A\mathbf{x}(t) + B\mathbf{u}(t), \tag{29}$$

where $\mathbf{x}(t) = (x_1(t), x_2(t), \ldots, x_N(t))^\top$ denotes the state of a network consisting of N nodes, and $\mathbf{u}(t) = (u_1(t), u_2(t), \ldots, u_m(t))^\top$ represents the m control inputs. This selection method is mainly based on maximum matching in graph theory and structural controllability in control theory. In [513], it has been claimed that the topology of a network is strongly correlated with certain control properties, i.e., the number of required control inputs and the functional origin of each control input. Furthermore, the fundamental structures of the topology in a network, which provide the explanation for the basis of this correlation, are presented individually, via exploiting the selection method in [507]. It follows that the connectivity of communication graphs can affect the signal propagation of the state evolution in complex networks. Subsequently, we briefly review recent advances of control on networks from static and dynamic topology perspectives, respectively.

3.4.1. Static topology

It is a fundamental issue to investigate the static connection case in network science, i.e., permanent interactions between adjacent nodes. The linear control theory is utilized to derive accurate closed-form expressions, which relate the specific connections (those linking driver nodes to non-driver nodes) to the minimum energy $E(\mathbf{u}(t))$ that is required to control networked systems (29) [514], where $E(\mathbf{u}(t))$ is defined as

$$E(\mathbf{u}(t)) = \sum_{i=1}^{N} \int_0^T \|u_i(t)\| dt.$$

To improve the accuracy of depicting the connections in a topology, an effective approach of modeling graph is introduced [515], i.e., a weighted graph where the nonlinear logical redundancy is captured in the context of biochemical network regulation, signaling, and control. This modeling approach is extended from the traditional representation of biochemical networks as binary interaction graphs, such that an important feature of biochemical multivariate systems is accurately presented: the efficiency of propagating control signals can be improved via some specific pathways in the topology of a network.

Submodular optimization approaches provide a novel idea to investigate driver/input node selection in networks [516], so as to identify appropriate nodes to deliver control signals in a network effectively. Submodularity is a property of set functions, analogous to the concavity of continuous functions. Submodular structures enable the development of polynomial-time input/node selection algorithms with provable optimality bounds. In addition, the controllability relationship between linear and nonlinear cases in complex networks is studied via the nodal importance ranked by means of the degree distribution [517]. Specifically, the nonlinear nodal importance is quantified by the ability of individual nodes to make the system resilient from the aftermath of a tipping-point transition, and the linear nodal importance is quantified by the ratio of the times of the node appearing in the configurations of the minimum controller sets to the total number of these configurations.

3.4.2. Dynamic topology

It is increasingly recognized that most real networked systems can be captured by dynamic networks, i.e., the connections of a network are changing over time. In Fig. 21, an example is provided to illustrate the property of dynamic topology for a control of networks. An analytical framework for temporal networks is presented in [25] based on the dynamics:

$$\dot{\mathbf{x}}(t) = A_M\mathbf{x}(t) + B_M\mathbf{u}_M(t),$$

for $t \in [t_{M-1}, t_{M-1} + \tau_M)$, where τ_M denotes the time interval between two snapshots $M-1$ and M. In that case, it is shown that compared to the static counterparts, temporal networks can reach controllability faster, with less control energy E_f and more compact control trajectories. Note that E_f is defined as follows,

$$E_f = \frac{1}{2}\mathbf{d}^\top \mathbf{W}_{eff}^{-1}\mathbf{d},$$

where $\mathbf{d} = \mathbf{x}_f - e^{A_M\tau_M}\cdots e^{A_1\tau_1}\mathbf{x}_0 \in \mathbb{R}^N$ is the difference vector between the desired final state and the natural final state that the system reaches without control inputs, and $\mathbf{W}_{eff}^{-1} \in \mathbb{R}^{N\times N}$ encodes the energy structure of the temporal network.

The limit, i.e., the knowledge of the network dynamics while designing control algorithms for networks, has been overcome via developing a data-driven framework to control complex networks optimally [518]. Moreover, the minimum energy control of network ensembles is investigated for networks typically affected by high levels of uncertainty [519], where the common assumption of perfect knowledge of the system in the field of optimal control has been removed. On the other hand, the antagonistic interactions have also been considered, which may be caused by adversarial attacks or corrupted signals, are usually represented by negative edge weights on a communication graph, and would result in

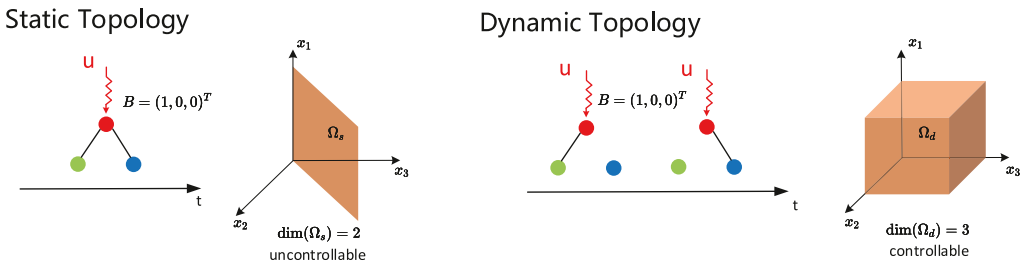

Fig. 21. It is shown that the network in this example is controllable under the dynamic topology situation, while it is uncontrollable in the static topology case with the same control input configuration [25], where Ω_s and Ω_d denote the controllable spaces corresponding to the above-mentioned cases under static topology and dynamic topology, respectively. $\dim(\Omega_s)$ and $\dim(\Omega_d)$ denote the dimensions of Ω_s and Ω_d, which depict the controllability of corresponding controllable spaces, respectively.
Source: Adapted from [25].

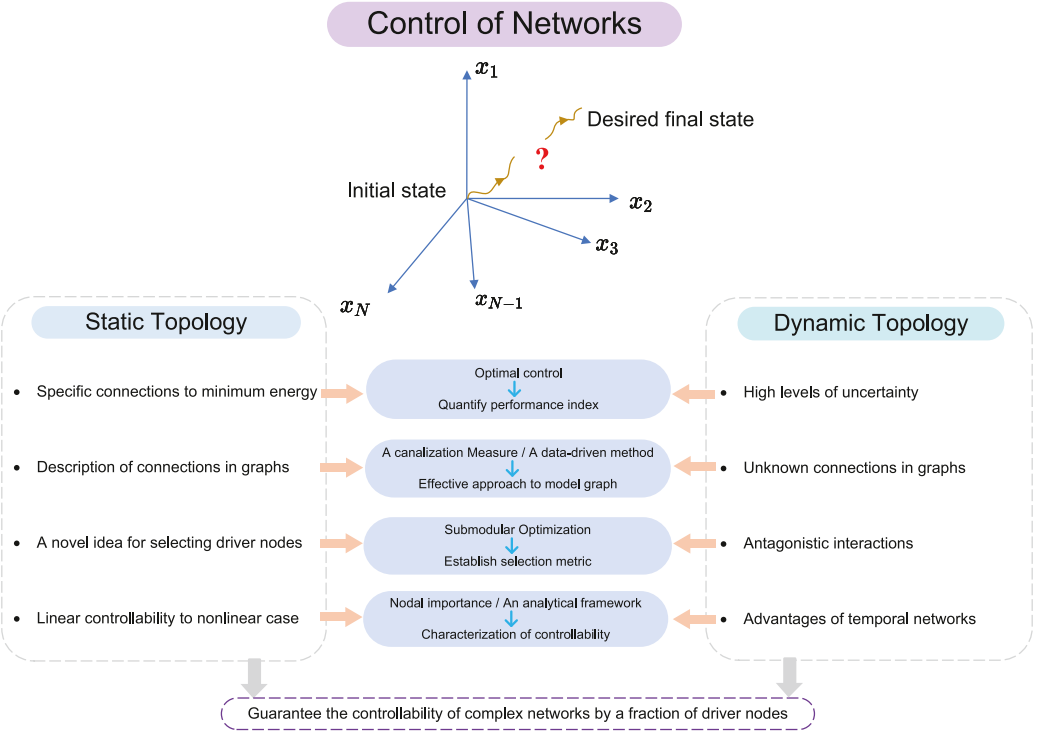

Fig. 22. This flow depicts the structure of this brief review on the control of networks.
Source: Adapted from [507].

hampering or even preventing desired collective performances. Specifically, a scheme to identify input nodes is proposed via the submodular optimization method to guarantee the consensus of high-order multiagent systems under switching topologies with antagonistic interactions [520].

In addition to the above-mentioned significant works on control of networks (a related flow is listed in Fig. 22), the interested reader can refer to [28,521] with respect to the review of network controllability and control of brain network, respectively. The stability of multi-dimensional switching networks in an open environment is well analyzed and its application to multi-agent systems is proposed in [522]. The stability for impulsive stochastic time-varying networks is analyzed in [523] and some sufficient conditions related to the average impulsive interval are also given. In addition, for semi-Markov jump stochastic nonlinear networks, some interesting results on their stability analysis are provided in [524], which are also closely related to the average impulsive interval. Besides, the applications of network control is increasingly growing. For example, it is posited that network control fundamentally relates to mind control (delivered by devices implanted in the subject's brain to regulate neurophysiological processes causing a change of mental state), and this relationship underlines important fields for empirical research in the future and offers opportunities to translate this knowledge into various practical domains [525]. Besides, a combination of computational approaches (graph theory

and network control theory) is applied to identifying brain regions that are the most influential in some particular transitions [526,527].

3.5. Graph neural networks

Graphs are widespread across physics (e.g., studies in quantum system [528–530] and non-equilibrium dynamics [531–533]), biology (e.g., analyses of brain [534–539], metabolic [540–542], and protein [543–545] networks), social science (e.g., scientific community [546–548] and opinion formation [549–551]), and computer science (e.g., analyses of internet [552–554] and information flow [555,556]), etc. Numerous challenging tasks can be addressed by studying graphs, which implies the rapid progress of graph theories [119]. The obstacles in concrete graph analyses lie in that real graphs can be irregular (i.e., lack clear topology patterns) or incomplete (i.e., there exist missing nodes or edges) and, therefore, put daunting challenges to analytic theories [557]. Consequently, data-driven approaches are becoming increasingly popular, among which, graph neural network may be the most non-negligible one [557,558].

Ever since an early version was proposed in [559], the potential for graph neural networks (GNN) to learn optimal representations of graphs have been demonstrated and promoted by extensive follow-up works. One can see [557,558,560] for comprehensive reviews of the technical and benchmark details of diverse GNN. In general, GNN can be classified into four classes according to their computational designs [557]:

(1) Recurrent GNN are earliest versions of GNN. These models are designed to learn node representations under the assumption of homogeneity, i.e., each node persistently interacts with its neighbors (e.g., exchanges information) until the system reaches a stable equilibrium [561–564].
(2) Convolutional GNN generalize the idea used in convolutional neural networks into graphs. Specifically, convolutional GNN learn the optimal representation of a node by aggregating the features of this node and the features of its neighbors (e.g., by spectral methods [565,566] or spatial aggregation methods [567,568]), which is similar to the operation of convolution. By stacking multiple convolution layers, convolutional GNN are more efficient in extracting high-level representations of nodes.
(3) Graph autoencoders (GAEs) are unsupervised learners that encode nodes or graphs into latent representations and decode nodes or graphs from latent space. These models can learn latent embedding space or generative distributions of graphs through the dual optimization of encoding and decoding [569–571].
(4) Spatial–temporal GNN learn the spatial and temporal dependency among nodes simultaneously. They are efficient in dealing with dynamic graphs that evolve across time (e.g., traffic networks) [572–574].

By learning optimal representations of graphs or nodes, GNN can be used for node classification, graph classification, graph compression, graph complement, and dynamic graph modeling [557,558,560]. Combining these elementary applications, physicists are enabled to represent and predict complex systems in data-driven ways. Such an idea has recently seen success in particle physics [575] and condensed matter physics [576].

4. Network time series analysis techniques

A fundamental question in the data-driven analysis of complex systems is to address, to which extent, two components (variables) are related given observational data from that process. (See Fig. 23 for a visual illustration.) For example, questions such as are the population dynamics of two species related in an ecosystem [577], or are two regions of the brain related in their dynamical activities [28], essentially rely upon some accurate and reliable measure of pairwise dependence [578,579]. Based on the type of systems and processes under consideration, various sets of theory and computational methods have been developed to serve as tools for analyzing dependencies between components in a system [26]. These tools range from basic linear correlation measures to more sophisticated information-theoretical quantities (Section 4.1), forming the cornerstone of extracting structural backbone of complex networked dynamics (Section 4.2).

4.1. Information transfer and nonlinear correlation tools

To facilitate a technical discussion with mathematical abstraction, we introduce some standard notation here. Consider two sequences $\boldsymbol{x} = (x_1, \ldots, x_t, \ldots)$ and $\boldsymbol{y} = (y_1, \ldots, y_t, \ldots)$, where $x_t \in \mathbb{D}^{(X)}$ and $y_t \in \mathbb{D}^{(Y)}$. For convenience of presentation, unless otherwise noted we assume that $\mathbb{D}^{(X)} = \mathbb{D}^{(Y)} = \mathbb{R}$ and simply refer to the two sequences as (scalar) time series. This representation is useful in a number of practical applications, for instance in the monitoring and detecting subtle patterns in the earth climate, in financial and economic data analysis and in the signal processing of physical waves. Being able to determine cross-dependencies is crucial for developing approximate models.

Linear correlations. The Pearson correlation is a standard statistical measure of the pairwise dependence between two random variables X and Y, given by

$$\rho(X;Y) = \mathrm{Corr}(X,Y) = \frac{\mathrm{cov}(X,Y)}{\sigma_X \sigma_Y}, \tag{30}$$

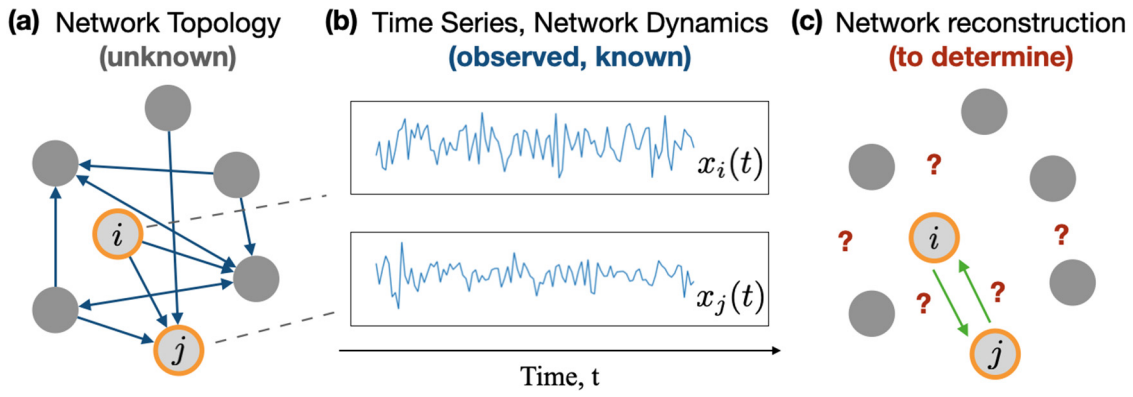

Fig. 23. Much of the modern research in complex systems requires understanding the dynamics of interacting components. In particular, when provided with time series observations from a system whose underlying interaction network is unknown (a–b), an important question is how to refer the structure of those interactions (c) — for instance, does node i influence j and vice versa?.
Source: Adapted from [580].

where $\mu_X = \mathbb{E}(X)$ and $\mu_Y = \mathbb{E}(Y)$ denote the mean of X and Y and the respective covariance and standard deviations are represented as $\text{cov}(X, Y) = \mathbb{E}[(X - \mu_X)(Y - \mu_Y)]$, $\sigma_X = \sqrt{\mathbb{E}[X^2] - (\mathbb{E}[X])^2}$ and $\sigma_Y = \sqrt{\mathbb{E}[Y^2] - (\mathbb{E}[Y])^2}$.

If we interpret time series $\boldsymbol{x} = (x_1, \ldots, x_T)$ and $\boldsymbol{y} = (y_1, \ldots, y_T)$ as iid data samples from the respective random variables X and Y, we can estimate their linear correlation coefficient from the data, for instance using the sample mean and sample (co)variances: $\hat{\mu}_X = \frac{1}{T}\sum_t x_t$, $\hat{\mu}_Y = \frac{1}{T}\sum_t y_t$, $\hat{\sigma}_X = \sqrt{\frac{1}{T-1}\sum_{t=1}^{T}(x_t - \hat{\mu}_X)^2}$, $\hat{\sigma}_Y = \sqrt{\frac{1}{T-1}\sum_{t=1}^{T}(y_t - \hat{\mu}_Y)^2}$.

What does the Pearson correlation $\text{Corr}(X, Y)$ measure? In fact, if both X and Y are Gaussians that are related by a linear model

$$Y = aX + b, \tag{31}$$

it follows that $a = \text{Corr}(X, Y)$, in other words the Pearson correlation coefficient gives the weight parameter of the linear model that relates the underlying variables assuming both are Gaussians. Interestingly, simple as it seems the linear model has a deep root in information theory and statistical physics. In fact, if we assume that the time series jointly forms a Gaussian process — which is not unreasonable if we follow the Maximum Entropy (MaxEnt) Principle enforcing the first and second moment constraints, then the correlation coefficient is exactly the parameter in this process. In other words, under the MaxEnt framework, we can explicitly model the behavior of the two time series as Gaussian processes, and the correlation coefficient is an estimation of the model parameter.

Limitations of standard linear correlation. The widely used standard linear correlation measure fails to capture much of the rich features common in practical applications. So what might go wrong with a linear correlation analysis? In fact, there are several aspects. (i) First, the standard correlation measure does not capture the history or memory effect of the process. For example, the effect of X on Y might be effective after some time delay but such delayed dependence is not accounted for by the standard correlation coefficient. (ii) Secondly, time series can be nonlinearly related while only exhibiting a very weak and even diminishing linear correlation. Without a proper measure of delayed and nonlinear dependence, much of the hidden relationships might go undetected in a complex system. (iii) Thirdly, even though pairwise dependence measures are useful and fundamental, they typically present within a complex network system where other processes can interact with one or both of them. This ultimately causes difficulties in untangling the pairwise correlation from effects imposed by other parts of the system (See Fig. 24).

For the reminder of Section 4.1 we survey works that address the first two challenges, leaving the third point as well as its further complication due to the cause-and-effect relations to Section 4.2.

Delayed correlation. Several existing works make it possible to address the issue of delayed dependence and correlation. Under the linear model framework, a commonly used tool is called cross-correlation function which is widely used in signal processing applications. The idea is to measure the linear correlation with one of the two variable time shifted, effectively defining a delayed correlation as

$$\rho_\tau(X; Y) = \text{Corr}(X(t - \tau), Y(t)) = \frac{\text{cov}(X(t - \tau), Y(t))}{\sigma_X \sigma_Y}. \tag{32}$$

In signal processing this type of tool often generalizes to continuous functions using convolutional methods and tools [581]. In practice, when the proper time delay is unknown, we can scan over a range of the delays to try to select the best one. For example, take a time delayed linear model $Y = aX(t - 5) + \xi$ as used in Fig. 24(b), we compute the delayed correlation $\rho_\tau(X; Y)$ for a range of τ. As shown in Fig. 25(a), the delayed correlation reaches its maximum at $\tau = 5$ which coincides with the delay parameter that generates the data.

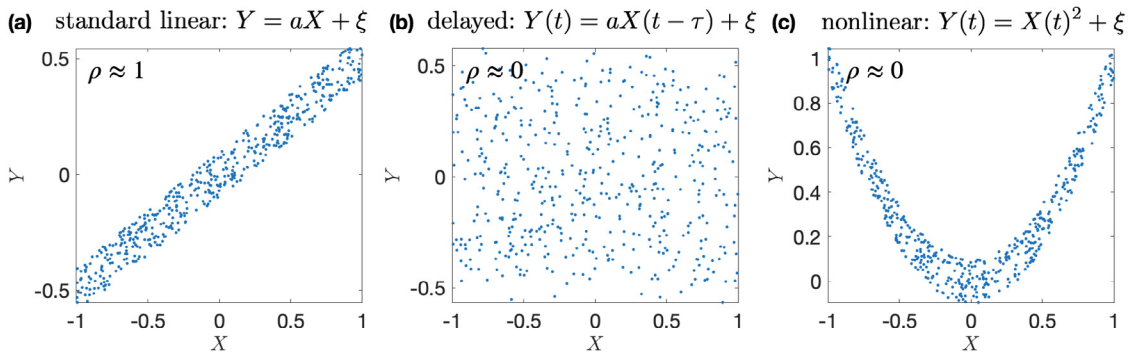

Fig. 24. Challenges and limitation of linear correlation measures in detecting pairwise dependencies. (a) In a standard linear model $Y = aX + \xi$, the linear correlation measure adequately captures the dependence between the two variables X and Y. (b) When the influence from X to Y is delayed, e.g., $Y(t) = aX(t-\tau) + \xi$, the standard use of the linear correlation coefficient fails to detect the proper pairwise dependence. (c) Under nonlinear effects, e.g., $Y(t) = f(X(t)) + \xi$ - here using $f(x) = x^2$ as an example, the linear correlation might fail. Here we generate X and ξ independently from the uniform distributions in the intervals $(-1, 1)$ and $(-0.1, 0.1)$ respectively. Other model parameters are $a = 0.5$, $\tau = 5$. For the instance as shown in the figure, $T = 500$ points are generated for each variable and the measured linear correlation coefficients are $\rho = \mathrm{Corr(X,Y)} = 0.98$ (a), $\rho = 0.0013$ (b) and $\rho = 0.0040$ (c).

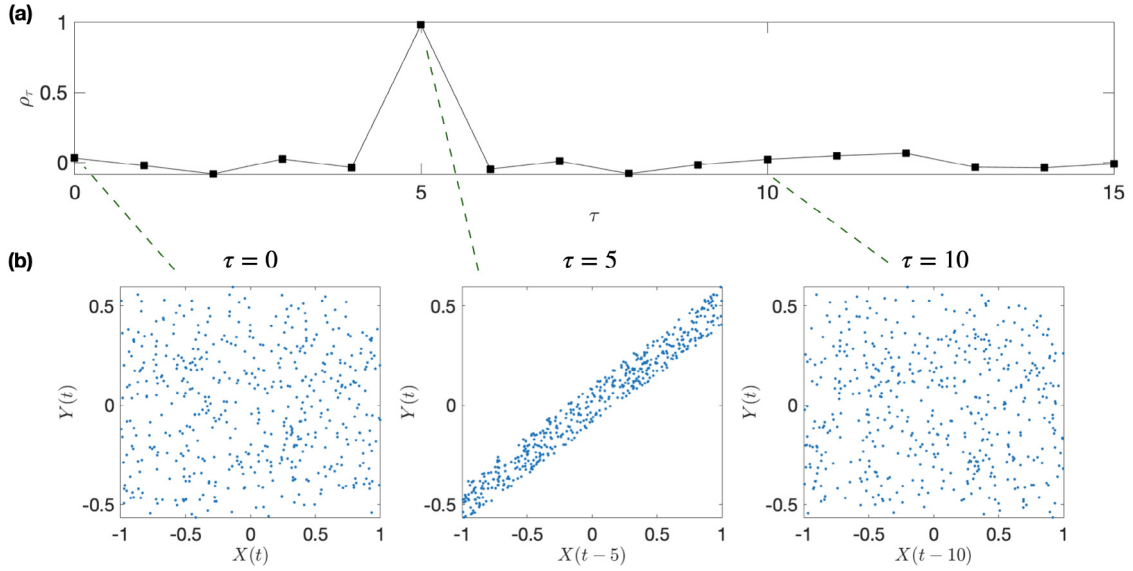

Fig. 25. Delayed correlation $\rho_\tau(X; Y)$ for time series data generated from the linear delay model $Y = aX(t-5) + \xi$ as used in Fig. 24(b).

Nonlinear correlation. To determine the dependence between two time series beyond linear measures, there are generally two types of approaches, namely model-based approach and model-free approach.

(i) In the model-based approach, one assumes that the nonlinear model form $Y = f(X; \mu)$ is known but the model parameter, here denoted as μ, need to be estimated from data. In this scenario the challenge is to deal with unknown parameters and noise in order to property quantify the possible dependence. Once the model parameter(s) are determined, one can read off and completely analyze the dependency within the model. For instance, consider a nonlinear model $Y(t) = aX(t)^2 + b\xi$, where the parameters a and b are unknown. If we are supplied with time series data $(X(t); Y(t))$, we can first apply a nonlinear transformation $Z = X^2$ which yields a linear model $Y = aZ + b\xi$, and then by using standard linear correlation measures to estimate a and b, thus completely determining the dependencies among the variables and noise.

(ii) In the second, model-free approach, the form of model is unknown *a priori*, in which case the question of measuring dependency becomes impossible within the parametric statistics context. Instead, one typically needs to resort to tools from information theory and information geometry [582]. In particular, for two random variables, there is a rigorous way of detecting whether or not they are statistically independent by measuring their mutual information — in fact, entropy and mutual information together form a type of metric for representing the interdependences among variables [583]. To

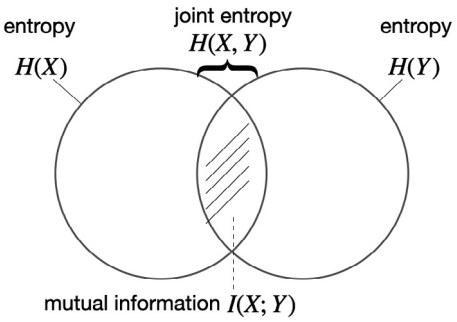

Fig. 26. Information Venn diagram that visualizes the relation between entropy, joint entropy and mutual information.

be concrete, note that the mutual information between two random variables is given by

$$I(X;Y) = H(X) + H(Y) - H(X;Y), \tag{33}$$

where the entropy and joint entropy are defined as $H(Z) = \mathbb{E}[-\log(p(Z))]$. The relation between entropy, joint entropy and mutual information can be conveniently understood through the information Venn diagram as depicted in Fig. 26. Substituting in $Z = X$, $Z = Y$ and $Z = (X, Y)$ with the corresponding probability mass (or density) function $p(X)$, $p(Y)$ and $p(X, Y)$ respectively gives rise to $H(X)$, $H(Y)$ and $H(X; Y)$, referred to as the entropy of X, entropy of Y and joint entropy of (X, Y), respectively [584]. It follows that for discrete random variables,

$$0 \leq I(X;Y) \leq \max(H(X), H(Y)), \tag{34}$$

with $I(X; Y) = 0$ if and only if $p(x, y) = p(x)p(y)$, i.e., X and Y are *independent*. Thus, by measuring the value of $I(X; Y)$ one can in principle detect the statistical dependence between two random variables — without having to assume that the variables are linearly related.

Statistical estimation for discrete and continuous-valued variables. In order to compute entropy and mutual information from data, one needs to resort to statistical estimation techniques, if the variables under consideration are discrete, For continuous-valued processes, which are common in practice, one in fact needs to deal with the issue of building up the "right" discretization. Several lines of work address this [585]. The naive uniform binning is typically inefficient and often replaced by some sort of optimal binning, by imposing uniformity on the measure rather than space. Another interesting piece of work shows that one can in fact define and solve an optimization problem in order to determine the right version of discrete mutual information as an approximation for the true continuous MI [586].

Transfer entropy and information flow. A natural question arises as for whether several of the challenges outlined above, namely (1) delayed correlation and (2) nonlinearity can be jointly resolved, in a single quantity. This was made possible by realizing that one can indeed compute a delayed version of mutual information, or so-called transfer entropy (named by Schreiber [587], around the same time proposed as a type of conditional mutual information and synchronization measure by Palus et al. [588]). In transfer entropy, one assumes that data originates from a Markov process (of some finite order), and defines the TE from one process to the other as:

$$\mathrm{TE}_{X\to Y} = H(Y_t|Y_{t^-}) - H(Y_t|X_{t^-}, Y_{t^-}), \tag{35}$$

where the processes X_t and Y_t are assumed to be stationary, with X_{t^-} denoting the semi-infinite joint variable $X_{t^-} = (X_{t-1}, X_{t-2}, \dots)$, and the conditional entropy $H(Y|X)$ is given by $H(Y|X) = H(X, Y) - H(X)$. Similarly, one can quantify the information transfer from Y_t to X_t using the transfer entropy in the reverse direction, as in Fig. 27

$$\mathrm{TE}_{Y\to X} = H(X_t|X_{t^-}) - H(X_t|X_{t^-}, Y_{t^-}). \tag{36}$$

Because of its unique capabilities of detecting nonlinear and delayed dependencies in random processes, transfer entropy after its initial introduction soon became a popular approach used in diverse field of applications including neurophysiology [589–591], quantitative finance [592,593], chemical processes [594], climate dynamics [595] and social science [596].

Practical considerations. Note that the (idealized) definition of transfer entropy cannot be applied because it requires estimating entropies from the infinite-dimensional variable X_{t^-} and/or Y_{t^-}. In practice one typically needs to *truncate* the model order. In most works one replaces X_{t^-} with X_{t-1} and Y_{t^-} with Y_{t-1}, implicitly assuming that X and Y jointly form a Markov process (with no memory). Caution needs to be exercised, however, since such an assumption can fail in practice and for processes with long memory truncating into the lowest order can have significant impact on the quality of computations [597].

Information flow in continuous-time dynamics. For signal-processing applications where observations come from sampling a continuous-time physical process, an important question is whether the estimated and computed quantities of

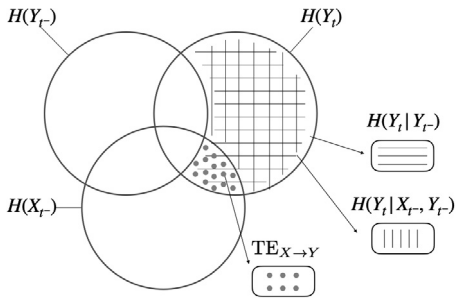

Fig. 27. Transfer entropy as visualized in the form of an information diagram.

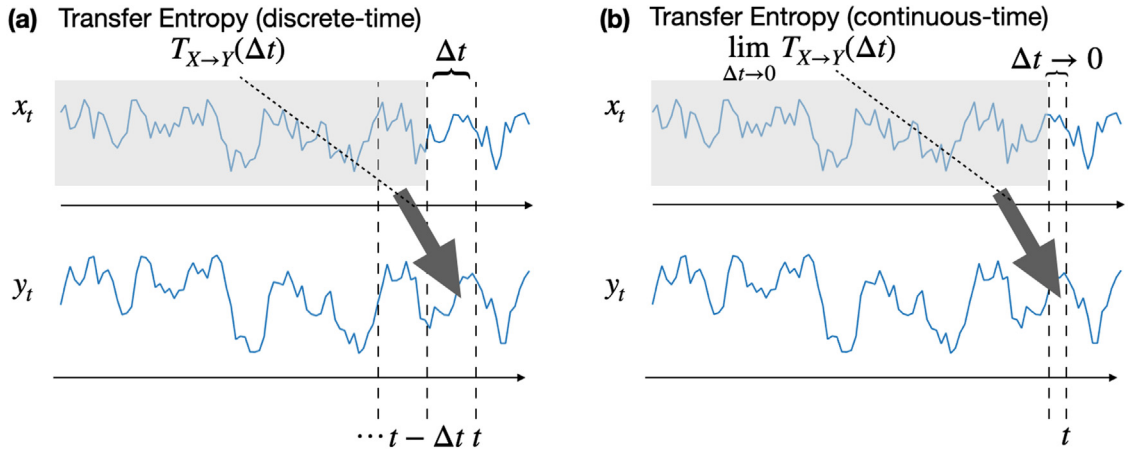

Fig. 28. Transfer entropy for discrete-time (a) versus for continuous-time processes (b), the latter type of processes naturally arise in physical systems.

information transfer are in fact meaningful, which requires defining and quantifying the flow of information in continuous-time processes. See Fig. 28. This question was elegantly addressed by Liang and Kleeman in their seminal work which led to the notion of Liang–Kleeman information flow [598,599]. Using the Liouville operator, they show that an analogous concept of transfer entropy can indeed be rigorously defined for continuous-time dynamics, proving a principled way of analyzing information flow in more general systems.

Detection of abrupt changes in time series. In building up statistical models and measures for time series, one often tactically assumes that data comes from some stationary process under which the relevant statistical quantities are computed by adequate "averaging" (statistical estimation) techniques. In practice, a dynamic process can undergo sudden changes breaking such stationarity assumption. How to detect abrupt changes is thus a very important problem. It essentially is about how to partition a time series into stationary segments. For linear processes, one can formulate a dynamic programming problem to detect those so-called structural breaks (see Fig. 29) [600,601], while for processes that include both linear trends and seasonal cycles more advanced approaches become necessary such as sparse modeling and optimization [602] (see Fig. 30). Generally, for nonlinear processes, a principled method is still lacking — heuristic approaches include those that are devoted into early-warning signals (EWS) [603] and more recent works based on nonlinear predictability [604].

In the important application area of structural health monitoring [605], in addition to addressing the issue of change-point detection in scalar time series, there is the more complex scenario, where we are presented a set of multivariate time series from which we wish to detect possible changes and failures, an important task in transforming traditional human-based system monitoring and risk analysis to a smart automated system in Fig. 31. While the majority of existing methods rely on linear and Gaussian process assumptions, there has already been some preliminary attempt to utilize nonlinear network modeling and applied it to multivariate sensor data observed from a real bridge in Fig. 32 [606].

4.2. Network reconstruction

Following a pairwise correlation analysis, one can further address issues such as how are multiple components in a system dynamically interacting [607]. At the heart of this question is a fundamental and challenging problem faced

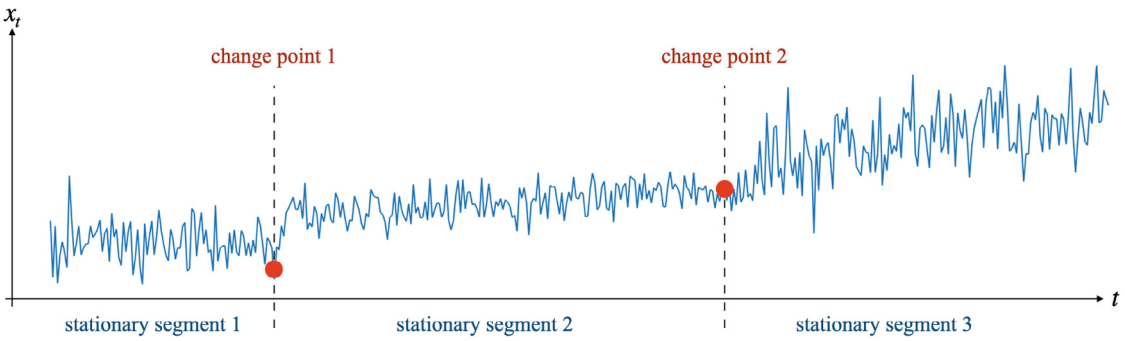

Fig. 29. Change point detection in time series, with the ultimate goal of partitioning the time series into stationary segments.

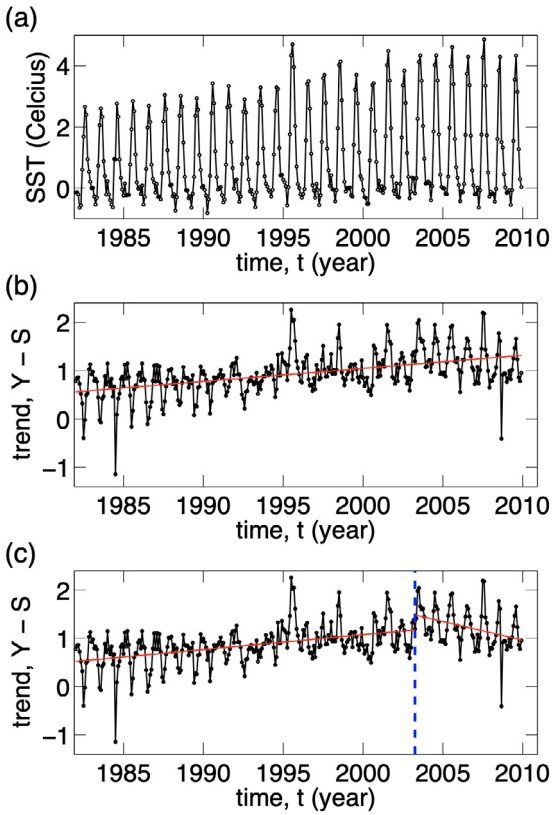

Fig. 30. The Arctic sea surface temperature (monthly) time series from Jan 1983 to Dec 2009 (a), and the structural breaks identified under two set of parameters (b–c).
Source: Adapted from [602].

in today's data analytics research, the question of determining cause-and-effect relationships. (See Fig. 33 for potential application and challenges in global climate modeling.) Traditionally, this was done by conveniently assuming a model form and converts the problem of causal inference to parameter estimation. However, in the modern era of complexity in the underlying process and massive amount of data often deviate significantly from known models. Developing model-free approaches that are not data-hungry becomes crucial. See Fig. 34.

Granger causality and transfer entropy. Among existing approaches, a widely adopted method of determining causality is through the Granger causality (GC) analysis. Consider a pair of time series, the working definition of GC can be summarized as follows [608,609]

$$\mathrm{GC}_{X\to Y} = \delta(Y_t; Y_{t^-}) - \delta(Y_t; X_{t^-}, Y_{t^-}), \tag{37}$$

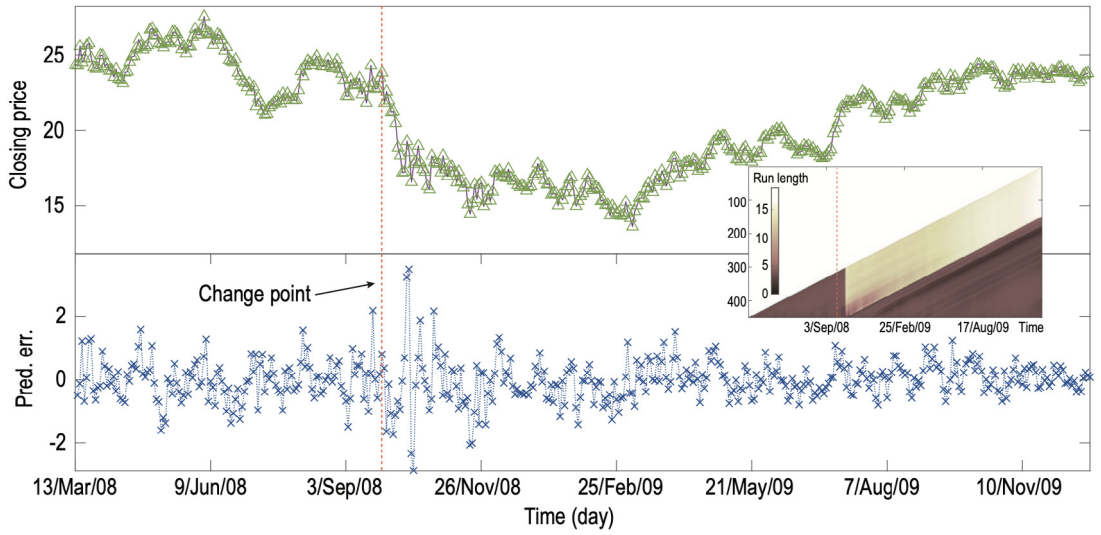

Fig. 31. Example of using model-free nonlinear prediction for change-point detection, applied to the stock market time series during the 2008 economic crisis.
Source: Adapted from [604].

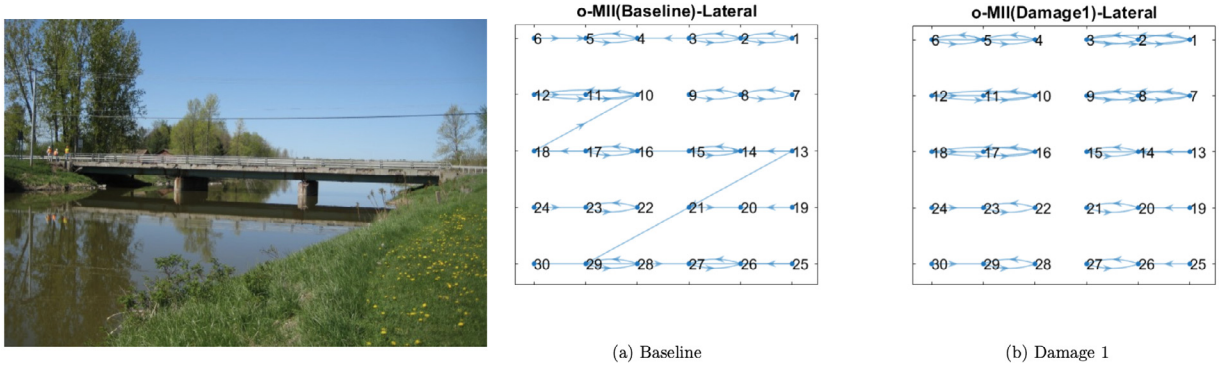

Fig. 32. Using nonlinear network dynamics modeling approach to detect structural changes from data measured on the Waddington Bridge — upper state New York.
Source: Adapted from [606].

where $\delta(Y;X) = \min_{\mathcal{L}} \|Y - \mathcal{L}(X)\|$, with $\mathcal{L}$ denoting a *linear* transformation. In simple words, the first term represents the error by using a linear regression model on Y_t, whereas the second terms represents the regression error when both X_{t^-} and Y_{t^-} are used in the linear regression model. The GC is non-negative which measures the error reduction when data from X_{t^-} is used to draw predictions of Y_t in addition to using the past of Y_t itself. Transfer entropy can be seen as a generalization of GC, where the linear regression error is replaced by the more general conditional entropy measures (see Fig. 35).

The reason GC requires a linear model is to define a computable quantity. But the linear model assumption clearly limits the applicability of GC. To resolve its limitation, TE is often used in settings where the Gaussian assumption is violated. For a long time, GC and TE are default options when trying to quantify cause-and-effect from observational data. Although the working definition of GC requires a linear model and is valid only for a bivariate processes, it merely represents a particular version of the general concept of causality as envisioned by Granger. In fact, Granger himself gave a much broader definition that does not rely upon a linear model [608,609] as follows: (i) The cause occurs before the effect. (ii) The cause should contain information about the caused that is not available otherwise.

What transfer entropy captures is a kind of temporal coherence in causal channels, which is related to, rather than equivalent to, causality [610]. In the interval of $(-\infty, \infty)$ where time series are distributed, the maximum entropy principle with constraints on the first and second moment implies the equivalence relation between transfer entropy and GC [611]. This property is favorable in statistical analysis but should be treated with cautions, especially when strict causal relations are targeted properties to analyze [610]. The main limitation on transfer entropy and information flow approaches is their essential dependence on the stationary assumption of dynamic processes, i.e., the probability

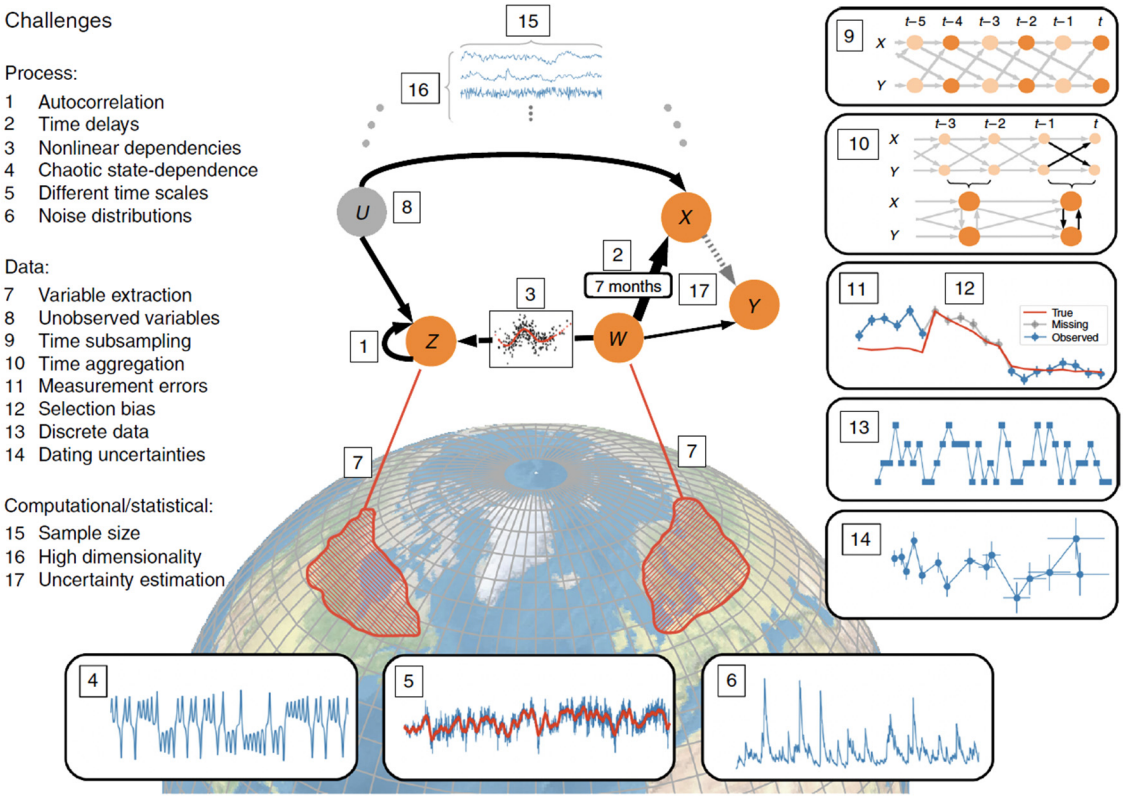

Fig. 33. Opportunities and challenges of causal network modeling of the global climate.
Source: Adapted from [27].

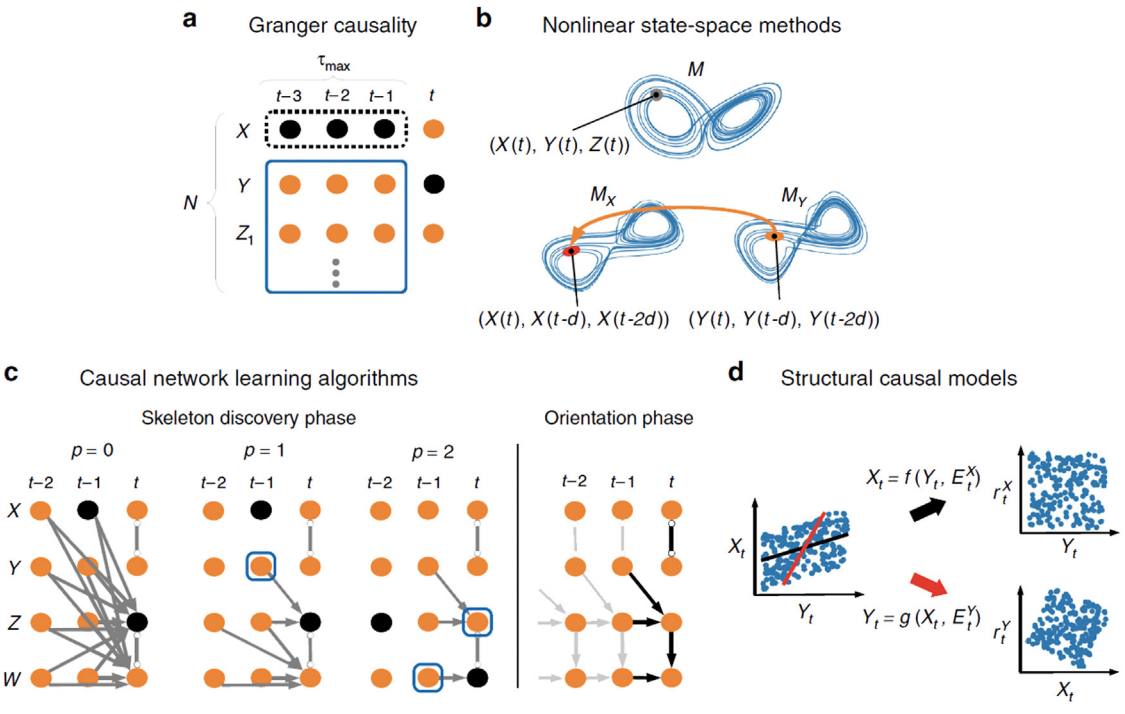

Fig. 34. Causal network inference problems and visualization of the conceptually different types of existing approaches.
Source: Adapted from [27].

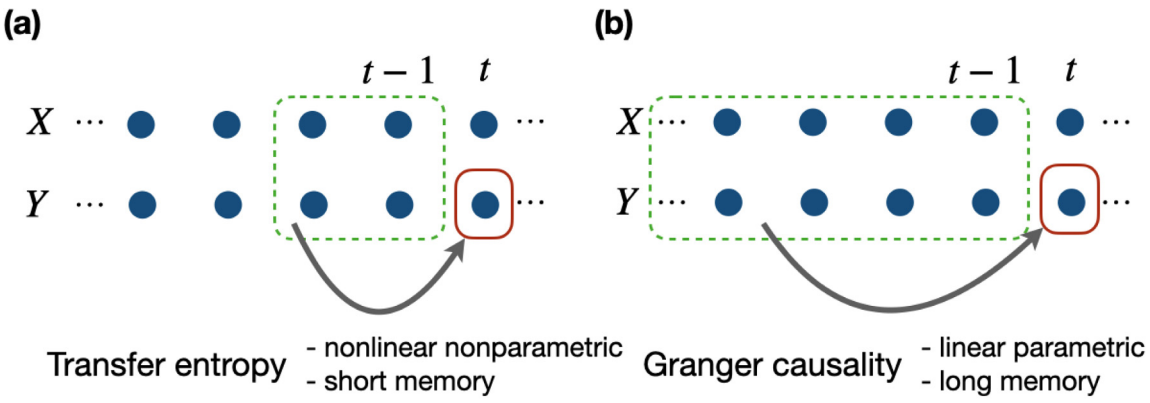

Fig. 35. Transfer entropy versus Granger causality.

distribution is time invariant. This limitation arises from the requirements of probability density estimation in these methods. In applications, transfer entropy [612] and the related GC [613] have been generalized to the Fourier domain to approximatively reflect the time–frequency distribution of causality-related properties, where the stationary assumption of dynamic processes can be principally relaxed. However, more theoretical explorations are necessary to resolve such a limitation.

Causation entropy and causal network inference. When considering a system with more-than-two variables, neither GC nor TE is guaranteed to identify the right causal models. One of the reasons is that variables other than the pair under consideration can impact the causal computations [27,583,614,615]. The following example, taken from Ref. [614], shows that even when a virtually unlimited amount of data is provided, using TE alone without accounting for confounding factors such as indirect couplings and dominance of neighbors effects can lead to the serious issue of detecting false causation relations (Fig. 36).

To address the problem of inferring the "right" causal network, one typically needs to combine some pairwise causation computation together with iterative algorithms to determine the correct causal topology underlying a multivariate process. In the same work that recognized the limitation of purely pairwise causation measures, the concept of causation entropy was proposed to define a statistical measure that is applicable to time series data from a network stochastic process, enabling to deduct the amount of information brought by indirect variables when assessing the causality between two nodes in a network [614]. Then, in a follow-up publication, a rigorous mathematical framework of optimal causation entropy was developed, giving rise to a precise and quantifiable way of defining causal network from a multivariable stochastic process, namely, the *direct causal neighbors of a node is the minimal set of nodes that maximizes the causation entropy (to the given node)*. Source: Adapted from [580], also see Fig. 37.

The optimal causation entropy problem was shown to be solvable in principle following a two-stage algorithm, as described in Ref. [580] (see Fig. 38) which extends the PC algorithm previously used for Bayesian networks but are too inefficient due to their combinatorial nature [616]. The optimal causation entropy algorithm was later compared against other related approaches, showing both its practical effectiveness and fast run-time and limitations in lack of sufficient statistical detection power [615] (Fig. 39).

Cross-mapping techniques. An alternative view and modeling framework for time series is by considering time series as outcomes from a dynamical system. From this perspective, several interesting approaches have been proposed to infer and quantify causal relations within. The convergent cross mapping (CCM) approach utilizes intrinsic (sub) manifolds embedded within coupled dynamical systems and was shown to be a promising method when dealing with data that are seemingly chaotic in particular those from ecosystems (Fig. 40) [577]. The initially developed CCM approach was later improved to enable (more) accurate account for indirect couplings, referred to as the partial cross mapping approach [617]. Also, the theories for the CMM approach and its improved variants were established empirically or/and rigorously in a series of efforts [618–620].

From structural to functional reconstruction. Beyond learning the structure of network interactions, one can further ask the question of functioning, or effectively what is the form of (coupled) dynamics that characterize the behavior of the network system. This question is challenging due to a combination of the difficulties from network structure learning (as discussed in the above parts) as well as unknown dynamics and coupling function the latter itself can be very hard to address [579].

Using causal network as a stepstone, one can further ask the question of how one can construct a model for the dynamics of a given system? This is crucially important as a way to automate dynamical modeling. Traditionally this problem was usually addressed by using either a linear modeling approach or via some pre-fixed transformation that defines a set of nonlinear basis and combine them linearly. Recently it was shown that utilizing causal network as

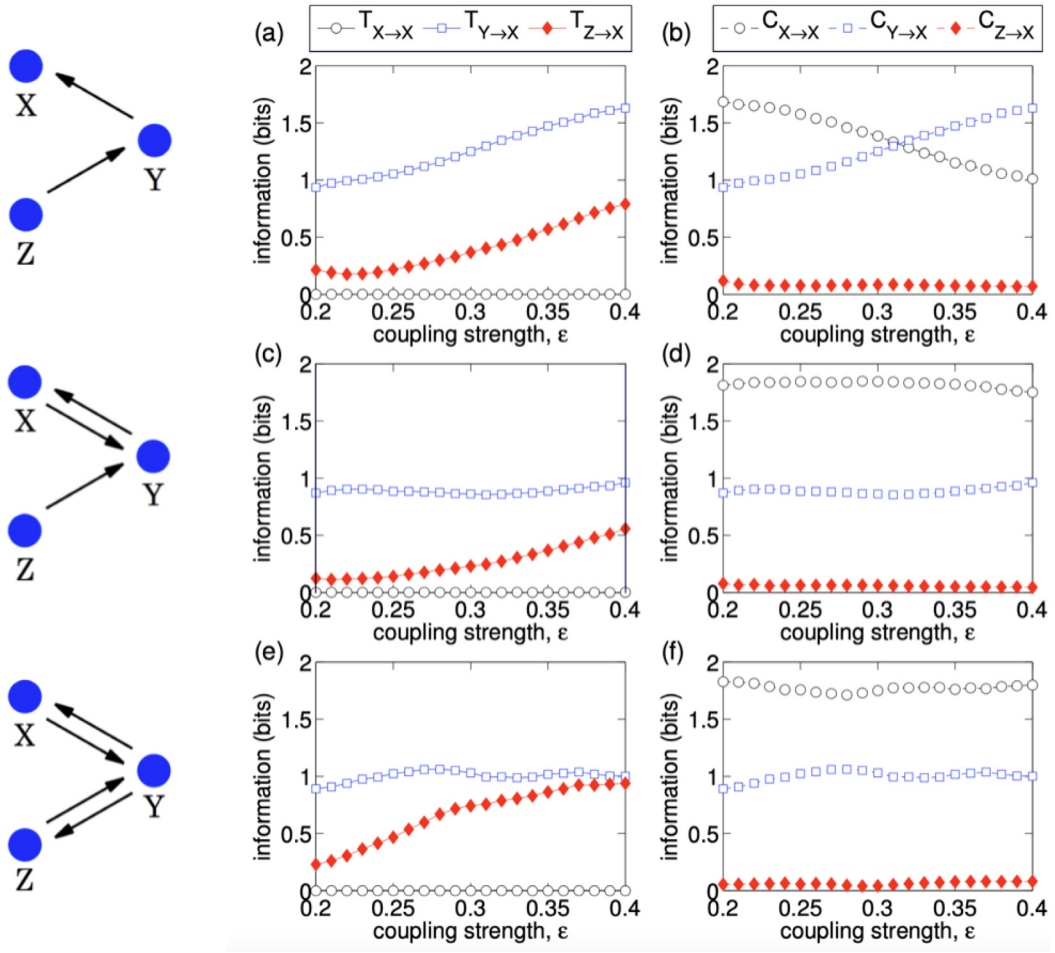

Fig. 36. Transfer entropy and causation entropy computations of detecting the causal neighbors of node/variable x in simple, three-node networks. In each row, a structure of the ground-truth network is shown on the left, whose state dynamics follows a coupled network system $x_{t+1}^{(i)} = f[x_t^{(i)}] + \epsilon \sum_{j\neq i} c_{ij} g[x_t^{(i)}, x_t^{(j)}]$ with $f(x) = 4x(1-x)$ and $g(x,y) = f(y) - f(x)$ (details in Ref. [614]).
Source: Adapted from [614].

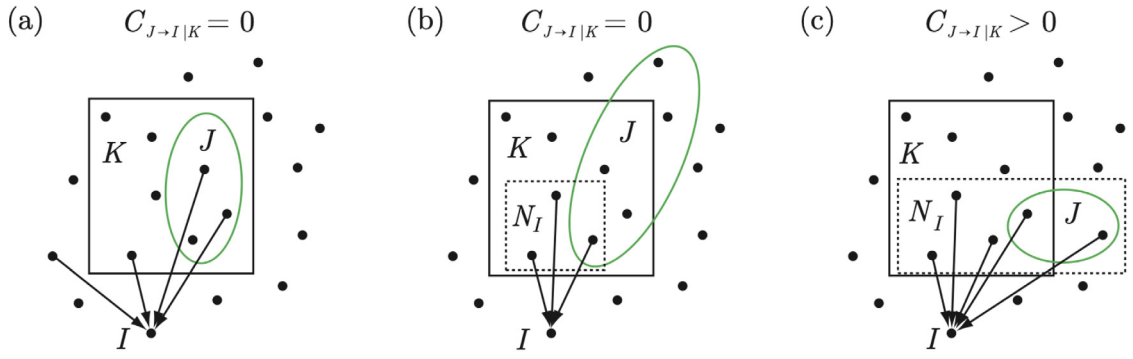

Fig. 37. Mathematical properties of causation entropy and its consequence leading to the optimal causation entropy principle for uniquely defining the causal network underlying a multivariate stochastic process.
Source: Adapted from [580].

an intermediate step can help *regularize* the solution of the problem especially when large noise is contained within the observational data. In such cases by first detecting the backbone network structure one can significantly reduce

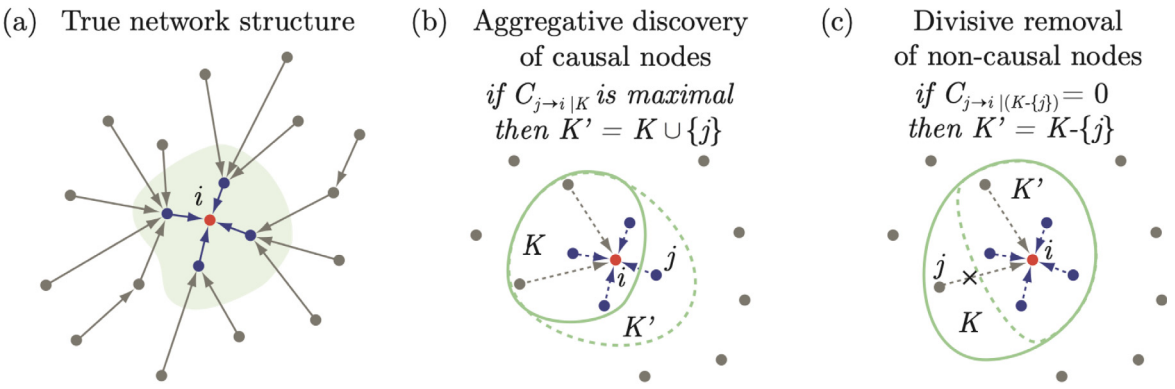

Fig. 38. Mathematical properties of causation entropy and its consequence leading to the optimal causation entropy principle for uniquely defining the causal network underlying a multivariate stochastic process.
Source: Adapted from [580].

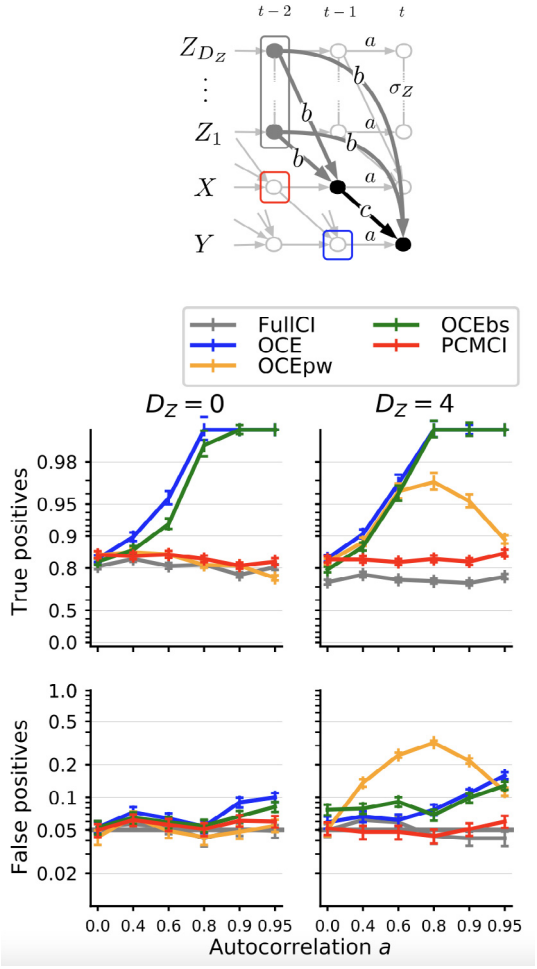

Fig. 39. Comparison of several different nonlinear causal network inference approaches. For details see Ref. [615].
Source: Adapted from [615].

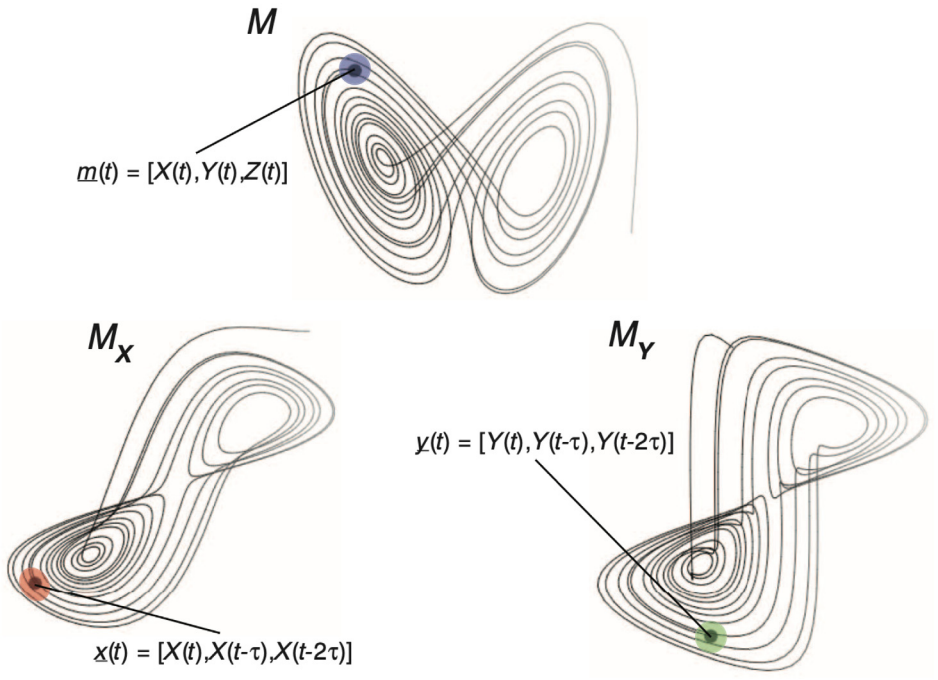

Fig. 40. Comparison of several different nonlinear causal network inference approaches. For details see Ref. [577]. *Source:* Adapted from [577].

the parameter search and optimization space to those network links, effectively reducing the challenge of noise and generalizability [621], see Fig. 41; also see Ref. [622].

Operator-theoretical techniques — Koopman Operators. Parallel to cross-mapping techniques, another kind of dynamical-system-based approach, referred to as the Koopman-based model, has become increasingly popular due to its high computational practicality and solid mathematical foundations [623]. In general, Koopman-based models approximate a simple but powerful theorem: any finite-dimensional dynamic system, irrespective of being linear, nonlinear, or even chaotic, corresponds to an infinite-dimensional linear operator that governs the evolution of scalar functions (e.g., the observation of the dynamic system) [623,624] (see Fig. 42 for illustrations). This theorem suggests an intriguing perspective to identify latent mathematical structures of dynamic systems from empirical data by computational approximation of specific linear operators. It provides a valuable opportunity to combine the advantages of mathematics, i.e., analytic analysis, and machine learning, i.e., efficient approximation. Unfortunately, the infinite-dimensional linear operator, referred to as the Koopman operator, is not computable in computers. Therefore, scientists always turn to searching the Koopman invariant subspace, which is a finite-dimensional subspace of the Koopman operator. To achieve this objective, one can consider two families of computational approaches of Koopman Embedding. The first family realizes approximation via matrix computation [625–627], which matures after the well-known dynamic mode decomposition (DMD) is proposed [625,626]. The second family, differing from the first one because of the using of neural networks, tickles the question following similar ideas [628–631]. Their ideas are rather straightforward in the context of autoencoder [628–631]. In practice, intrinsic connections between these two families of computational works and low-rank models are discovered as key guarantees of their efficiency in the data-driven modeling of dynamic systems [623,626,632]. The main limitation of classic Koopman embedding approaches, no matter what kind of computation techniques they depend on, lies in their intrinsic dependence on the autonomous property of dynamic systems (i.e., the evolution mapping that governs the dynamic system is time-invariant and deterministic) [623,626]. In real cases, non-autonomous or stochastic dynamic systems are much more common [623,626]. To meet the application demands in these cases, researchers have explored the generalization of Koopman embedding theorem to non-autonomous and stochastic systems [633–635]. This idea has seen substantial success in developing neural-network-based solvers of partial differential equations to capture the long-term dynamics of equation solutions [636,637].

4.3. Source localization and link prediction

In real world, the structure and function of most systems are inherently time-varying. Therefore, complex networks whose node properties and topologies change over time are provided to describe real systems, such as communication

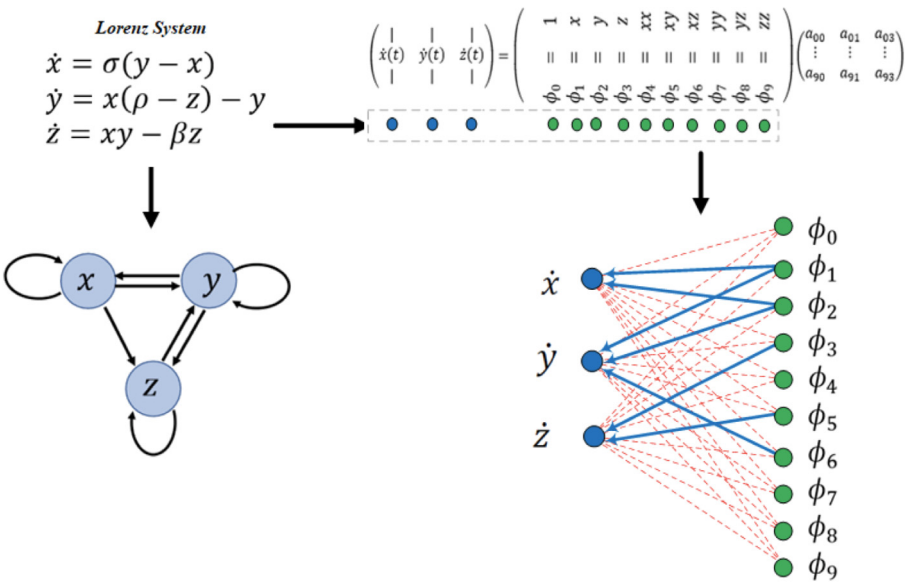

Fig. 41. Entropic regression: Integrating causal network techniques with regression approaches offers a principled way of addressing the question of learning the full network dynamics from noisy observational data.
Source: Adapted from [621].

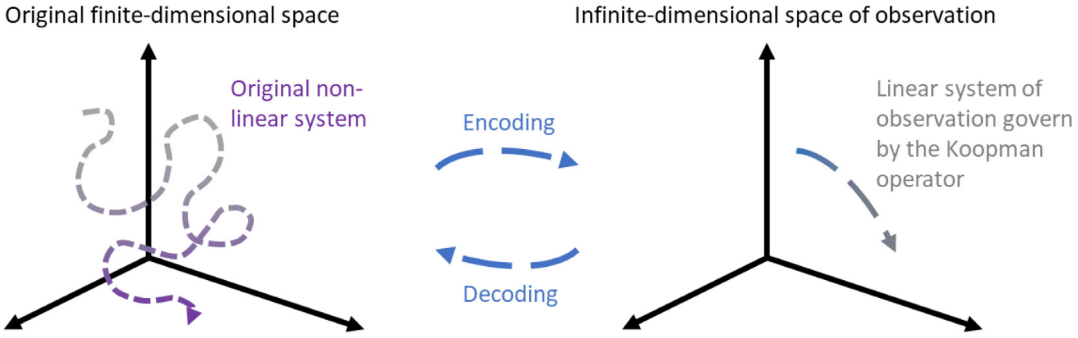

Fig. 42. General idea of the Koopman operator.

networks, social networks, or protein interaction networks. As depicted in Fig. 43, a time-varying complex network is a combination of a static network and time information. To abstract the time-varying characteristics of complex systems more accurately, time series analysis techniques are provided as methods for modeling and analysis of complex systems, and the studies of time series analysis techniques in complex networks have presented great theoretical significance and extensive practical value [29–31]. Time series analysis techniques, such as link prediction and source localization depicted in Fig. 44, have been widely applied in many fields, such as computer worms, rumors in social networks and epidemics [29]. For instance, in social networks, link prediction is to forecast whether the link in the social network would occur at future time by analyzing the topological structure of the social network and the attributes of the nodes in the network at current time, which reveals the spread of rumors in social networks. Source localization utilizes network time series information to trace the source of rumors in social networks, and we review these two common time series analysis techniques in time-varying complex networks in this part.

4.3.1. Link prediction

Link prediction is usually provided to forecast the possibility of connecting edges between two unconnected nodes when the present network topology and label information have been determined. Generally, link prediction algorithms are divided into two categories: unsupervised and supervised methods [30,31]. (i) A common unsupervised method is to use the topology information of the network to predict the links between nodes by calculating the similarity of node attributes or network structure at different time, which is called similarity-based algorithm [639]. The core of this algorithm is the design of similarity index. Different scholars put forward corresponding similarity indices considering the characteristics of

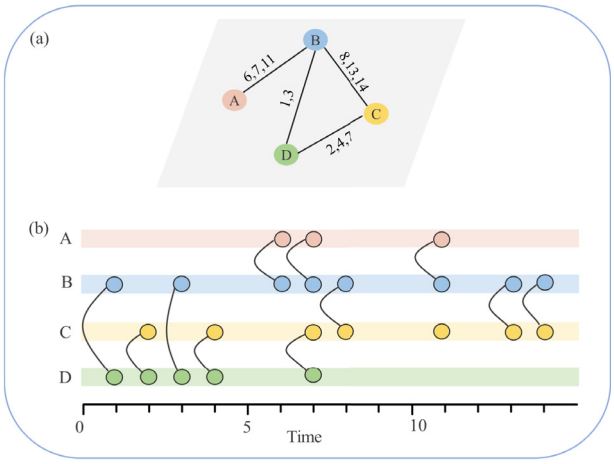

Fig. 43. Time-varying complex networks. (a). Time-varying complex networks, where A, B C, and D are the nodes. The numbers on the links between these adjacent nodes represent the occurrence moment of these contacts. (b). The sequence of contacts among four nodes, capturing, for example, the connection patterns between four individuals. We draw a line between two nodes if they interact with each other during a 1 s interval [25].
Source: Adapted from [25].

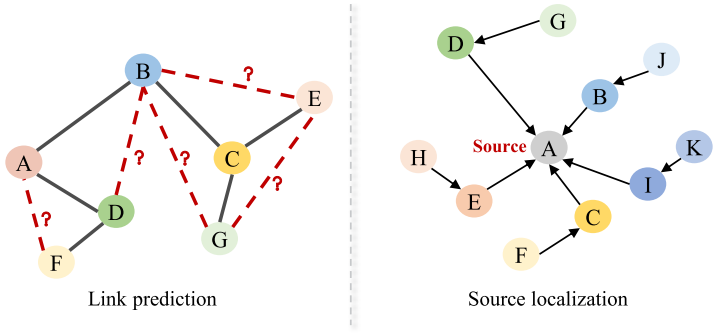

Fig. 44. Link prediction and source localization.
Source: Adapted from [638].

different types of networks. For example, the correlation or strength of the interaction between a pair of nodes is viewed as the similarity index in [30], and an unsupervised mixed strategy is proposed to predicate the link weight in social and biological networks. In multiple social media networks (SMNs), to determine whether given accounts on different SMNs belong to the same user, the traditional embedding-based method is applied to obtain the degree of consistency between the vectors representing the unmatched nodes, and a proposed distance consistency index based on the positions of nodes in each latent space provides additional clues for prediction [639]. As for protein–protein interaction networks, which consist of rich quadrangles, two quadrangle coefficients are proposed in [640] to quantify quadrangle formation in networks, which are further extended to weighted networks to analyze their correlations with node degree. It is worth noting that different networks have different topologies, and a single similarity index according to their characteristics is not universal. Another common unsupervised method is the likelihood algorithm, which assumes that the evolution of a network is determined. A likelihood estimation method for stochastic networks is proposed in [641] to predict missing connections in partly known networks with high accuracy. Normally, implementing such an algorithm requires to choose the appropriate likelihood function, and its applicability robustness to different types of networks is relatively low. Considering the differences of dynamic and topology properties in different time-varying complex networks, unsupervised methods design a similarity index or specific likelihood function to predict the links of a specific network, which is not adaptive.

(ii) Supervised methods use currently available network information as a labeled sample to update and iterate the algorithms, thus revealing the evolution mechanism of different networks. For instance, in [642], the authors investigate internal and external factors that affect the formation of links and propose a three-level hidden Bayesian link prediction model by integrating the user behavior as well as user relationships to link prediction. With the success of deep learning in different fields, a number of scholars have applied this technology to link prediction recently [643–646]. Considering the excellent performance of long short-term memory (LSTM) in processing time series, the LSTM is used for dynamic

network link prediction [643,644]. A novel encoder-LSTM-decoder deep learning model is proposed in [643] to predict dynamic links end to end, which can handle long-term prediction problems and suit the networks of different scales with fine-tuned structure. To capture the spatial–temporal patterns and high nonlinearity of dynamic networks, a graph convolutional network (GCN) is usually applied to automatically learn the spatial features [644,645]. A novel generative framework is proposed in [644] to tackle the challenging temporal link prediction task efficiently, which simultaneously models the spatial and temporal features in the dynamic networks via deep learning techniques such as GCN, the temporal matrix factorization, the LSTM, and the generative adversarial network (GAN). Similarly, combined with recurrent neural network (RNN), GCN is also used for better capturing both rich structural and evolutional information of complex information networks in [645]. Besides, in the industrial field, a cooperative link prediction model using a stacked denoising autoencoder is proposed in [646] to predict links of the Industrial Internet of Things-based mobile devices at the next moment through historical link information. All the aforementioned methods based on deep learning have a core, i.e., to extract, classify and predict the features of the time-varying complex networks.

4.3.2. Source localization

Source localization is another common application of network time series analysis techniques, which refers to find the source of wireless sensor networks, disease or information dissemination using incomplete available information based on known network structure.

In disease dissemination, rapid and accurate tracking of aggregate population flows may therefore be epidemiologically informative [647]. Human-mediated parasite importations have affected the landscape of malaria and led to spatial and temporal heterogeneity, so mobility estimates derived from mobile phone data and spatial malaria prevalence data are used to identify travel routes and sources of malaria transmission in Madagascar in [648]. Similarly, mobile phone data is also used to accurately predict the relative frequency and geographical distribution of infections with the severe acute respiratory syndrome coronavirus 2 (SARS-CoV-2), and a spatio-temporal risk source model is proposed in [647], which leverages population flow data not only to forecast the distribution of confirmed cases, but also to identify regions that have a high risk of transmission at an early stage. Besides, due to the dynamic role of source locations, it is critical to explore geographical and time-varying trends of source locations. For example, a modeling framework is proposed in [649] to estimate the time window in which early local outbreaks may have been initiated from China and signal heterogeneities in the extent and the exact source of introduced COVID-19 cases in the African locations, in which the authors firstly estimate the number of airplane passengers from China to global destinations and daily prevalence of COVID-19 in 18 Chinese cities, then predict exported case counts to African countries and contribution of different locations in China to globally imported cases.

In information dissemination of social networks, it is an important problem to identify the geolocation of social media users in a wide range of applications, spanning from emergency detection, local event recommendation, to fake news localization, online marketing planning, and even crime control and prevention [650,651]. For instance, it is desirable for police to identify on-site users of an event, from whom we could gather valuable source information, so a fused feature Gaussian process regression model is proposed in [652] to estimate the distance between a user and a social event, which exploits three influential factors in social networks for on-site user identification: mobility influence, content similarity, and social relationship. Similarly, both social media content and user network information are available for geotagging Twitter messages. Gaussian mixture models are used in [653] to map the raw spatial distribution of the model features to a predicted field, and the model features consist of Twitter content and network information jointly. Moreover, in reality, a very few samples are available and prediction models are not easy to be generalized for users from new regions. A meta-learning-based general framework for identifying user geolocation is proposed in [650] to quickly adapt the prediction toward users from new locations.

In wireless sensor networks, the localization methods can be divided into two kinds: Time of Arrival (TOA) and Time Difference of Arrival (TDOA) according to different time series parameters. TOA measurements give the distances between sources and sensors, and TDOA measurements give the differences among these distances. Thus, TOA-based or TDOA-based joint source and sensor localization can be understood as the estimation of source and sensor positions when noisy distances between sources and sensors or the differences among these distances are measured [654]. However, the performance of TOA and TDOA methods for source localization is affected by some conditions, including synchronization between the source and the sensors, stability of measured signal, as well as the ability of sensor networks to receive and process information [655–657]. Once these conditions are not established, the performance of source localization will be degraded. For instance, if the source and the sensors are asynchronous, the TOA measurement model has an unknown start transmission time in addition to the unknown source location. To solve this problem, the authors in [655] propose two different formulations to jointly estimate the start transmission time and the source location. Besides, resource-limited sensor networks with stringent power and communication bandwidth constraints also affect the performance of source localization. A novel channel-aware source localization method based on quantized asynchronous TOA measurements is proposed in [657] to save sensor energy and communication bandwidth in a resource-limited sensor network, where the quantization errors as well as the imperfect communication link between each sensor and the fusion center are considered.

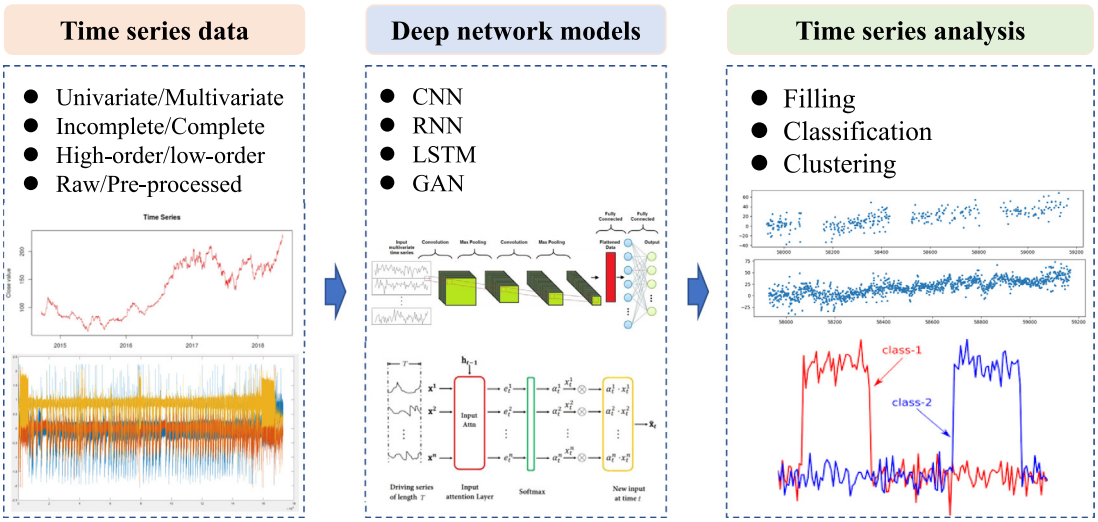

Fig. 45. Framework diagram for time series analysis [663,664].
Source: Adapted from [663,664].

4.4. AI driven time series analysis

Analyzing time series data and forecasting the future state of complex systems are among the most important research topics that analysts face in many fields, such as, in the financial field, to predict economic trends and plan policies of different institutions [658]; in social public opinion, to monitor the evolution of public opinion; in the climate field, to predict future weather changes and extreme events [659]; in biology, to understand and reveal the law of species interaction [660]; in medicine, to predict the spread of diseases and assess the risk of transmission [661]. As the scale of complex systems in practical applications continues to increase, the scale of collected time series data also continues to grow. This trend will make it difficult to guarantee the approximate performance of traditional time series data analysis methods [662]. At the same time, due to the continuous development of AI technology, its advantages in processing big data, achieving high precision and dealing with small sample data problem, AI technology has been gradually applied to time series analysis and forecasting tasks. Therefore, some research results using AI technology to realize time series analysis and forecasting will be summarized in this subsection.

4.4.1. Time series processing

Data-driven modeling of time series is a major topic in academic research and industrial applications, and is a key component in various fields such as climate modeling [665], patient monitoring, industrial maintenance, and decision-making-finance [666]. The two main components in time series analysis are processing and broadcasting, and these two components are usually performed in this order. Processing involves filling, classification and clustering the raw data, which are mainly overviewed in this subsection and depicted in Fig. 45.

Time series filling. The purpose of time series filling is to fill in missing data as accurately as possible, thereby eliminating the problem of unstable data characteristics caused by missing data. According to different prediction criteria, such as the interaction relationship in complex systems [667] and the characteristics of historical data series [668,669], various algorithms based on artificial intelligence (AI) technologies are designed to achieve missing data complementation.

The interaction between nodes in a complex network affects the evolution of each node, so it can be used as a basis for predicting the missing data of nodes. Inspired by the above ideas, a real-time filling method for time series based on GAN is proposed in [667]. This method first utilizes the Graph Embedding (GE) method to obtain the structure representation of the complex network, and then uses the interaction structure and historical data of the nodes in the complex network to generate the missing data through the GAN.

For some types of time series data, such as the time series state data of pipeline networks, the similarity of the same-level properties of the data features can also be used to recover incomplete time series data. Therefore, a three-network-based form of generative adversarial network (tnGAN) is proposed in [668] to deal with the incompleteness of pipeline network time-series data. The main component of the method is a bi-discriminative network architecture that can generate missing data by computing the similarity of latent features of samples, while facilitating the integration of existing information.

Most data imputation-based methods have limitations when a continuous amount of time series data is missing and training data is insufficient. Therefore, for the problem of lacking a continuous amount of data and insufficient training

data, a new sequence-to-sequence imputation model is proposed in [669], whose main components are the long short-term memory network and variable-length sliding window generation module. The long short-term memory networks can alleviate the reliance on large contiguous quantities of time-series data by leveraging past and future information at a given time. The variable-length sliding window generation algorithm can generate a large number of training samples to solve the difficulty of insufficient training data.

Time series classification. Different from traditional classification problems, time series classification needs to process data with time series characteristics, which means more information and brings stronger classification difficulties. Time series classification can provide a data basis for feature analysis to realize time series forecasting [670], and has been widely used in the fields such as medicine, sports, and economics.

For the time series classification problem, a new deep learning method is proposed in [671], which mainly consists of a convolutional neural network and a self-attention module. The method is applied to the task of satellite image time series classification, which not only improves in accuracy, but also significantly reduces processing time and memory requirements.

When the time series data to be classified is high-dimensional, multivariate and cross-domain, most deep learning-based methods can only effectively learn low-dimensional features in the single domain and lack the utilization of high-dimensional and cross-domain features. Therefore, a novel multivariate time series classification model incorporating an attention module is proposed in [672]. The model incorporates a random group permutation method for multi-layer convolutional networks, and can simultaneously learn low-dimensional and high-dimensional features in multiple domains from multivariate time series data.

Concerning the time series classification problem, there are few studies considering the existence of adversarial samples in time series data, and the adversarial samples are likely to damage the security of the model. To address the adversarial example problem, an adversarial transformation network-based time series classification model is proposed in [673]. This model utilizes the distillation model as a proxy to simulate the behavior of the classical time series classification model under attack, and utilizes a simple defense mechanism to reduce the proportion of successful adversarial examples, thereby improving the model against adversarial examples elasticity.

Time series clustering. Different from time series classification, time series clustering does not have predetermined category information in advance, and it is carried out completely according to the similarity between samples [674]. To describe the similarity between series, there are some popular measures, including Euclidean distance, short time series distance and minimum description length, which are usually utilized in AI based methods. Time series clustering is very important for the mining of time series features and the analysis of the evolution of complex systems.

The increasing scale of collected time series data in complex systems makes it difficult to guarantee the performance of traditional time series data analysis methods based on standard expert models. To avoid the reliance on standard expert models and enable cluster analysis of large-scale time series data, a framework based on deep scattering networks, Gaussian mixture models and unsupervised machine learning is presented in [675].

The above model and some mainstream methods all rely heavily on the assumption of data integrity, which is difficult to be guaranteed in practical applications. Aiming at the problem of incomplete large-scale time series data, a cluster representation learning (CRLI) method by jointly optimizing the imputation and clustering process is proposed in [676], which is different from the traditional time series data completion strategy. CRLI is able to impute more discriminative values for the clusters, making the learned representations having good clustering properties.

Similar to missing data, the missing labels of time series data can also cause data incompleteness and bring challenges to time series analysis. To address the problem of missing time series labels, an unsupervised saliency subsequence learning model (USL) is proposed in [677]. USL combines the advantages of saliency subsequence (shapelet) learning of time series, shapelet regularization, spectral analysis and pseudo-labeling, and iteratively solves by coordinate descent algorithm, which can better cluster unlabeled time series.

Different from the above methods, the temporal dynamics of time series, the interaction of feature extraction and clustering tasks are further considered in [678] to improve data analysis performance. A time series clustering framework named Self-Supervised Time Series Clustering Network (STCN) is proposed in [678]. In STCN, the RNN is used for one-step time series prediction, which is reconstructed as input data to capture the temporal dynamics and preserve the local structure of the time series.

4.4.2. Time series forecasting

Time series forecasting, which is a key research topic in the analysis of critical characteristics for complex systems, depicts the information dissemination characteristics and internal evolution laws among the components of the complex system. By mining the statistical characteristics and causal relationships contained in the historical data sampled from the complex system, time series forecasting can predict the future evolution trend of the complex system [662].

For the time series denoted by $\{z_1^{(i:T_i)} = \left(z_1^{(i)}, z_2^{(i)}, \ldots, z_{T_i}^{(i)}\right)\}_{i=1}^{M}$, where $z_t^{(i)}$ represents the value of the ith time series at time t. The goal of time series probability forecasting is to generate a set of probability distributions for future time series based on past time series data,

$$P = \left(z_{T_i+1:T_i+\eta}^{(i)} \mid z_{1:T_i}^{(i)}, \Phi\right),$$

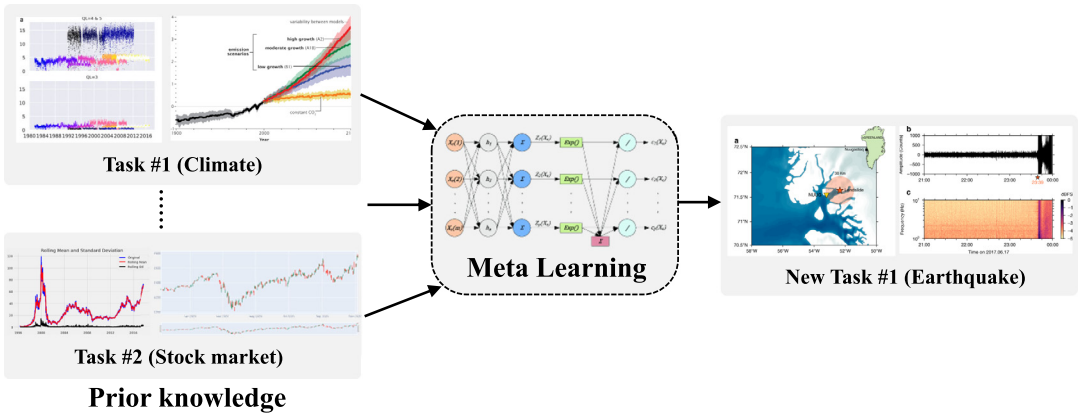

Fig. 46. Meta learning in time series forecasting.
Source: Adapted from [675,683].

where Φ represents a set of learnable parameters in the forecasting model, $z^{(i)}_{T_i+1:T_i+\eta}$ defines a future time series, and η represents the length of time for the forecasting.

Because the large-scale signal propagation process makes complex systems having various coupling mechanisms and evolution dynamics, and at the same time profoundly affects the critical properties of complex systems, time series forecasting is affected by signal propagation. Since deep learning has obvious advantages at the feature extraction level, it is widely used in time series prediction tasks. In this subsection, we focus on two mainstream approaches, graph convolutional neural networks and meta-learning, corresponding to regular forecasting tasks and few-shot prediction tasks, respectively.

Graph convolutional network. The statistical characteristics and evolution characteristics of large-scale complex systems contained in the sampled data are more diverse and complex. Thus traditional statistical analysis based methods cannot effectively process large-scale data to achieve good prediction results [662]. However, by incorporating custom architectural assumptions or inductive biases that reflect the nuances of the underlying dataset, GNN are able to learn complex data representations, so GNN based methods can also be used to predict time series.

For the prediction and early warning of tsunami, a time series prediction model based on convolutional neural network is proposed in [679], which can effectively mine the relationship between time series observation data and the tsunami waveform. Further considering the problem of highly nonlinear and complex dynamic spatiotemporal correlations in some practical applications such as traffic flow prediction, an attention-based spatiotemporal graph convolutional network model (ASTGCN) is proposed in [680]. ASTGCN is mainly composed of three independent modules, which perform feature analysis on three time attributes of time series. Each module consists of a spatiotemporal attention mechanism and a spatiotemporal convolutional layer. Aiming at the heterogeneity of time series data that cannot be solved by the above methods, a time series prediction model, called spatiotemporal synchronous graph convolutional network (STSGCN), is proposed in [681]. STSGCN contains multiple modules for different time intervals, which can effectively capture complex local spatiotemporal correlations and capture heterogeneity in local spatiotemporal graphs. Multivariate time series forecasting is a challenging problem because it needs to consider both intra-series temporal correlations and inter-series correlations. A multivariate time series forecasting model, called Spectral Temporal Graph Neural Network (StemGNN), is proposed in [682]. StemGNN further improves the accuracy of multivariate time series forecasting by jointly capturing inter-series correlations and time-dependent performance.

Meta learning. In many practical application scenarios, due to the difficulty of data collection and other reasons, the prediction of time series can only rely on extremely rare sample data. In addition, considering the diversity of tasks in practical complex system applications and the cost of model training, the transferability of prediction methods has also received extensive attention. Owing to the better generalization learning ability, meta-learning depicted in Fig. 46 is an effective method to deal with the above problems.

For the problem of small number of available samples, a meta-learning-based time series forecasting framework (N-BEATS) is proposed in [684]. The structure of N-BEATS is proved to conform to the basic training framework of meta-learning, which can realize time series forecasting for zero-sample univariate, and also shows the feasibility of deep learning in zero-sample time series forecasting.

In order to further mine the time series feature information in small sample data, a new meta-learning framework composed of convolutional neural network (CNN) and LSTM is proposed in [685], where LSTM is used for extracting the time series feature information in the small sample data. The method is currently applied to the problem of classification and prediction of brain states under anesthesia. Considering the influence of the spatiotemporal features of complex systems on the time series prediction problem, a spatiotemporal meta-learning prediction model is proposed in [686] to

jointly model the static spatial features of complex systems. The meta representation greatly improves the expressiveness of the model in a few cases.

Though the above-introduced techniques of AI driven time series analytics are extremely useful in their applications to real-world datasets, these techniques, akin to the most of the methods driven by AI frameworks, need further physical interpretations and mathematical demonstrations. Utilization of physical or/and mathematical principles to achieving time series analytics has many advantages including small-sampling-data and lower-resource-consumption. These advances can be found in a series of recent works [687–689].

5. Applications

As reported in previous sections, signal propagation has become a commonly used metric to discern the spatio-temporal process of collective behavior in complex networks. There are two different approaches to study signal propagation, one is modeling-driven (see Sections 2 and 3) and the other is data-driven (see Section 4). In this section, we review some applications in different fields, such as epidemic, social dynamics, neuroscience, power grids and robot swarms.

5.1. Epidemic

5.1.1. Agent-based models

Two decades ago, a stochastic influenza simulation model (agent-based/ABM) was used for rural Southeast Asia [50] to study the efficacy of targeted antiviral prophylaxis and pre-vaccination strategy to contain the influenza strain (Highly pathogenic avian influenza A (subtype H5N1)) at the source. The Thai census data of 2000 were used to measure the population's age structure and household size distribution. A mixing of groups is constructed based on a network study of the Nang Rong District in rural Thailand [690]. Marta Luisa et al. studied the Influenza pandemic in Italy [74]. Here SEIR dynamics on a global scale are coupled with the individual-based modeling (ABM) on a local (municipality level) scale. Under different R_0 values, the impact of pre-pandemic and pandemic vaccines, social distancing, air-travel restrictions, and age effects among cohorts have been studied. The socio-demographic structure of the Italian population is used to characterize the contact networks among individuals [81]. Viral endemic diseases like hepatitis A are studied in affected areas of Italy through an ABM approach incorporating individuals' death, birth, and careers of individuals [76]. Using the contact networks of Italy [81] the epidemic transmission model is developed. Direct and indirect transmission (due to the ingestion of contaminated seafood) and mobility to high endemicity areas are considered to study the propagation of such infections. An age-structured, socio-demographic heterogeneous ABM is used to study the transmission of tuberculosis (TB) infection in low-burden settings [82], in Arkansas covering 1% population of USA. In contrast to the ODE mode, which overestimates the reinfection, the heterogeneous ABM closely predicts the reactivated cases. The maximum impact of household contact tracing for TB in a moderate-burden setting [691] is further investigated. A spatial ABM is developed to study the EBOLA transmission in Liberia [692]. It is estimated that almost 38% of infections emerged from hospitals, and 10% were acquired from funerals. Safe burials and proper distribution of household protection kits are suggestible measures for the containment of EBOLA infections. A ten-week projection from December 21, 2014, is done using ABMS in Liberia and Sierra Leone [693]. In another ABM setup, the spreading of cholera in the Dadaab refugee camp in Kenya is studied [694]. The individual agent represents each refugee as a myopic agent who cannot differentiate between clean and contaminated water and thus becomes exposed to cholera infection. Here ABM shows that cholera grows radially from the source (contaminated water), and environmental effects such as seasonal rain can reemerge the disease. It is further used to develop multi-agent simulation (MAS) for vector-borne disease (malaria) [84] at Camargue in southern France. Here movements of humans as well as mosquito movements, and temporal and spatial fluctuations in the rate of actual human biting (ABR) are also taken into account. Recently, Aleta et al. [695] have collected real-time mobility data from New York and Seattle metropolitan areas from February 2020 to June 2020. Based on the collection of interaction in different layers (schools, workplaces, etc.), a synthetic population is constructed for each area, and agent-based simulation (incorporating the stochastic epidemic model) is performed on the time-dependent contact networks to capture the transmission of SARS-CoV-2. Only 18% of individuals are estimated as responsible for most of the infections. They have also examined the probability of the emergence of super spreading events (SSE) by observing the number of infections produced by each person in each place. Recently, to ascertain whether the sequencing can identify the problematic connections among the populations in Australia, an agent-based simulation is compared with real-time genome sequencing of SARS-CoV-2 in a subgroup of infected patients during the first ten weeks of COVID-19 [696].

Intervention strategy using ABMs. To combat sexually transmitted diseases, pairwise-approximation methods on ABMS are developed to study the impact of contact tracing [697]. This is essential for heterogeneous networks containing core groups or super-spreaders to eradicate the disease. Smallpox transmission and control in Great Britain is investigated through individual-based stochastic modeling. Contact tracing with vaccination and isolation can vastly reduce the ongoing epidemics [698]. Several Non-pharmaceutical interventions (NPI: quarantine, symptom monitoring, contact tracing etc.) for containing infectious disease outbreaks, including Ebola, SARS, smallpox, and influenza strains with pandemic potential, have been compared by using agent-based branching model [19] through a susceptible–exposed–infectious–recovered disease process. The number of secondary infections is extracted from the negative binomial

distribution with the mean equal to the product of the reproduction number and relative infectiousness, which follows a triangular distribution. Simulation confirms that quarantine is less beneficial than symptom monitoring for EBOLA and SARS but works well for smallpox. To replicate the environment and malaria transmission activities in a made-up, remote African hamlet, a spatial individual-based model has been developed, where long-lasting insecticidal nets and outdoor attractive toxic sugar bait were installed for indoor and outdoor intervention strategy [699]. For influenza spreading, the impact of school holidays is studied in Belgium. An agent-based stochastic metapopulation model is developed [700], and it has been observed that holidays may delay the infection peak of seasonal influenza. This ABM approach is further used to control the COVID-19 pandemic by using the isolation scheme and contact tracing [701]. The simulation confirms that If the reproduction number is around 1.5, for different numbers of initial infections, the disease can be controlled if 50% contact tracing is possible. In contrast, for $R_0 \sim 2.5$, the contact tracing percentage should be increased to 70%. The same method is used to investigate the effectiveness of facemasks in combination with a lock-down [702]. The observations suggest that a continuous use of facemasks in public places can flatten the secondary and tertiary waves. For a review of the modeling and effectiveness of facemasks, one can look into [703]. Another agent-based (publicly available) model was developed a decade ago to study the influenza epidemic in the USA. It incorporates mobility and different social contact rates [704]. This simulation is further used to study the SARS-CoV-2 in Singapore [705], where a combined intervention strategy including social distancing, isolation, and school closure is advised to reduce the number of infected individuals. During the SARS-CoV-2 pandemic, Aleta et al. have provided a sophisticated agent-based simulator for investigating the role of multiple intervention strategies on transmission in the area of Boston [441]. The intervention strategies include contact tracing, strict social distancing, and large-scale testing. A combined effect of all of them can keep the disease under control. Aleta et al. [695] have further investigated the impact of NPIs encoded in the mobility data to study the transmission of SARS-CoV-2. They have hypothetically shown that a one-week delay in the implementation of the NPI can have doubled the peak of the death tolls in New York and Seattle. The height of the death toll could be reduced by a factor of 3 if the NPI strategies were implemented one week before. Another ABM approach encoding different intervention strategies (air-travel restrictions, isolation, school closures etc.) is also used to understand the transmission and control of the COVID-19 pandemic in Australia (AMTraC-19) [706]. The authors suggest that a combined effect of home isolation, travel restriction and a moderate level of social distancing can reduce the severity of the disease. Regarding school closure, an agent-based simulation suggests that repeated screening of students using antigen tests can reduce the severity of the COVID-19 burden [707]. For further review on the application of ABM, see [708].

5.1.2. Metapopulation models

A stochastic spatial metapopulation dynamics on rat dynamics is developed to understand emerging and remerging bubonic pleague [709]. A five-dimensional model describing the dynamics of rats is encoded into a 25 subpopulation of a square lattice, and random movement of fleas and rats is considered. The model predicts that a small rodent population can persist in the disease. The impact of the movement of workers from one ward to another and the permanent movement of cattle from one farm to another is investigated for infection dynamics, and it has been established that the commuters who create the network links may have a significant impact on the infection spreading [710]. This metapopulation formalism was used to infer the spatiotemporal spread of dengue cases reported in Santiago de Cali (Colombia) during 2015–2016 [711]. Also, an age-stratified mobility-based metapopulation (Markov chain based) is developed, and the spatiotemporal pattern of COVID-19 in Spain is successfully verified [57]. The model can capture the time-dependent adequate reproduction number. People's bidirectional movement that does not require tracking every individual separately or several compartments is encoded in a metapopulation network for the city map of Israel [712] and successfully used to track the infection trend.

Intervention strategy. This type of modeling using metapopulation networks can be applied to implementing suitable intervention strategies. Such as it can be used as a prevalence indicator that can rearrange the patches according to their infection risks. Recently this framework has been used to predict SARS-CoV-2 in the United States [713]. Exploiting this MMCA approach, the authors provide an optimal control strategy, where the vulnerable cities are identified and flow entering those cities is advised to be restricted. However, the usual mobility pattern inside the city can be continued. A spatial metapopulation patch model is developed to mitigate the smallpox outbreak [714]. Here the six compartments are provided; susceptible (S), latent (E_U), prodromal (P_U), symptomatic (I), recovered (R) and dead (D). Intervention starts when the I crosses the baseline. In the deterministic multi-dimensional dynamical setup, the transmission term depends on the mobility of susceptible and symptomatic individuals from one district to another. Against this backdrop, the authors suggest that mass vaccines should be targeted in highly infected districts for higher reproduction numbers. A test-kit based intervention strategy was recently developed to study the reduction of final outbreak size in a metapopulation network of a five compartmental model: susceptible (S), exposed (E), infected (I), hospitalized (H), and recovered (R) [715]. The investigation confirms that test kits should be applied to nodes with a higher degree or higher node betweenness. A metapopulation setup is used to detect the suitable patches for applying optimal intervention strategy for vector-borne disease (dengue) in Kolkata [716]. Note that an efficient calculation of arrival time is also possible if someone assumes the exportation of the infectious population between two patches follows a homogeneous Poisson process and a small fraction moves when the disease prevalence is still growing. In this setup, Wang et al. [717] develops a framework based on a stochastic process that captures the arrival time for the 2014 Ebola Epidemic and 2009 influenza pandemic.

GLEaM Model. Based on a Monte Carlo Maximum Likelihood analysis, the GLEaM simulator is successfully used to predict the early phase of the 2009 H1N1 pandemic [40,56]. The peak timing of the pandemic is also estimated and

validated with real data. The integration of a multiscale structure to the epidemic model can be used as a test-bed for Influenza-like pandemic diseases, and the spread of the disease (the peak and the peak time) can be well captured if the initial infection strength, onset zone, and the multiscale network structures are provided. The same tools are also used to understand the propagation of mosquito-borne epidemics. In particular, propagation of the ZIKA virus (ZIKV) is analyzed in the Americas [718]. GLEaM model is further used for an ensemble forecast of the EBOLA virus transmission in WEST Africa [719]. The structure of Global mobility through air transportation networks also enabled the prediction of the infection spread on a global scale. Each subpopulation follows a SEIR compartmental dynamics, where the chain of binomial or multinomial processes determines the transition from one compartment to the other ones. Recently, the GLEaM has been used to demonstrate a mechanistic understanding of SARS-temporal CoV-2's pattern, the onset of local transmission in Europe, and the early dissemination of infection in the United States [720]. According to the model, the community transmission of SARS-CoV-2 was evident (by early March) in many parts of Europe and the USA, and only about 4% of the original data. Note that GLEaM ignores the differential transmissibility across age structures and does not encompass the pre-symptomatic transmission, which may affect the future prediction of infection fatality rate [721]. Deep spatiotemporal forecasting uncertainty is now being explored from frequentist, and Bayesian viewpoints [722]. To train the DeepGLEAM model, a residual is calculated between the reported mortality in the USA and the related GLEAM forecasts. As a general rule, Bayesian approaches are more reliable at predicting the mean, while frequentist methods are better at assess the variability.

Intervention strategy. Using the same approach, the role of travel restrictions during the early propagation of COVID-19 in mainland China has been studied [723]. On a local scale, the ground mobility data of 30 countries are extracted from the statistics office (Baidu location-based services (LBS) for China). The Official Aviation Guide (OAG) and International Air Transport Association(IATA) databases (updated in 2019) were used for mobility on a global scale. To reflect the trend of COVID-19 transmission from human to human within each node, compartmental modeling, including the following states: susceptible, latent, infectious, and removed, is considered. The model predicts that the Wuhan travel ban will at first decrease the number of cases reported from overseas but that after two to three weeks, the number of infections outside mainland China will increase. The model also demonstrates that stricter travel restrictions (up to 90% of traffic) have minimal effect unless combined with public health initiatives that can slow the spread of diseases, such as early detection, isolation, and public awareness campaigns.

5.2. Social dynamics

Although many applications of signal propagation in complex networks to social dynamics are covered well in recent [724] and somewhat less recent reviews [725–727], we here nevertheless review the most recent advances for completeness and comprehensiveness of this review. In what follows, we will touch upon opinion dynamics, human cooperation, and related models of social dynamics.

5.2.1. Opinion formation

Models of opinion dynamics were amongst the very first to form the basis of what is today sociophysics or social physics, and where social dynamics thus comes into play. Already in 1971, Weidlich was the first physicist to design an opinion dynamics model [728]. A good decade later, Galam et al. [729] introduced the Ising model as suitable for studying opinion dynamics, specifically by considering spin–spin coupling to represent pairwise interactions between agents, a magnetic field to represent cultural majority or propaganda, and individual fields to represent personal preferences towards one or the other option [730]. Yet another good decade later, the Sznajd model was developed under the premise that changing the opinion of somebody is easier if two or more people already adopt the new opinion than if just a single person does so [731]. A popular review of these advances is due to Hegselmann and Krause [732].

It is now another good two decades later, and opinion dynamics is still a vibrant and relevant field of research, with many recent publications building upon past seminal advances [724,733]. For example, a model-based opinion dynamics approach has recently been used to tackle vaccine hesitancy. Uncovering the mechanisms underlying the diffusion of vaccine hesitancy is crucial in fighting epidemic spreading [734], and research done by Ancona et al. [735] has shown that treating vaccine hesitancy as an opinion that may diffuse in a social group can provide important new insights. A mathematical model was ultimately proposed that, when calibrated with survey data, was able to predict the modification of the pre-existing willingness of individuals to vaccinate, as well as to estimate the fraction of a population that is expected to adhere to an immunization program.

From a more theoretical perspective, Hickok et al. [736] have upgraded the bounded-confidence model of opinion dynamics to hypergraphs, where a link no longer connects just a pair of nodes but can also connect more individuals at once. This is an important advance in line with recent research trends which are revealing that a paradigm shift in the way we model human interactions in groups is necessary and indeed urgent. Thus the birth of higher-order social networks, where a single link can connect more than two people. Although a simple change in principle, research across the board shows that this has important implications for better understanding collective human behavior, from opinion formation to cooperation to vaccination and climate inaction [15,737]. Research by Hickok et al. [736], for example, and in line with this reasoning, shows that a hypergraph bounded-confidence model converges to consensus for a wide range of initial conditions for the opinions of the nodes, including for nonuniform and asymmetric initial opinion distributions. Moreover,

under suitable conditions, echo chambers can form on hypergraphs with community structure, and the opinions of nodes can sometimes jump from one opinion cluster to another in a single time step – a phenomenon called "opinion jumping" by the authors. Several of these results are not possible in standard dyadic bounded-confidence models, thus underlining the need to consider higher-order interactions separately and in depth when studying opinion dynamics in groups.

Another important, and fairly recent, application of opinion dynamics models is to determine how misinformation and fake news affect our values and decision making [738,739]. To that goal, Guo et al. [740] have proposed a game theoretic approach that can discern the effects of disinformation propagation on opinion dynamics. In particular, an opinion framework was formulated where repeated, incomplete information games model the subjective opinions of online social network users. Research has shown how a subjective logic model – a belief model explicitly handling opinion uncertainty – can be employed to uncover deception strategies, opinion updates, and the influences of misinformation through the network.

As the above short overview of very recent research shows, opinion dynamics continues to pique the interest of the complex network and complexity science communities, and it continues to find innovative applications and theoretical upgrades to remain relevant to a broad range of research fields, ranging from epidemiology to physics.

5.2.2. Human cooperation

Comprehensive cooperation among unrelated individuals is almost unique to humans. Although ants and bees and some species of bird and fish cooperate as well, the depth of our cooperation is unrivaled. Indeed, the argument has often times been made that the very essence of our evolutionary success is due to our unparalleled other-regarding abilities [741]. Since cooperation is deeply rooted in collective behavior across social networks, methods of physics and network science have, in the past two decades, evolved to play an important role in helping us to better understand the evolution of cooperation and its upkeeping in the face of natural selection and selfishness.

Monte Carlo methods and the theory of collective behavior of interacting particles near phase transition points, in particular, have proven to be very valuable for understanding counterintuitive evolutionary outcomes. By studying models of human cooperation as classical spin models, a physicist can draw on familiar settings from statistical physics. However, unlike pairwise interactions among particles that typically govern solid-state physics systems, interactions among humans often involve group interactions, and they also involve a larger number of possible states even for the most simplified description of reality. The complexity of solutions therefore often surpasses that observed in physical systems. This has been reviewed and emphasized already in 2017 by Perc et al. [742], but since then a number of noteworthy developments and progress have been made.

Similarly as by opinion dynamics, for human cooperation too higher-order networks have been considered in [743]. Since we live and cooperate in networks, it was noted that since links in networks only allow for pairwise interactions, the framework is suitable only for dyadic games, but not for games that are played in groups of more than two players. To remedy this, Alvarez-Rodriguez et al. [743] have introduced higher-order interactions to a public goods, first on a uniform hypergraph, showing that it corresponds to the replicator dynamics in the well-mixed limit, and thus providing an exact theoretical foundation to study cooperation in networked groups. The analysis was then extended also to heterogeneous hypergraphs that describe interactions of groups of different sizes, and the evolution of cooperation in such cases was studied as well. This new framework has been applied to study the nature of group dynamics in real systems, showing how to extract the actual dependence of the synergy factor on the size of a group from data on large communities of international collaborations.

Others have also considered higher-order interactions and the evolution of cooperation. In particular, Burgio et al. [744] have studied the evolution of cooperation in the presence of higher-order interactions, showing that, likewise to network reciprocity, group interactions also promote cooperation. More importantly, by means of an invasion analysis in which the conditions for a strategy to survive were studied, they have shown how, in heterogeneously-structured populations, reciprocity among players is expected to grow with the increasing of the order of the interactions. This was noted to be due to the heterogeneity of connections, especially the presence of individuals standing out as hubs in the population.

Another important recent development concerns the broadening of the scope of human cooperation to other forms of moral behavior, which include, for example, altruism, truth-telling, altruistic punishment, and trustworthiness [745]. One-shot anonymous unselfishness in economic games has commonly been explained by social preferences, which assume that people care about the monetary payoffs of others. However, during the last ten years, research has shown that different types of unselfish behavior are in fact better explained by preferences for following one's own personal norms — internal standards about what is right or wrong in a given situation. Beyond better organizing various forms of unselfish behavior, this moral preference hypothesis has recently also been used to increase charitable donations, simply by means of interventions that make the morality of an action salient. Experimental and theoretical work dedicated to this rapidly growing field of research has been recently reviewed in [745], where also mathematical foundations for moral preferences that can be used in future models to better understand selfless human actions and to adjust policies accordingly have been described. Moreover, it was noted that these foundations could also be used by artificial intelligence to better navigate the complex landscape of human morality.

Taken together, the propagation of cooperation in complex networks continues to play an important role for better understanding this crucial and fascinating aspect of our biology, and especially the interplay of higher-order interactions and models beyond social dilemmas and the public goods game constitutes promising ground for future research based on recent-most advances.

5.2.3. Other models

The scope of social dynamics is increasing continuously since the inception of the field, with new models being proposed and existing models modified at a significant pace. Indeed, an overview of the majority of these models certainly requires a specifically dedicated review that goes beyond signal propagation in complex networks, and indeed such a review has recently been published [724]. Nonetheless, we note notable recent advances that concern social dynamics for the sake of completeness.

An interesting model was recently proposed and studied by Giambiagi Ferrari et al. [746], who have coupled epidemiological models with social dynamics, in particular the susceptible–infectious–susceptible model with a continuous opinion dynamics model. A two dimensional set of ordinary differential equations describing the dynamic of the proportion of the number of infected individuals and the mean value of the effort parameter have been derived based on simple rules to model the propagation of behaviors that affect the dynamics of the disease.

Social dynamics modeling has recently also been used to study overtourism. Antoci et al. [747] have written a paper beautifully titled "Preying on beauty? The complex social dynamics of overtourism", where a simple mathematical model that analyzes the dynamics of the populations of residents and tourists when there is competition for the access to local services and resources has been introduced. Since the needs of the two mentioned populations are partly mutually incompatible, research has focused to determine under what conditions a stable equilibrium between residents and tourists can exist, and what are the conditions for tourists to take over the city and to expel residents. Akin to many models of social dynamics, Antoci et al. [747] have also found that even small changes in key parameters may bring about very different outcomes, and they have concluded that policymakers should thus be aware that a sound knowledge of the structural properties of the dynamics is important when taking measures to avoid unintended consequence and counterproductive actions.

Determinants of sustainable tourism have also been studied by means of an asymmetric game with mobility by Chica et al. [748], where local stakeholders and tourists can either cooperate or defect in a spatially structured setting, the point being that sustainable tourism is primarily determined by an optimal tradeoff between economic benefits of the stakeholders and their costs related to the application of sustainability policies. In agreement with observations worldwide, research has identified decreasing population densities in tourist areas in terms of both, stakeholders and tourists, to be a key aid to greater cooperation and overall sustainability of tourism.

Another recent application area of social dynamics has been the study of diffusion of neologisms – newly coined words or expressions (see e.g. [749]) – over social networks. Würschinger [750], in his aptly titled paper "Social Networks of Lexical Innovation" has investigated the social dynamics of diffusion of neologisms on Twitter, in particular a longitudinal study of the spread of 99 English neologisms to study their degrees and pathways of diffusion. Since previous work on lexical innovation has almost exclusively relied on usage frequency for investigating the spread of new words, Würschinger has used frequency-based measures to study temporal aspects of diffusion and network analyses for a more detailed and accurate investigation of the sociolinguistic dynamics of diffusion. Research has revealed that frequency counts can serve as an approximate indicator for overall degrees of diffusion, yet they might miss important information about the temporal usage profiles of lexical innovations. In particular, neologisms with similar total frequency can exhibit significantly different degrees of diffusion, and analyzing these differences in their temporal dynamics of use with regard to their age, trends in usage intensity, and volatility contributes to a more accurate account of their diffusion. The inclusion of temporal and social information has thus been deemed of particular importance for the study of lexical innovation since neologisms exhibit high degrees of temporal volatility and social indexicality [750].

From epidemiology of a tourism to sociolinguistic research, the applications of signal propagation in complex networks to topics related to social dynamics are indeed vast, and only time will tell what the future holds. For certain, the prospects for innovative applications only increase, not least with the rapidly expanding application of artificial intelligence and data collection that already now pervade virtually all facets of our social being.

5.3. Neuroscience

Anatomical connectivity stays relatively stable in a matured brain, while the functional dynamic patterns vary significantly to enable adaptive behaviors [751,752]. Generating flexible neural functions from dynamic signal propagation is the key to the emergence of human intelligence. In the past decade, with the rapidly improved large-scale neural recording techniques, neural signal propagation has been described deeply from both spatial and temporal axes [753–755]. Extracting the principles underlying spatial–temporal propagation could pave the path to understanding the brain and developing tools for curing cognitive disorders.

5.3.1. Circuit neuroscience

Spatially, nodes in the neural network are studied at multiple levels, ranging from the microscale level of single neurons to the macroscale level of brain areas that compose massive neurons. Circuit neuroscience becomes critical due to its mesoscale aspect, filling the gap between micro- and macro-dynamics. Circuit neuroscience focuses on characterizing signal propagation between pairs of neurons within or across brain regions; in other words, the aim is to identify edges with local or long-range connections. The direct propagation between local and remote pairs of neurons is considered as building blocks for the mechanistic understanding of the emergence of brain functions [756–758].

Both correlation and causality approaches are used for characterizing neural circuits. High-density electrodes record action potential from groups of neurons in local brain regions and provide the opportunity to infer directional connections between neuron-pairs [759]. Cross-correlograms (CCG) enable us to identify neuronal pairs [760]. Within a short latency, sharp peaks or troughs in the CCG are used to infer monosynaptic excitatory or inhibitory connections between neurons. Statistics are performed on CCG from the original dataset and surrogate datasets to determine the significance of activity correlation between connected neurons from randomly correlated activities. Surrogate datasets can be generated from 'jittered' spike trains, meaning the timing of each spike was shifted randomly and independently within a uniform interval [761]. From a large number of cell pairs (62,408), 55% and 24% of pairs were characterized as excitatory (peaks) and inhibitory (troughs) connections. Transmission efficacy has been defined as the increased probability of firing at short latencies between the pre-and post-synaptic neurons [760].

Causal evidence of a monosynaptic connection is vital for characterizing direct signal propagations. Three technical advances complementarily measure the direct connectivity for circuit neuroscience: functional perturbation tools, anatomical tracing techniques, and genetic approach. (i) Functional perturbations control individual edges without disturbing the state of the rest edges from the network. For example, optogenetic activation/inhibition can specifically activate/inhibit synapses between two neurons [762]. Suppose an optogenetic activation on a single neuron triggers a reliable neural signal in another neuron, with minimum power of light and within a short latency. In that case, we consider the propagation is mediated through a direct synaptic connection (monosynaptic) rather than indirectly through multiple layers of relays in the network (polysynaptic). (ii) Anatomical tracing aims to send probes (usually molecules showing fluorescent signals) from one cell to the other across synapses; thus, detecting probes in the second cell indicates an anatomical connection between them [763]. Perturbation and tracing results provide complementary evidence from functional and anatomical aspects and identify edges between nodes. (iii) The genetic approach targets specific nodes – certain types of neurons or synapses – and allows specific expression of tools for the perturbation and tracing in those nodes [764,765].

Three approaches jointly reveal direct information flow from one node to the other. From a reductionist perspective, these direct propagations could be the key to the emergence of elementary functions at the behavioral and cognitive levels. Ideally, these perturbation experiments can answer two critical questions: (1) if a directed or an undirected connection exists between two neurons; (2) how the signal arising from a single node propagates in the entire network and impacts behavioral functions. However, the second aim is still hardly achievable, because the activity of all the nodes cannot be monitored simultaneously, and the framework for large-scale analysis is still lacking. Integrating biological data with large-scale recording and mathematic analysis methods from the complex system will be essential to dissect brain-wide propagation patterns and the underlying mechanisms.

5.3.2. Propagation directions: Bottom-up, top-down

The directional edges connect the nodes and form a functional brain. The edges start from a single or a group of presynaptic neurons and point to the downstream postsynaptic neurons. The neural signal propagates among brain regions through a hierarchical network structure defined by different aspects. For example, sensory- and motor-related brain regions can be considered as early and late stages of information processing, respectively (Fig. 47) [22,766]. At the same time, sensory representation and decision-making areas can be regarded as lower and higher functional centers. An influential framework of directional propagations is based on the categories: bottom-up and top-down, which are proposed and applied in characterizing the information flow and their corresponding brain functions [767–769].

The visual information flow well demonstrates a bottom-up signal propagation among different brain regions [768]. It enters the nervous system through the retina. Within the retina, an up-to-ten-layered neural network starts from photoreceptor cells and reaches retina ganglion cells (RGC). In this local propagation, light information is translated into voltage changes in photoreceptor cells and leaves the retina as electrical pulses in RGC axons, which directly deliver the visual signal to the brain [770]. In mammals, this RGC-conveyed information reaches the relayed structures, LGN, and superior colliculus and then enters the neocortex regions [771]. In the neocortex, visual information propagates in two main streams: the dorsal and ventral pathways, characterized as the 'where' and 'what' pathways [772,773]. The dorsal stream flows along the neocortex of V1-V2-DM (dorsalmedial area) - MT (medial temporal area) - posterior parietal cortex and sequentially processes visually-guided-action-related information. The ventral stream flows from V1-V2-V4-IT (inferior temporal cortex) and processes object-related information.

This bottom-up visual pathway exemplifies a hierarchical and parallelly processing structure for processing information. In the meantime, top-down propagation streams along the same pathway and provides an opposite direction of information flow for the feedback control [769]. The following question is how the bottom-up and top-down propagation coordinate or compete, e.g., whether the flow direction changes when the two information streams collide.

Brain functions, such as memory or decision-making, emerge from broadly distributed brain regions rather than compartmentalized functions from isolated areas and require the co-existing of both directional propagations. Datasets with single-cell resolution and whole-brain coverage will be necessary to characterize this brain function-related signal propagation framework. In the past ten years, large-scale neural recordings have initiated a journey that integrates experimental with analysis approaches and establishes a brain-wide framework to unify the pieces of knowledge of various brain functions. In decision-making, which integrates sensory perception, task recognition, and motor generation functions, both bottom-up and top-down propagations occur during a single decision-making process [768]. From the bottom-up direction, sensory information flows feed-forwardly from MT and V4, two visual cortex regions, to LIP, IT, FEF,

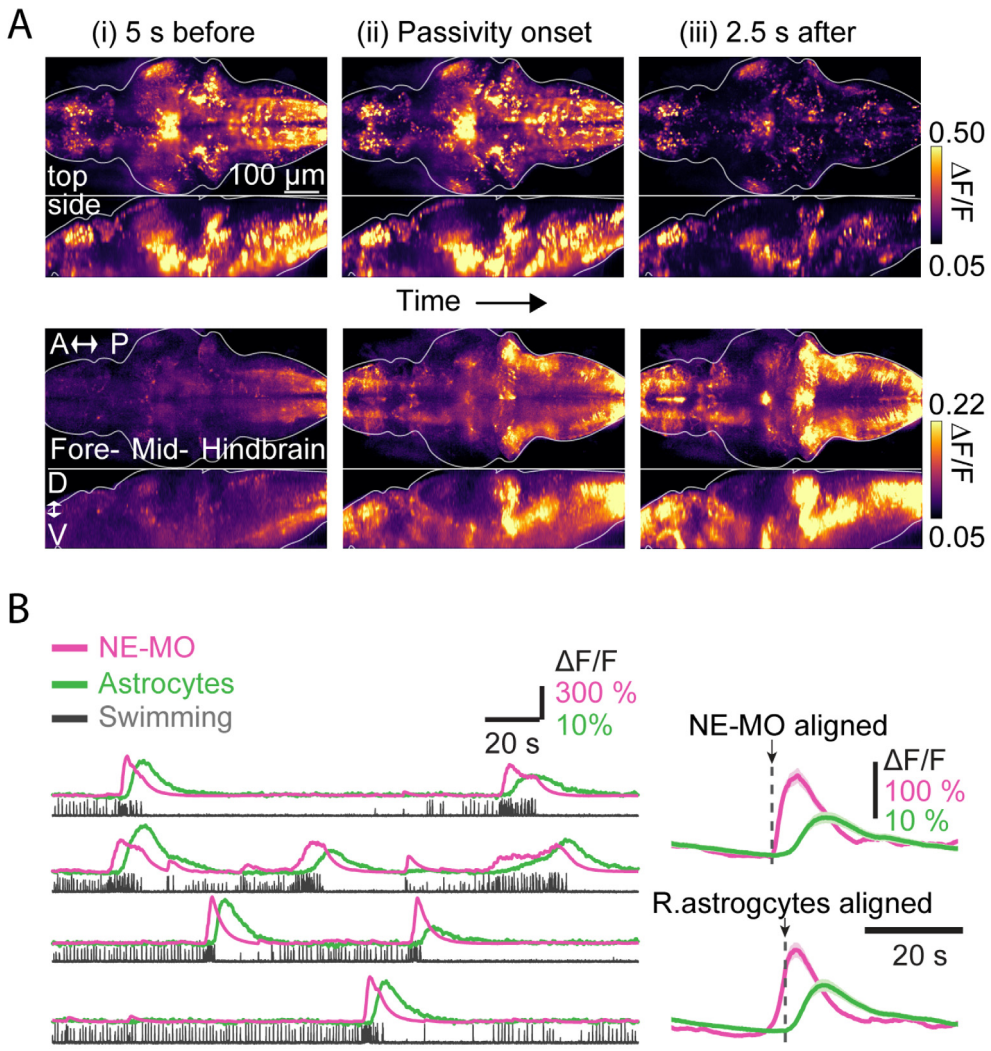

Fig. 47. Brain-wide sensorimotor transformation in zebrafish. Top, whole-brain activity propagation in all neurons and astrocytes. Bottom, sequential activation of the norepinephrine cluster of the medulla oblongata (NE-MO) and astrocytes, leading to the behavioral state switch to passivity.
Source: Adapted from [766].

and PFC, regions involved in the decision, motor, and cognitive functions. Simultaneously, task information, evoked from a memory system, exhibits both directional propagations: at an early phase, bottom-up propagation starts from V4 and IT and reaches PFC and LIP, and at a later step, top-down flow of sustained information flow from PFC and LIP to FEF and visual cortex, indicating that the task information modulates both sensory processing stage and motor generation stage. Lastly, choice signals show top-down propagation from PFC and LIP to FEF and the visual cortex.

5.3.3. Propagation in time: Sequential activation

Temporally, the propagation generates a sustained and evolving neural signal. Sequential and recurrent activation of chains of neural nodes supported such sustained propagation. Two critical neural functions emerge from the chain-structured propagations — the sequence of movements and the maintenance of information.

Sequential motor acts refer to organized behaviors with structures on time, ranging from continuous limb movements to speech or music. Birdsong is a model system to study how the brain generates temporally structured neural activity and sequential behaviors. A birdsong is composed of a 0.5–1.0-s motif, which contains multiple 100 ms syllables. Each motif's different syllables are organized in a fixed order and produced sequentially [774]. Hierarchically, signal propagation is proposed to generate both the sequence of syllables and their corresponding sequential neural activities [775]. Electrophysiological recording and calcium imaging show chain-like firings in the premotor region HVC and propagated to motor cortical structure RA (robust nucleus of the arcopallium) [776]. Perturbation experiments by cooling the HVC – slower signal propagation in a lower-temperature network – slow down the song, which contains prolonged syllables

and enlarges the intervals between syllables. But cooling in the RA cannot change the timing of the song, indicating that the activity sequence in HVC determines the temporal sequence but not in RA [774].

Another model system is the sequential limb movements which generate locomotion. The rhythmic alternation of right-left and flexor–extensor movements is believed to originate from a push-pull motif [777]. However, a recent study showed that rotational neural dynamics could cause alternating movements. In a rotational neural space, activities cycled through all phases. Based on this observation, a state called balanced sequence generator (BSG) was proposed for modeling the movement output. In the BSG model, a subset of neurons was connected based on their phase in the dominant eigenmode and generated sequential activity for movements. Flexible movements with speed regulation, force control, and multiple functions emerge from BSG [778].

Sequential propagation can preserve information and form memory, and an influential theory of 'cell assembly sequences' has been proposed to implement such propagation [751,779,780]. There are three key components: the nodes are the 'cell assemblies' composed of strongly interconnected neurons, the edges are the connections between different cell assemblies, and the propagation refers to the activity transition between assemblies with specific probabilities. In this theory, each transition only activates one downstream node, and each node can be activated multiple times in the sequence (recurring transitions). During a memory task, in the hippocampus, assembly sequences are detected to be correlated with the task-related sensory information, and essential for memory [760,781,782]. This sequential propagation can be regulated by two factors facilitating the transmission efficacy, the firing pattern and the coincident firing of pre-synaptic neurons [760].

Modeling studies suggest that neural plasticity could be the neural mechanism to generate and modify the sequential propagation in both the sequential movement and the memory maintenance [780,783]. A popular model proposes that pre-wired feedforward/asymmetric connections support sequential propagation. Novel sequential propagation is gradually developed through training. When conditioning the visual cortex with sequential sensory stimulation – a bright spot continuously and repeatedly moving along the same trajectory – the neural ensemble responding to the stimulus forms a sequential propagation pattern [784]. After the conditioning, activation at the 'start' node of the sequence can sufficiently trigger the propagation towards the 'end' node. This conditioning process is hypothesized to be mediated by spike timing-dependent plasticity (STDP). Training-induced sequential propagation disappears when blocking the NMDA receptor, which is essential for STDP. The STDP rule bi-directionally modifies the strength of the synapses between cells within the ensemble. It generates the feedforward/asymmetric connections: strengthening those edges following and weakening the ones against the conditioning direction. In both experimental and computational studies, this model has been applied in other systems displaying sequential propagation [783,785–787]. Unlike regulating the majority of synapses of the ensemble and changing the feedforward connection, other models propose that altering a small fraction of synapses is enough to generate sequential propagation. For example, cooperation of recurrent synaptic interaction and external input in randomly connected neurons can efficiently generate sequential propagations, showing that input-dependent and non-interfering propagation sequences can emerge from the unstructured network architectures [788].

5.4. Power grids

As one of the most critical infrastructures, power grids are essential for economy and people's daily life. Requirements for stable power supply increase with the increase of the growing dependency on, e.g., society. However, the stability-analysis complexity lies not only in the internal transmission between power plants, but also in unpredictable external factors like extreme weather and renewable energy sources. Perturbations may cause redistribution of power, system desynchronization, or even blackout. Much research has been devoted to the analysis of stability against perturbations by means of statistical physics, nonlinear dynamics and network science. Here, we focus on recent progress in dynamical and structural perturbations to the power grids with alternating current (AC): (1) dynamical perturbations referring to adjusting the parameters in the system (10) or additional noises as fluctuations, and (2) structural perturbations referring to the alteration of the underlying connectivity network.

In an AC power network, each generator $i = 1, 2, \ldots, N$ has the voltage $V_i = |V_i|e^{i\theta_i}$ with phase θ_i and magnitude $|V_i|$, and the effective input ω_i. During the transmission between each pair of connected generators i and j, maximum power $\lambda_{ij} = |V_i||V_j|Y_{ij}$, where Y_{ij} is the reduced admittance, represents the coupling strength, while the phase shift φ_{ij} corresponds to the energy loss. For simplification, consider the system in coarse scale with the assumption of homogeneous generator properties (inertial and damping parameter), homogeneous voltage magnitudes and line reactance (global coupling strength), as well as lossless transmission ($\varphi_{ij} = 0$) [789]. Each machine i rotates at the same frequency $\Omega = 2\pi \times 50$ Hz or $\Omega = 2\pi \times 60$ Hz with the phase difference θ_i. In this case, the dynamics of generator i can be governed by the second-order Kuramoto model, Eq. (10) [789–793]. Despite the simplicity, the model is sufficient to capture the typical dynamics and exhibits complex phenomena of AC power grids. The model with heterogeneous coupling strength and nonzero phase shift has been discussed deeply in [794].

5.4.1. Dynamical perturbations

Dynamical perturbations can be induced during the transmission of energy from renewable power resources like the wind or solar one as well as outputs to consumers. Here, we focus on two types of dynamical perturbations: phase disturbances and power fluctuations.

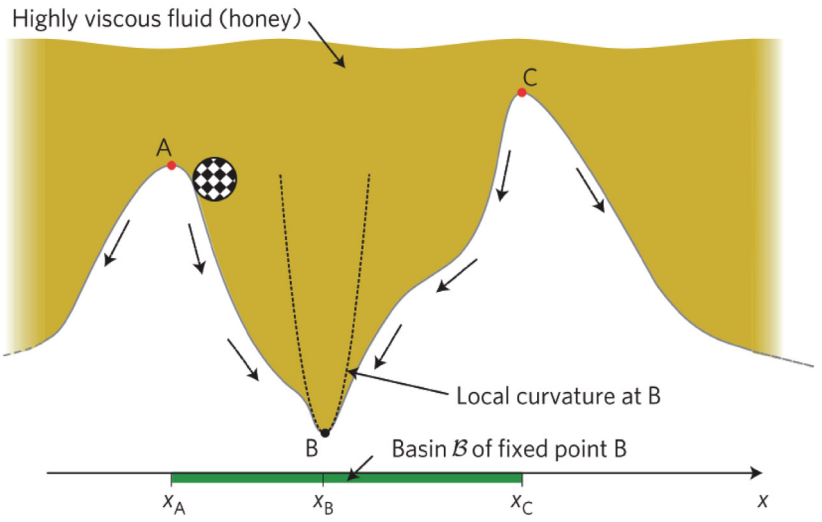

Fig. 48. Basin stability. Illustration of the basin stability with the analogy of marble track. Points A, B and C stand for fixed points but only B is stable. Arrows indicate the direction that the marble will roll to from different positions. The green bar below represents the basin attraction of point B, i.e. the marble always returns to point B after it is perturbed from B to a state within the region of Basin attraction.
Source: Adapted from [796].

Phase Disturbances: Disturbances imposed on each node are usually modeled with phase or frequency displacements. The propagation dynamics of such perturbation is rather complex: it may either spread globally throughout the system or just stay localized, depending on the network structure, maximal power capacity and the geographical distribution of power [795].

Basin stability is one of the typical metrics for large phase/frequency disturbances [796]. It quantifies the likelihood that a system will retain a stable state after perturbation, complementing the limitation of traditional linear stability. After perturbation on disturbed node k, it is defined as

$$\mathcal{BS}_k = \int \mathcal{X}(\theta_k, \nu_k)\rho_{\mathrm{p}}(\theta_k, \nu_k)d\theta_k d\nu_k, \tag{38}$$

where $\mathcal{X}(\theta_k, \nu_k)$ is the indicator function with $\mathcal{X}(\theta_k, \nu_k) = 1$ if (θ_k, ν_k) belongs to the basin attraction of the synchronous state, or $\mathcal{X}(\theta_k, \nu_k) = 0$ otherwise. $\rho_{\mathrm{p}}(\theta_k, \nu_k)$ denotes the perturbation density function satisfying $\int \rho_{\mathrm{p}}(\theta_k, \nu_k)d\theta_k d\nu_k = 1$. The value of $\mathcal{BS}_k \in [0, 1]$ depends on the property of node k with $\mathcal{BS}_k = 0$ if k is totally unstable and $\mathcal{BS}_k = 1$ when k is globally stable. Therefore, it measures the system robustness against disturbances imposed on nodes, and it allows the identification of the topological weakness of the system. The illustration of basin attraction is shown in Fig. 48. Numerically, basin stability could be estimated through the Monte-Carlo method, i,e, the ratio between the number of times that the system returns to the synchronous state after perturbation and the total number of independent simulations with different initial conditions are drawn from the distribution with density function ρ_{p} [797]. Generalizations of basin stability, like introduction of time dependency [798] or the one corresponding to multiple nodes [799], provide deeper insights of the disturbances dynamics in power grids.

The investigation of basin stability reveals how a network structure influences the system when dealing with phase disturbances. Nodes, with neighbors with larger average degree, have higher value of stability, especially those with degree larger than 2 [800]. Dead ends, as nodes with only one edge connected to the whole network, are confirmed to be extremely fragile [797]. Moreover, when one node directly or indirectly connecting several dead ends (a local structure called dead tree) is perturbed, the perturbation tends to spread to those dead ends and diminishes the system stability. While, from the design of real power grids, connecting a new power plant to the existing grids through a single transmission line is often the cheapest way. Therefore, this result implies the trade-off between construction costs and system stability. Vulnerability of structure of bottleneck was discussed in [801]. In contrast, nodes, in triangles with low betweenness centrality called detour nodes, haves high value of basin stability, indicating the robustness of local three-cycle motifs [802]. Additionally, conditions, which are simplified during the derivation of the swing equation, may also influence the dynamics of phase disturbances. For example, the presence of transmission losses φ_{ij} may create a new solitary state tending to destabilize the neighboring nodes and lead to desynchronization [803]. With the increase of losses, the size of desynchronized part of the network induced by perturbation becomes larger. This motivates researchers to reconsider to what extent the simplified equation reflects the realistic behaviors of power grids.

Methods for prior prevention and timely reaction have also been exploited. From the perspective of enhancing the system stability against phase disturbances, tuning the systemic parameters, like damping coefficient according to the

individual properties of each node, facilitates returning to the stable state of synchronization after perturbation [804]. Since the synchronous state is stable if and only if the real part of the Lyapunov exponents determined by the system is negative, there exists an optimization of such adjustment, characterizing the process of resynchronization with the highest speed. To control the spread of disturbances, a time-delayed feedback was introduced [805], given by

$$\frac{d^2\theta_i}{dt^2} + \alpha\frac{d\theta_i}{dt} = P_i + \sum_j A_{ij}\sin(\theta_j - \theta_i) - \frac{g_i\alpha}{\tau}[\theta_i(t) - \theta_i(t-\tau)], \tag{39}$$

where g_i is the control gain of node i and τ is the length of delay. In fact, the control term represents the average frequency during the delay window $\frac{1}{\tau}[\theta_i(t)-\theta_i(t-\tau)] = \frac{1}{\tau}\int_{t-\tau}^{t}\dot{\theta}(t')dt' = \langle\omega_i\rangle_t$, and aims to stabilize the frequency of the disturbed node. Difference among various control strategies lies in the choice of the subset of nodes to apply the control scheme.

Power Perturbation: The balance between supply and demand is essential for the operation of power grids. In a system containing N power plants, a steady state exists only if $\sum_i^N P_i = 0$. In other words, the power generated by plants with $P_i > 0$ is required to meet the consumption of those absorbing machines with $P_i < 0$.

A sudden but transient reset of power generation or consumption breaks the balance as well as the stead state, which may occur in real systems as a short circuit fault. Such a perturbation on a simple network structure was analyzed in [789]. By considering consumers connected to several generators requiring more power than under normal operation with the magnitude ΔP for a short while, it turns out that system could either withstand the perturbation under small ΔP or lose its stability even after the stop of the perturbation under relatively large ΔP. Such transition is then determined by a critical point, representing the robustness of the system against power reset. Further numerical simulations confirm that this critical point raises with the increase of coupling strength and the decrease of dissipation α. Besides, the behavior exhibits nonlinearity for perturbations with short duration but linearity for rather long pulse. This result implies that if the system has enough time to reach a new stable state, prolonged perturbation loses its influence in deciding the dynamics. The vulnerability of power grids, when facing perturbations modeled as transiently increased power demand with short-term and large-amplitude, was later confirmed in complex topology of real power grids [790]. Moreover, by replacing large power plants with several small ones, the critical point of perturbation magnitude shrinks, suggesting a negative impact of decentralization on the dynamic stability of power grids.

For sustained time-varying power fluctuations, the system dynamics becomes much more complicated than a temporary power reset. The generalized dynamics of the AC power grids with fluctuation term $\xi_i(t)$ and intensity ϵ_i is governed by

$$\frac{d^2\theta_i}{dt^2} + \alpha\frac{d\theta_i}{dt} = P_i + \lambda\sum_j A_{ij}\sin(\theta_j - \theta_i) + \epsilon_i\xi_i(t). \tag{40}$$

Related work has investigated different types of power fluctuations with their unique dynamical influence. Taking the nodal harmonic fluctuation ($F_i(t) = \delta_{ik}e^{i\phi t+\varphi}$) as an example, the amplitude of nodes' response to the fluctuation exhibits strong heterogeneity, according to which one could identify those with a large amplitude of response as vulnerable ones [806].

Fluctuations in the form of Gaussian white noise have also been well studied thanks to its simplicity. Interdependent Gaussian white noise $\{\xi_i(t)\}$ satisfies $\langle\xi_i\rangle = 0$ and $\langle\xi_i(t)\xi_j(s)\rangle = \delta_{ij}\delta(t-s)$. Although noises with high intensity prevent the system from approaching synchronization [807], it was found that noises with appropriate intensity can play constructive role not only in eliminating unstable intermediate states like traveling waves from the synchronization transition profile, but also in decreasing the critical coupling strength for partial synchronization [808,809]. Moreover, the break of stable synchronization induced by fluctuation provides insight into critical parts of the system. Nodal Gaussian white noise causes a systemic deviation from both frequency synchronization and equilibrium, the extent of which could be taken as the criticality of node against fluctuations [810]. Criticality exhibits significant correlation with nodes' degree. From the perspective of transmission line, the difference between phases of end nodes measures the vulnerability of links, implying the process of escaping the basin of attraction [811].

A recent work established a theoretical framework with the combination of the frequency distribution $p(\nu)$ and the underlying power fluctuations ξ [803]. The framework shows that the losses can fundamentally alter the dynamical behavior of the network coupling system, and it is almost impossible to use theoretical results on the system stability without losses for the design of future power systems. This remarkable result explains how the frequency distribution, observed in real power system, inherits the property of heavy tails and asymmetry, classical non-Gaussian natures, from the power fluctuations caused by solar and wind. To eliminate negative impacts of power fluctuation, various control strategies have also been proposed. Additional communication layer providing control signals for each power plants helps to improve the frequency synchronization under power fluctuations, with the highest efficiency reached when both frequency difference between the connected nodes and sum of neighbors' frequency are considered in the control scheme [812,813]. Efforts have also been devoted to improving the practicability of traditional proportional–integral control [814] in real power systems, such as distributed averaging-based integral control [815] and decentralized leaky integral control [816].

5.4.2. Structural perturbation

Structural perturbation, i.e., removal or addition of nodes/links, causes the redistribution of power flow and may induce further failures due to overload effect and end in a large-scale blackout. With the failure of even one single transmission element, cascading of power grids could be triggered [817–820]. In practical electrical systems, such initial failure usually represents malfunction due to exogenous events, such as lightning strike and extreme temperature. The successive failures in power grids involve more complicated mechanisms, including not only the underlying network topology and the statistic redistribution of power flow, but also the collective dynamics of the electrical system. On the other hand, addition of extra links could impact the emergence of system synchrony. In this subsection, we will review a popular model for cascading failures in power grids, features of the realistic process and various factors that may influence the process.

The process of cascading failures in power grids is as follows. Initially, the system (10) is in stable state and all lines have power loads lower than their capacity. The stable state is characterized by the fixed points of $\{\theta_i^*\}$ obeying $0 = P_i + \sum_{j=1}^{N} A_{ij} \sin(\theta_j^* - \theta_i^*)$. After the initial failure modeled as the removal of one or several links, the system evolves until a new stable state is reached. All transmission lines with flow beyond their capacity are removed, and power flow is redistributed to approach another stable state. This process is repeated until at least one of the following conditions is satisfied: no overload effect takes place any longer or the whole network is departed into unconnected subgrids. The consequence of cascades is quantified by the failure size, the number of consumers which cannot be supplied by the available generators. Simulations matched well with empirically observed power-law failure size distributions on high voltage power grids including the German grid [821], the US grid and the Hungarian grid [822].

Studying the influence of network structure as well as the layout of generators and consumers on the system robustness against such structural perturbations is of large practical significance. Although the increase of the capacity of existing transmission lines directly avoids large-scale cascades, designing the grid topology motivated by theoretical results is a sustainable way. The existence of large clusters of generators and consumers makes the system vulnerable [821]. Decentralized generator distributions were found more favorable than the centralized ones, implying the necessity of monitoring time-varying distribution of generation and demand caused by seasonal changes, diurnal variation and user habits [823]. Local redundancy, referring to a lot of short detours, provides sufficient options for rerouting and hence decreases the likelihood of large-scale cascading [824]. Therefore, a well-designed grid topology is characterized by a strong localization for both connectivity and plants layout, ensuring that a single link failure of the majority of transmission lines could only induce local effects.

Identifying critical links, on the other hand, emphasizes the vulnerable exponents in power grids. The combination of network structure and power flow dynamics in propagation of structural perturbation, compared to traditional measures solely relying on topological connectivity or steady state of the system like edge betweenness or heavy load invalid, provides a deeper and more comprehensive insight. A relatively simple algorithm is based on quantification of redundant capacity [825]. Considering the failure of a link (a, b), its flow F_{ab} has to redistribute to alternative paths. As links along these paths have limited residual capacity $C_{ij} - F_{ij}$ to take over part of F_{ab}, the redundant capacity C_{ab}^{res} of link (a, b) is defined as the maximum flow from nodes a to b through all links except (a, b), and it is approximated by

$$C_{ab}^{\text{res}} = \sum_{\text{paths } a\to b} \min_{(i,j)\in a\to b} (C_{ij} - F_{ij}), \tag{41}$$

which involves both flow distribution and network connectivity. The criticality of the link (a, b) is quantified by the ratio of its flow and redundant capacity $F_{ab}/C_{ab}^{\text{res}}$ determining whether there is sufficient vacant capacity for rerouting the flow. Other measures include estimating the flow rerouting based on the linear response theory [825] and the one involving the impact of transient dynamics with the order of seconds [16].

For the situation for addition of links, one may expect that such perturbation is always beneficial for the system operation. However, similar to Braess's paradox originally found in traffic networks [826], where closing a street may relieve the congestion of whole traffic, adding new links could either promote or destroy system synchrony of power grids [791]. The possible negative influence originates from the new cycles caused by additional links. In fact, phase differences along each cycle require the adjustment of multiples of 2π such that all phases are well-defined:

$$\sum_{(i,j)\in\text{cyclic path}} (\theta_j - \theta_i) = \sum_{(i,j)\in\text{cyclic path}} \arcsin(F_{ji}/K_{ji}) = 0 \ (\text{mod } 2\pi), \tag{42}$$

while the new cycles break the balance and call for new consistency conditions. Besides, additional links could also trigger the cascading failures with similar mechanism mentioned above for removing links [827]. These counter-intuitive phenomena should be taken into consideration when upgrading the power grids to avoid destabilizing the synchronization or inducing large-scale cascades.

5.5. Robot swarms

5.5.1. Collective behaviors in robot swarms

The study of the collective behavior of robotic swarms is largely inspired from the self-organization collectives in nature, such as flocking of birds, fish schools, and insect colonies. The common characteristic of these swarms is that a large number of simple individuals coordinating with each other through local interactions can generate impressive

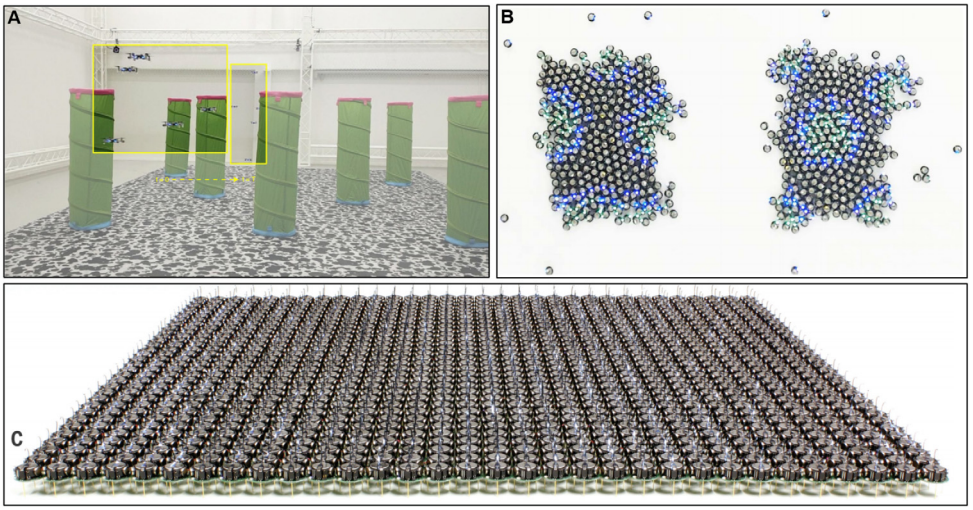

Fig. 49. Explicit interaction of collective behaviors. (A. The swarm of quadrotors in cluttered environments [831]. B. Morphogenesis in robot swarms [832]. C. The 1024 Kilobot swarm experiment [833].).
Source: Adapted from [831–833].

and complicated global behaviors. In the past few decades, scientists and engineers strived to figure out the relationship between local information transmission and collective behaviors to understand the mechanism on the natural collective intelligence and the artificial robot [828–830]. In different scenarios of collective behavior in robotic swarms, robots generally interact and transmit the messages to their neighbors through an explicit or implicit way in the existing studies.

Collective behaviors for explicit communication. The explicit way means that robots are capable of communicating in the swarm network by infrared signals, Wi-Fi signals, or other radio signals [831–833] as shown in Fig. 49. For example, a collective behavior to create a self-assembly robot swarm is shown in [833] that can be programmed to form complex two-dimensional shapes with a thousand simple robots. The robot can transmit the distance information to neighbors by sensing the infrared light intensity of the received signals, although this information is noisy. It is shown that a flexible self-assembly thousand-robot swarm relies entirely on local interactions and sensing can achieve a highly complex collective behavior. However, it relies on the hierarchical control principle, and each robot has an explicit image of the final shape that will be created. Thus, this collective shaping is not fully emergent. An emergent morphology is studied in a large robotic swarm [832]. This robotic swarm consisting of tiny robots can achieve self-organizing without any localization and only rely entirely on local interactions with neighbors instead, which is robust to intrinsic noise and adaptable to changing environments. The communication among the tiny kilobots is performed by passing only 8–9 bytes infrared messages which is limited to a range less than 10 cm. This collective behavior of robotic swarm is controlled by gene regulatory networks (GRNs) that are identical in every robot. The GRN is comprised of two virtual molecules, i.e., U and V. Each robot will track its own concentrations of U and V. The change in concentration of each molecule is given by the reaction–diffusion (RD) equation [832],

$$\begin{aligned}
\frac{\partial u}{\partial t} &= Rf(u,v) + \mathbf{D}_u \nabla^2 u, \\
\frac{\partial v}{\partial t} &= Rg(u,v) + \mathbf{D}_v \nabla^2 v, \\
f(u,v) &= (\mathbf{A}u + \mathbf{B}v + \mathbf{C}) - \gamma_u u, \\
g(u,v) &= (\mathbf{E}u - \mathbf{F}) - \gamma_v v,
\end{aligned}$$

where u, v represents the current values of the molecule U acted as an activator and the molecule V acts as an inhibitor, R, D_u and D_v are positive parameters. Based on GRNs, an experiment is demonstrated on 300 real kilobots, which achieves a shape-forming behavior of the collective swarm, even when some of the individual robots are unreliable. Other emergence behaviors such as aggregating [834], covering space [835], and moving coordinately [836] have also been investigated recently. Different from these emergence behaviors, the emergence of cognitive abilities also attracts researchers' interest [837,838]. A robot swarm called TS-swarm that can collectively sequence tasks is shown in [837] whose order of execution is priori unknown. This complex cognitive ability will emerge at the swarm level via the interaction of reactive individuals. Each robot can receive the messages of a failure or success in executing a task from task abstraction modules via an infrared signal [837].

Communication capacity plays an important role in realizing the emergence behavior in robotic swarms. The requirement of communication abilities is simple in the above research. While, in the swarm of the 3D aerial domain, the

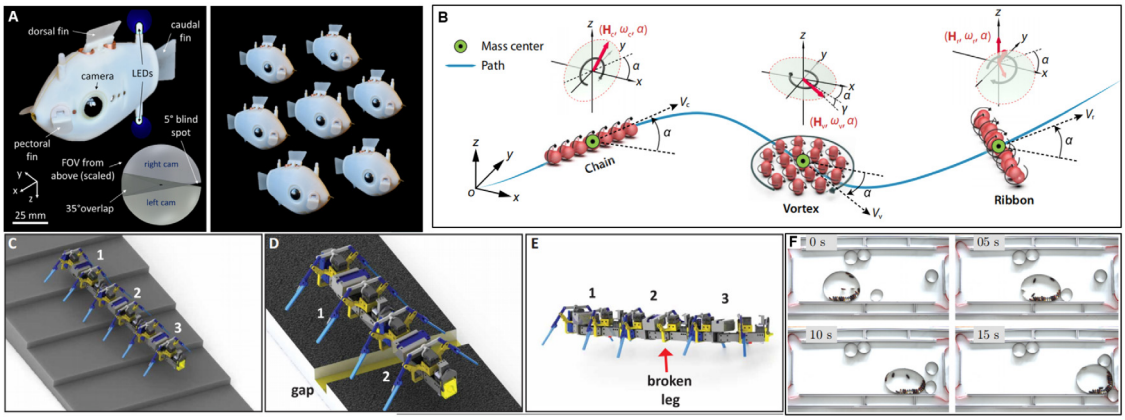

Fig. 50. Implicit interaction of collective behaviors. (A. Blueswarm platform [847]. B. Reconfigurable magnetic microrobot swarm of the chain, vortex, and ribbon [848]. C. Terrestrial swarms: Stair climbing with three chained robots [17]. D. Gap traversal with two chained robots [17]. E Transporting a broken-legged robot (middle) with the help of two other robots (front and back) [17]. F. Rod-like robots confined in a flexible scaffold [849].). *Source:* Adapted from [17,847–849].

requirements of hardware are relatively higher than the robots on the ground, especially for completing the task in a complex and unknown environment [831,839,840]. To deal with the navigation and obstacle avoidance of aerial swarms in a cluttered environment, the predictive model incorporates the local principles of potential field models in objective functions, which guarantees the separation, propulsion, and directional movement of the aerial swarm [831]. The cost function of the nonlinear model predicted control problem is formulated as follows,

$$\min_{\mathbf{x}(k),\mathbf{U}(k)} \sum_{i=1}^{N} \left(J_{\text{sep},i}(k) + J_{\text{prop},i}(k) + J_{\text{dir},i}(k) + J_{u,i}(k) \right),$$

where $J_{\text{sep},i}$, $J_{\text{prop},i}$, $J_{\text{dir},i}$, $J_{u,i}$ represent the separation, propulsion, and direction term, and the control effort, respectively. $\mathbf{X}(k) \in \mathbb{R}^{6NP}$ is the stacked sequence of the predicted states $\mathbf{x}(k+l/k)$ over the horizon $l \in \{1, \ldots, P\}$ and $\mathbf{U}(k) \in \mathbb{R}^{3NP}$ is the stacked sequence of the predicted control inputs $\mathbf{u}(p|k)$ over the horizon $l \in \{0, \ldots, P-1\}$. By solving the above problem, the behavior of each drone is governed by the knowledge of its neighbors and its own states. A central computing node will generate the acceleration command and broadcast it to the swarms through a radio link with small communication delays. It demonstrates that this aerial swarm can generate a faster flight, while guaranteeing safe navigation in an indoor environment with diverse obstacles, and is scalable to the dynamic changes in the swarm speed and inter-agent distance. Note that this control scheme is executed in a centralized manner. A decentralized flocking model for autonomous drone swarms is proposed in a confined environment with obstacles, communication delays, and perturbations [839]. By giving the number of drones and the flocking speed, the collision-free and coherent collective behavior is reached based on the decentralized flocking algorithm using evolutionary optimization. In the flocking model, each drone is equipped with two independent wireless modules in the 2.4 GHz range for inter-agent communication. The position and velocity signals are obtained by the onboard GNSS receivers. A real flight experiment with a self-organized swarm of 30 quadcopters is achieved in a bounded and cluttered environment. The tiny swarm robot holds a great potential for the unknown environment search, monitoring, and exploration. The state-of-art solutions, such as simultaneous localization and mapping, are source demanding in computation and communication. A major concern is to seek a high efficient swarm algorithm [840,841]. It should be noted that communication resources in tiny robotic swarms or other scenarios like micro-satellite swarms are usually limited, which motivates research on efficient information transmission scheme. A novel sampled-data based communication scheme has been deeply studied in the past decades [842], such as event-triggered mechanism [843] and quantization mechanism [844], which show the priority in reducing the communication consumption in robotic swarms. For multiple rigid body systems, which are usually to model the robot swarms, an effective event-triggered attitude synchronization method without velocity measurements is provided in [845]. In addition, over fixed and switching topologies, two different interesting event-triggered fixed-time attitude consensus algorithms are designed in [846].

Collective behaviors for implicit communication. The implicit communication way means that robots do not communicate with others directly by exchanging the data in swarms. They transmit or share the information over the swarm network through physical or chemical interaction and visual observation instead [17,847,848,850] as illustrated in Fig. 50. For example, terrestrial swarm robots with a self-reconfigurable multilegged structure are reported in [17] that can be linked on demand and autonomously. These legged robots are made up of reversibly chainable modular units with appropriate passive perturbation management mechanisms. The terradynamic interactions can be built through the physical contact between the individuals and can improve the locomotor capabilities of swarm robots in complex terrestrial terrain. This

Table 1
Summary of collective behaviors for robotic swarms.
Source: Adapted from [831–833,837,839,840,845–848].

	Communication		Communication setting				Domain			External assistance		Swarm scale		
			Distance		Bandwidth									
	Implicit	Explicit	Long (>1m)	Short (<1m)	High	Low	Aerial	Ground	Under water	Yes	No	<10	10^1 - 10^2	> 10^3
Kilobot [825]		√		√		√		√		√				√
Kilobot [824]		√		√		√		√			√		√	
E-puck robots [829]		√		√		√		√			√		√	
Crazyflie2.1 [823]		√		√			√			√		√		
Pixhawk quadrotors [831]		√	√		√		√				√		√	
Crazyflie2.0 [832]		√	√		√		√				√	√		
multilegged robot swarms [839]	√			√		√		√			√	√		
Superstructure robot [840]	√			√		√		√			√	√		
Magnetic microrobots [838]	√			√		√		√		√			√	
Bluebots [837]	√			√		√			√		√	√		

terrestrial swarm robot is capable of obstacle traversal and object transport in rough terrain by establishing the physical interactions of relatively simple units. Despite the self-configuration structure, the use of scaffolds made of rigid or flexible boundaries enclosing several robots is a promising structure to create complex behaviors. A superstructure consisting of a swarm rod-like robots is introduced in [849], which is confined in a deformable scaffold. The motion of this superstructure is related to the self-organization of the robots and these rod-like robots interact with each other through force conduction. A cluster of self-propelled rods inside the scaffold aligns parallel to each other to generate a driving force perpendicular to the scaffold wall to control the direction of the movement. Ways are shown for this superstructure robot to execute different tasks such as pulling loads, moving through an obstacle, cleaning up an arena, and interacting with each other.

The self-organizing dynamic structure provides insights for understanding the complex collective behaviors [17,849]. However, regulating a swarm of micro- and nanobot systems with high flexibility in the dynamic environment and tasks is still a challenging problem [850]. A magnetic microrobot swarm with high flexibility is proposed in response to the environmental changes and task variations [848]. This magnetic microrobot swarm is made up of self-propelled colloidal individuals via physical interactions rather than informatic communications. The colloidal particles can be programmed by using alternating magnetic fields into liquid, chain, vortex, and ribbon-like swarm formations and enabled to complete fast and reversible transformation among them. The reconfigurable magnetic microrobot swarm shows the high adaptability and functionality in several tasks such as complex locomotion in confined narrow paths, coordinated handling of heavy loads beyond an individual's capability, and synchronized manipulation in large areas.

Aquatic environments impose a substantial challenge on sensing and information transmitting since traditional above-ground communication methods such as radio and localizing methods using GPSs are not available. An implicit coordination mechanism is proposed for 3D underwater collective behaviors with a fish-inspired robot swarm [847,851]. This fish-like robot, called Blue-bot, achieves local sensing and interaction with neighbors only relies on a combination of cameras and blue-light LEDs. It can be shown that the multiple kinds of 3D collective behaviors underwater such as synchronization, controlled dispersion, and dynamic motion can be achieved through this simple mode of vision-based communication and without any external position sensing or control. The interaction force F_{ij} between robots based on the relative distance is calculated by taking the derivative of the artificial potential, the Lennard-Jones potential V_{ij} with respect to their distances $|r_{ij}|$. Hence, the movement vector $\mathbf{p}_i$ of robot i is determined as follows,

$$\mathbf{p}_i = \frac{1}{N}\sum_{j=1}^{N} F_{ij} r_{ij} = \frac{1}{N}\sum_{j=1}^{N} \frac{\partial V_{ij}}{\partial |r_{ij}|} r_{ij} = \frac{1}{N}\sum_{j=1}^{N} -\frac{1}{|r_{ij}|}\left[a\left(\frac{d_t}{|r_{ij}|}\right)^a - 2b\left(\frac{d_t}{|r_{ij}|}\right)^b \right] r_{ij}, \forall j \neq i, \tag{43}$$

where d_t, a, b are parameters needed to be determined in real experiments. An experiment of self-organized circle formation, collective research, gathering, and alert is demonstrated in this 3D underwater robot swarm. A summary of collective behaviors for robotic swarms is shown in Table 1.

5.5.2. Swarm attack

Many studies have been conducted around swarm robots, and most of them assume a benign operating environment for robot swarms. In a benign operating environment, the robot swarms can propagate signals without any obstacle, which

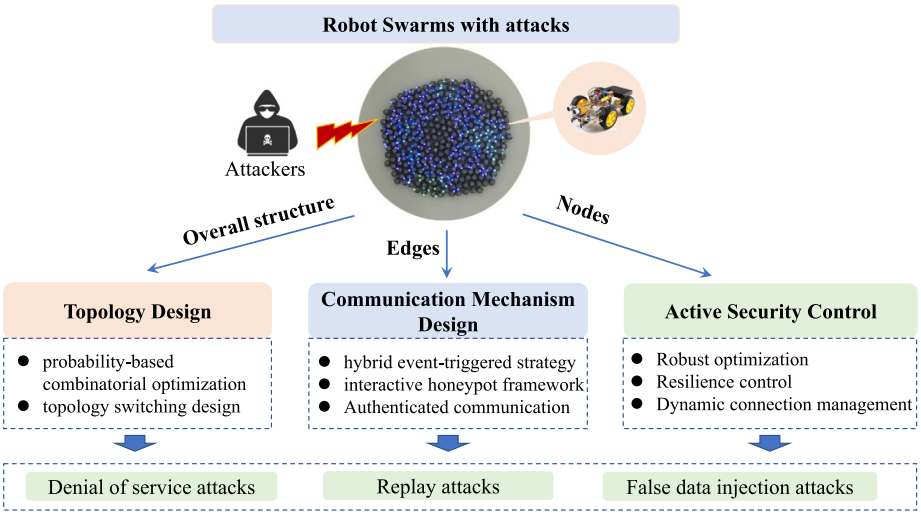

Fig. 51. The overall structure of swarm attack subsection.
Source: Adapted from [833].

is the basis and key to realizing the cooperative behavior of the swarm. However, in practical applications such as military confrontation, it is difficult to guarantee a benign communication environment, and potential adversarial factors such as false data injection, denial of service attacks, packet drops, etc. usually exist. For example, the effect of random time delays and packet drops is well analyzed and modeled in [852] and a LQG control method is proposed for discrete-time networked control systems. Therefore, it is of great significance to study the defense strategy for robot swarm attacks. According to the difference in the signal propagation process in the robot swarm, the existing research on the defense strategy design for robot swarm attacks can be divided into three categories: topology design based, communication mechanism based and active security control based. The overall structure of this subsection is shown as Fig. 51.

Topology design for swarm attacks. The key for robot swarms to realize cooperative behavior is the signal propagation among robots, and the communication network of robot swarms is the most critical underlying foundation for realizing signal propagation, which is usually represented by topology. Therefore, there exist various cyber attacks against target nodes (robots) and edges (signal propagation channels) in the communication topology of robot swarms. Considering that cyber attacks spread their risks through the communication topology, which can be freely designed to determine the signal propagation, the most direct defense strategy is to design a corresponding communication topology based on the targets of various cyber attacks, so as to reduce or even eliminate the risk of cyber attacks. A lot of current research works are based on this idea to design defense methods, including the probability-based combinatorial optimization, communication topology switching and so on.

To model the uncertainty of information interaction in robot swarms, the probability distribution is utilized in [853] to describe whether there exists an edge or not. Probability expressions are derived based on disjoint paths and sub-cuts that define safety probabilities and accurate probabilities for a multi-robot system are calculated using binary decision graphs. To reduce computational complexity, an efficient defense topology is designed by solving a safe probability-based combinatorial optimization problem. Different from the safety probability optimization, a more direct approach is to design communication topology switching signals. A defense method for robot swarms is proposed in [854], which uses the physical properties of wireless transmission to design communication topology switching signals. The generation of the handover signals relies on information extracted from the wireless channel, randomly excluding potentially untrusted transmissions from consensus and selectively ignoring data transmissions from untrusted agents. This defense method, based on the design of communication topology switching, differs from previous works, which allows arbitrary malicious node values and is insensitive to the initial topology of the network. Aiming at robot swarms in practical applications, such as drone formations, a secure robot swarm model is proposed in [855] that takes the robot's location as input and enables multiple robots to form a wireless mesh network by moving with the help of a centralized computing unit. After the wireless mesh network is formed, the A* search method is used to calculate the shortest communication path between robots to obtain the communication network topology. In addition, the model utilizes encryption techniques such as Advanced Encryption Standard (AES) and Blowfish to further enhance the security of the robot swarms. Further, the system-wide attacks and resilient design for robot swarms are considered in [856]. Based on the above concepts, a defense method is given in [856], which is based on topology design. This method can achieve the minimum communication between robots while guaranteeing the security defense of the approximate optimal solution against any number of denial-of-service attacks and failures.

Communication mechanism design for swarm attacks. The defense strategy based on topology design against cyber attack in the robot swarms is the most direct method. However, this approach has limitations when considering the communication structure constraints in practical applications. Therefore, many experts and scholars start from the channel in the communication topology, and study the defense strategy based on the design for communication mechanism. Compared with the defense strategy based on topology design, the defense strategy based on communication mechanism pays more attention to signal propagation in the channel, which is more flexible and achievable.

In order to deal with hidden attacks in cooperative multi-robot systems, a runtime monitoring framework is proposed in [857] to guarantee the safe operation of the communication mechanism. The cumulative sign detector in this framework takes the signed residuals into account, defined as expected and received information to identify and isolate unexpected non-random behavior in multi-robot systems. The control problem of robot swarm formation with nonlinear characteristics under the denial of service attacks is considered in [858]. The distributed hybrid event-triggered strategy (HETS) proposed in [858] utilizes a hybrid communication topology and the corresponding control strategy to limit the propagation of errors caused by denial-of-service attacks, and at the same time uses an event-triggered mechanism to limit the communication frequency of the robot to save communication resource. To deal with potential long-range attacks in networked robot swarm systems, [859] leverages HoneyPhy, a physics-aware honeypot framework, to create HoneyBot, the first software-hybrid interactive honeypot designed specifically for networked robot systems. HoneyBot can attempt to trick attackers into believing their attack was successful by simulating insecure operations and physical execution, while recording all communications for attacker attribution and threat model creation. To develop new models that ensure safe cooperation in large robot swarms, a way to encapsulate cobot tasks in an authenticated data structure called a Merkle tree is devised in [860]. Using this approach based on the design of communication mechanisms, operators can provide a "blueprint" of swarm missions without revealing their raw data. In other words, data validation can be separated from the data itself. Robots applying this communication-mechanism-based approach must prove their integrity to their peers by exchanging cryptographic proofs when performing cooperative tasks. Against potential spoofing attacks in robot swarms, a class of consensus-based defense strategies called Weighted Average Subsequence Reduction (W-MSR) are devised in [861]. This communication mechanism-based approach further provides spoofing resilience by incorporating physical-layer authentication, where legitimate agents can identify and isolate malicious agents attempting spoofing attacks by comparing the physical fingerprints of received signals. A special advantage of this method is that the worst-case misclassification probability can be quantified using the distribution-robust Chebyshev bound computed by semi-definite programming when the physical fingerprints of the received signal are random.

Active security control for swarm attacks. Although defense methods based on topology design and communication mechanism can effectively deal with cyber attacks targeting signal propagation in communication networks for robot swarms, they cannot solve the cases where cyber attacks directly target individual nodes and may have already begun to take effect. At this time, it is necessary to design a defense strategy that can effectively handle the single-point attack from the perspective of the control for a single robot, that is, active security control. Active security control ensures the resistance and recoverability of a single robot or robot swarm from the perspective of control signal design, and effectively eliminates the risk of swarm attack [862].

Aiming at DoS attacks in robot swarms, a general distributed active security control based defense algorithm named distributed robust maximization (DRM) is proposed in [863], which can achieve robust optimization of large-scale robot swarms, and only depends on local communication. DRM utilizes the divide-and-conquer idea to distribute the problem among K groups of robots. Factions are optimized in parallel independently of each other. At the same time, DRM also ensures computational acceleration that differs from centralized algorithms, which depend on the communication range of the robot swarms. DRM achieves near-optimal control performance while maintaining defensive performance. In order to ensure the resilience to robot failures, the elastic coverage maximization problem is considered in [864], and two approximation algorithms are proposed, namely the ordered greedy algorithm and the local search algorithm, which can realize the fast computation of collaborative active security control signals. Both algorithms empirically outperform state-of-the-art solutions in terms of accuracy and runtime. In the presence of non-cooperative robots in a robot swarm, an active security control strategy is designed in [865] that can realize the elastic formation control of the robot swarms. The proposed active security control strategy relies on dynamic connection management, utilizing a management matrix to characterize the metrics of the robustness of the communication network topology. Different from previous work, the proposed strategy can ensure that the network is above a critical resiliency threshold to ensure that the collaborative task of the robot swarm can be completed. How to trace the source of the attack signal transmission in the robot group is also a key issue to ensure the information security of the robot group.

6. Conclusion

In this Review, we offered a comprehensive survey covering a number of important and contemporary research topics related to signal propagation in complex networks. Signal propagation, broadly regarded as a key element in understanding the emergence of collective behaviors, has received much attention in recent years from both theoretical and applied domains. This Review serves to provide a broad yet structured overview of recent progress as well as bringing up some open challenges.

In the Introduction part, we gave an overview of some recent discoveries of the universal features of dynamical processes and signal propagation in various fields of applications. Furthermore, we pointed out the importance of the

current survey, linking it with various research topics ranging from dynamical modeling and topological structures via time series analysis, to applications.

In Section 2, we started with the multiscale modeling of disease spread. In this scenario individual-based stochastic modeling and reaction–diffusion-based sophisticated metapopulation dynamics are the fundamental building blocks of the corresponding studies. Such multiscale modeling to capture propagation from a source requires more attention, as detailed interactions between pathogens on a down-scale and interactions between individuals on an up-scale must be carefully embedded. Next, we presented emergence conditions of traveling wave state in Kuramoto model as well as diffusion dynamics in the context of social, biological, and technological factors. In particular, analytical studies of diffusion dynamics reveal the emergence of the classic Turing instability in a reaction–diffusion process in complex networks. While, the role of higher-order interactions has not been fully-explored regarding Turing instability, signal spreading across temporal walks deserves further investigation. Finally, we focused on signal propagation in the neuronal dynamics and its importance for the central nervous system of Larval zebrafish. Neural signal propagations can be described at multiple scales. At the microscopic scale, detailed biological measurements enable the modeling of interactions between neurons: At the macroscopic scale, on the other hand, limited spatial and temporal resolutions of observations generally prevent attempts of the discovery of neural signal propagation accurately. Recently, whole-brain imaging techniques such as those prototype demos in zebrafish provide a unique and exciting opportunity to integrate analysis tools from complex systems to neural dynamics underlying various brain functions.

In Section 3, we first reviewed the spread of disease in temporal networks suggesting that a coarse-grained static version of temporal networks often cannot reflect the true spreading pattern. Two types of complex time-varying interactions, namely activity-driven and neighborhood exchange, are both investigated in this section. Understanding signal propagation in time-varying topology remains challenging and demands future study in particular regarding infections spreading in temporal networks and systems. We then reviewed a recently-proposed theoretical framework for signal propagation through complex networks. Under this framework, the intrinsic dynamics of each node, the interaction between neighboring nodes jointly determine how signals propagate from a given source to far-off target nodes. Furthermore, the dynamical propagation rules may vary across systems with locally perturbed high-dimensional chaotic dynamics, but a complete perturbation analysis has yet to be developed. The impact of higher-order interactions on signal propagation for a large class of dynamical models remains to be further explored. In addition, we addressed the role of multilayer structure in epidemic spreading and provided insights towards revealing the essence of control on complex networks. Specifically, we show that the connectivity with specific static structures and dynamic properties can efficiently affect the propagation of control signals in communication graphs. Further investigation could be devoted to the issues of robustness analysis on network controllability, multiplex networks, and node dynamics with diverse categories.

In Section 4, we focus on the problem of reconstructing the structure and dynamics of observed signal propagation from complex networks. We start by reviewing analytical and statistical tools for computing pairwise correlation measures from both a regression viewpoint and later generalized to information transfer via information-theoretic measures, enabling the determination of causality from time series using methods such as Granger causality and transfer entropy. Advanced nonlinear embedding and prediction approaches are also surveyed, in particular Koopman operator analysis. These pairwise measures of correlation and causality form the building block for reconstructing causal networks from time series observations, which we discussed from the perspective of dynamical systems and information theory. Then, we summarize existing methods of link prediction from the perspective of supervised and unsupervised techniques, and enumerate the application of source localization in different types of complex networks, such as disease dissemination, social, and wireless sensor networks. We note that it is valuable to combine time series analysis techniques with cutting-edge artificial intelligence approaches such as meta-learning, few-shot learning, etc., as summarized towards the end of this section, recent progress and methods based on artificial intelligence. In addition to improving the accuracy and performance of existing time series analysis methods for single task scenarios, the data problems (few samples and poor data quality) and mobility performance for cross/multiple tasks scenarios deserve special attention for practical applications of time series analysis methods.

In Section 5, we presented various applications. We first described the application of agent-based modeling and metapopulation modeling to infectious diseases, e.g., Ebola, COVID-19, and Dengue/Malaria, offering computational methods and insights for designing intervention strategies to mitigate the spread. Next, we note that signal propagation is key to understanding the power grid in particular for its stability analysis from dynamical and structural perspectives. The dynamics of signal propagation in nervous systems is also crucial for the generation of flexible and adaptive brain functions. At the spatial level, detailed nodes and edges have been identified in circuit neuroscience; whereas at the temporal level, various patterns of directional and sequential have been revealed in system neuroscience. These two research directions have produced fruitful results for integrating advanced and suitable methods from complex systems. Such a multi-disciplinary research field may uncover the rules underlying the unique properties of the brain, such as probabilistic and robust computation or invariant representations. In addition, owing to the wide potential applications of robotic swarms, studies of collective behavior and swarming dynamics where the robots communicate in a threatening environment, are rapidly gaining interest. Noting that the fundamental mechanism of the emergence and evolution of swarm intelligence remain unclear in particular, future research needs to be devoted to the investigation of the learning algorithm of individual robots.

Declaration of competing interest

The authors declare that they have no known competing financial interests or personal relationships that could have appeared to influence the work reported in this paper.

Acknowledgments

We would like to thank Mr. Subrata Ghosh, Mr. Arpit Kumar and Ms. Shitong Zhao for fruitful suggestions and discussion. P.J. is supported by STI2030-Major Projects (2021ZD0204500) and the NSFC (62076071). J.Y. is supported by the NSFC (12147101) and Shanghai Municipal Science and Technology Major Project (2018SHZDZX01). Y. M. is supported by STI2030-Major Projects (2021ZD0203700, 2021ZD0204500). W.L. is supported by the NSFC (No. 11925103) and by the STCSM (Nos. 22JC1401402, 2021SHZDZX0103, and 2023ZKZD04). C.H. is supported by DST-INSPIRE Faculty Grant No. IFA17-PH193. M.P. is supported by the Slovenian Research Agency (Javna agencija zaraziskovalno dejavnost RS) (Grant Nos. P1-0403 and J1-2457). Y.T. is supported by the NSFC (61988101, 62293502, 62233005) and Shanghai AI Laboratory.

References

[1] R. Albert, A.-L. Barabási, Statistical mechanics of complex networks, Rev. Modern Phys. 74 (2002) 47–97.
[2] S. Boccaletti, V. Latora, Y. Moreno, M. Chavez, D.U. Hwang, Complex networks: Structure and dynamics, Phys. Rep. 424 (2006) 175–308.
[3] Stefano Boccaletti, Ginestra Bianconi, Regino Criado, Charo I Del Genio, Jesús Gómez-Gardenes, Miguel Romance, Irene Sendina-Nadal, Zhen Wang, Massimiliano Zanin, The structure and dynamics of multilayer networks, Phys. Rep. 544 (1) (2014) 1–122.
[4] Mikko Kivelä, Alex Arenas, Marc Barthelemy, James P Gleeson, Yamir Moreno, Mason A Porter, Multilayer networks, J. Complex Netw. 2 (3) (2014) 203–271.
[5] D.J. Watts, S.H. Strogatz, Collective dynamics of 'small world' networks, Nature 393 (1998) 440–442.
[6] A.-L. Barabási, R. Albert, Emergence of scaling in random networks, Science 286 (1999) 509–512.
[7] Steven H. Strogatz, Exploring complex networks, Nature 410 (2001) 268–276.
[8] A. Pikovsky, M. Rosenblum, J. Kurths, Synchronization: a Universal Concept in Nonlinear Sciences, in: Cambridge Nonlinear Scrience Series 12, Cambridge University Press, 2003.
[9] Alex Arenas, Albert Díaz-Guilera, Jurgen Kurths, Yamir Moreno, Changsong Zhou, Synchronization in complex networks, Phys. Rep. 469 (3) (2008) 93–153.
[10] Chittaranjan Hens, Uzi Harush, Simi Haber, Reuven Cohen, Baruch Barzel, Spatiotemporal signal propagation in complex networks, Nat. Phys. 15 (4) (2019) 403–412.
[11] Xiaozhu Zhang, Sarah Hallerberg, Moritz Matthiae, Dirk Witthaut, Marc Timme, Fluctuation-induced distributed resonances in oscillatory networks, Sci. Adv. 5 (7) (2019) eaav1027.
[12] Xiaozhu Zhang, Dirk Witthaut, Marc Timme, et al., Topological determinants of perturbation spreading in networks, Phys. Rev. Lett. 125 (21) (2020) 218301.
[13] Xiaoge Bao, Qitong Hu, Peng Ji, Wei Lin, Jürgen Kurths, Jan Nagler, Impact of basic network motifs on the collective response to perturbations, Nature Commun. 13 (1) (2022) 1–8.
[14] Yang Yang, Takashi Nishikawa, Adilson E. Motter, Small vulnerable sets determine large network cascades in power grids, Science 358 (6365) (2017) eaan3184.
[15] Federico Battiston, Giulia Cencetti, Iacopo Iacopini, Vito Latora, Maxime Lucas, Alice Patania, Jean-Gabriel Young, Giovanni Petri, Networks beyond pairwise interactions: structure and dynamics, Phys. Rep. 874 (2020) 1–92.
[16] Benjamin Schäfer, Dirk Witthaut, Marc Timme, Vito Latora, Dynamically induced cascading failures in power grids, Nature Commun. 9 (1) (2018) 1–13.
[17] Yasemin Ozkan-Aydin, Daniel I. Goldman, Self-reconfigurable multilegged robot swarms collectively accomplish challenging terradynamic tasks, Science Robotics 6 (56) (2021) eabf1628.
[18] Armin Bahl, Florian Engert, Neural circuits for evidence accumulation and decision making in larval zebrafish, Nature Neurosci. 23 (1) (2020) 94–102.
[19] Corey M Peak, Lauren M Childs, Yonatan H Grad, Caroline O Buckee, Comparing nonpharmaceutical interventions for containing emerging epidemics, Proc. Natl. Acad. Sci. 114 (15) (2017) 4023–4028.
[20] Hyunsuk Hong, Steven H. Strogatz, Kuramoto model of coupled oscillators with positive and negative coupling parameters: an example of conformist and contrarian oscillators, Phys. Rev. Lett. 106 (5) (2011) 054102.
[21] Thomas Peron, Discordant synchronization patterns on directed networks of identical phase oscillators with attractive and repulsive couplings, Phys. Rev. E 103 (4) (2021) 042210.
[22] Xiuye Chen, Yu Mu, Yu Hu, Aaron T Kuan, Maxim Nikitchenko, Owen Randlett, Alex B Chen, Jeffery P Gavornik, Haim Sompolinsky, Florian Engert, et al., Brain-wide organization of neuronal activity and convergent sensorimotor transformations in larval zebrafish, Neuron 100 (4) (2018) 876–890.
[23] Ingo Scholtes, Nicolas Wider, René Pfitzner, Antonios Garas, Claudio J Tessone, Frank Schweitzer, Causality-driven slow-down and speed-up of diffusion in non-Markovian temporal networks, Nature Commun. 5 (1) (2014) 1–9.
[24] Jean-Charles Delvenne, Renaud Lambiotte, Luis E.C. Rocha, Diffusion on networked systems is a question of time or structure, Nature Commun. 6 (1) (2015) 1–10.
[25] Aming Li, Sean P Cornelius, Y Y Liu, Long Wang, A-L Barabási, The fundamental advantages of temporal networks, Science 358 (6366) (2017) 1042–1046.
[26] Holger Kantz, Thomas Schreiber, Nonlinear Time Series Analysis, Vol. 7, Cambridge University Press, 2004.
[27] Jakob Runge, Sebastian Bathiany, Erik Bollt, Gustau Camps-Valls, Dim Coumou, Ethan Deyle, Clark Glymour, Marlene Kretschmer, Miguel D Mahecha, Jordi Muñoz-Marí, et al., Inferring causation from time series in Earth system sciences, Nature Commun. 10 (1) (2019) 1–13.
[28] Christopher W. Lynn, Danielle S. Bassett, The physics of brain network structure, function and control, Nat. Rev. Phys. 1 (5) (2019) 318–332.
[29] Brunella Spinelli, L. Elisa Celis, Patrick Thiran, A general framework for sensor placement in source localization, IEEE Trans. Netw. Sci. Eng. 6 (2) (2019) 86–102.
[30] Zhiwei Cao, Yichao Zhang, Jihong Guan, Shuigeng Zhou, Guanrong Chen, Link weight prediction using weight perturbation and latent factor, IEEE Trans. Cybern. 52 (3) (2022) 1785–1797.

[31] Chenbo Fu, Minghao Zhao, Lu Fan, Xinyi Chen, Jinyin Chen, Zhefu Wu, Yongxiang Xia, Qi Xuan, Link weight prediction using supervised learning methods and its application to yelp layered network, IEEE Trans. Knowl. Data Eng. 30 (8) (2018) 1507–1518.
[32] Matt J. Keeling, Pejman Rohani, Estimating spatial coupling in epidemiological systems: a mechanistic approach, Ecol. Lett. 5 (1) (2002) 20–29.
[33] Matt J. Keeling, Pejman Rohani, Modeling Infectious Diseases in Humans and Animals, Princeton University Press, 2011.
[34] Ilkka Hanski, et al., Metapopulation Ecology, Oxford University Press, 1999.
[35] Remo Ryser, Myriam R Hirt, Johanna Häussler, Dominique Gravel, Ulrich Brose, Landscape heterogeneity buffers biodiversity of simulated meta-food-webs under global change through rescue and drainage effects, Nature Commun. 12 (1) (2021) 1–9.
[36] Sedigheh Yagoobi, Arne Traulsen, Fixation probabilities in network structured meta-populations, Sci. Rep. 11 (1) (2021) 1–9.
[37] Shi Chen, Cristina Lanzas, Chihoon Lee, Gabriel L Zenarosa, Ahmed A Arif, Michael Dulin, Metapopulation model from pathogen's perspective: A versatile framework to quantify pathogen transfer and circulation between environment and hosts, Sci. Rep. 9 (1) (2019) 1–11.
[38] Lisa C McManus, Edward W Tekwa, Daniel E Schindler, Timothy E Walsworth, Madhavi A Colton, Michael M Webster, Timothy E Essington, Daniel L Forrest, Stephen R Palumbi, Peter J Mumby, et al., Evolution reverses the effect of network structure on metapopulation persistence, Ecology 102 (7) (2021) e03381.
[39] Alessandro Vespignani, Predicting the behavior of techno-social systems, Science 325 (5939) (2009) 425–428.
[40] Duygu Balcan, Vittoria Colizza, Bruno Gonçalves, Hao Hu, José J Ramasco, Alessandro Vespignani, Multiscale mobility networks and the spatial spreading of infectious diseases, Proc. Natl. Acad. Sci. 106 (51) (2009) 21484–21489.
[41] Lars Hufnagel, Dirk Brockmann, Theo Geisel, Forecast and control of epidemics in a globalized world, Proc. Natl. Acad. Sci. 101 (42) (2004) 15124–15129.
[42] Duygu Balcan, Hao Hu, Bruno Goncalves, Paolo Bajardi, Chiara Poletto, Jose J Ramasco, Daniela Paolotti, Nicola Perra, Michele Tizzoni, Wouter Van den Broeck, et al., Seasonal transmission potential and activity peaks of the new influenza A (h1n1): a Monte Carlo likelihood analysis based on human mobility, BMC Med. 7 (1) (2009) 1–12.
[43] Frank Ball, Tom Britton, Thomas House, Valerie Isham, Denis Mollison, Lorenzo Pellis, Gianpaolo Scalia Tomba, Seven challenges for metapopulation models of epidemics, including households models, Epidemics 10 (2015) 63–67.
[44] Zhen Wang, Chris T Bauch, Samit Bhattacharyya, Alberto d'Onofrio, Piero Manfredi, Matjaž Perc, Nicola Perra, Marcel Salathé, Dawei Zhao, Statistical physics of vaccination, Phys. Rep. 664 (2016) 1–113.
[45] Leon Danon, Ashley P Ford, Thomas House, Chris P Jewell, Matt J Keeling, Gareth O Roberts, Joshua V Ross, Matthew C Vernon, Networks and the epidemiology of infectious disease, Interdiscip. Perspect. Infect. Dis. 2011 (2011).
[46] Theodore J. Gordon, A simple agent model of an epidemic, Technol. Forecast. Soc. Change 70 (5) (2003) 397–417.
[47] Liliana Perez, Suzana Dragicevic, An agent-based approach for modeling dynamics of contagious disease spread, Int. J. Health Geogr. 8 (1) (2009) 1–17.
[48] Stephen Eubank, Hasan Guclu, VS Anil Kumar, Madhav V Marathe, Aravind Srinivasan, Zoltan Toroczkai, Nan Wang, Modelling disease outbreaks in realistic urban social networks, Nature 429 (6988) (2004) 180–184.
[49] Neil M Ferguson, Derek AT Cummings, Simon Cauchemez, Christophe Fraser, Steven Riley, Aronrag Meeyai, Sopon Iamsirithaworn, Donald S Burke, Strategies for containing an emerging influenza pandemic in Southeast Asia, Nature 437 (7056) (2005) 209–214.
[50] Ira M Longini Jr., Azhar Nizam, Shufu Xu, Kumnuan Ungchusak, Wanna Hanshaoworakul, Derek AT Cummings, M Elizabeth Halloran, Containing pandemic influenza at the source, Science 309 (5737) (2005) 1083–1087.
[51] Rebecca A Kelly, Anthony J Jakeman, Olivier Barreteau, Mark E Borsuk, Sondoss ElSawah, Serena H Hamilton, Hans Jørgen Henriksen, Sakari Kuikka, Holger R Maier, Andrea Emilio Rizzoli, et al., Selecting among five common modelling approaches for integrated environmental assessment and management, Environ. Model. Softw. 47 (2013) 159–181.
[52] Lander Willem, Frederik Verelst, Joke Bilcke, Niel Hens, Philippe Beutels, Lessons from a decade of individual-based models for infectious disease transmission: a systematic review (2006–2015), BMC Infect. Dis. 17 (1) (2017) 1–16.
[53] Christopher L Barrett, Keith R Bisset, Stephen G Eubank, Xizhou Feng, Madhav V Marathe, Episimdemics: an efficient algorithm for simulating the spread of infectious disease over large realistic social networks, in: SC'08: Proceedings of the 2008 ACM/IEEE Conference on Supercomputing, IEEE, 2008, pp. 1–12.
[54] Kathleen M Carley, Douglas B Fridsma, Elizabeth Casman, Alex Yahja, Neal Altman, Li-Chiou Chen, Boris Kaminsky, Démian Nave, BioWar: scalable agent-based model of bioattacks, IEEE Trans. Syst., Man, Cybern.- A 36 (2) (2006) 252–265.
[55] Vittoria Colizza, Alain Barrat, Marc Barthélemy, Alessandro Vespignani, Predictability and epidemic pathways in global outbreaks of infectious diseases: the SARS case study, BMC Med. 5 (1) (2007) 1–13.
[56] Michele Tizzoni, Paolo Bajardi, Chiara Poletto, José J Ramasco, Duygu Balcan, Bruno Gonçalves, Nicola Perra, Vittoria Colizza, Alessandro Vespignani, Real-time numerical forecast of global epidemic spreading: case study of 2009 A/H1N1pdm, BMC Med. 10 (1) (2012) 1–31.
[57] Alex Arenas, Wesley Cota, Jesús Gómez-Gardeñes, Sergio Gómez, Clara Granell, Joan T Matamalas, David Soriano-Paños, Benjamin Steinegger, Modeling the spatiotemporal epidemic spreading of COVID-19 and the impact of mobility and social distancing interventions, Phys. Rev. X 10 (4) (2020) 041055.
[58] Moritz UG Kraemer, Chia-Hung Yang, Bernardo Gutierrez, Chieh-Hsi Wu, Brennan Klein, David M Pigott, Open COVID-19 Data Working Group, Louis du Plessis, Nuno R Faria, Ruoran Li, et al., The effect of human mobility and control measures on the COVID-19 epidemic in China, Science 368 (6490) (2020) 493–497.
[59] Vittoria Colizza, Romualdo Pastor-Satorras, Alessandro Vespignani, Reaction–diffusion processes and metapopulation models in heterogeneous networks, Nat. Phys. 3 (4) (2007) 276–282.
[60] Vittoria Colizza, Alessandro Vespignani, Epidemic modeling in metapopulation systems with heterogeneous coupling pattern: Theory and simulations, J. Theoret. Biol. 251 (3) (2008) 450–467.
[61] Vincent A.A. Jansen, Alun L. Lloyd, Local stability analysis of spatially homogeneous solutions of multi-patch systems, J. Math. Biol. 41 (3) (2000) 232–252.
[62] Aurélien Gautreau, Alain Barrat, Marc Barthélemy, Arrival time statistics in global disease spread, J. Stat. Mech. Theory Exp. 2007 (09) (2007) L09001.
[63] Aurélien Gautreau, Alain Barrat, Marc Barthelemy, Global disease spread: statistics and estimation of arrival times, J. Theoret. Biol. 251 (3) (2008) 509–522.
[64] Dirk Brockmann, Dirk Helbing, The hidden geometry of complex, network-driven contagion phenomena, Science 342 (6164) (2013) 1337–1342.
[65] Flavio Iannelli, Andreas Koher, Dirk Brockmann, Philipp Hövel, Igor M Sokolov, Effective distances for epidemics spreading on complex networks, Phys. Rev. E 95 (1) (2017) 012313.
[66] Dirk Brockmann, Lars Hufnagel, Theo Geisel, The scaling laws of human travel, Nature 439 (7075) (2006) 462–465.
[67] Marta C. Gonzalez, Cesar A. Hidalgo, Albert-Laszlo Barabasi, Understanding individual human mobility patterns, Nature 453 (7196) (2008) 779–782.
[68] Vitaly Belik, Theo Geisel, Dirk Brockmann, Natural human mobility patterns and spatial spread of infectious diseases, Phys. Rev. X 1 (1) (2011) 011001.

[69] David Soriano-Paños, Wesley Cota, Silvio C Ferreira, Gourab Ghoshal, Alex Arenas, Jesús Gómez-Gardeñes, Modeling communicable diseases, human mobility, and epidemics: A review, Ann. Phys. (2022) 2100482.
[70] D Soriano-Paños, L Lotero, A Arenas, J Gómez-Gardeñes, Spreading processes in multiplex metapopulations containing different mobility networks, Phys. Rev. X 8 (3) (2018) 031039.
[71] Jesús Gómez-Gardeñes, David Soriano-Paños, Alex Arenas, Critical regimes driven by recurrent mobility patterns of reaction–diffusion processes in networks, Nat. Phys. 14 (4) (2018) 391–395.
[72] Suman Saha, Arindam Mishra, Syamal K Dana, Chittaranjan Hens, Nandadulal Bairagi, Infection spreading and recovery in a square lattice, Phys. Rev. E 102 (5) (2020) 052307.
[73] Joshua M Epstein, Derek AT Cummings, Shubha Chakravarty, Ramesh M Singha, Donald S Burke, Toward a Containment Strategy for Smallpox Bioterror: An Individual-Based Computational Approach, Brookings Institution Press, 2004.
[74] Marta Luisa Ciofi degli Atti, Stefano Merler, Caterina Rizzo, Marco Ajelli, Marco Massari, Piero Manfredi, Cesare Furlanello, Gianpaolo Scalia Tomba, Mimmo Iannelli, Mitigation measures for pandemic influenza in Italy: an individual based model considering different scenarios, PLoS One 3 (3) (2008) e1790.
[75] Marco Ajelli, Bruno Gonçalves, Duygu Balcan, Vittoria Colizza, Hao Hu, José J Ramasco, Stefano Merler, Alessandro Vespignani, Comparing large-scale computational approaches to epidemic modeling: agent-based versus structured metapopulation models, BMC Infect. Dis. 10 (1) (2010) 1–13.
[76] Marco Ajelli, Stefano Merler, An individual-based model of hepatitis A transmission, J. Theoret. Biol. 259 (3) (2009) 478–488.
[77] Elizabeth Hunter, Brian Mac Namee, John D. Kelleher, A taxonomy for agent-based models in human infectious disease epidemiology, J. Artif. Soc. Soc. Simul. 20 (3) (2017).
[78] M.C. González, H.J. Herrmann, Scaling of the propagation of epidemics in a system of mobile agents, Phys. A 340 (4) (2004) 741–748.
[79] Fernando Peruani, Gustavo J. Sibona, Dynamics and steady states in excitable mobile agent systems, Phys. Rev. Lett. 100 (16) (2008) 168103.
[80] Jie Zhou, Zonghua Liu, Epidemic spreading in communities with mobile agents, Phys. A 388 (7) (2009) 1228–1236.
[81] Marco Ajelli, Stefano Merler, The impact of the unstructured contacts component in influenza pandemic modeling, PLoS One 3 (1) (2008) e1519.
[82] Giorgio Guzzetta, Marco Ajelli, Zhenhua Yang, Stefano Merler, Cesare Furlanello, Denise Kirschner, Modeling socio-demography to capture tuberculosis transmission dynamics in a low burden setting, J. Theoret. Biol. 289 (2011) 197–205.
[83] Neal R Smith, James M Trauer, Manoj Gambhir, Jack S Richards, Richard J Maude, Jonathan M Keith, Jennifer A Flegg, Agent-based models of malaria transmission: a systematic review, Malar. J. 17 (1) (2018) 1–16.
[84] Catherine Linard, Nicolas Ponçon, Didier Fontenille, Eric F Lambin, A multi-agent simulation to assess the risk of malaria re-emergence in southern France, Ecol. Model. 220 (2) (2009) 160–174.
[85] Yoshiki Kuramoto, International symposium on mathematical problems in theoretical physics, Lecture Notes Phys. 30 (1975) 420.
[86] Yoshiki Kuramoto, Chemical Oscillations, Waves, and Turbulence, Springer, New York, 1984.
[87] Steven H. Strogatz, From Kuramoto to Crawford: exploring the onset of synchronization in populations of coupled oscillators, Physica D 143 (1–4) (2000) 1–20.
[88] Juan A Acebrón, Luis L Bonilla, Conrad J Pérez Vicente, Félix Ritort, Renato Spigler, The Kuramoto model: A simple paradigm for synchronization phenomena, Rev. Modern Phys. 77 (1) (2005) 137.
[89] Francisco A Rodrigues, Thomas K DM Peron, Peng Ji, Jürgen Kurths, The Kuramoto model in complex networks, Phys. Rep. 610 (2016) 1–98.
[90] David Sherrington, Scott Kirkpatrick, Solvable model of a spin-glass, Phys. Rev. Lett. 35 (26) (1975) 1792.
[91] Christoph Börgers, Nancy Kopell, Synchronization in networks of excitatory and inhibitory neurons with sparse, random connectivity, Neural Comput. 15 (3) (2003) 509–538.
[92] L.S. Tsimring, N.F. Rulkov, M.L. Larsen, Michael Gabbay, Repulsive synchronization in an array of phase oscillators, Phys. Rev. Lett. 95 (1) (2005) 014101.
[93] Hyunsuk Hong, Kevin P. O'Keeffe, Steven H. Strogatz, Phase coherence induced by correlated disorder, Phys. Rev. E 93 (2) (2016) 022219.
[94] Roberto C Budzinski, Tung T Nguyen, Jacqueline Doan, Jan Minac, Terrence J Sejnowski, Lyle E Muller, A simple geometry unites synchrony, chimeras, and waves in nonlinear oscillator networks, 2021, arXiv preprint arXiv:2111.02560.
[95] Hyunsuk Hong, Steven H. Strogatz, Conformists and contrarians in a Kuramoto model with identical natural frequencies, Phys. Rev. E 84 (4) (2011) 046202.
[96] Bernard Sonnenschein, Thomas K DM Peron, Francisco A Rodrigues, Jürgen Kurths, Lutz Schimansky-Geier, Collective dynamics in two populations of noisy oscillators with asymmetric interactions, Phys. Rev. E 91 (6) (2015) 062910.
[97] Edward Ott, Thomas M. Antonsen, Low dimensional behavior of large systems of globally coupled oscillators, Chaos 18 (3) (2008) 037113.
[98] Edward Ott, Thomas M. Antonsen, Long time evolution of phase oscillator systems, Chaos 19 (2) (2009) 023117.
[99] Hyunsuk Hong, Steven H. Strogatz, Mean-field behavior in coupled oscillators with attractive and repulsive interactions, Phys. Rev. E 85 (5) (2012) 056210.
[100] Dmytro Iatsenko, Spase Petkoski, PVE McClintock, A Stefanovska, Stationary and traveling wave states of the Kuramoto model with an arbitrary distribution of frequencies and coupling strengths, Phys. Rev. Lett. 110 (6) (2013) 064101.
[101] Spase Petkoski, Dmytro Iatsenko, Lasko Basnarkov, Aneta Stefanovska, Mean-field and mean-ensemble frequencies of a system of coupled oscillators, Phys. Rev. E 87 (3) (2013) 032908.
[102] Tian Qiu, Stefano Boccaletti, Ivan Bonamassa, Yong Zou, Jie Zhou, Zonghua Liu, Shuguang Guan, Synchronization and Bellerophon states in conformist and contrarian oscillators, Sci. Rep. 6 (1) (2016) 1–16.
[103] Di Yuan, Mei Zhang, Junzhong Yang, Dynamics of the Kuramoto model in the presence of correlation between distributions of frequencies and coupling strengths, Phys. Rev. E 89 (1) (2014) 012910.
[104] Di Yuan, Fang Lin, Limei Wang, Danyang Liu, Junzhong Yang, Yi Xiao, Multistable states in a system of coupled phase oscillators with inertia, Sci. Rep. 7 (1) (2017) 1–9.
[105] Jinha Park, B. Kahng, Metastable state en route to traveling-wave synchronization state, Phys. Rev. E 97 (2) (2018) 020203.
[106] Ping Ju, Qionglin Dai, Hongyan Cheng, Junzhong Yang, Dynamics in the Sakaguchi-Kuramoto model with two subpopulations, Phys. Rev. E 90 (1) (2014) 012903.
[107] Hidetsugu Sakaguchi, Yoshiki Kuramoto, A soluble active rotater model showing phase transitions via mutual entertainment, Progr. Theoret. Phys. 76 (3) (1986) 576–581.
[108] Di Yuan, Haitao Cui, Junlong Tian, Yi Xiao, Yingxin Zhang, Dynamics in the Kuramoto model with a bi-harmonic coupling function, Commun. Nonlinear Sci. Numer. Simul. 38 (2016) 23–29.
[109] Di Yuan, Jun-Long Tian, Fang Lin, Dong-Wei Ma, Jing Zhang, Hai-Tao Cui, Yi Xiao, Periodic synchronization in a system of coupled phase oscillators with attractive and repulsive interactions, Front. Phys. 13 (3) (2018) 1–7.
[110] Damián H. Zanette, Propagation of small perturbations in synchronized oscillator networks, Europhys. Lett. 68 (3) (2004) 356.
[111] Damián H. Zanette, Disturbing synchronization: Propagation of perturbations in networks of coupled oscillators, Eur. Phys. J. B 43 (1) (2005) 97–108.

[112] Bard Ermentrout, An adaptive model for synchrony in the firefly Pteroptyx malaccae, J. Math. Biol. 29 (6) (1991) 571–585.
[113] Jason Hindes, Philippe Jacquod, Ira B. Schwartz, Network desynchronization by non-Gaussian fluctuations, Phys. Rev. E 100 (5) (2019) 052314.
[114] Jonas Wassmer, Dirk Witthaut, Franz Kaiser, Targeted suppression of failure spreading in multistable oscillator networks, J. Phys.: Complexity 2 (3) (2021) 035003.
[115] Jiachen Ye, Thomas Peron, Wei Lin, Jürgen Kurths, Peng Ji, Performance measures after perturbations in the presence of inertia, Commun. Nonlinear Sci. Numer. Simul. 97 (2021) 105727.
[116] Manuel Gomez-Rodriguez, Jure Leskovec, Andreas Krause, Inferring networks of diffusion and influence, ACM Trans. Knowl. Discov. Data (TKDD) 5 (4) (2012) 1–37.
[117] Shlomo Havlin, Daniel Ben-Avraham, Diffusion in disordered media, Adv. Phys. 36 (6) (1987) 695–798.
[118] Naoki Masuda, Mason A. Porter, Renaud Lambiotte, Random walks and diffusion on networks, Phys. Rep. 716 (2017) 1–58.
[119] Stefano Boccaletti, Vito Latora, Yamir Moreno, Martin Chavez, D-U Hwang, Complex networks: Structure and dynamics, Phys. Rep. 424 (4–5) (2006) 175–308.
[120] Letizia Milli, Giulio Rossetti, Dino Pedreschi, Fosca Giannotti, Active and passive diffusion processes in complex networks, Appl. Netw. Sci. 3 (1) (2018) 1–15.
[121] Zi-Ke Zhang, Chuang Liu, Xiu-Xiu Zhan, Xin Lu, Chu-Xu Zhang, Yi-Cheng Zhang, Dynamics of information diffusion and its applications on complex networks, Phys. Rep. 651 (2016) 1–34.
[122] Sergio Gomez, Albert Diaz-Guilera, Jesus Gomez-Gardenes, Conrad J Perez-Vicente, Yamir Moreno, Alex Arenas, Diffusion dynamics on multiplex networks, Phys. Rev. Lett. 110 (2) (2013) 028701.
[123] Matjaž Perc, Diffusion dynamics and information spreading in multilayer networks: An overview, Eur. Phys. J. Spec. Top. 228 (11) (2019) 2351–2355.
[124] Oliver Ibe, Markov Processes for Stochastic Modeling, Newnes, 2013.
[125] Fabrizio Gabbiani, Steven J. Cox, Mathematics for Neuroscientists, Academic Press, 2017.
[126] Andrea Avena-Koenigsberger, Xiaoran Yan, Artemy Kolchinsky, Martijn P van den Heuvel, Patric Hagmann, Olaf Sporns, A spectrum of routing strategies for brain networks, PLoS Comput. Biol. 15 (3) (2019) e1006833.
[127] Takamitsu Watanabe, Geraint Rees, Brain network dynamics in high-functioning individuals with autism, Nature Commun. 8 (1) (2017) 1–14.
[128] Carson Ingo, Richard L Magin, Luis Colon-Perez, William Triplett, Thomas H Mareci, On random walks and entropy in diffusion-weighted magnetic resonance imaging studies of neural tissue, Magn. Reson. Med. 71 (2) (2014) 617–627.
[129] Nicolas E Humphries, Nuno Queiroz, Jennifer RM Dyer, Nicolas G Pade, Michael K Musyl, Kurt M Schaefer, Daniel W Fuller, Juerg M Brunnschweiler, Thomas K Doyle, Jonathan DR Houghton, et al., Environmental context explains Lévy and Brownian movement patterns of marine predators, Nature 465 (7301) (2010) 1066–1069.
[130] Gandhimohan M Viswanathan, Marcos GE Da Luz, Ernesto P Raposo, H Eugene Stanley, The Physics of Foraging: an Introduction to Random Searches and Biological Encounters, Cambridge University Press, 2011.
[131] Edward A. Codling, Michael J. Plank, Simon Benhamou, Random walk models in biology, J. R. Soc. Interface 5 (25) (2008) 813–834.
[132] Yannis P Papastamatiou, Carl G Meyer, Felipe Carvalho, Jonathon J Dale, Melanie R Hutchinson, Kim N Holland, Telemetry and random-walk models reveal complex patterns of partial migration in a large marine predator, Ecology 94 (11) (2013) 2595–2606.
[133] David A Raichlen, Brian M Wood, Adam D Gordon, Audax ZP Mabulla, Frank W Marlowe, Herman Pontzer, Evidence of Lévy walk foraging patterns in human hunter–gatherers, Proc. Natl. Acad. Sci. 111 (2) (2014) 728–733.
[134] Nicolas E Humphries, Henri Weimerskirch, Nuno Queiroz, Emily J Southall, David W Sims, Foraging success of biological Lévy flights recorded in situ, Proc. Natl. Acad. Sci. 109 (19) (2012) 7169–7174.
[135] Lysanne Snijders, Ralf HJM Kurvers, Stefan Krause, Indar W Ramnarine, Jens Krause, Individual-and population-level drivers of consistent foraging success across environments, Nat. Ecol. Evol. 2 (10) (2018) 1610–1618.
[136] Théo Michelot, Roland Langrock, Toby A. Patterson, moveHMM: an R package for the statistical modelling of animal movement data using hidden Markov models, Methods Ecol. Evolut. 7 (11) (2016) 1308–1315.
[137] Cristina Dimidov, Giuseppe Oriolo, Vito Trianni, Random walks in swarm robotics: an experiment with kilobots, in: International Conference on Swarm Intelligence, Springer, 2016, pp. 185–196.
[138] Adam Schroeder, Subramanian Ramakrishnan, Manish Kumar, Brian Trease, Efficient spatial coverage by a robot swarm based on an ant foraging model and the Lévy distribution, Swarm Intell. 11 (1) (2017) 39–69.
[139] Karthik Elamvazhuthi, Spring Berman, Mean-field models in swarm robotics: A survey, Bioinspiration Biomim. 15 (1) (2019) 015001.
[140] Simon O Obute, Philip Kilby, Mehmet R Dogar, Jordan H Boyle, Swarm foraging under communication and vision uncertainties, IEEE Trans. Autom. Sci. Eng. (2022).
[141] Emma Milner, Mahesh Sooriyabandara, Sabine Hauert, Stochastic behaviours for retrieval of storage items using simulated robot swarms, Artif. Life Robot. 27 (2) (2022) 264–271.
[142] Agata Fronczak, Piotr Fronczak, Biased random walks in complex networks: The role of local navigation rules, Phys. Rev. E 80 (1) (2009) 016107.
[143] Benjamin F. Maier, Dirk Brockmann, Cover time for random walks on arbitrary complex networks, Phys. Rev. E 96 (4) (2017) 042307.
[144] Moreno Bonaventura, Vincenzo Nicosia, Vito Latora, Characteristic times of biased random walks on complex networks, Phys. Rev. E 89 (1) (2014) 012803.
[145] Jae Dong Noh, Heiko Rieger, Random walks on complex networks, Phys. Rev. Lett. 92 (11) (2004) 118701.
[146] Naoki Masuda, Renaud Lambiotte, A Guide To Temporal Networks, World Scientific, 2016.
[147] Wen-Xu Wang, Bing-Hong Wang, Chuan-Yang Yin, Yan-Bo Xie, Tao Zhou, Traffic dynamics based on local routing protocol on a scale-free network, Phys. Rev. E 73 (2) (2006) 026111.
[148] Alejandro P. Riascos, José L. Mateos, Random walks on weighted networks: a survey of local and non-local dynamics, J. Complex Netw. 9 (5) (2021) cnab032.
[149] Mark Newman, Networks, Oxford University Press, 2018.
[150] Zdzislaw Burda, Jarek Duda, Jean-Marc Luck, Bartek Waclaw, Localization of the maximal entropy random walk, Phys. Rev. Lett. 102 (16) (2009) 160602.
[151] Roberta Sinatra, Jesús Gómez-Gardenes, Renaud Lambiotte, Vincenzo Nicosia, Vito Latora, Maximal-entropy random walks in complex networks with limited information, Phys. Rev. E 83 (3) (2011) 030103.
[152] Shi-Jie Yang, Exploring complex networks by walking on them, Phys. Rev. E 71 (1) (2005) 016107.
[153] Christopher Sebastian Hidalgo Calva, Alejandro P. Riascos, Optimal exploration of random walks with local bias on networks, Phys. Rev. E 105 (4) (2022) 044318.
[154] Xiang Ling, Mao-Bin Hu, Rui Jiang, Qing-Song Wu, Global dynamic routing for scale-free networks, Phys. Rev. E 81 (1) (2010) 016113.
[155] Shengyong Chen, Wei Huang, Carlo Cattani, Giuseppe Altieri, Traffic dynamics on complex networks: a survey, Math. Probl. Eng. 2012 (2012).
[156] Manlio De Domenico, Albert Solé-Ribalta, Sergio Gómez, Alex Arenas, Navigability of interconnected networks under random failures, Proc. Natl. Acad. Sci. 111 (23) (2014) 8351–8356.

[157] Steven Riley, Ken Eames, Valerie Isham, Denis Mollison, Pieter Trapman, Five challenges for spatial epidemic models, Epidemics 10 (2015) 68–71.
[158] Moez Draief, Ayalvadi Ganesh, A random walk model for infection on graphs: spread of epidemics & rumours with mobile agents, Discrete Event Dyn. Syst. 21 (1) (2011) 41–61.
[159] Nilanjana Datta, Tony C. Dorlas, Random walks on a complete graph: a model for infection, J. Appl. Probab. 41 (4) (2004) 1008–1021.
[160] Tassos Dimitriou, Sotiris Nikoletseas, Paul Spirakis, The infection time of graphs, Discrete Appl. Math. 154 (18) (2006) 2577–2589.
[161] Takuya Ohwa, Exact computation for meeting times and infection times of random walks on graphs, Pac. J. Math. Ind. 7 (1) (2015) 1–9.
[162] Daniel Figueiredo, Giulio Iacobelli, Seva Shneer, The end time of SIS epidemics driven by random walks on edge-transitive graphs, J. Stat. Phys. 179 (3) (2020) 651–671.
[163] Oskar Hallatschek, Daniel S. Fisher, Acceleration of evolutionary spread by long-range dispersal, Proc. Natl. Acad. Sci. 111 (46) (2014) E4911–E4919.
[164] François Baccelli, Nithin Ramesan, A computational framework for evaluating the role of mobility on the propagation of epidemics on point processes, J. Math. Biol. 84 (1) (2022) 1–40.
[165] Michael Bestehorn, Alejandro P Riascos, Thomas M Michelitsch, Bernard A Collet, A Markovian random walk model of epidemic spreading, Contin. Mech. Thermodyn. 33 (4) (2021) 1207–1221.
[166] Arturo Buscarino, Luigi Fortuna, Mattia Frasca, Alessandro Rizzo, Dynamical network interactions in distributed control of robots, Chaos 16 (1) (2006) 015116.
[167] Mattia Frasca, Arturo Buscarino, Alessandro Rizzo, Luigi Fortuna, Stefano Boccaletti, Dynamical network model of infective mobile agents, Phys. Rev. E 74 (3) (2006) 036110.
[168] Mattia Frasca, Arturo Buscarino, Alessandro Rizzo, Luigi Fortuna, Stefano Boccaletti, Synchronization of moving chaotic agents, Phys. Rev. Lett. 100 (4) (2008) 044102.
[169] Naoya Fujiwara, Jürgen Kurths, Albert Díaz-Guilera, Synchronization in networks of mobile oscillators, Phys. Rev. E 83 (2) (2011) 025101.
[170] Sayantan Nag Chowdhury, Soumen Majhi, Mahmut Ozer, Dibakar Ghosh, Matjaž Perc, Synchronization to extreme events in moving agents, New J. Phys. 21 (7) (2019) 073048.
[171] Sayantan Nag Chowdhury, Soumen Majhi, Dibakar Ghosh, Distance dependent competitive interactions in a frustrated network of mobile agents, IEEE Trans. Netw. Sci. Eng. 7 (4) (2020) 3159–3170.
[172] Sayantan Nag Chowdhury, Srilena Kundu, Maja Duh, Matjaž Perc, Dibakar Ghosh, Cooperation on interdependent networks by means of migration and stochastic imitation, Entropy 22 (4) (2020) 485.
[173] Yunhan Huang, Li Ding, Yun Feng, Jiangtian Pan, Epidemic spreading in random walkers with heterogeneous interaction radius, J. Stat. Mech. Theory Exp. 2016 (10) (2016) 103501.
[174] S. Triambak, D.P. Mahapatra, A random walk Monte Carlo simulation study of COVID-19-like infection spread, Phys. A 574 (2021) 126014.
[175] Benjamin F. Maier, Dirk Brockmann, Effective containment explains subexponential growth in recent confirmed COVID-19 cases in China, Science 368 (6492) (2020) 742–746.
[176] D.P. Mahapatra, S. Triambak, Towards predicting COVID-19 infection waves: A random-walk Monte Carlo simulation approach, Chaos Solitons Fractals 156 (2022) 111785.
[177] Andrew Chu, Greg Huber, Aaron McGeever, Boris Veytsman, David Yllanes, A random-walk-based epidemiological model, Sci. Rep. 11 (1) (2021) 1–11.
[178] Santo Fortunato, Community detection in graphs, Phys. Rep. 486 (3–5) (2010) 75–174.
[179] Martin Rosvall, Carl T. Bergstrom, Maps of random walks on complex networks reveal community structure, Proc. Natl. Acad. Sci. 105 (4) (2008) 1118–1123.
[180] Caio Seguin, Olaf Sporns, Andrew Zalesky, Fernando Calamante, et al., Network communication models narrow the gap between the modular organization of structural and functional brain networks, NeuroImage (2022) 119323.
[181] Joaquín Goñi, Martijn P Van Den Heuvel, Andrea Avena-Koenigsberger, Nieves Velez de Mendizabal, Richard F Betzel, Alessandra Griffa, Patric Hagmann, Bernat Corominas-Murtra, Jean-Philippe Thiran, Olaf Sporns, Resting-brain functional connectivity predicted by analytic measures of network communication, Proc. Natl. Acad. Sci. 111 (2) (2014) 833–838.
[182] Samuel P Fraiberger, Roberta Sinatra, Magnus Resch, Christoph Riedl, Albert-László Barabási, Quantifying reputation and success in art, Science 362 (6416) (2018) 825–829.
[183] Martin Rosvall, Alcides V Esquivel, Andrea Lancichinetti, Jevin D West, Renaud Lambiotte, Memory in network flows and its effects on spreading dynamics and community detection, Nature Commun. 5 (1) (2014) 1–13.
[184] Austin R. Benson, David F. Gleich, Lek-Heng Lim, The spacey random walk: A stochastic process for higher-order data, SIAM Rev. 59 (2) (2017) 321–345.
[185] Renaud Lambiotte, Martin Rosvall, Ingo Scholtes, From networks to optimal higher-order models of complex systems, Nat. Phys. 15 (4) (2019) 313–320.
[186] Timoteo Carletti, Federico Battiston, Giulia Cencetti, Duccio Fanelli, Random walks on hypergraphs, Phys. Rev. E 101 (2) (2020) 022308.
[187] Timoteo Carletti, Duccio Fanelli, Renaud Lambiotte, Random walks and community detection in hypergraphs, J. Phy.: Complexity 2 (1) (2021) 015011.
[188] Sayan Mukherjee, John Steenbergen, Random walks on simplicial complexes and harmonics, Random Struct. Algorithms 49 (2) (2016) 379–405.
[189] Austin R Benson, Rediet Abebe, Michael T Schaub, Ali Jadbabaie, Jon Kleinberg, Simplicial closure and higher-order link prediction, Proc. Natl. Acad. Sci. 115 (48) (2018) E11221–E11230.
[190] Michael T Schaub, Austin R Benson, Paul Horn, Gabor Lippner, Ali Jadbabaie, Random walks on simplicial complexes and the normalized Hodge 1-Laplacian, SIAM Rev. 62 (2) (2020) 353–391.
[191] Ajay Kumar, Shashank Sheshar Singh, Kuldeep Singh, Bhaskar Biswas, Link prediction techniques, applications, and performance: A survey, Phys. A 553 (2020) 124289.
[192] Pu Wang, Marta C González, César A Hidalgo, Albert-László Barabási, Understanding the spreading patterns of mobile phone viruses, Science 324 (5930) (2009) 1071–1076.
[193] E.J. Crampin, P.K. Maini, Reaction-diffusion models for biological pattern formation, Methods Appl. Anal. 8 (3) (2001) 415–428.
[194] James Dickson Murray, Mathematical Biology: I. an Introduction, Springer, 2002.
[195] Argha Mondal, Sanjeev Kumar Sharma, Ranjit Kumar Upadhyay, MA Aziz-Alaoui, Prosenjit Kundu, Chittaranjan Hens, Diffusion dynamics of a conductance-based neuronal population, Phys. Rev. E 99 (4) (2019) 042307.
[196] Mark C. Cross, Pierre C. Hohenberg, Pattern formation outside of equilibrium, Rev. Modern Phys. 65 (3) (1993) 851.
[197] J.A. Scott Kelso, Dynamic Patterns: The Self-Organization of Brain and Behavior, MIT Press, 1995.
[198] Michael Taylor, Partial Differential Equations II: Qualitative Studies of Linear Equations, Vol. 116, Springer Science & Business Media, 2013.
[199] James D. Murray, Philip K. Maini, Robert T. Tranquillo, Mechanochemical models for generating biological pattern and form in development, Phys. Rep. 171 (2) (1988) 59–84.
[200] A.M. Turing, The chemical basis of mokphogenesis, Philos. Trans. R. Soc. Lond. Ser. B 237 (641) (1952) 37–72.

[201] G.F. Oster, J.D. Murray, A.K. Harris, Mechanical aspects of mesenchymal morphogenesis, J. Embryol. Exp. Morphol. 78 (1983) 83–125.
[202] J.D. Murray, G.F. Oster, A.K. Harris, A mechanical model for mesenchymal morphogenesis, J. Math. Biol. (Print) 17 (1) (1983) 125–129.
[203] Graham Griffiths, William E. Schiesser, Traveling Wave Analysis of Partial Differential Equations: Numerical and Analytical Methods with MATLAB and Maple, Academic Press, 2010.
[204] Philip K Maini, Thomas E Woolley, Ruth E Baker, Eamonn A Gaffney, S Seirin Lee, Turing's model for biological pattern formation and the robustness problem, Interface focus 2 (4) (2012) 487–496.
[205] Alfred Gierer, Hans Meinhardt, A theory of biological pattern formation, Kybernetik 12 (1) (1972) 30–39.
[206] Shigeru Kondo, Takashi Miura, Reaction-diffusion model as a framework for understanding biological pattern formation, Science 329 (5999) (2010) 1616–1620.
[207] Igor S. Aranson, Lorenz Kramer, The world of the complex Ginzburg-Landau equation, Rev. Modern Phys. 74 (1) (2002) 99.
[208] Rushikesh Sheth, Luciano Marcon, M Félix Bastida, Marisa Junco, Laura Quintana, Randall Dahn, Marie Kmita, James Sharpe, Maria A Ros, Hox genes regulate digit patterning by controlling the wavelength of a Turing-type mechanism, Science 338 (6113) (2012) 1476–1480.
[209] Nicola Bellomo, Abdelghani Bellouquid, Youshan Tao, Michael Winkler, Toward a mathematical theory of Keller–Segel models of pattern formation in biological tissues, Math. Models Methods Appl. Sci. 25 (09) (2015) 1663–1763.
[210] Tobias Reichenbach, Mauro Mobilia, Erwin Frey, Noise and correlations in a spatial population model with cyclic competition, Phys. Rev. Lett. 99 (23) (2007) 238105.
[211] Attila Szolnoki, Mauro Mobilia, Luo-Luo Jiang, Bartosz Szczesny, Alastair M Rucklidge, Matjaž Perc, Cyclic dominance in evolutionary games: a review, J. R. Soc. Interface 11 (100) (2014) 20140735.
[212] György Szabó, István Borsos, Evolutionary potential games on lattices, Phys. Rep. 624 (2016) 1–60.
[213] Sahil Islam, Argha Mondal, Mauro Mobilia, Sirshendu Bhattacharyya, Chittaranjan Hens, Effect of mobility in the rock-paper-scissor dynamics with high mortality, Phys. Rev. E 105 (1) (2022) 014215.
[214] Ulrich Dobramysl, Mauro Mobilia, Michel Pleimling, Uwe C Täuber, Stochastic population dynamics in spatially extended predator–prey systems, J. Phys. A 51 (6) (2018) 063001.
[215] Hiroya Nakao, Alexander S. Mikhailov, Turing patterns in network-organized activator–inhibitor systems, Nat. Phys. 6 (7) (2010) 544–550.
[216] Hans G. Othmer, L.E. Scriven, Instability and dynamic pattern in cellular networks, J. Theoret. Biol. 32 (3) (1971) 507–537.
[217] Malbor Asllani, Joseph D Challenger, Francesco Saverio Pavone, Leonardo Sacconi, Duccio Fanelli, The theory of pattern formation on directed networks, Nature Commun. 5 (1) (2014) 1–9.
[218] Nikos E. Kouvaris, Shigefumi Hata, Albert Díaz Guilera, Pattern formation in multiplex networks, Sci. Rep. 5 (1) (2015) 1–9.
[219] Chen Liu, Shupeng Gao, Mingrui Song, Yue Bai, Lili Chang, Zhen Wang, Optimal control of the reaction–diffusion process on directed networks, Chaos 32 (6) (2022) 063115.
[220] Shupeng Gao, Lili Chang, Ivan Romić, Zhen Wang, Marko Jusup, Petter Holme, Optimal control of networked reaction–diffusion systems, J. R. Soc. Interface 19 (188) (2022) 20210739.
[221] Lili Chang, Chen Liu, Guiquan Sun, Zhen Wang, Zhen Jin, Delay-induced patterns in a predator–prey model on complex networks with diffusion, New J. Phys. 21 (7) (2019) 073035.
[222] Moran Duan, Lili Chang, Zhen Jin, Turing patterns of an SI epidemic model with cross-diffusion on complex networks, Phys. A 533 (2019) 122023.
[223] Lili Chang, Moran Duan, Guiquan Sun, Zhen Jin, Cross-diffusion-induced patterns in an SIR epidemic model on complex networks, Chaos 30 (1) (2020) 013147.
[224] Linhe Zhu, Xuewei Wang, Huihui Zhang, Shuling Shen, Yimin Li, Yudong Zhou, Dynamics analysis and optimal control strategy for a SIRS epidemic model with two discrete time delays, Phys. Scr. 95 (3) (2020) 035213.
[225] Alberto d'Onofrio, Malay Banerjee, Piero Manfredi, Spatial behavioural responses to the spread of an infectious disease can suppress Turing and Turing–Hopf patterning of the disease, Phys. A 545 (2020) 123773.
[226] Andrew L Krause, Eamonn A Gaffney, Philip K Maini, Václav Klika, Modern perspectives on near-equilibrium analysis of Turing systems, Phil. Trans. R. Soc. A 379 (2213) (2021) 20200268.
[227] Juan A. Almendral, Albert Díaz-Guilera, Dynamical and spectral properties of complex networks, New J. Phys. 9 (6) (2007) 187.
[228] Adilson E. Motter, Changsong Zhou, Jürgen Kurths, Network synchronization, diffusion, and the paradox of heterogeneity, Phys. Rev. E 71 (1) (2005) 016116.
[229] Vincent D Blondel, Julien M Hendrickx, Alex Olshevsky, John N Tsitsiklis, Convergence in multiagent coordination, consensus, and flocking, in: Proceedings of the 44th IEEE Conference on Decision and Control, IEEE, 2005, pp. 2996–3000.
[230] Ming Li, Run-Ran Liu, Linyuan Lü, Mao-Bin Hu, Shuqi Xu, Yi-Cheng Zhang, Percolation on complex networks: Theory and application, Phys. Rep. 907 (2021) 1–68.
[231] Stephen B. Seidman, Network structure and minimum degree, Social Networks 5 (3) (1983) 269–287.
[232] Béla Bollobás, Graph Theory and Combinatorics: Proceedings of the Cambridge Combinatorial Conference in Honour of Paul ErdÖS,[Trinity College, Cambridge, 21-25 March 1983], Academic Press, 1984.
[233] Boris Pittel, Joel Spencer, Nicholas Wormald, Sudden emergence of a giantk-core in a random graph, J. Combin. Theory Ser. B 67 (1) (1996) 111–151.
[234] A.B. Harris, T.C. Lubensky, Field theoretic approaches to biconnectedness in percolating systems, J. Phys. A: Math. Gen. 16 (11) (1983) L365.
[235] Sergey N Dorogovtsev, Alexander V Goltsev, Jose Ferreira F Mendes, K-core organization of complex networks, Phys. Rev. Lett. 96 (4) (2006) 040601.
[236] Alexander V Goltsev, Sergey N Dorogovtsev, Jose Ferreira F Mendes, k-core (bootstrap) percolation on complex networks: Critical phenomena and nonlocal effects, Phys. Rev. E 73 (5) (2006) 056101.
[237] M.E.J. Newman, Gourab Ghoshal, Bicomponents and the robustness of networks to failure, Phys. Rev. Lett. 100 (13) (2008) 138701.
[238] John Chalupa, Paul L. Leath, Gary R. Reich, Bootstrap percolation on a Bethe lattice, J. Phys. C: Solid State Phys. 12 (1) (1979) L31.
[239] Yong Zhu, Xiaosong Chen, Revealing the phase transition behaviors of k-core percolation in random networks, 2017, arXiv preprint arXiv:1710.02959.
[240] P. Kim, D.-S. Lee, B. Kahng, Phase transition in the biconnectivity of scale-free networks, Phys. Rev. E 87 (2) (2013) 022804.
[241] Hendrik Schawe, Alexander K. Hartmann, Large-deviation properties of the largest biconnected component for random graphs, Eur. Phys. J. B 92 (4) (2019) 1–9.
[242] Xin Yuan, Yang Dai, H. Eugene Stanley, Shlomo Havlin, k-core percolation on complex networks: Comparing random, localized, and targeted attacks, Phys. Rev. E 93 (6) (2016) 062302.
[243] N. Azimi-Tafreshi, J. Gómez-Gardenes, S.N. Dorogovtsev, k-core percolation on multiplex networks, Phys. Rev. E 90 (3) (2014) 032816.
[244] Nagendra K Panduranga, Jianxi Gao, Xin Yuan, H Eugene Stanley, Shlomo Havlin, Generalized model for k-core percolation and interdependent networks, Phys. Rev. E 96 (3) (2017) 032317.
[245] Yilun Shang, Generalized k-core percolation on correlated and uncorrelated multiplex networks, Phys. Rev. E 101 (4) (2020) 042306.

[246] Kexian Zheng, Ying Liu, Yang Wang, Wei Wang, k-core percolation on interdependent and interconnected multiplex networks, Europhys. Lett. 133 (4) (2021) 48003.
[247] Yilun Shang, Generalized K-Core percolation in networks with community structure, SIAM J. Appl. Math. 80 (3) (2020) 1272–1289.
[248] Wei Wang, Wenyao Li, Tao Lin, Tao Wu, Liming Pan, Yanbing Liu, Generalized k-core percolation on higher-order dependent networks, Appl. Math. Comput. 420 (2022) 126793.
[249] Gareth J Baxter, Sergey N Dorogovtsev, Alexander V Goltsev, José FF Mendes, Heterogeneous k-core versus bootstrap percolation on complex networks, Phys. Rev. E 83 (5) (2011) 051134.
[250] Davide Cellai, Aonghus Lawlor, Kenneth A Dawson, James P Gleeson, Tricritical point in heterogeneous k-core percolation, Phys. Rev. Lett. 107 (17) (2011) 175703.
[251] Davide Cellai, Aonghus Lawlor, Kenneth A Dawson, James P Gleeson, Critical phenomena in heterogeneous k-core percolation, Phys. Rev. E 87 (2) (2013) 022134.
[252] Davide Cellai, James P. Gleeson, Singularities in ternary mixtures of k-core percolation, in: Complex Networks IV, Springer, 2013, pp. 165–172.
[253] Huiseung Chae, Soon-Hyung Yook, Yup Kim, Complete set of types of phase transition in generalized heterogeneous k-core percolation, Phys. Rev. E 89 (5) (2014) 052134.
[254] Joan Adler, Amnon Aharony, Diffusion percolation. I. Infinite time limit and bootstrap percolation, J. Phys. A: Math. Gen. 21 (6) (1988) 1387.
[255] Duncan J. Watts, A simple model of global cascades on random networks, Proc. Natl. Acad. Sci. 99 (9) (2002) 5766–5771.
[256] Michael Aizenman, Joel L. Lebowitz, Metastability effects in bootstrap percolation, J. Phys. A: Math. Gen. 21 (19) (1988) 3801.
[257] Raphaël Cerf, Emilio N.M. Cirillo, Finite size scaling in three-dimensional bootstrap percolation, Ann. Probab. 27 (4) (1999) 1837–1850.
[258] Raphaël Cerf, Francesco Manzo, The threshold regime of finite volume bootstrap percolation, Stochastic Process. Appl. 101 (1) (2002) 69–82.
[259] Alexander E. Holroyd, Sharp metastability threshold for two-dimensional bootstrap percolation, Probab. Theory Related Fields 125 (2) (2003) 195–224.
[260] Alexander Holroyd, The metastability threshold for modified bootstrap percolation in d dimensions, Electron. J. Probab. 11 (2006) 418–433.
[261] József Balogh, Béla Bollobás, Bootstrap percolation on the hypercube, Probab. Theory Related Fields 134 (4) (2006) 624–648.
[262] József Balogh, Béla Bollobás, Hugo Duminil-Copin, Robert Morris, The sharp threshold for bootstrap percolation in all dimensions, Trans. Amer. Math. Soc. 364 (5) (2012) 2667–2701.
[263] József Balogh, Yuval Peres, Gábor Pete, Bootstrap percolation on infinite trees and non-amenable groups, Combin. Probab. Comput. 15 (5) (2006) 715–730.
[264] József Balogh, Boris G. Pittel, Bootstrap percolation on the random regular graph, Random Struct. Algorithms 30 (1–2) (2007) 257–286.
[265] Luiz R.G. Fontes, Roberto H. Schonmann, Bootstrap percolation on homogeneous trees has 2 phase transitions, J. Stat. Phys. 132 (5) (2008) 839–861.
[266] Hamed Amini, Nikolaos Fountoulakis, Bootstrap percolation in power-law random graphs, J. Stat. Phys. 155 (1) (2014) 72–92.
[267] Gareth J Baxter, Sergey N Dorogovtsev, Alexander V Goltsev, José FF Mendes, Bootstrap percolation on complex networks, Phys. Rev. E 82 (1) (2010) 011103.
[268] Svante Janson, Tomasz Łuczak, Tatyana Turova, Thomas Vallier, Bootstrap percolation on the random graph $G_{n,p}$, Ann. Appl. Probab. 22 (5) (2012) 1989–2047.
[269] Matías A Di Muro, Lucas D Valdez, H Eugene Stanley, Sergey V Buldyrev, Lidia A Braunstein, Insights into bootstrap percolation: Its equivalence with k-core percolation and the giant component, Phys. Rev. E 99 (2) (2019) 022311.
[270] Matías A Di Muro, Sergey V Buldyrev, Lidia A Braunstein, Reversible bootstrap percolation: Fake news and fact checking, Phys. Rev. E 101 (4) (2020) 042307.
[271] Svante Janson, On percolation in random graphs with given vertex degrees, Electron. J. Probab. 14 (2009) 86–118.
[272] Joel C. Miller, Equivalence of several generalized percolation models on networks, Phys. Rev. E 94 (3) (2016) 032313.
[273] Ruifeng Yan, Tapan Kumar Saha, Feifei Bai, Huajie Gu, et al., The anatomy of the 2016 South Australia blackout: A catastrophic event in a high renewable network, IEEE Trans. Power Syst. 33 (5) (2018) 5374–5388.
[274] Adilson E. Motter, Ying-Cheng Lai, Cascade-based attacks on complex networks, Phys. Rev. E 66 (6) (2002) 065102.
[275] K.-I. Goh, Byungnam Kahng, Doochul Kim, Universal behavior of load distribution in scale-free networks, Phys. Rev. Lett. 87 (27) (2001) 278701.
[276] Paolo Crucitti, Vito Latora, Massimo Marchiori, Model for cascading failures in complex networks, Phys. Rev. E 69 (4) (2004) 045104.
[277] Yosef Kornbluth, Gilad Barach, Yaakov Tuchman, Benjamin Kadish, Gabriel Cwilich, Sergey V Buldyrev, Network overload due to massive attacks, Phys. Rev. E 97 (5) (2018) 052309.
[278] Jichang Zhao, Daqing Li, Hillel Sanhedrai, Reuven Cohen, Shlomo Havlin, Spatio-temporal propagation of cascading overload failures in spatially embedded networks, Nature Commun. 7 (1) (2016) 1–6.
[279] Yang Yang, Takashi Nishikawa, Adilson E. Motter, Vulnerability and cosusceptibility determine the size of network cascades, Phys. Rev. Lett. 118 (4) (2017) 048301.
[280] Dirk Witthaut, Marc Timme, Nonlocal effects and countermeasures in cascading failures, Phys. Rev. E 92 (3) (2015) 032809.
[281] Jeff Ash, David Newth, Optimizing complex networks for resilience against cascading failure, Phys. A 380 (2007) 673–683.
[282] Rui Yang, Wen-Xu Wang, Ying-Cheng Lai, Guanrong Chen, Optimal weighting scheme for suppressing cascades and traffic congestion in complex networks, Phys. Rev. E 79 (2) (2009) 026112.
[283] Baharan Mirzasoleiman, Mahmoudreza Babaei, Mahdi Jalili, MohammadAli Safari, Cascaded failures in weighted networks, Phys. Rev. E 84 (4) (2011) 046114.
[284] Yucheng Hao, Yanhui Wang, Limin Jia, Zhichao He, Cascading failures in networks with the harmonic closeness under edge attack strategies, Chaos Solitons Fractals 135 (2020) 109772.
[285] Wen-Xu Wang, Guanrong Chen, Universal robustness characteristic of weighted networks against cascading failure, Phys. Rev. E 77 (2) (2008) 026101.
[286] Mirko Schäfer, Jan Scholz, Martin Greiner, Proactive robustness control of heterogeneously loaded networks, Phys. Rev. Lett. 96 (10) (2006) 108701.
[287] Bing Wang, Beom Jun Kim, A high-robustness and low-cost model for cascading failures, Europhys. Lett. 78 (4) (2007) 48001.
[288] Ding-Xue Zhang, Dan Zhao, Zhi-Hong Guan, Yonghong Wu, Ming Chi, Gui-Lin Zheng, Probabilistic analysis of cascade failure dynamics in complex network, Phys. A 461 (2016) 299–309.
[289] Jianwei Wang, Robustness of complex networks with the local protection strategy against cascading failures, Saf. Sci. 53 (2013) 219–225.
[290] Zhong-Yuan Jiang, Jian-Feng Ma, An efficient local cascade defense method in complex networks, Internat. J. Modern Phys. C 28 (03) (2017) 1750031.
[291] Jianwei Wang, Mitigation strategies on scale-free networks against cascading failures, Phys. A 392 (9) (2013) 2257–2264.
[292] Adilson E. Motter, Cascade control and defense in complex networks, Phys. Rev. Lett. 93 (9) (2004) 098701.
[293] Sen Nie, Xuwen Wang, Haifeng Zhang, Qilang Li, Binghong Wang, Robustness of controllability for networks based on edge-attack, PLoS One 9 (2) (2014) e89066.

[294] Thomas C. Schelling, Hockey helmets, concealed weapons, and daylight saving: A study of binary choices with externalities, J. Confl. Resolut. 17 (3) (1973) 381–428.
[295] James P. Gleeson, Diarmuid J. Cahalane, Seed size strongly affects cascades on random networks, Phys. Rev. E 75 (5) (2007) 056103.
[296] Run-Ran Liu, Wen-Xu Wang, Ying-Cheng Lai, Bing-Hong Wang, Cascading dynamics on random networks: Crossover in phase transition, Phys. Rev. E 85 (2) (2012) 026110.
[297] M.E.J. Newman, Assortative mixing in networks, Phys. Rev. Lett. 89 (2002) 208701.
[298] Aram Galstyan, Paul Cohen, Cascading dynamics in modular networks, Phys. Rev. E 75 (3) (2007) 036109.
[299] James P. Gleeson, Cascades on correlated and modular random networks, Phys. Rev. E 77 (4) (2008) 046117.
[300] Peter Sheridan Dodds, Joshua L. Payne, Analysis of a threshold model of social contagion on degree-correlated networks, Phys. Rev. E 79 (6) (2009) 066115.
[301] Mark E.J. Newman, Random graphs with clustering, Phys. Rev. Lett. 103 (5) (2009) 058701.
[302] Adam Hackett, Sergey Melnik, James P. Gleeson, Cascades on a class of clustered random networks, Phys. Rev. E 83 (5) (2011) 056107.
[303] Damon Centola, Víctor M. Eguíluz, Michael W. Macy, Cascade dynamics of complex propagation, Phys. A 374 (1) (2007) 449–456.
[304] Charles D. Brummitt, Kyu-Min Lee, K.-I. Goh, Multiplexity-facilitated cascades in networks, Phys. Rev. E 85 (4) (2012) 045102.
[305] Taro Takaguchi, Naoki Masuda, Petter Holme, Bursty communication patterns facilitate spreading in a threshold-based epidemic dynamics, PLoS One 8 (7) (2013) e68629.
[306] Fariba Karimi, Petter Holme, Threshold model of cascades in empirical temporal networks, Phys. A 392 (16) (2013) 3476–3483.
[307] Ville-Pekka Backlund, Jari Saramäki, Raj Kumar Pan, Effects of temporal correlations on cascades: Threshold models on temporal networks, Phys. Rev. E 89 (6) (2014) 062815.
[308] Eva A Naumann, James E Fitzgerald, Timothy W Dunn, Jason Rihel, Haim Sompolinsky, Florian Engert, From whole-brain data to functional circuit models: the zebrafish optomotor response, Cell 167 (4) (2016) 947–960.
[309] Dimitry Fisher, Itsaso Olasagasti, David W Tank, Emre RF Aksay, Mark S Goldman, A modeling framework for deriving the structural and functional architecture of a short-term memory microcircuit, Neuron 79 (5) (2013) 987–1000.
[310] Michael D Fox, Abraham Z Snyder, Justin L Vincent, Maurizio Corbetta, David C Van Essen, Marcus E Raichle, The human brain is intrinsically organized into dynamic, anticorrelated functional networks, Proc. Natl. Acad. Sci. 102 (27) (2005) 9673–9678.
[311] Stephen G. Lisberger, Visual guidance of smooth-pursuit eye movements: sensation, action, and what happens in between, Neuron 66 (4) (2010) 477–491.
[312] Andrew JP Fink, Katherine R Croce, Z Josh Huang, LF Abbott, Thomas M Jessell, Eiman Azim, Presynaptic inhibition of spinal sensory feedback ensures smooth movement, Nature 509 (7498) (2014) 43–48.
[313] Peiran Gao, Surya Ganguli, On simplicity and complexity in the brave new world of large-scale neuroscience, Curr. Opin. Neurobiol. 32 (2015) 148–155.
[314] Timothy O'Leary, Alexander C. Sutton, Eve Marder, Computational models in the age of large datasets, Curr. Opin. Neurobiol. 32 (2015) 87–94.
[315] Kong-Fatt Wong, Xiao-Jing Wang, A recurrent network mechanism of time integration in perceptual decisions, J. Neurosci. 26 (4) (2006) 1314–1328.
[316] Xiaohan Lin, Xiaolong Zou, Zilong Ji, Tiejun Huang, Si Wu, Yuanyuan Mi, A brain-inspired computational model for spatio-temporal information processing, Neural Netw. 143 (2021) 74–87.
[317] Fatima Abbas, Marcus A Triplett, Geoffrey J Goodhill, Martin P Meyer, A three-layer network model of direction selective circuits in the optic tectum, Front. Neural Circuits 11 (2017) 88.
[318] Wolfram Erlhagen, Gregor Schöner, Dynamic field theory of movement preparation, Psychol. Rev. 109 (3) (2002) 545.
[319] Hidehiko K Inagaki, Lorenzo Fontolan, Sandro Romani, Karel Svoboda, Discrete attractor dynamics underlies persistent activity in the frontal cortex, Nature 566 (7743) (2019) 212–217.
[320] Mark M Churchland, John P Cunningham, Matthew T Kaufman, Justin D Foster, Paul Nuyujukian, Stephen I Ryu, Krishna V Shenoy, Neural population dynamics during reaching, Nature 487 (7405) (2012) 51–56.
[321] Michael B. Orger, Gonzalo G. de Polavieja, Zebrafish behavior: opportunities and challenges, Annu. Rev. Neurosci. 40 (2017) 125–147.
[322] Misha B Ahrens, Michael B Orger, Drew N Robson, Jennifer M Li, Philipp J Keller, Whole-brain functional imaging at cellular resolution using light-sheet microscopy, Nature Methods 10 (5) (2013) 413–420.
[323] Jeremy Freeman, Nikita Vladimirov, Takashi Kawashima, Yu Mu, Nicholas J Sofroniew, Davis V Bennett, Joshua Rosen, Chao-Tsung Yang, Loren L Looger, Misha B Ahrens, Mapping brain activity at scale with cluster computing, Nature Methods 11 (9) (2014) 941–950.
[324] Thomas O Auer, Karine Duroure, Anne De Cian, Jean-Paul Concordet, Filippo Del Bene, Highly efficient CRISPR/Cas9-mediated knock-in in zebrafish by homology-independent DNA repair, Genome Res. 24 (1) (2014) 142–153.
[325] Lorenzo Chicchi, Gloria Cecchini, Ihusan Adam, Giuseppe de Vito, Roberto Livi, Francesco Saverio Pavone, Ludovico Silvestri, Lapo Turrini, Francesco Vanzi, Duccio Fanelli, Reconstruction scheme for excitatory and inhibitory dynamics with quenched disorder: application to zebrafish imaging, J. Comput. Neurosci. 49 (2) (2021) 159–174.
[326] Dominic RW Burrows, Giovanni Diana, Birgit Pimpel, Friederike Moeller, Mark P Richardson, Danielle S Bassett, Martin P Meyer, Richard E Rosch, Single-cell networks reorganise to facilitate whole-brain supercritical dynamics during epileptic seizures, 2021, BioRxiv.
[327] Marcus A. Triplett, Lilach Avitan, Geoffrey J. Goodhill, Emergence of spontaneous assembly activity in developing neural networks without afferent input, PLoS Comput. Biol. 14 (9) (2018) e1006421.
[328] Michael Breakspear, Dynamic models of large-scale brain activity, Nature Neurosci. 20 (3) (2017) 340–352.
[329] Pedro J Gonçalves, Aristides B Arrenberg, Bastian Hablitzel, Herwig Baier, Christian K Machens, Optogenetic perturbations reveal the dynamics of an oculomotor integrator, Front. Neural Circuits 8 (2014) 10.
[330] Sophia Karpenko, Sebastien Wolf, Julie Lafaye, Guillaume Le Goc, Thomas Panier, Volker Bormuth, Raphaël Candelier, Georges Debrégeas, From behavior to circuit modeling of light-seeking navigation in zebrafish larvae, Elife 9 (2020) e52882.
[331] Drew N. Robson, Jennifer M. Li, A dynamical systems view of neuroethology: Uncovering stateful computation in natural behaviors, Curr. Opin. Neurobiol. 73 (2022) 102517.
[332] João C Marques, Meng Li, Diane Schaak, Drew N Robson, Jennifer M Li, Internal state dynamics shape brainwide activity and foraging behaviour, Nature 577 (7789) (2020) 239–243.
[333] Timothy W Dunn, Yu Mu, Sujatha Narayan, Owen Randlett, Eva A Naumann, Chao-Tsung Yang, Alexander F Schier, Jeremy Freeman, Florian Engert, Misha B Ahrens, Brain-wide mapping of neural activity controlling zebrafish exploratory locomotion, Elife 5 (2016) e12741.
[334] Nikita Vladimirov, Yu Mu, Takashi Kawashima, Davis V Bennett, Chao-Tsung Yang, Loren L Looger, Philipp J Keller, Jeremy Freeman, Misha B Ahrens, Light-sheet functional imaging in fictively behaving zebrafish, Nature Methods 11 (9) (2014) 883–884.
[335] Philippa J Karoly, Levin Kuhlmann, Daniel Soudry, David B Grayden, Mark J Cook, Dean R Freestone, Seizure pathways: A model-based investigation, PLoS Comput. Biol. 14 (10) (2018) e1006403.
[336] Kyesam Jung, Jiyoung Kang, Seungsoo Chung, Hae-Jeong Park, Dynamic causal modeling for calcium imaging: Exploration of differential effective connectivity for sensory processing in a barrel cortical column, Neuroimage 201 (2019) 116008.

[337] José Luis Iribarren, Esteban Moro, Impact of human activity patterns on the dynamics of information diffusion, Phys. Rev. Lett. 103 (3) (2009) 038702.
[338] José Luis Iribarren, Esteban Moro, Branching dynamics of viral information spreading, Phys. Rev. E 84 (4) (2011) 046116.
[339] Herbert W. Hethcote, The mathematics of infectious diseases, SIAM Rev. 42 (4) (2000) 599–653.
[340] Romualdo Pastor-Satorras, Claudio Castellano, Piet Van Mieghem, Alessandro Vespignani, Epidemic processes in complex networks, Rev. Modern Phys. 87 (3) (2015) 925.
[341] Juliette Stehlé, Nicolas Voirin, Alain Barrat, Ciro Cattuto, Vittoria Colizza, Lorenzo Isella, Corinne Régis, Jean-François Pinton, Nagham Khanafer, Wouter Van den Broeck, et al., Simulation of an SEIR infectious disease model on the dynamic contact network of conference attendees, BMC Med. 9 (1) (2011) 1–15.
[342] Albert-Laszlo Barabasi, The origin of bursts and heavy tails in human dynamics, Nature 435 (7039) (2005) 207–211.
[343] Alexei Vázquez, Joao Gama Oliveira, Zoltán Dezsö, Kwang-Il Goh, Imre Kondor, Albert-László Barabási, Modeling bursts and heavy tails in human dynamics, Phys. Rev. E 73 (3) (2006) 036127.
[344] Alexei Vazquez, Balazs Racz, Andras Lukacs, Albert-Laszlo Barabasi, Impact of non-Poissonian activity patterns on spreading processes, Phys. Rev. Lett. 98 (15) (2007) 158702.
[345] Byungjoon Min, K.-I. Goh, Alexei Vazquez, Spreading dynamics following bursty human activity patterns, Phys. Rev. E 83 (3) (2011) 036102.
[346] Márton Karsai, Nicola Perra, Alessandro Vespignani, Time varying networks and the weakness of strong ties, Sci. Rep. 4 (1) (2014) 1–7.
[347] Márton Karsai, Mikko Kivelä, Raj Kumar Pan, Kimmo Kaski, János Kertész, A-L Barabási, Jari Saramäki, Small but slow world: How network topology and burstiness slow down spreading, Phys. Rev. E 83 (2) (2011) 025102.
[348] Luis E.C. Rocha, Fredrik Liljeros, Petter Holme, Information dynamics shape the sexual networks of internet-mediated prostitution, Proc. Natl. Acad. Sci. 107 (13) (2010) 5706–5711.
[349] Luis E.C. Rocha, Fredrik Liljeros, Petter Holme, Simulated epidemics in an empirical spatiotemporal network of 50,185 sexual contacts, PLoS Comput. Biol. 7 (3) (2011) e1001109.
[350] Luis E.C. Rocha, Vincent D. Blondel, Bursts of vertex activation and epidemics in evolving networks, PLoS Comput. Biol. 9 (3) (2013) e1002974.
[351] Hang-Hyun Jo, Juan I Perotti, Kimmo Kaski, János Kertész, Analytically solvable model of spreading dynamics with non-Poissonian processes, Phys. Rev. X 4 (1) (2014) 011041.
[352] Giovanna Miritello, Esteban Moro, Rubén Lara, Dynamical strength of social ties in information spreading, Phys. Rev. E 83 (4) (2011) 045102.
[353] Michele Starnini, Andrea Baronchelli, Alain Barrat, Romualdo Pastor-Satorras, Random walks on temporal networks, Phys. Rev. E 85 (5) (2012) 056115.
[354] Nicola Perra, Bruno Gonçalves, Romualdo Pastor-Satorras, Alessandro Vespignani, Activity driven modeling of time varying networks, Sci. Rep. 2 (1) (2012) 1–7.
[355] Michele Starnini, Romualdo Pastor-Satorras, Topological properties of a time-integrated activity-driven network, Phys. Rev. E 87 (6) (2013) 062807.
[356] Sarah De Nigris, Anthony Hastir, Renaud Lambiotte, Burstiness and fractional diffusion on complex networks, Eur. Phys. J. B 89 (5) (2016) 1–7.
[357] Martin Gueuning, Renaud Lambiotte, Jean-Charles Delvenne, Backtracking and mixing rate of diffusion on uncorrelated temporal networks, Entropy 19 (10) (2017) 542.
[358] Renaud Lambiotte, Vsevolod Salnikov, Martin Rosvall, Effect of memory on the dynamics of random walks on networks, J. Complex Netw. 3 (2) (2015) 177–188.
[359] Hyewon Kim, Meesoon Ha, Hawoong Jeong, Scaling properties in time-varying networks with memory, Eur. Phys. J. B 88 (12) (2015) 1–8.
[360] Takayuki Hiraoka, Hang-Hyun Jo, Correlated bursts in temporal networks slow down spreading, Sci. Rep. 8 (1) (2018) 1–12.
[361] Oriol Artime, José J. Ramasco, Maxi San Miguel, Dynamics on networks: competition of temporal and topological correlations, Sci. Rep. 7 (1) (2017) 1–10.
[362] Oliver E. Williams, Fabrizio Lillo, Vito Latora, Effects of memory on spreading processes in non-Markovian temporal networks, New J. Phys. 21 (4) (2019) 043028.
[363] Petter Holme, Jari Saramäki, Temporal networks, Phys. Rep. 519 (3) (2012) 97–125.
[364] Jack Leitch, Kathleen A. Alexander, Srijan Sengupta, Toward epidemic thresholds on temporal networks: a review and open questions, Appl. Netw. Sci. 4 (1) (2019) 1–21.
[365] Jessica T Davis, Nicola Perra, Qian Zhang, Yamir Moreno, Alessandro Vespignani, Phase transitions in information spreading on structured populations, Nat. Phys. 16 (5) (2020) 590–596.
[366] Petter Holme, Modern temporal network theory: a colloquium, Eur. Phys. J. B 88 (9) (2015) 1–30.
[367] Jean-Pierre Eckmann, Elisha Moses, Danilo Sergi, Entropy of dialogues creates coherent structures in e-mail traffic, Proc. Natl. Acad. Sci. 101 (40) (2004) 14333–14337.
[368] David Liben-Nowell, Jon Kleinberg, Tracing information flow on a global scale using internet chain-letter data, Proc. Natl. Acad. Sci. 105 (12) (2008) 4633–4638.
[369] Julie Fournet, Alain Barrat, Contact patterns among high school students, PLoS One 9 (9) (2014) e107878.
[370] Lorenzo Isella, Juliette Stehlé, Alain Barrat, Ciro Cattuto, Jean-François Pinton, Wouter Van den Broeck, What's in a crowd? Analysis of face-to-face behavioral networks, J. Theoret. Biol. 271 (1) (2011) 166–180.
[371] Ed Bullmore, Olaf Sporns, Complex brain networks: graph theoretical analysis of structural and functional systems, Nat. Rev. Neurosci. 10 (3) (2009) 186–198.
[372] Mikail Rubinov, Olaf Sporns, Complex network measures of brain connectivity: uses and interpretations, Neuroimage 52 (3) (2010) 1059–1069.
[373] Kaspar A Schindler, Stephan Bialonski, Marie-Therese Horstmann, Christian E Elger, Klaus Lehnertz, Evolving functional network properties and synchronizability during human epileptic seizures, Chaos 18 (3) (2008) 033119.
[374] Klaus Lehnertz, Gerrit Ansmann, Stephan Bialonski, Henning Dickten, Christian Geier, Stephan Porz, Evolving networks in the human epileptic brain, Physica D 267 (2014) 7–15.
[375] Romualdo Pastor-Satorras, Alessandro Vespignani, Epidemic spreading in scale-free networks, Phys. Rev. Lett. 86 (14) (2001) 3200.
[376] István Z Kiss, Joel C Miller, Péter L Simon, et al., Mathematics of Epidemics on Networks, Vol. 598, Springer, Cham, 2017, p. 31.
[377] Vedran Sekara, Arkadiusz Stopczynski, Sune Lehmann, Fundamental structures of dynamic social networks, Proc. Natl. Acad. Sci. 113 (36) (2016) 9977–9982.
[378] Arkadiusz Stopczynski, Vedran Sekara, Piotr Sapiezynski, Andrea Cuttone, Mette My Madsen, Jakob Eg Larsen, Sune Lehmann, Measuring large-scale social networks with high resolution, PLoS One 9 (4) (2014) e95978.
[379] Thilo Gross, Carlos J. Dommar D'Lima, Bernd Blasius, Epidemic dynamics on an adaptive network, Phys. Rev. Lett. 96 (20) (2006) 208701.
[380] Andreas Koher, Hartmut HK Lentz, James P Gleeson, Philipp Hövel, Contact-based model for epidemic spreading on temporal networks, Phys. Rev. X 9 (3) (2019) 031017.
[381] Erik Volz, Lauren Ancel Meyers, Susceptible–infected–recovered epidemics in dynamic contact networks, Proc. R. Soc. B Biol. Sci. 274 (1628) (2007) 2925–2934.

[382] Erik Volz, Lauren Ancel Meyers, Epidemic thresholds in dynamic contact networks, J. R. Soc. Interface 6 (32) (2009) 233–241.
[383] Lauren Ancel Meyers, MEJ Newman, Michael Martin, Stephanie Schrag, Applying network theory to epidemics: control measures for Mycoplasma pneumoniae outbreaks, Emerg. Infect. Diseases 9 (2) (2003) 204.
[384] Lauren Ancel Meyers, Babak Pourbohloul, Mark EJ Newman, Danuta M Skowronski, Robert C Brunham, Network theory and SARS: predicting outbreak diversity, J. Theoret. Biol. 232 (1) (2005) 71–81.
[385] Lorenzo Zino, Alessandro Rizzo, Maurizio Porfiri, An analytical framework for the study of epidemic models on activity driven networks, J. Complex Netw. 5 (6) (2017) 924–952.
[386] Renat M Yulmetyev, Natalya A Emelyanova, Sergey A Demin, Fail M Gafarov, Peter Hänggi, Dinara G Yulmetyeva, Non-Markov stochastic dynamics of real epidemic process of respiratory infections, Phys. A 331 (1–2) (2004) 300–318.
[387] M Saeedian, M Khalighi, N Azimi-Tafreshi, GR Jafari, Marcel Ausloos, Memory effects on epidemic evolution: The susceptible-infected-recovered epidemic model, Phys. Rev. E 95 (2) (2017) 022409.
[388] Matthieu Nadini, Alessandro Rizzo, Maurizio Porfiri, Epidemic spreading in temporal and adaptive networks with static backbone, IEEE Trans. Netw. Sci. Eng. 7 (1) (2018) 549–561.
[389] Yanjun Lei, Xin Jiang, Quantong Guo, Yifang Ma, Meng Li, Zhiming Zheng, Contagion processes on the static and activity-driven coupling networks, Phys. Rev. E 93 (3) (2016) 032308.
[390] Mian-Xin Liu, Wei Wang, Ying Liu, Ming Tang, Shi-Min Cai, Hai-Feng Zhang, Social contagions on time-varying community networks, Phys. Rev. E 95 (5) (2017) 052306.
[391] Matthieu Nadini, Kaiyuan Sun, Enrico Ubaldi, Michele Starnini, Alessandro Rizzo, Nicola Perra, Epidemic spreading in modular time-varying networks, Sci. Rep. 8 (1) (2018) 1–11.
[392] Lorenzo Zino, Alessandro Rizzo, Maurizio Porfiri, Modeling memory effects in activity-driven networks, SIAM J. Appl. Dyn. Syst. 17 (4) (2018) 2830–2854.
[393] Jalil Hasanyan, Lorenzo Zino, Daniel Alberto Burbano Lombana, Alessandro Rizzo, Maurizio Porfiri, Leader–follower consensus on activity-driven networks, Proc. R. Soc. Lond. Ser. A Math. Phys. Eng. Sci. 476 (2233) (2020) 20190485.
[394] Alessandro Rizzo, Biagio Pedalino, Maurizio Porfiri, A network model for Ebola spreading, J. Theoret. Biol. 394 (2016) 212–222.
[395] Mahbubul H Riad, Musa Sekamatte, Felix Ocom, Issa Makumbi, Caterina M Scoglio, Risk assessment of ebola virus disease spreading in Uganda using a two-layer temporal network, Sci. Rep. 9 (1) (2019) 1–17.
[396] Eugenio Valdano, Michele Re Fiorentin, Chiara Poletto, Vittoria Colizza, Epidemic threshold in continuous-time evolving networks, Phys. Rev. Lett. 120 (6) (2018) 068302.
[397] Eugenio Valdano, Luca Ferreri, Chiara Poletto, Vittoria Colizza, Analytical computation of the epidemic threshold on temporal networks, Phys. Rev. X 5 (2) (2015) 021005.
[398] Mostafa Salehi, Rajesh Sharma, Moreno Marzolla, Matteo Magnani, Payam Siyari, Danilo Montesi, Spreading processes in multilayer networks, IEEE Trans. Netw. Sci. Eng. 2 (2) (2015) 65–83.
[399] Alberto Aleta, Yamir Moreno, Multilayer networks in a nutshell, Annu. Rev. Condens. Matter Phys. 10 (2019) 45–62.
[400] Alexandre Darbon, Davide Colombi, Eugenio Valdano, Lara Savini, Armando Giovannini, Vittoria Colizza, Disease persistence on temporal contact networks accounting for heterogeneous infectious periods, R. Soc. Open Sci. 6 (1) (2019) 181404.
[401] Andrey Y Lokhov, Marc Mézard, Hiroki Ohta, Lenka Zdeborová, Inferring the origin of an epidemic with a dynamic message-passing algorithm, Phys. Rev. E 90 (1) (2014) 012801.
[402] Brian Karrer, Mark E.J. Newman, Message passing approach for general epidemic models, Phys. Rev. E 82 (1) (2010) 016101.
[403] Anne-Sophie Ruget, Gianluigi Rossi, P Theo Pepler, Gaël Beaunée, Christopher J Banks, Jessica Enright, Rowland R Kao, Multi-species temporal network of livestock movements for disease spread, Appl. Netw. Sci. 6 (1) (2021) 1–20.
[404] Naoki Masuda, Joel C. Miller, Petter Holme, Concurrency measures in the era of temporal network epidemiology: a review, J. R. Soc. Interface 18 (179) (2021) 20210019.
[405] Baruch Barzel, Albert-László Barabási, Universality in network dynamics, Nat. Phys. 9 (10) (2013) 673–681.
[406] Baruch Barzel, Yang-Yu Liu, Albert-László Barabási, Constructing minimal models for complex system dynamics, Nature Commun. 6 (1) (2015) 1–8.
[407] Uzi Harush, Baruch Barzel, Dynamic patterns of information flow in complex networks, Nature Commun. 8 (1) (2017) 1–11.
[408] Marc Timme, Jan Nagler, Propagation patterns unravelled, Nat. Phys. 15 (4) (2019) 308–309.
[409] Marc Timme, Malte Schröder, Disentangling scaling arguments to empower complex systems analysis, Nat. Phys. 16 (11) (2020) 1086–1088.
[410] Peng Ji, Wei Lin, Jürgen Kurths, Asymptotic scaling describing signal propagation in complex networks, Nat. Phys. 16 (11) (2020) 1082–1083.
[411] Chittaranjan Hens, Uzi Harush, Simcha Haber, Reuven Cohen, Baruch Barzel, Reply to: Asymptotic scaling describing signal propagation in complex networks, Nat. Phys. 16 (11) (2020) 1084–1085.
[412] Justine Wolter, Benedict Lünsmann, Xiaozhu Zhang, Malte Schröder, Marc Timme, Quantifying transient spreading dynamics on networks, Chaos 28 (6) (2018) 063122.
[413] Malte Schröder, Xiaozhu Zhang, Justine Wolter, Marc Timme, Dynamic perturbation spreading in networks, IEEE Trans. Netw. Sci. Eng. 7 (3) (2019) 1019–1026.
[414] Manlio De Domenico, Clara Granell, Mason A Porter, Alex Arenas, The physics of spreading processes in multilayer networks, Nat. Phys. 12 (10) (2016) 901–906.
[415] Clara Granell, Sergio Gómez, Alex Arenas, Dynamical interplay between awareness and epidemic spreading in multiplex networks, Phys. Rev. Lett. 111 (12) (2013) 128701.
[416] Clara Granell, Sergio Gómez, Alex Arenas, Competing spreading processes on multiplex networks: awareness and epidemics, Phys. Rev. E 90 (1) (2014) 012808.
[417] Sergio Gómez, Jesús Gómez-Gardenes, Yamir Moreno, Alex Arenas, Nonperturbative heterogeneous mean-field approach to epidemic spreading in complex networks, Phys. Rev. E 84 (3) (2011) 036105.
[418] Sergio Gómez, Alexandre Arenas, Javier Borge-Holthoefer, Sandro Meloni, Yamir Moreno, Discrete-time Markov chain approach to contact-based disease spreading in complex networks, Europhys. Lett. 89 (3) (2010) 38009.
[419] Zhishuang Wang, Quantong Guo, Shiwen Sun, Chengyi Xia, The impact of awareness diffusion on SIR-like epidemics in multiplex networks, Appl. Math. Comput. 349 (2019) 134–147.
[420] Chengyi Xia, Zhishuang Wang, Chunyuan Zheng, Quantong Guo, Yongtang Shi, Matthias Dehmer, Zengqiang Chen, A new coupled disease-awareness spreading model with mass media on multiplex networks, Inform. Sci. 471 (2019) 185–200.
[421] Emanuele Cozzo, Raquel A Banos, Sandro Meloni, Yamir Moreno, Contact-based social contagion in multiplex networks, Phys. Rev. E 88 (5) (2013) 050801.
[422] Yu-Jhe Huang, Jonq Juang, Yu-Hao Liang, Hsin-Yu Wang, Global stability for epidemic models on multiplex networks, J. Math. Biol. 76 (6) (2018) 1339–1356.
[423] Quantong Guo, Xin Jiang, Yanjun Lei, Meng Li, Yifang Ma, Zhiming Zheng, Two-stage effects of awareness cascade on epidemic spreading in multiplex networks, Phys. Rev. E 91 (1) (2015) 012822.

[424] Quantong Guo, Yanjun Lei, Chengyi Xia, Lu Guo, Xin Jiang, Zhiming Zheng, The role of node heterogeneity in the coupled spreading of epidemics and awareness, PLoS One 11 (8) (2016) e0161037.
[425] Yaohui Pan, Zhijun Yan, The impact of individual heterogeneity on the coupled awareness-epidemic dynamics in multiplex networks, Chaos 28 (6) (2018) 063123.
[426] Faryad Darabi Sahneh, Caterina Scoglio, Competitive epidemic spreading over arbitrary multilayer networks, Phys. Rev. E 89 (6) (2014) 062817.
[427] Joaquín Sanz, Cheng-Yi Xia, Sandro Meloni, Yamir Moreno, Dynamics of interacting diseases, Phys. Rev. X 4 (4) (2014) 041005.
[428] David Soriano-Paños, Quantong Guo, Vito Latora, Jesús Gómez-Gardeñes, Explosive transitions induced by interdependent contagion-consensus dynamics in multiplex networks, Phys. Rev. E 99 (6) (2019) 062311.
[429] Piotr Bródka, Katarzyna Musial, Jaroslaw Jankowski, Interacting spreading processes in multilayer networks: a systematic review, IEEE Access 8 (2020) 10316–10341.
[430] Anna Saumell-Mendiola, M. Ángeles Serrano, Marián Boguná, Epidemic spreading on interconnected networks, Phys. Rev. E 86 (2) (2012) 026106.
[431] Huijuan Wang, Qian Li, Gregorio D'Agostino, Shlomo Havlin, H Eugene Stanley, Piet Van Mieghem, Effect of the interconnected network structure on the epidemic threshold, Phys. Rev. E 88 (2) (2013) 022801.
[432] Yong Min, Jiaren Hu, Weihong Wang, Ying Ge, Jie Chang, Xiaogang Jin, Diversity of multilayer networks and its impact on collaborating epidemics, Phys. Rev. E 90 (6) (2014) 062803.
[433] Shenyu Zhou, Shuangdie Xu, Lin Wang, Zhixin Liu, Guanrong Chen, Xiaofan Wang, Propagation of interacting diseases on multilayer networks, Phys. Rev. E 98 (1) (2018) 012303.
[434] Ginestra Bianconi, Epidemic spreading and bond percolation on multilayer networks, J. Stat. Mech. Theory Exp. 2017 (3) (2017) 034001.
[435] Guilherme Ferraz de Arruda, Emanuele Cozzo, Tiago P Peixoto, Francisco A Rodrigues, Yamir Moreno, Disease localization in multilayer networks, Phys. Rev. X 7 (1) (2017) 011014.
[436] L.G. Zuzek, Harry Eugene Stanley, Lidia A. Braunstein, Epidemic model with isolation in multilayer networks, Sci. Rep. 5 (1) (2015) 1–7.
[437] LD Valdez, HH Aragão Rêgo, HE Stanley, S Havlin, LA Braunstein, The role of bridge nodes between layers on epidemic spreading, New J. Phys. 20 (12) (2018) 125003.
[438] Juan G Calvo, Fabio Sanchez, Luis A Barboza, Yury E García, Paola Vásquez, A multilayer network model implementation for Covid-19, 2021, arXiv preprint arXiv:2103.08843.
[439] Yury E García, Gustavo Mery, Paola Vásquez, Juan G Calvo, Luis A Barboza, Tania Rivas, Fabio Sanchez, Projecting the impact of Covid-19 variants and vaccination strategies in disease transmission using a multilayer network model in costa rica, Sci. Rep. 12 (1) (2022) 1–9.
[440] Adrià Plazas, Irene Malvestio, Michele Starnini, Albert Díaz-Guilera, Modeling partial lockdowns in multiplex networks using partition strategies, Appl. Netw. Sci. 6 (1) (2021) 1–15.
[441] Alberto Aleta, David Martin-Corral, Ana Pastore y Piontti, Marco Ajelli, Maria Litvinova, Matteo Chinazzi, Natalie E Dean, M Elizabeth Halloran, Ira M Longini Jr., Stefano Merler, et al., Modelling the impact of testing, contact tracing and household quarantine on second waves of COVID-19, Nat. Hum. Behav. 4 (9) (2020) 964–971.
[442] Alessandro Vespignani, The fragility of interdependency, Nature 464 (7291) (2010) 984–985.
[443] Sergey V. Buldyrev, Roni Parshani, Gerald Paul, H. Eugene Stanley, Shlomo Havlin, Catastrophic cascade of failures in interdependent networks, Nature 464 (2010) 1025–1028.
[444] Vittorio Rosato, Limor Issacharoff, Fabio Tiriticco, Sandro Meloni, S Porcellinis, Roberto Setola, Modelling interdependent infrastructures using interacting dynamical models, Int. J. Crit. Infrastruct. 4 (1–2) (2008) 63–79.
[445] Dong Zhou, Amir Bashan, Reuven Cohen, Yehiel Berezin, Nadav Shnerb, Shlomo Havlin, Simultaneous first-and second-order percolation transitions in interdependent networks, Phys. Rev. E 90 (1) (2014) 012803.
[446] Maksim Kitsak, Alexander A Ganin, Daniel A Eisenberg, Pavel L Krapivsky, Dmitri Krioukov, David L Alderson, Igor Linkov, Stability of a giant connected component in a complex network, Phys. Rev. E 97 (1) (2018) 012309.
[447] Seung-Woo Son, Peter Grassberger, Maya Paczuski, Percolation transitions are not always sharpened by making networks interdependent, Phys. Rev. Lett. 107 (19) (2011) 195702.
[448] Seung-Woo Son, Golnoosh Bizhani, Claire Christensen, Peter Grassberger, Maya Paczuski, Percolation theory on interdependent networks based on epidemic spreading, Europhys. Lett. 97 (2012) 16006.
[449] Run-Ran Liu, Ming Li, Chun-Xiao Jia, Cascading failures in coupled networks: The critical role of node-coupling strength across networks, Sci. Rep. 6 (1) (2016) 1–6.
[450] Lucas D Valdez, Louis Shekhtman, Cristian E La Rocca, Xin Zhang, Sergey V Buldyrev, Paul A Trunfio, Lidia A Braunstein, Shlomo Havlin, Cascading failures in complex networks, J. Complex Netw. 8 (2) (2020) cnaa013.
[451] Xuqing Huang, Shuai Shao, Huijuan Wang, Sergey V Buldyrev, H Eugene Stanley, Shlomo Havlin, The robustness of interdependent clustered networks, Europhys. Lett. 101 (1) (2013) 18002.
[452] Shuai Shao, Xuqing Huang, H Eugene Stanley, Shlomo Havlin, Robustness of a partially interdependent network formed of clustered networks, Phys. Rev. E 89 (3) (2014) 032812.
[453] Lixin Tian, Yi Huang, Gaogao Dong, Ruijin Du, Liu Shi, Robustness of interdependent and interconnected clustered networks, Phys. A 412 (2014) 120–126.
[454] Louis M. Shekhtman, Saray Shai, Shlomo Havlin, Resilience of networks formed of interdependent modular networks, New J. Phys. 17 (12) (2015) 123007.
[455] Louis M. Shekhtman, Shlomo Havlin, Percolation of hierarchical networks and networks of networks, Phys. Rev. E 98 (5) (2018) 052305.
[456] D. Zhou, H.E. Stanley, G. D'Agostino, A. Scala, Assortativity decreases the robustness of interdependent networks, Phys. Rev. E 86 (2012) 066103.
[457] Byungjoon Min, Su Do Yi, Kyu-Min Lee, K.-I. Goh, Network robustness of multiplex networks with interlayer degree correlations, Phys. Rev. E 89 (4) (2014) 042811.
[458] Shunsuke Watanabe, Yoshiyuki Kabashima, Cavity-based robustness analysis of interdependent networks: Influences of intranetwork and internetwork degree-degree correlations, Phys. Rev. E 89 (1) (2014) 012808.
[459] M. Ángeles Serrano, L'uboš Buzna, Marián Boguná, Escaping the avalanche collapse in self-similar multiplexes, New J. Phys. 17 (5) (2015) 053033.
[460] Davide Cellai, Eduardo López, Jie Zhou, James P Gleeson, Ginestra Bianconi, Percolation in multiplex networks with overlap, Phys. Rev. E 88 (2013) 052811.
[461] Yanqing Hu, Dong Zhou, Rui Zhang, Zhangang Han, Céline Rozenblat, Shlomo Havlin, Percolation of interdependent networks with intersimilarity, Phys. Rev. E 88 (5) (2013) 052805.
[462] Byungjoon Min, Sangchul Lee, Kyu-Min Lee, K.-I. Goh, Link overlap, viability, and mutual percolation in multiplex networks, Chaos Solitons Fractals 72 (2015) 49–58.
[463] Davide Cellai, Sergey N. Dorogovtsev, Ginestra Bianconi, Message passing theory for percolation models on multiplex networks with link overlap, Phys. Rev. E 94 (3) (2016) 032301.

[464] Xueming Liu, H. Eugene Stanley, Jianxi Gao, Breakdown of interdependent directed networks, Proc. Natl. Acad. Sci. 113 (5) (2016) 1138–1143.
[465] Xueming Liu, Linqiang Pan, H. Eugene Stanley, Jianxi Gao, Multiple phase transitions in networks of directed networks, Phys. Rev. E 99 (1) (2019) 012312.
[466] Jia Shao, Sergey V. Buldyrev, Shlomo Havlin, H. Eugene Stanley, Cascade of failures in coupled network systems with multiple support-dependence relations, Phys. Rev. E 83 (2011) 036116.
[467] Matias Alberto Di Muro, Lucas Daniel Valdez, HH Aragão Rêgo, SV Buldyrev, HE Stanley, Lidia Adriana Braunstein, Cascading failures in interdependent networks with multiple supply-demand links and functionality thresholds, Sci. Rep. 7 (1) (2017) 1–10.
[468] Tianqiao Zhang, Yang Zhang, Xuzhen Zhu, Junliang Chen, Cascading failures on interdependent networks with star dependent links, Phys. A 535 (2019) 122222.
[469] Roni Parshani, Sergey V. Buldyrev, Shlomo Havlin, Interdependent networks: Reducing the coupling strength leads to a change from a first to second order percolation transition, Phys. Rev. Lett. 105 (2010) 048701.
[470] Christian M Schneider, Nuri Yazdani, Nuno AM Araújo, Shlomo Havlin, Hans J Herrmann, Towards designing robust coupled networks, Sci. Rep. 3 (1) (2013) 1–7.
[471] Lucas Daniel Valdez, Pablo Alejandro Macri, L.A. Braunstein, A triple point induced by targeted autonomization on interdependent scale-free networks, J. Phys. A 47 (5) (2014) 055002.
[472] Yangyang Liu, Chengli Zhao, Dongyun Yi, H Eugene Stanley, Robustness of partially interdependent networks under combined attack, Chaos 29 (2) (2019) 021101.
[473] Jianxi Gao, Sergey V Buldyrev, Shlomo Havlin, H Eugene Stanley, Robustness of a network of networks, Phys. Rev. Lett. 107 (19) (2011) 195701.
[474] Jianxi Gao, Sergey V. Buldyrev, H. Eugene Stanley, Shlomo Havlin, Networks formed from interdependent networks, Nat. Phys. 8 (2012) 40–48.
[475] Jianxi Gao, Sergey V Buldyrev, Shlomo Havlin, H Eugene Stanley, Robustness of a network formed by n interdependent networks with a one-to-one correspondence of dependent nodes, Phys. Rev. E 85 (6) (2012) 066134.
[476] Jianxi Gao, Sergey V Buldyrev, H Eugene Stanley, Xiaoming Xu, Shlomo Havlin, Percolation of a general network of networks, Phys. Rev. E 88 (6) (2013) 062816.
[477] Ginestra Bianconi, Sergey N. Dorogovtsev, Multiple percolation transitions in a configuration model of a network of networks, Phys. Rev. E 89 (6) (2014) 062814.
[478] S. Havlin, D.Y. Kenett, A. Bashan, J. Gao, H.E. Stanley, Vulnerability of network of networks, Eur. Phys. J. Spec. Top. 223 (11) (2014) 2087–2106.
[479] Ginestra Bianconi, Sergey N. Dorogovtsev, José F.F. Mendes, Mutually connected component of networks of networks with replica nodes, Phys. Rev. E 91 (1) (2015) 012804.
[480] M. Barthélemy, Spatial networks, Phys. Rep. 499 (2011) 1–101.
[481] W. Li, A. Bashan, S.V. Buldyrev, Cascading failures in interdependent lattice networks: The critical role of the length of dependency links, Phys. Rev. Lett. 108 (2012) 228702.
[482] Amir Bashan, Yehiel Berezin, Sergey V Buldyrev, Shlomo Havlin, The extreme vulnerability of interdependent spatially embedded networks, Nat. Phys. 9 (10) (2013) 667–672.
[483] Michael M Danziger, Amir Bashan, Yehiel Berezin, Shlomo Havlin, Percolation and cascade dynamics of spatial networks with partial dependency, J. Complex Netw. 2 (4) (2014) 460–474.
[484] Louis M Shekhtman, Yehiel Berezin, Michael M Danziger, Shlomo Havlin, Robustness of a network formed of spatially embedded networks, Phys. Rev. E 90 (1) (2014) 012809.
[485] Yehiel Berezin, Amir Bashan, Michael M Danziger, Daqing Li, Shlomo Havlin, Localized attacks on spatially embedded networks with dependencies, Sci. Rep. 5 (1) (2015) 1–5.
[486] Michael M Danziger, Louis M Shekhtman, Yehiel Berezin, Shlomo Havlin, The effect of spatiality on multiplex networks, Europhys. Lett. 115 (3) (2016) 36002.
[487] Dana Vaknin, Michael M. Danziger, Shlomo Havlin, Spreading of localized attacks in spatial multiplex networks, New J. Phys. 19 (7) (2017) 073037.
[488] Weifei Zang, Xinsheng Ji, Shuxin Liu, Haitao Li, An interdependent network coupling strategy based on overlapping link structure against targeted attack, Internat. J. Modern Phys. C 32 (08) (2021) 2150101.
[489] Zhengcheng Dong, Yanjun Fang, Meng Tian, Rong Zhang, Approaches to improve the robustness on interdependent networks against cascading failures with load-based model, Modern Phys. Lett. B 29 (32) (2015) 1550210.
[490] Meng Tian, Xianpei Wang, Zhengcheng Dong, Guowei Zhu, Jiachuang Long, Dangdang Dai, Qilin Zhang, Cascading failures of interdependent modular scale-free networks with different coupling preferences, Europhys. Lett. 111 (1) (2015) 18007.
[491] Xingpei Ji, Bo Wang, Dichen Liu, Guo Chen, Fei Tang, Daqian Wei, Lian Tu, Improving interdependent networks robustness by adding connectivity links, Phys. A 444 (2016) 9–19.
[492] Pengshuai Cui, Peidong Zhu, Ke Wang, Peng Xun, Zhuoqun Xia, Enhancing robustness of interdependent network by adding connectivity and dependence links, Phys. A 497 (2018) 185–197.
[493] Marcell Stippinger, János Kertész, Enhancing resilience of interdependent networks by healing, Phys. A 416 (2014) 481–487.
[494] Marcell Stippinger, János Kertész, Universality and scaling laws in the cascading failure model with healing, Phys. Rev. E 98 (4) (2018) 042303.
[495] Cristian E. La Rocca, H. Eugene Stanley, Lidia A. Braunstein, Strategy for stopping failure cascades in interdependent networks, Phys. A 508 (2018) 577–583.
[496] Antonio Majdandzic, Lidia A Braunstein, Chester Curme, Irena Vodenska, Sary Levy-Carciente, H Eugene Stanley, Shlomo Havlin, Multiple tipping points and optimal repairing in interacting networks, Nature Commun. 7 (1) (2016) 1–10.
[497] Matias Alberto Di Muro, Cristian Ernesto La Rocca, Harry Eugene Stanley, S Havlin, Lidia Adriana Braunstein, Recovery of interdependent networks, Sci. Rep. 6 (1) (2016) 1–11.
[498] Renjian Lyu, Min Zhang, Xiao-Juan Wang, Tie-Jun Wang, Recovery strategy of multilayer network against cascading failure, Internat. J. Modern Phys. C 33 (03) (2022) 2250039.
[499] Antonio Majdandzic, Boris Podobnik, Sergey V Buldyrev, Dror Y Kenett, Shlomo Havlin, H Eugene Stanley, Spontaneous recovery in dynamical networks, Nat. Phys. 10 (2014) 34.
[500] Antonio Scala, Pier Giorgio De Sanctis Lucentini, Guido Caldarelli, Gregorio D'Agostino, Cascades in interdependent flow networks, Physica D 323 (2016) 35–39.
[501] Yingrui Zhang, Osman Yağan, Modeling and analysis of cascading failures in interdependent cyber-physical systems, in: 2018 IEEE Conference on Decision and Control, CDC, IEEE, 2018, pp. 4731–4738.
[502] Yingrui Zhang, Alex Arenas, Osman Yağan, Cascading failures in interdependent systems under a flow redistribution model, Phys. Rev. E 97 (2) (2018) 022307.
[503] M.A. Di Muro, S.V. Buldyrev, H.E. Stanley, L.A. Braunstein, Cascading failures in interdependent networks with finite functional components, Phys. Rev. E 94 (4) (2016) 042304.
[504] Xin Yuan, Yanqing Hu, H. Eugene Stanley, Shlomo Havlin, Eradicating catastrophic collapse in interdependent networks via reinforced nodes, Proc. Natl. Acad. Sci. 114 (13) (2017) 3311–3315.

[505] C.D. Brummitt, R.M. D'Souza, E.A. Leicht, Suppressing cascades of load in interdependent networks, Proc. Natl. Acad. Sci. 109 (2012) E680–E689.
[506] Michael M Danziger, Ivan Bonamassa, Stefano Boccaletti, Shlomo Havlin, Dynamic interdependence and competition in multilayer networks, Nat. Phys. 15 (2) (2019) 178–185.
[507] Yangyu Liu, Jean Jacques Slotine, Albert-László Barabási, Controllability of complex networks, Nature 473 (7346) (2011) 167–173.
[508] Yang Tang, Feng Qian, Huijun Gao, Jürgen Kurths, Synchronization in complex networks and its application – A survey of recent advances and challenges, Annu. Rev. Control 38 (2014) 184–198.
[509] Henri Weimerskirch, Julien Martin, Yannick Clerquin, Peggy Alexandre, Sarka Jiraskova, Energy saving in flight formation - Pelicans flying in a 'V' can glide for extended periods using the other birds' air streams, Nature 413 (6857) (2001) 697–698.
[510] Iain D. Couzin, Jens Krause, Nigel R. Franks, Simon A. Levin, Effective leadership and decision-making in animal groups on the move, Nature 433 (7025) (2005) 513–516.
[511] Adrian Cho, Scientific link-up yields 'control panel' for networks, Science 332 (6031) (2011) 777.
[512] Xiaofan Wang, Guanrong Chen, Pinning control of scale-free dynamical networks, Physica A 310 (3–4) (2002) 521–531.
[513] Justin Ruths, Derek Ruths, Control profiles of complex networks, Science 343 (6177) (2014) 1373–1376.
[514] Jason Z Kim, Jonathan M Soffer, Ari E Kahn, Jean M Vettel, Fabio Pasqualetti, Danielle S Bassett, Role of graph architecture in controlling dynamical networks with applications to neural systems, Nat. Phys. 14 (1) (2018) 91–98.
[515] Alexander J Gates, Rion Brattig Correia, Xuan Wang, Luis M Rocha, The effective graph reveals redundancy, canalization, and control pathways in biochemical regulation and signaling, Proc. Natl. Acad. Sci. 118 (12) (2021).
[516] Andrew Clark, Basel Alomair, Linda Bushnell, Radha Poovendran, Submodularity in input node selection for networked linear systems: Efficient algorithms for performance and controllability, IEEE Control Syst. Mag. 37 (6) (2017) 52–74.
[517] Junjie Jiang, Yingcheng Lai, Irrelevance of linear controllability to nonlinear dynamical networks, Nature Commun. 10 (1) (2019) 1–10.
[518] Giacomo Baggio, Danielle S. Bassett, Fabio Pasqualetti, Data-driven control of complex networks, Nature Commun. 12 (1) (2021) 1–13.
[519] Isaac Klickstein, Francesco Sorrentino, Controlling network ensembles, Nature Commun. 12 (1) (2021) 1–10.
[520] Kaile Chen, Wangli He, Qing-Long Han, Mengqi Xue, Yang Tang, Leader selection in networks under switching topologies with antagonistic interactions, Automatica 142 (2022) 110334.
[521] Linying Xiang, Fei Chen, Wei Ren, Guanrong Chen, Advances in network controllability, IEEE Circuits Syst. Mag. 19 (2) (2019) 8–32.
[522] Mengqi Xue, Yang Tang, Wei Ren, Feng Qian, Stability of multi-dimensional switched systems with an application to open multi-agent systems, Automatica 146 (2022) 110644.
[523] Xiaotai Wu, Wei Xing Zheng, Yang Tang, Xin Jin, Stability analysis for impulsive stochastic time-varying systems, IEEE Trans. Automat. Control (2022) 1–8.
[524] Xiaotai Wu, Peng Shi, Yang Tang, Shuai Mao, Feng Qian, Stability analysis of semi-Markov jump stochastic nonlinear systems, IEEE Trans. Automat. Control 67 (4) (2021) 2084–2091.
[525] John D Medaglia, Perry Zurn, Walter Sinnott-Armstrong, Danielle S Bassett, Mind control as a guide for the mind, Nat. Hum. Behav. 1 (6) (2017) 1–8.
[526] Yang Tang, Huijun Gao, Kurths Jürgen, Multiobjective identification of controlling areas in neuronal networks, IEEE/ACM Trans. Comput. Biol. Bioinform. 10 (3) (2013) 708–720.
[527] Julia K Brynildsen, Kyla D Mace, Eli J Cornblath, Carmen Weidler, Fabio Pasqualetti, Danielle S Bassett, Julie A Blendy, Gene coexpression patterns predict opiate-induced brain-state transitions, Proc. Natl. Acad. Sci. 117 (32) (2020) 19556–19565.
[528] Jacob Biamonte, Mauro Faccin, Manlio De Domenico, Complex networks from classical to quantum, Commun. Phys. 2 (1) (2019) 1–10.
[529] Oliver Mülken, Alexander Blumen, Continuous-time quantum walks: Models for coherent transport on complex networks, Phys. Rep. 502 (2–3) (2011) 37–87.
[530] Ginestra Bianconi, Quantum statistics in complex networks, Phys. Rev. E 66 (5) (2002) 056123.
[531] Yasser Roudi, John Hertz, Mean field theory for nonequilibrium network reconstruction, Phys. Rev. Lett. 106 (4) (2011) 048702.
[532] Sergey N Dorogovtsev, Alexander V Goltsev, José FF Mendes, Critical phenomena in complex networks, Rev. Modern Phys. 80 (4) (2008) 1275.
[533] Alejandro D Sánchez, Juan M López, Miguel A Rodriguez, Nonequilibrium phase transitions in directed small-world networks, Phys. Rev. Lett. 88 (4) (2002) 048701.
[534] Michael N. Hallquist, Frank G. Hillary, Graph theory approaches to functional network organization in brain disorders: A critique for a brave new small-world, Netw. Neurosci. 3 (1) (2018) 1–26.
[535] Kun Zhao, Qiang Zheng, Tongtong Che, Martin Dyrba, Qiongling Li, Yanhui Ding, Yuanjie Zheng, Yong Liu, Shuyu Li, Regional radiomics similarity networks (R2SNs) in the human brain: Reproducibility, small-world properties and a biological basis, Netw. Neurosci. 5 (3) (2021) 783–797.
[536] Barbara Benigni, Arsham Ghavasieh, Alessandra Corso, Valeria d'Andrea, Manlio De Domenico, Persistence of information flow: A multiscale characterization of human brain, Netw. Neurosci. 5 (3) (2021) 831–850.
[537] Roberto C Sotero, Lazaro M Sanchez-Rodriguez, Narges Moradi, Mehdy Dousty, Estimation of global and local complexities of brain networks: A random walks approach, Netw. Neurosci. 4 (3) (2020) 575–594.
[538] Shota Shirai, Susant Kumar Acharya, Saurabh Kumar Bose, Joshua Brian Mallinson, Edoardo Galli, Matthew D Pike, Matthew D Arnold, Simon Anthony Brown, Long-range temporal correlations in scale-free neuromorphic networks, Netw. Neurosci. 4 (2) (2020) 432–447.
[539] Yang Tian, Pei Sun, Percolation may explain efficiency, robustness, and economy of the brain, Netw. Neurosci. (2022) 1–42.
[540] Hawoong Jeong, Bálint Tombor, Réka Albert, Zoltan N Oltvai, A-L Barabási, The large-scale organization of metabolic networks, Nature 407 (6804) (2000) 651–654.
[541] Andreas Wagner, David A. Fell, The small world inside large metabolic networks, Proc. R. Soc. B 268 (1478) (2001) 1803–1810.
[542] Reiko Tanaka, Scale-rich metabolic networks, Phys. Rev. Lett. 94 (16) (2005) 168101.
[543] Hawoong Jeong, Sean P Mason, A-L Barabási, Zoltan N Oltvai, Lethality and centrality in protein networks, Nature 411 (6833) (2001) 41–42.
[544] Soon-Hyung Yook, Zoltán N Oltvai, Albert-László Barabási, Functional and topological characterization of protein interaction networks, Proteomics 4 (4) (2004) 928–942.
[545] Andreas Wagner, The yeast protein interaction network evolves rapidly and contains few redundant duplicate genes, Mol. Biol. Evol. 18 (7) (2001) 1283–1292.
[546] Mark E.J. Newman, The structure of scientific collaboration networks, Proc. Natl. Acad. Sci. 98 (2) (2001) 404–409.
[547] Constantino Tsallis, Marcio P. de Albuquerque, Are citations of scientific papers a case of nonextensivity? Eur. Phys. J. B 13 (4) (2000) 777–780.
[548] F. Menczer, Correlated topologies in citation networks and the web, Eur. Phys. J. B 38 (2) (2004) 211–221.
[549] Katarzyna Sznajd-Weron, Jozef Sznajd, Opinion evolution in closed community, Internat. J. Modern Phys. C 11 (06) (2000) 1157–1165.
[550] Alessandro Pluchino, Vito Latora, Andrea Rapisarda, Changing opinions in a changing world: A new perspective in sociophysics, Internat. J. Modern Phys. C 16 (04) (2005) 515–531.
[551] Dietrich Stauffer, Hildegard Meyer-Ortmanns, Simulation of consensus model of Deffuant et al. on a Barabasi–Albert network, Internat. J. Modern Phys. C 15 (02) (2004) 241–246.

[552] Alexei Vázquez, Romualdo Pastor-Satorras, Alessandro Vespignani, Large-scale topological and dynamical properties of the internet, Phys. Rev. E 65 (6) (2002) 066130.
[553] Romualdo Pastor-Satorras, Alessandro Vespignani, Evolution and Structure of the Internet: A Statistical Physics Approach, Cambridge University Press, Cambridge, U.K., 2007.
[554] Byungnam Kahng, Y. Park, Hawoong Jeong, Robustness of the in-degree exponent for the world-wide web, Phys. Rev. E 66 (4) (2002) 046107.
[555] M. Argollo De Menezes, A.-L. Barabási, Fluctuations in network dynamics, Phys. Rev. Lett. 92 (2) (2004) 028701.
[556] M. Argollo de Menezes, A.-L. Barabási, Separating internal and external dynamics of complex systems, Phys. Rev. Lett. 93 (6) (2004) 068701.
[557] Zonghan Wu, Shirui Pan, Fengwen Chen, Guodong Long, Chengqi Zhang, S Yu Philip, A comprehensive survey on graph neural networks, IEEE Trans. Neural Netw. Learn. Syst. 32 (1) (2020) 4–24.
[558] Keyulu Xu, Weihua Hu, Jure Leskovec, Stefanie Jegelka, How powerful are graph neural networks? 2018, arXiv preprint arXiv:1810.00826.
[559] Alessandro Sperduti, Antonina Starita, Supervised neural networks for the classification of structures, IEEE Trans. Neural Netw. 8 (3) (1997) 714–735.
[560] Vijay Prakash Dwivedi, Chaitanya K Joshi, Thomas Laurent, Yoshua Bengio, Xavier Bresson, Benchmarking graph neural networks, 2020, arXiv preprint arXiv:2003.00982.
[561] Franco Scarselli, Marco Gori, Ah Chung Tsoi, Markus Hagenbuchner, Gabriele Monfardini, The graph neural network model, IEEE Trans. Neural Netw. 20 (1) (2008) 61–80.
[562] Claudio Gallicchio, Alessio Micheli, Graph echo state networks, in: The 2010 International Joint Conference on Neural Networks, IJCNN, IEEE, 2010, pp. 1–8.
[563] Yujia Li, Daniel Tarlow, Marc Brockschmidt, Richard Zemel, Gated graph sequence neural networks, 2015, arXiv preprint arXiv:1511.05493.
[564] Hanjun Dai, Zornitsa Kozareva, Bo Dai, Alex Smola, Le Song, Learning steady-states of iterative algorithms over graphs, in: International Conference on Machine Learning, PMLR, 2018, pp. 1106–1114.
[565] Mikael Henaff, Joan Bruna, Yann LeCun, Deep convolutional networks on graph-structured data, 2015, arXiv preprint arXiv:1506.05163.
[566] Joan Bruna, Wojciech Zaremba, Arthur Szlam, Yann LeCun, Spectral networks and locally connected networks on graphs, 2013, arXiv preprint arXiv:1312.6203.
[567] Alessio Micheli, Neural network for graphs: A contextual constructive approach, IEEE Trans. Neural Netw. 20 (3) (2009) 498–511.
[568] James Atwood, Don Towsley, Diffusion-convolutional neural networks, Adv. Neural Inf. Process. Syst. 29 (2016).
[569] Shaosheng Cao, Wei Lu, Qiongkai Xu, Deep neural networks for learning graph representations, in: Proceedings of the AAAI Conference on Artificial Intelligence, Vol. 30, 2016.
[570] Daixin Wang, Peng Cui, Wenwu Zhu, Structural deep network embedding, in: Proceedings of the 22nd ACM SIGKDD International Conference on Knowledge Discovery and Data Mining, 2016, pp. 1225–1234.
[571] Yujia Li, Oriol Vinyals, Chris Dyer, Razvan Pascanu, Peter Battaglia, Learning deep generative models of graphs, 2018, arXiv preprint arXiv:1803.03324.
[572] Youngjoo Seo, Michaël Defferrard, Pierre Vandergheynst, Xavier Bresson, Structured sequence modeling with graph convolutional recurrent networks, in: International Conference on Neural Information Processing, Springer, 2018, pp. 362–373.
[573] Yaguang Li, Rose Yu, Cyrus Shahabi, Yan Liu, Diffusion convolutional recurrent neural network: Data-driven traffic forecasting, 2017, arXiv preprint arXiv:1707.01926.
[574] Ashesh Jain, Amir R Zamir, Silvio Savarese, Ashutosh Saxena, Structural-rnn: Deep learning on spatio-temporal graphs, in: Proceedings of the Ieee Conference on Computer Vision and Pattern Recognition, 2016, pp. 5308–5317.
[575] Jonathan Shlomi, Peter Battaglia, Jean-Roch Vlimant, Graph neural networks in particle physics, Mach. Learn.: Sci. Technol. 2 (2) (2020) 021001.
[576] Johannes Allotey, Keith T. Butler, Jeyan Thiyagalingam, Entropy-based active learning of graph neural network surrogate models for materials properties, J. Chem. Phys. 155 (17) (2021) 174116.
[577] George Sugihara, Robert May, Hao Ye, Chih-hao Hsieh, Ethan Deyle, Michael Fogarty, Stephan Munch, Detecting causality in complex ecosystems, Science 338 (6106) (2012) 496–500.
[578] Katerina Hlaváčková-Schindler, Milan Paluš, Martin Vejmelka, Joydeep Bhattacharya, Causality detection based on information-theoretic approaches in time series analysis, Phys. Rep. 441 (1) (2007) 1–46.
[579] Tomislav Stankovski, Tiago Pereira, Peter VE McClintock, Aneta Stefanovska, Coupling functions: universal insights into dynamical interaction mechanisms, Rev. Modern Phys. 89 (4) (2017) 045001.
[580] Jie Sun, Dane Taylor, Erik M. Bollt, Causal network inference by optimal causation entropy, SIAM J. Appl. Dyn. Syst. 14 (1) (2015) 73–106.
[581] John A. Gubner, Probability and Random Processes for Electrical and Computer Engineers, Cambridge University Press, 2006.
[582] Claude Elwood Shannon, A mathematical theory of communication, Bell Syst. Tech. J. 27 (3) (1948) 379–423.
[583] KR Pilkiewicz, BH Lemasson, MA Rowland, A Hein, J Sun, A Berdahl, ML Mayo, J Moehlis, M Porfiri, E Fernández-Juricic, et al., Decoding collective communications using information theory tools, J. R. Soc. Interface 17 (164) (2020) 20190563.
[584] Thomas M. Cover, Elements of Information Theory, John Wiley & Sons, 1999.
[585] Angeliki Papana, Dimitris Kugiumtzis, Evaluation of mutual information estimators for time series, Int. J. Bifurcation Chaos 19 (12) (2009) 4197–4215.
[586] David N Reshef, Yakir A Reshef, Hilary K Finucane, Sharon R Grossman, Gilean McVean, Peter J Turnbaugh, Eric S Lander, Michael Mitzenmacher, Pardis C Sabeti, Detecting novel associations in large data sets, Science 334 (6062) (2011) 1518–1524.
[587] Thomas Schreiber, Measuring information transfer, Phys. Rev. Lett. 85 (2) (2000) 461.
[588] Milan Paluš, Vladimír Komárek, Zbyněk Hrnčíř, Katalin Štěrbová, Synchronization as adjustment of information rates: Detection from bivariate time series, Phys. Rev. E 63 (4) (2001) 046211.
[589] Cornelis J. Stam, Nonlinear dynamical analysis of EEG and MEG: review of an emerging field, Clin. Neurophysiol. 116 (10) (2005) 2266–2301.
[590] Ernesto Pereda, Rodrigo Quian Quiroga, Joydeep Bhattacharya, Nonlinear multivariate analysis of neurophysiological signals, Prog. Neurobiol. 77 (1–2) (2005) 1–37.
[591] Raul Vicente, Michael Wibral, Michael Lindner, Gordon Pipa, Transfer entropy—a model-free measure of effective connectivity for the neurosciences, J. Comput. Neurosci. 30 (1) (2011) 45–67.
[592] Eric Gilbert, Karrie Karahalios, Widespread worry and the stock market, in: Fourth International AAAI Conference on Weblogs and Social Media, 2010.
[593] Robert Marschinski, Holger Kantz, Analysing the information flow between financial time series, Eur. Phys. J. B 30 (2) (2002) 275–281.
[594] Margret Bauer, John W Cox, Michelle H Caveness, James J Downs, Nina F Thornhill, Finding the direction of disturbance propagation in a chemical process using transfer entropy, IEEE Trans. Control Syst. Technol. 15 (1) (2006) 12–21.
[595] Jakob Runge, Jobst Heitzig, Vladimir Petoukhov, Jürgen Kurths, Escaping the curse of dimensionality in estimating multivariate transfer entropy, Phys. Rev. Lett. 108 (25) (2012) 258701.
[596] Greg Ver Steeg, Aram Galstyan, Information transfer in social media, in: Proceedings of the 21st International Conference on World Wide Web, 2012, pp. 509–518.

[597] Carlo Cafaro, Warren M. Lord, Jie Sun, Erik M. Bollt, Causation entropy from symbolic representations of dynamical systems, Chaos 25 (4) (2015) 043106.
[598] X. San Liang, Richard Kleeman, Information transfer between dynamical system components, Phys. Rev. Lett. 95 (24) (2005) 244101.
[599] X. San Liang, The Liang-Kleeman information flow: Theory and applications, Entropy 15 (1) (2013) 327–360.
[600] Jushan Bai, Pierre Perron, Estimating and testing linear models with multiple structural changes, Econometrica (1998) 47–78.
[601] Jushan Bai, Pierre Perron, Computation and analysis of multiple structural change models, J. Appl. Econometrics 18 (1) (2003) 1–22.
[602] Bing Wang, Jie Sun, Adilson E. Motter, Detecting structural breaks in seasonal time series by regularized optimization, 2015, arXiv preprint arXiv:1505.04305.
[603] Marten Scheffer, Jordi Bascompte, William A Brock, Victor Brovkin, Stephen R Carpenter, Vasilis Dakos, Hermann Held, Egbert H Van Nes, Max Rietkerk, George Sugihara, Early-warning signals for critical transitions, Nature 461 (7260) (2009) 53–59.
[604] Jia-Wen Hou, Huan-Fei Ma, Dake He, Jie Sun, Qing Nie, Wei Lin, Harvesting random embedding for high-frequency change-point detection in temporal complex systems, Natl. Sci. Rev. 9 (4) (2022) nwab228.
[605] Charles R. Farrar, Keith Worden, An introduction to structural health monitoring, Phil. Trans. R. Soc. A 365 (1851) (2007) 303–315.
[606] Amila Sudu Ambegedara, Jie Sun, Kerop Janoyan, Erik Bollt, Information-theoretical noninvasive damage detection in bridge structures, Chaos 26 (11) (2016) 116312.
[607] Yong Zou, Reik V Donner, Norbert Marwan, Jonathan F Donges, Jürgen Kurths, Complex network approaches to nonlinear time series analysis, Phys. Rep. 787 (2019) 1–97.
[608] Clive W.J. Granger, Investigating causal relations by econometric models and cross-spectral methods, Econometrica (1969) 424–438.
[609] Clive W.J. Granger, Some recent development in a concept of causality, J. Econometrics 39 (1–2) (1988) 199–211.
[610] Joseph T. Lizier, Mikhail Prokopenko, Differentiating information transfer and causal effect, Eur. Phys. J. B 73 (4) (2010) 605–615.
[611] Lionel Barnett, Adam B. Barrett, Anil K. Seth, Granger causality and transfer entropy are equivalent for Gaussian variables, Phys. Rev. Lett. 103 (23) (2009) 238701.
[612] Yang Tian, Yaoyuan Wang, Ziyang Zhang, Pei Sun, Fourier-domain transfer entropy spectrum, Phys. Rev. Res. 3 (4) (2021) L042040.
[613] Mukeshwar Dhamala, Govindan Rangarajan, Mingzhou Ding, Estimating Granger causality from Fourier and wavelet transforms of time series data, Phys. Rev. Lett. 100 (1) (2008) 018701.
[614] Jie Sun, Erik M. Bollt, Causation entropy identifies indirect influences, dominance of neighbors and anticipatory couplings, Physica D 267 (2014) 49–57.
[615] Jakob Runge, Causal network reconstruction from time series: From theoretical assumptions to practical estimation, Chaos 28 (7) (2018) 075310.
[616] Peter Spirtes, Clark N Glymour, Richard Scheines, David Heckerman, Causation, Prediction, and Search, MIT Press, 2000.
[617] Siyang Leng, Huanfei Ma, Jürgen Kurths, Ying-Cheng Lai, Wei Lin, Kazuyuki Aihara, Luonan Chen, Partial cross mapping eliminates indirect causal influences, Nature Commun. 11 (1) (2020) 1–9.
[618] Daniel Harnack, Erik Laminski, Maik Schünemann, Klaus Richard Pawelzik, Topological causality in dynamical systems, Phys. Rev. Lett. 119 (9) (2017) 098301.
[619] José M. Amigó, Yoshito Hirata, Detecting directional couplings from multivariate flows by the joint distance distribution, Chaos 28 (7) (2018) 075302.
[620] Xiong Ying, Si-Yang Leng, Huan-Fei Ma, Qing Nie, Ying-Cheng Lai, Wei Lin, Detecting directional couplings from multivariate flows by the joint distance distribution, Research 2022 (2022) 9870149.
[621] Abd AlRahman R. AlMomani, Jie Sun, Erik Bollt, How entropic regression beats the outliers problem in nonlinear system identification, Chaos 30 (1) (2020) 013107.
[622] Ying-Cheng Lai, Finding nonlinear system equations and complex network structures from data: A sparse optimization approach, Chaos 31 (8) (2021) 082101.
[623] Steven L. Brunton, Marko Budišić, Eurika Kaiser, J Nathan Kutz, Modern Koopman theory for dynamical systems, 2021, arXiv preprint arXiv:2102.12086.
[624] Bernard O. Koopman, Hamiltonian systems and transformation in Hilbert space, Proc. Natl. Acad. Sci. 17 (5) (1931) 315–318.
[625] Peter J. Schmid, Dynamic mode decomposition of numerical and experimental data, J. Fluid Mech. 656 (2010) 5–28.
[626] J Nathan Kutz, Steven L Brunton, Bingni W Brunton, Joshua L Proctor, Dynamic Mode Decomposition: Data-Driven Modeling of Complex Systems, SIAM, 2016.
[627] Matthew O. Williams, Ioannis G. Kevrekidis, Clarence W. Rowley, A data–driven approximation of the koopman operator: Extending dynamic mode decomposition, J. Nonlinear Sci. 25 (6) (2015) 1307–1346.
[628] Jeremy Morton, Freddie D. Witherden, Mykel J. Kochenderfer, Deep variational koopman models: Inferring koopman observations for uncertainty-aware dynamics modeling and control, 2019, arXiv preprint arXiv:1902.09742.
[629] Bethany Lusch, J. Nathan Kutz, Steven L. Brunton, Deep learning for universal linear embeddings of nonlinear dynamics, Nature Commun. 9 (1) (2018) 1–10.
[630] Omri Azencot, N Benjamin Erichson, Vanessa Lin, Michael Mahoney, Forecasting sequential data using consistent koopman autoencoders, in: International Conference on Machine Learning, PMLR, 2020, pp. 475–485.
[631] Samuel E. Otto, Clarence W. Rowley, Linearly recurrent autoencoder networks for learning dynamics, SIAM J. Appl. Dyn. Syst. 18 (1) (2019) 558–593.
[632] Madeleine Udell, Corinne Horn, Reza Zadeh, Stephen Boyd, et al., Generalized low rank models, Found. Trends® Mach. Learn. 9 (1) (2016) 1–118.
[633] Nelida Črnjarić-Žic, Senka Maćešić, Igor Mezić, Koopman operator spectrum for random dynamical systems, J. Nonlinear Sci. 30 (5) (2020) 2007–2056.
[634] Sebastian Peitz, Stefan Klus, Koopman operator-based model reduction for switched-system control of PDEs, Automatica 106 (2019) 184–191.
[635] Senka Macesic, Nelida Crnjaric-Zic, Igor Mezic, Koopman operator family spectrum for nonautonomous systems, SIAM J. Appl. Dyn. Syst. 17 (4) (2018) 2478–2515.
[636] Wei Xiong, Muyuan Ma, Pei Sun, Yang Tian, Koopmanlab: machine learning for solving complex physics equations, 2023, arXiv preprint arXiv:2301.01104.
[637] Wei Xiong, Xiaomeng Huang, Ziyang Zhang, Ruixuan Deng, Pei Sun, Yang Tian, Koopman neural operator as a mesh-free solver of non-linear partial differential equations, 2023, arXiv preprint arXiv:2301.10022.
[638] Mikhail Galkin, Max Berrendorf, Charles Tapley Hoyt, An open challenge for inductive link prediction on knowledge graphs, 2022, arXiv preprint arXiv:2203.01520.
[639] Rui Tang, Zhenxiong Miao, Shuyu Jiang, Xingshu Chen, Haizhou Wang, Wei Wang, Interlayer link prediction in multiplex social networks based on multiple types of consistency between embedding vectors, IEEE Trans. Cybern. (2021) 1–14.
[640] Mingshan Jia, Bogdan Gabrys, Katarzyna Musial, Measuring quadrangle formation in complex networks, IEEE Trans. Netw. Sci. Eng. 9 (2) (2022) 538–551.

[641] Aaron Clauset, Cristopher Moore, Mark E.J. Newman, Hierarchical structure and the prediction of missing links in networks, Nature 453 (7191) (2008) 98–101.
[642] Yunpeng Xiao, Xixi Li, Haohan Wang, Ming Xu, Yanbing Liu, 3-HBP: A three-level hidden Bayesian link prediction model in social networks, IEEE Trans. Comput. Soc. Syst. 5 (2) (2018) 430–443.
[643] Jinyin Chen, Jian Zhang, Xuanheng Xu, Chenbo Fu, Dan Zhang, Qingpeng Zhang, Qi Xuan, E-LSTM-D: A deep learning framework for dynamic network link prediction, IEEE Trans. Syst. Man Cybern. 51 (6) (2021) 3699–3712.
[644] Min Yang, Junhao Liu, Lei Chen, Zhou Zhao, Xiaojun Chen, Ying Shen, An advanced deep generative framework for temporal link prediction in dynamic networks, IEEE Trans. Cybern. 50 (12) (2020) 4946–4957.
[645] Phu Pham, Loan T.T. Nguyen, Ngoc Thanh Nguyen, Witold Pedrycz, Unil Yun, Bay Vo, ComGCN: Community-driven graph convolutional network for link prediction in dynamic networks, IEEE Trans. Syst. Man Cybern. (2021) 1–13.
[646] Lanlan Rui, Yu Zhu, Zhipeng Gao, Xuesong Qiu, CLPM: A cooperative link prediction model for industrial internet of things using partitioned stacked denoising autoencoder, IEEE Trans. Ind. Inform. 17 (5) (2021) 3620–3629.
[647] Jayson S Jia, Xin Lu, Yun Yuan, Ge Xu, Jianmin Jia, Nicholas A Christakis, Population flow drives spatio-temporal distribution of COVID-19 in China, Nature 582 (7812) (2020) 389–394.
[648] Felana Angella Ihantamalala, Vincent Herbreteau, Feno MJ Rakotoarimanana, Jean Marius Rakotondramanga, Simon Cauchemez, Bienvenue Rahoilijaona, Gwenaëlle Pennober, Caroline O Buckee, Christophe Rogier, Charlotte Jessica Eland Metcalf, et al., Estimating sources and sinks of malaria parasites in Madagascar, Nature Commun. 9 (1) (2018) 1–8.
[649] Tigist F Menkir, Taylor Chin, James A Hay, Erik D Surface, Pablo M De Salazar, Caroline O Buckee, Alexander Watts, Kamran Khan, Ryan Sherbo, Ada WC Yan, et al., Estimating internationally imported cases during the early COVID-19 pandemic, Nature Commun. 12 (1) (2021) 1–10.
[650] Fan Zhou, Xiuxiu Qi, Kunpeng Zhang, Goce Trajcevski, Ting Zhong, MetaGeo: A general framework for social user geolocation identification with few-shot learning, IEEE Trans. Neural Netw. Learn. Syst. (2022) 1–15.
[651] Xin Zheng, Jialong Han, Aixin Sun, A survey of location prediction on Twitter, IEEE Trans. Knowl. Data Eng. 30 (9) (2018) 1652–1671.
[652] Zhiwen Yu, Fei Yi, Qin Lv, Bin Guo, Identifying on-site users for social events: Mobility, content, and social relationship, IEEE Trans. Mob. Comput. 17 (9) (2018) 2055–2068.
[653] Jordan Bakerman, Karl Pazdernik, Alyson Wilson, Geoffrey Fairchild, Rian Bahran, Twitter geolocation: A hybrid approach, ACM Trans. Knowl. Discov. Data (TKDD) 12 (3) (2018) 1–17.
[654] Trung-Kien Le, Nobutaka Ono, Closed-form and near closed-form solutions for TDOA-based joint source and sensor localization, IEEE Trans. Signal Process. 65 (5) (2017) 1207–1221.
[655] Gang Wang, Shu Cai, Youming Li, Ming Jin, Second-order cone relaxation for TOA-based source localization with unknown start transmission time, IEEE Trans. Veh. Technol. 63 (6) (2014) 2973–2977.
[656] T. Li, A. Ekpenyong, Y.-F. Huang, Source localization and tracking using distributed asynchronous sensors, IEEE Trans. Signal Process. 54 (10) (2006) 3991–4003.
[657] Yongsheng Yan, Ge Yang, Haiyan Wang, Xiaohong Shen, Semidefinite relaxation for source localization with quantized ToA measurements and transmission uncertainty in sensor networks, IEEE Trans. Commun. 69 (2) (2021) 1201–1213.
[658] Omer Berat Sezer, Mehmet Ugur Gudelek, Ahmet Murat Ozbayoglu, Financial time series forecasting with deep learning: A systematic literature review: 2005–2019, Appl. Soft Comput. 90 (2020) 106181.
[659] Fengzhen Jia, Chun-Chun Chen, Emotional characteristics and time series analysis of internet public opinion participants based on emotional feature words, Int. J. Adv. Robot. Syst. 17 (1) (2020) 1729881420904213.
[660] Shinsuke Uda, Application of information theory in systems biology, Biophys. Rev. 12 (2) (2020) 377–384.
[661] Greice Madeleine Ikeda do Carmo, Catherine Yen, Jennifer Cortes, Alessandra Araujo Siqueira, Wanderson Kleber de Oliveira, Juan Jose Cortez-Escalante, Ben Lopman, Brendan Flannery, Lucia Helena de Oliveira, Eduardo Hage Carmo, et al., Decline in diarrhea mortality and admissions after routine childhood rotavirus immunization in Brazil: a time-series analysis, PLoS Med. 8 (4) (2011) e1001024.
[662] Bryan Lim, Stefan Zohren, Time-series forecasting with deep learning: a survey, Phil. Trans. R. Soc. A 379 (2194) (2021) 20200209.
[663] Biswadeb Dutta, Andreas Krichel, Marie-Paule Odini, The challenge of zero touch and explainable AI, J. ICT Stand. (2021) 147–158.
[664] Yao Qin, Dongjin Song, Haifeng Cheng, Wei Cheng, Guofei Jiang, Garrison W. Cottrell, A dual-stage attention-based recurrent neural network for time series prediction, in: IJCAI '17, AAAI Press, 2017, pp. 2627–2633.
[665] Olivier Pieters, Emiel Deprost, Jonas Van Der Donckt, Lore Brosens, Pieter Sanczuk, Pieter Vangansbeke, Tom De Swaef, Pieter De Frenne, Francis Wyffels, MIRRA: A modular and cost-effective microclimate monitoring system for real-time remote applications, Sensors 21 (13) (2021) 4615.
[666] Stephen J. Taylor, Modelling Financial Time Series, World Scientific, 2008.
[667] Dongwei Xu, Chenchen Wei, Peng Peng, Qi Xuan, Haifeng Guo, GE-GAN: A novel deep learning framework for road traffic state estimation, Transp. Res. C 117 (2020) 102635.
[668] Xuguang Hu, Huaguang Zhang, Dazhong Ma, Rui Wang, A tnGAN-based leak detection method for pipeline network considering incomplete sensor data, IEEE Trans. Instrum. Meas. 70 (2020) 1–10.
[669] Yi-Fan Zhang, Peter J. Thorburn, Wei Xiang, Peter Fitch, SSIM—A deep learning approach for recovering missing time series sensor data, IEEE Internet Things J. 6 (4) (2019) 6618–6628.
[670] Hassan Ismail Fawaz, Germain Forestier, Jonathan Weber, Lhassane Idoumghar, Pierre-Alain Muller, Deep learning for time series classification: a review, Data Min. Knowl. Discov. 33 (4) (2019) 917–963.
[671] Vivien Sainte Fare Garnot, Loic Landrieu, Sebastien Giordano, Nesrine Chehata, Satellite image time series classification with pixel-set encoders and temporal self-attention, in: Proceedings of the IEEE/CVF Conference on Computer Vision and Pattern Recognition, 2020, pp. 12325–12334.
[672] Xuchao Zhang, Yifeng Gao, Jessica Lin, Chang-Tien Lu, Tapnet: Multivariate time series classification with attentional prototypical network, in: Proceedings of the AAAI Conference on Artificial Intelligence, Vol. 34, 2020, pp. 6845–6852.
[673] Fazle Karim, Somshubra Majumdar, Houshang Darabi, Adversarial attacks on time series, IEEE Trans. Pattern Anal. Mach. Intell. 43 (10) (2020) 3309–3320.
[674] Mohd Yousuf Ansari, Amir Ahmad, Shehroz S Khan, Gopal Bhushan, et al., Spatiotemporal clustering: a review, Artif. Intell. Rev. 53 (4) (2020) 2381–2423.
[675] Léonard Seydoux, Randall Balestriero, Piero Poli, Maarten de Hoop, Michel Campillo, Richard Baraniuk, Clustering earthquake signals and background noises in continuous seismic data with unsupervised deep learning, Nature Commun. 11 (1) (2020) 1–12.
[676] Qianli Ma, Chuxin Chen, Sen Li, Garrison W. Cottrell, Learning representations for incomplete time series clustering, in: Proceedings of the AAAI Conference on Artificial Intelligence, Vol. 35, 2021, pp. 8837–8846.
[677] Qin Zhang, Jia Wu, Peng Zhang, Guodong Long, Chengqi Zhang, Salient subsequence learning for time series clustering, IEEE Trans. Pattern Anal. Mach. Intell. 41 (9) (2018) 2193–2207.
[678] Qianli Ma, Sen Li, Wanqing Zhuang, Jiabing Wang, Delu Zeng, Self-supervised time series clustering with model-based dynamics, IEEE Trans. Neural Netw. Learn. Syst. 32 (9) (2020) 3942–3955.

[679] Fumiyasu Makinoshima, Yusuke Oishi, Takashi Yamazaki, Takashi Furumura, Fumihiko Imamura, Early forecasting of tsunami inundation from tsunami and geodetic observation data with convolutional neural networks, Nature Commun. 12 (1) (2021) 1–10.
[680] Shengnan Guo, Youfang Lin, Ning Feng, Chao Song, Huaiyu Wan, Attention based spatial-temporal graph convolutional networks for traffic flow forecasting, in: Proceedings of the AAAI Conference on Artificial Intelligence, Vol. 33, 2019, pp. 922–929.
[681] Chao Song, Youfang Lin, Shengnan Guo, Huaiyu Wan, Spatial-temporal synchronous graph convolutional networks: A new framework for spatial-temporal network data forecasting, in: Proceedings of the AAAI Conference on Artificial Intelligence, Vol. 34, 2020, pp. 914–921.
[682] Defu Cao, Yujing Wang, Juanyong Duan, Ce Zhang, Xia Zhu, Congrui Huang, Yunhai Tong, Bixiong Xu, Jing Bai, Jie Tong, et al., Spectral temporal graph neural network for multivariate time-series forecasting, Adv. Neural Inf. Process. Syst. 33 (2020) 17766–17778.
[683] Shangfeng Chen, Bin Yu, Renguang Wu, Wen Chen, Linye Song, The dominant north Pacific atmospheric circulation patterns and their relations to Pacific SSTs: historical simulations and future projections in the IPCC AR6 models, Clim. Dynam. 56 (2021) 701–725.
[684] Boris N Oreshkin, Dmitri Carpov, Nicolas Chapados, Yoshua Bengio, Meta-learning framework with applications to zero-shot time-series forecasting, 2020, arXiv preprint arXiv:2002.02887.
[685] Qihang Wang, Feng Liu, Guihong Wan, Ying Chen, Inference of brain states under anesthesia with meta learning based deep learning models, IEEE Trans. Neural Syst. Rehabil. Eng. 30 (2022) 1081–1091.
[686] Huiling Qin, Songyu Ke, Xiaodu Yang, Haoran Xu, Xianyuan Zhan, Yu Zheng, Robust spatio-temporal purchase prediction via deep meta learning, in: Proceedings of the AAAI Conference on Artificial Intelligence, Vol. 35, 2021, pp. 4312–4319.
[687] Huanfei Ma, Siyang Leng, Kazuyuki Aihara, Wei Lin, Luonan Chen, Randomly distributed embedding making short-term high-dimensional data predictable, Proc. Natl. Acad. Sci. USA 115 (2018) E9994–10002.
[688] Qunxi Zhu, Huanfei Ma, Wei Lin, Detecting unstable periodic orbits based only on time series: When adaptive delayed feedback control meets reservoir computing, Chaos 29 (9) (2019) 093125.
[689] Qunxi Zhu, Yao Guo, Wei Lin, Neural delay differential equations, in: International Conference on Learning Representations, 2021, URL https://openreview.net/forum?id=Q1jmmQz72M2.
[690] George P Malanson, Ashton M Verdery, Stephen J Walsh, Yothin Sawangdee, Benjamin W Heumann, Philip M McDaniel, Brian G Frizzelle, Nathalie E Williams, Xiaozheng Yao, Barbara Entwisle, et al., Changing crops in response to climate: Virtual nang rong, thailand in an agent based simulation, Appl. Geogr. 53 (2014) 202–212.
[691] Parastu Kasaie, Jason R Andrews, W David Kelton, David W Dowdy, Timing of tuberculosis transmission and the impact of household contact tracing. An agent-based simulation model, Am. J. Respir. Crit. Care Med. 189 (7) (2014) 845–852.
[692] Stefano Merler, Marco Ajelli, Laura Fumanelli, Marcelo FC Gomes, Ana Pastore y Piontti, Luca Rossi, Dennis L Chao, Ira M Longini Jr., M Elizabeth Halloran, Alessandro Vespignani, Spatiotemporal spread of the 2014 outbreak of ebola virus disease in liberia and the effectiveness of non-pharmaceutical interventions: a computational modelling analysis, Lancet Infect. Dis. 15 (2) (2015) 204–211.
[693] Constantinos Siettos, Cleo Anastassopoulou, Lucia Russo, Christos Grigoras, Eleftherios Mylonakis, Modeling the 2014 ebola virus epidemic–agent-based simulations, temporal analysis and future predictions for liberia and sierra leone, PLoS Curr. 7 (2015).
[694] Andrew T. Crooks, Atesmachew B. Hailegiorgis, An agent-based modeling approach applied to the spread of cholera, Environ. Model. Softw. 62 (2014) 164–177.
[695] Alberto Aleta, David Martín-Corral, Michiel A Bakker, Ana Pastore y Piontti, Marco Ajelli, Maria Litvinova, Matteo Chinazzi, Natalie E Dean, M Elizabeth Halloran, Ira M Longini Jr., et al., Quantifying the importance and location of SARS-CoV-2 transmission events in large metropolitan areas, Proc. Natl. Acad. Sci. 119 (26) (2022) e2112182119.
[696] Rebecca J Rockett, Alicia Arnott, Connie Lam, Rosemarie Sadsad, Verlaine Timms, Karen-Ann Gray, John-Sebastian Eden, Sheryl Chang, Mailie Gall, Jenny Draper, et al., Revealing COVID-19 transmission in Australia by SARS-CoV-2 genome sequencing and agent-based modeling, Nature Med. 26 (9) (2020) 1398–1404.
[697] Ken T.D. Eames, Matt J. Keeling, Contact tracing and disease control, Proc. R. Soc. B 270 (1533) (2003) 2565–2571.
[698] Steven Riley, Neil M. Ferguson, Smallpox transmission and control: spatial dynamics in great britain, Proc. Natl. Acad. Sci. 103 (33) (2006) 12637–12642.
[699] Lin Zhu, Günter C Müller, John M Marshall, Kristopher L Arheart, Whitney A Qualls, WayWay M Hlaing, Yosef Schlein, Sekou F Traore, Seydou Doumbia, John C Beier, Is outdoor vector control needed for malaria elimination? An individual-based modelling study, Malar. J. 16 (1) (2017) 1–11.
[700] Giancarlo De Luca, Kim Van Kerckhove, Pietro Coletti, Chiara Poletto, Nathalie Bossuyt, Niel Hens, Vittoria Colizza, The impact of regular school closure on seasonal influenza epidemics: a data-driven spatial transmission model for Belgium, BMC Infect. Dis. 18 (1) (2018) 1–16.
[701] Joel Hellewell, Sam Abbott, Amy Gimma, Nikos I Bosse, Christopher I Jarvis, Timothy W Russell, James D Munday, Adam J Kucharski, W John Edmunds, Fiona Sun, et al., Feasibility of controlling COVID-19 outbreaks by isolation of cases and contacts, Lancet Glob. Health 8 (4) (2020) e488–e496.
[702] Richard O.J.H. Stutt, Renata Retkute, Michael Bradley, Christopher A. Gilligan, John Colvin, A modelling framework to assess the likely effectiveness of facemasks in combination with 'lock-down'in managing the COVID-19 pandemic, Proc. R. Soc. Lond. Ser. A Math. Phys. Eng. Sci. 476 (2238) (2020) 20200376.
[703] Jeremy Howard, Austin Huang, Zhiyuan Li, Zeynep Tufekci, Vladimir Zdimal, Helene-Mari van der Westhuizen, Arne von Delft, Amy Price, Lex Fridman, Lei-Han Tang, et al., An evidence review of face masks against COVID-19, Proc. Natl. Acad. Sci. 118 (4) (2021) e2014564118.
[704] Dennis L. Chao, M. Elizabeth Halloran, Valerie J. Obenchain, Ira M. Longini Jr., FluTE, a publicly available stochastic influenza epidemic simulation model, PLoS Comput. Biol. 6 (1) (2010) e1000656.
[705] Joel R. Koo, Alex R. Cook, Minah Park, Yinxiaohe Sun, Haoyang Sun, Jue Tao Lim, Clarence Tam, Borame L. Dickens, Interventions to mitigate early spread of SARS-CoV-2 in Singapore: a modelling study, Lancet Infect. Dis. 20 (6) (2020) 678–688.
[706] Sheryl L. Chang, Nathan Harding, Cameron Zachreson, Oliver M. Cliff, Mikhail Prokopenko, Modelling transmission and control of the COVID-19 pandemic in Australia, Nature Commun. 11 (1) (2020) 1–13.
[707] Quan-Hui Liu, Juanjuan Zhang, Cheng Peng, Maria Litvinova, Shudong Huang, Piero Poletti, Filippo Trentini, Giorgio Guzzetta, Valentina Marziano, Tao Zhou, et al., Model-based evaluation of alternative reactive class closure strategies against COVID-19, Nature Commun. 13 (1) (2022) 1–10.
[708] Cliff C. Kerr, Robyn M. Stuart, Dina Mistry, Romesh G. Abeysuriya, Katherine Rosenfeld, Gregory R. Hart, Rafael C. Núñez, Jamie A. Cohen, Prashanth Selvaraj, Brittany Hagedorn, et al., Covasim: an agent-based model of COVID-19 dynamics and interventions, PLoS Comput. Biol. 17 (7) (2021) e1009149.
[709] Matt J. Keeling, Chris A. Gilligan, Metapopulation dynamics of bubonic plague, Nature 407 (6806) (2000) 903–906.
[710] Matt J. Keeling, Leon Danon, Matthew C. Vernon, Thomas A. House, Individual identity and movement networks for disease metapopulations, Proc. Natl. Acad. Sci. 107 (19) (2010) 8866–8870.
[711] David Soriano-Paños, Juddy Heliana Arias-Castro, Adriana Reyna-Lara, Hector J. Martínez, Sandro Meloni, Jesús Gómez-Gardeñes, Vector-borne epidemics driven by human mobility, Phys. Rev. Res. 2 (2020) 013312.
[712] Azi Lipshtat, Roger Alimi, Yochai Ben-Horin, Commuting in metapopulation epidemic modeling, Sci. Rep. 11 (1) (2021) 1–8.

[713] Surendra Hazarie, David Soriano-Paños, Alex Arenas, Jesús Gómez-Gardeñes, Gourab Ghoshal, Interplay between population density and mobility in determining the spread of epidemics in cities, Commun. Phys. 4 (1) (2021) 1–10.
[714] I.M. Hall, Joseph R. Egan, I. Barrass, R. Gani, Stephen Leach, Comparison of smallpox outbreak control strategies using a spatial metapopulation model, Epidemiol. Infect. 135 (7) (2007) 1133–1144.
[715] Subrata Ghosh, Abhishek Senapati, Joydev Chattopadhyay, Chittaranjan Hens, Dibakar Ghosh, Optimal test-kit-based intervention strategy of epidemic spreading in heterogeneous complex networks, Chaos 31 (7) (2021) 071101.
[716] Abhishek Senapati, Tridip Sardar, Krishnendra Sankar Ganguly, Krishna Sankar Ganguly, Asis Kumar Chattopadhyay, Joydev Chattopadhyay, Impact of adult mosquito control on dengue prevalence in a multi-patch setting: a case study in Kolkata (2014–2015), J. Theoret. Biol. 478 (2019) 139–152.
[717] Lin Wang, Joseph T. Wu, Characterizing the dynamics underlying global spread of epidemics, Nature Commun. 9 (1) (2018) 1–11.
[718] Qian Zhang, Kaiyuan Sun, Matteo Chinazzi, Ana Pastore y Piontti, Natalie E. Dean, Diana Patricia Rojas, Stefano Merler, Dina Mistry, Piero Poletti, Luca Rossi, et al., Spread of Zika virus in the Americas, Proc. Natl. Acad. Sci. 114 (22) (2017) E4334–E4343.
[719] Marcelo F.C. Gomes, Ana Pastore y Piontti, Luca Rossi, Dennis Chao, Ira Longini, M. Elizabeth Halloran, Alessandro Vespignani, Assessing the international spreading risk associated with the 2014 West African Ebola outbreak, PLoS Curr. 6 (2014).
[720] Jessica T. Davis, Matteo Chinazzi, Nicola Perra, Kunpeng Mu, Ana Pastore y Piontti, Marco Ajelli, Natalie E. Dean, Corrado Gioannini, Maria Litvinova, Stefano Merler, et al., Cryptic transmission of SARS-CoV-2 and the first COVID-19 wave, Nature 600 (7887) (2021) 127–132.
[721] Fred S. Lu, Andre T. Nguyen, Nicholas B. Link, Mathieu Molina, Jessica T. Davis, Matteo Chinazzi, Xinyue Xiong, Alessandro Vespignani, Marc Lipsitch, Mauricio Santillana, Estimating the cumulative incidence of COVID-19 in the United States using influenza surveillance, virologic testing, and mortality data: Four complementary approaches, PLoS Comput. Biol. 17 (6) (2021) e1008994.
[722] Dongxia Wu, Liyao Gao, Matteo Chinazzi, Xinyue Xiong, Alessandro Vespignani, Yi-An Ma, Rose Yu, Quantifying uncertainty in deep spatiotemporal forecasting, in: Proceedings of the 27th ACM SIGKDD Conference on Knowledge Discovery & Data Mining, 2021, pp. 1841–1851.
[723] Matteo Chinazzi, Jessica T. Davis, Marco Ajelli, Corrado Gioannini, Maria Litvinova, Stefano Merler, Ana Pastore y Piontti, Kunpeng Mu, Luca Rossi, Kaiyuan Sun, et al., The effect of travel restrictions on the spread of the 2019 novel coronavirus (COVID-19) outbreak, Science 368 (6489) (2020) 395–400.
[724] Marko Jusup, Petter Holme, Kiyoshi Kanazawa, Misako Takayasu, Ivan Romić, Zhen Wang, Sunčana Geček, Tomislav Lipić, Boris Podobnik, Lin Wang, Wei Luo, Tin Klanjšček, Jingfang Fan, Stefano Boccaletti, Matjaž Perc, Social physics, Phys. Rep. 948 (2022) 1–148.
[725] Serge Galam, Sociophysics: A review of Galam models, Internat. J. Modern Phys. C 19 (2008) 409–440.
[726] C. Castellano, S. Fortunato, V. Loreto, Statistical physics of social dynamics, Rev. Modern Phys. 81 (2009) 591–646.
[727] Dirk Helbing, Dirk Brockmann, Thomas Chadefaux, Karsten Donnay, Ulf Blanke, Olivia Woolley-Meza, Mehdi Moussaid, Anders Johansson, Jens Krause, Matjaz Perc, Saving human lives: What complexity science and information systems can contribute, J. Stat. Phys. 158 (2015) 735–781.
[728] Wolfgang Weidlich, The statistical description of polarization phenomena in society, Br. J. Math. Stat. Psychol. 24 (1971) 251–266.
[729] Serge Galam, Yuval Gefen, Yonathan Shapir, Sociophysics: A new approach of sociological collective behaviour. I. mean-behaviour description of a strike, J. Math. Sociol. 9 (1982) 1–13.
[730] Serge Galam, Serge Moscovici, Towards a theory of collective phenomena: Consensus and attitude changes in groups, Eur. J. Soc. Psychol. 21 (1991) 49–74.
[731] Katarzyna Sznajd-Weron, Sznajd model and its applications, Acta Phys. Polon. B 36 (2005) 2537.
[732] Rainer Hegselmann, Ulrich Krause, et al., Opinion dynamics and bounded confidence models, analysis, and simulation, J. Artif. Soc. Soc. Simul. 5 (2002) 1.
[733] Katarzyna Sznajd-Weron, Józef Sznajd, Tomasz Weron, A review on the Sznajd model – 20 years after, Physica A 565 (2021) 125537.
[734] Tyll Krüger, Krzysztof Gogolewski, Marcin Bodych, Anna Gambin, Giulia Giordano, Sarah Cuschieri, Thomas Czypionka, Matjaž Perc, Elena Petelos, Magdalena Rosińska, Ewa Szczurek, Risk assessment of COVID-19 epidemic resurgence in relation to SARS-CoV-2 variants and vaccination passes, Commun. Med. 2 (2022) 23.
[735] Camilla Ancona, Francesco Lo Iudice, Franco Garofalo, Pietro De Lellis, A model-based opinion dynamics approach to tackle vaccine hesitancy, Sci. Rep. 12 (2022) 11835.
[736] Abigail Hickok, Yacoub Kureh, Heather Z. Brooks, Michelle Feng, Mason A. Porter, A bounded-confidence model of opinion dynamics on hypergraphs, SIAM J. Appl. Dyn. Syst. 21 (2022) 1–32.
[737] Soumen Majhi, Matjaž Perc, Dibakar Ghosh, Dynamics on higher-order networks: A review, J. R. Soc. Interface 19 (2022) 20220043.
[738] Gordon Pennycook, Ziv Epstein, Mohsen Mosleh, Antonio A. Arechar, Dean Eckles, David G. Rand, Shifting attention to accuracy can reduce misinformation online, Nature 592 (2021) 590–595.
[739] Gordon Pennycook, David G. Rand, The psychology of fake news, Trends Cogn. Sci. 25 (2021) 388–402.
[740] Zhen Guo, Jaber Valinejad, Jin-Hee Cho, Effect of disinformation propagation on opinion dynamics: A game theoretic approach, IEEE Trans. Netw. Sci. Eng. 9 (2022) 3775–3790.
[741] M.A. Nowak, R. Highfield, SuperCooperators: Altruism, Evolution, and Why We Need Each Other to Succeed, Free Press, New York, 2011.
[742] M. Perc, J.J. Jordan, D.G. Rand, Z. Wang, S. Boccaletti, A. Szolnoki, Statistical physics of human cooperation, Phys. Rep. 687 (2017) 1–51.
[743] Unai Alvarez-Rodriguez, Federico Battiston, Guilherme Ferraz de Arruda, Yamir Moreno, Matjaž Perc, Vito Latora, Evolutionary dynamics of higher-order interactions in social networks, Nat. Hum. Behav. 5 (2021) 586–595.
[744] Giulio Burgio, Joan T. Matamalas, Sergio Gómez, Alex Arenas, Evolution of cooperation in the presence of higher-order interactions: from networks to hypergraphs, Entropy 22 (2020) 744.
[745] Valerio Capraro, Matjaž Perc, Mathematical foundations of moral preferences, J. R. Soc. Interface 18 (2021) 20200880.
[746] Carlo Giambiagi Ferrari, Juan Pablo Pinasco, Nicolas Saintier, Coupling epidemiological models with social dynamics, Bull. Math. Biol. 83 (2021) 74.
[747] Angelo Antoci, Paolo Russu, Pier Luigi Sacco, Giorgio Tavano Blessi, Preying on beauty? The complex social dynamics of overtourism, J. Econ. Interact. Coord. 17 (2022) 379–400.
[748] Manuel Chica, Juan M. Hernández, Matjaž Perc, Sustainability in tourism determined by an asymmetric game with mobility, J. Clean. Prod. 355 (2022) 131662.
[749] Alexander M. Petersen, Joel N. Tenenbaum, Shlomo Havlin, H. Eugene Stanley, Matjaž Perc, Languages cool as they expand: Allometric scaling and the decreasing need for new words, Sci. Rep. 2 (2012) 943.
[750] Quirin Würschinger, Social networks of lexical innovation. Investigating the social dynamics of diffusion of neologisms on Twitter, Front. Artif. Intell. 4 (2021) 648583.
[751] György Buzsáki, Neural syntax: cell assemblies, synapsembles, and readers, Neuron 68 (3) (2010) 362–385.
[752] Yu Mu, Sujatha Narayan, Brett D. Mensh, Misha B. Ahrens, Brain-wide, scale-wide physiology underlying behavioral flexibility in zebrafish, Curr. Opin. Neurobiol. 64 (2020) 151–160.
[753] Anne E. Urai, Brent Doiron, Andrew M. Leifer, Anne K. Churchland, Large-scale neural recordings call for new insights to link brain and behavior, Nature Neurosci. 25 (1) (2022) 11–19.

[754] Albert Lin, Daniel Witvliet, Luis Hernandez-Nunez, Scott W. Linderman, Aravinthan D.T. Samuel, Vivek Venkatachalam, Imaging whole-brain activity to understand behaviour, Nat. Rev. Phys. 4 (5) (2022) 292–305.
[755] Philipp J. Keller, Misha B. Ahrens, Visualizing whole-brain activity and development at the single-cell level using light-sheet microscopy, Neuron 85 (3) (2015) 462–483.
[756] Rafael Yuste, Circuit neuroscience: the road ahead, Front. Neurosci. 2 (2008) 17.
[757] Liqun Luo, Architectures of neuronal circuits, Science 373 (6559) (2021) eabg7285.
[758] Nelly Daur, Farzan Nadim, Dirk Bucher, The complexity of small circuits: the stomatogastric nervous system, Curr. Opin. Neurobiol. 41 (2016) 1–7.
[759] Nicholas A. Steinmetz, Christof Koch, Kenneth D. Harris, Matteo Carandini, Challenges and opportunities for large-scale electrophysiology with Neuropixels probes, Curr. Opin. Neurobiol. 50 (2018) 92–100.
[760] Shigeyoshi Fujisawa, Asohan Amarasingham, Matthew T. Harrison, György Buzsáki, Behavior-dependent short-term assembly dynamics in the medial prefrontal cortex, Nature Neurosci. 11 (7) (2008) 823–833.
[761] N Hatsopoulos, Stuart Geman, Asohan Amarasingham, Elie Bienenstock, At what time scale does the nervous system operate? Neurocomputing 52 (2003) 25–29.
[762] Feng Zhang, Viviana Gradinaru, Antoine R. Adamantidis, Remy Durand, Raag D. Airan, Luis De Lecea, Karl Deisseroth, Optogenetic interrogation of neural circuits: technology for probing mammalian brain structures, Nat. Protoc. 5 (3) (2010) 439–456.
[763] Edward M. Callaway, Transneuronal circuit tracing with neurotropic viruses, Curr. Opin. Neurobiol. 18 (6) (2008) 617–623.
[764] Gregory S.X.E. Jefferis, Jean Livet, Sparse and combinatorial neuron labelling, Curr. Opin. Neurobiol. 22 (1) (2012) 101–110.
[765] Laura B. Motta-Mena, Anna Reade, Michael J. Mallory, Spencer Glantz, Orion D. Weiner, Kristen W. Lynch, Kevin H. Gardner, An optogenetic gene expression system with rapid activation and deactivation kinetics, Nat. Chem. Biol. 10 (3) (2014) 196–202.
[766] Yu Mu, Davis V. Bennett, Mikail Rubinov, Sujatha Narayan, Chao-Tsung Yang, Masashi Tanimoto, Brett D. Mensh, Loren L. Looger, Misha B. Ahrens, Glia accumulate evidence that actions are futile and suppress unsuccessful behavior, Cell 178 (1) (2019) 27–43.
[767] Fumi Katsuki, Christos Constantinidis, Bottom-up and top-down attention: different processes and overlapping neural systems, Neuroscientist 20 (5) (2014) 509–521.
[768] Markus Siegel, Timothy J. Buschman, Earl K. Miller, Cortical information flow during flexible sensorimotor decisions, Science 348 (6241) (2015) 1352–1355.
[769] Charles D. Gilbert, Wu Li, Top-down influences on visual processing, Nat. Rev. Neurosci. 14 (5) (2013) 350–363.
[770] Botond Roska, Markus Meister, The retina dissects the visual scene into distinct features, in: The New Visual Neurosciences, Vol. 843, MIT Press, Cambridge, MA, 2014, pp. 163–182.
[771] Edward M. Callaway, Structure and function of parallel pathways in the primate early visual system, J. Physiol. 566 (1) (2005) 13–19.
[772] Mortimer Mishkin, Leslie G. Ungerleider, Kathleen A. Macko, Object vision and spatial vision: two cortical pathways, Trends Neurosci. 6 (1983) 414–417.
[773] Dwight J. Kravitz, Kadharbatcha S. Saleem, Chris I. Baker, Mortimer Mishkin, A new neural framework for visuospatial processing, Nat. Rev. Neurosci. 12 (4) (2011) 217–230.
[774] Michael A. Long, Michale S. Fee, Using temperature to analyse temporal dynamics in the songbird motor pathway, Nature 456 (7219) (2008) 189–194.
[775] Kalman A. Katlowitz, Michel A. Picardo, Michael A. Long, Stable sequential activity underlying the maintenance of a precisely executed skilled behavior, Neuron 98 (6) (2018) 1133–1140.
[776] Kosuke Hamaguchi, Masashi Tanaka, Richard Mooney, A distributed recurrent network contributes to temporally precise vocalizations, Neuron 91 (3) (2016) 680–693.
[777] David A. McCrea, Ilya A. Rybak, Organization of mammalian locomotor rhythm and pattern generation, Brain Res. Rev. 57 (1) (2008) 134–146.
[778] Henrik Lindén, Peter C. Petersen, Mikkel Vestergaard, Rune W. Berg, Movement is governed by rotational neural dynamics in spinal motor networks, Nature (2022) 1–6.
[779] Donald Olding Hebb, The Organization of Behavior: A Neuropsychological Theory, Psychology Press, 2005.
[780] Mark S. Goldman, Memory without feedback in a neural network, Neuron 61 (4) (2009) 621–634.
[781] Eva Pastalkova, Vladimir Itskov, Asohan Amarasingham, Gyorgy Buzsaki, Internally generated cell assembly sequences in the rat hippocampus, Science 321 (5894) (2008) 1322–1327.
[782] Yingxue Wang, Sandro Romani, Brian Lustig, Anthony Leonardo, Eva Pastalkova, Theta sequences are essential for internally generated hippocampal firing fields, Nature Neurosci. 18 (2) (2015) 282–288.
[783] Ashok Litwin-Kumar, Brent Doiron, Formation and maintenance of neuronal assemblies through synaptic plasticity, Nature Commun. 5 (1) (2014) 1–12.
[784] Shengjin Xu, Wanchen Jiang, Mu-ming Poo, Yang Dan, Activity recall in a visual cortical ensemble, Nature Neurosci. 15 (3) (2012) 449–455.
[785] Michael A. Long, Dezhe Z. Jin, Michale S. Fee, Support for a synaptic chain model of neuronal sequence generation, Nature 468 (7322) (2010) 394–399.
[786] Johanni Brea, Walter Senn, Jean-Pascal Pfister, Matching recall and storage in sequence learning with spiking neural networks, J. Neurosci. 33 (23) (2013) 9565–9575.
[787] Ila R. Fiete, Walter Senn, Claude Z.H. Wang, Richard H.R. Hahnloser, Spike-time-dependent plasticity and heterosynaptic competition organize networks to produce long scale-free sequences of neural activity, Neuron 65 (4) (2010) 563–576.
[788] Kanaka Rajan, Christopher D. Harvey, David W. Tank, Recurrent network models of sequence generation and memory, Neuron 90 (1) (2016) 128–142.
[789] Giovanni Filatrella, Arne Hejde Nielsen, Niels Falsig Pedersen, Analysis of a power grid using a Kuramoto-like model, Eur. Phys. J. B 61 (4) (2008) 485–491.
[790] Martin Rohden, Andreas Sorge, Marc Timme, Dirk Witthaut, Self-organized synchronization in decentralized power grids, Phys. Rev. Lett. 109 (6) (2012) 064101.
[791] Dirk Witthaut, Marc Timme, Braess's paradox in oscillator networks, desynchronization and power outage, New J. Phys. 14 (8) (2012) 083036.
[792] Peng Ji, Thomas K.D.M Peron, Peter J. Menck, Francisco A. Rodrigues, Jürgen Kurths, Cluster explosive synchronization in complex networks, Phys. Rev. Lett. 110 (21) (2013) 218701.
[793] Florian Dörfler, Michael Chertkov, Francesco Bullo, Synchronization in complex oscillator networks and smart grids, Proc. Natl. Acad. Sci. 110 (6) (2013) 2005–2010.
[794] Florian Dorfler, Francesco Bullo, Synchronization and transient stability in power networks and nonuniform Kuramoto oscillators, SIAM J. Control Optim. 50 (3) (2012) 1616–1642.
[795] Stefan Kettemann, Delocalization of disturbances and the stability of ac electricity grids, Phys. Rev. E 94 (6) (2016) 062311.
[796] Peter J. Menck, Jobst Heitzig, Norbert Marwan, Jürgen Kurths, How basin stability complements the linear-stability paradigm, Nat. Phys. 9 (2) (2013) 89–92.

[797] Peter J. Menck, Jobst Heitzig, Jürgen Kurths, Hans Joachim Schellnhuber, How dead ends undermine power grid stability, Nature Commun. 5 (2014) 3969.
[798] Frank Hellmann, Paul Schultz, Carsten Grabow, Jobst Heitzig, Jürgen Kurths, Survivability of deterministic dynamical systems, Sci. Rep. 6 (1) (2016) 1–12.
[799] Chiranjit Mitra, Anshul Choudhary, Sudeshna Sinha, Jürgen Kurths, Reik V. Donner, Multiple-node basin stability in complex dynamical networks, Phys. Rev. E 95 (3) (2017) 032317.
[800] Peter J. Menck, Jürgen Kurths, Topological identification of weak points in power grids, in: NDES 2012; Nonlinear Dynamics of Electronic Systems, VDE, 2012, pp. 1–4.
[801] Heetae Kim, Mi Jin Lee, Sang Hoon Lee, Seung-Woo Son, On structural and dynamical factors determining the integrated basin instability of power-grid nodes, Chaos 29 (10) (2019) 103132.
[802] Paul Schultz, Jobst Heitzig, Jürgen Kurths, Detours around basin stability in power networks, New J. Phys. 16 (12) (2014) 125001.
[803] Frank Hellmann, Paul Schultz, Patrycja Jaros, Roman Levchenko, Tomasz Kapitaniak, Jürgen Kurths, Yuri Maistrenko, Network-induced multistability through lossy coupling and exotic solitary states, Nature Commun. 11 (1) (2020) 1–9.
[804] Adilson E. Motter, Seth A. Myers, Marian Anghel, Takashi Nishikawa, Spontaneous synchrony in power-grid networks, Nat. Phys. 9 (3) (2013) 191–197.
[805] Halgurd Taher, Simona Olmi, Eckehard Schöll, Enhancing power grid synchronization and stability through time-delayed feedback control, Phys. Rev. E 100 (6) (2019) 062306.
[806] Xiaozhu Zhang, Cheng Ma, Marc Timme, Vulnerability in dynamically driven oscillatory networks and power grids, Chaos 30 (6) (2020) 063111.
[807] Liudmila Tumash, Simona Olmi, Eckehard Schöll, Stability and control of power grids with diluted network topology, Chaos 29 (12) (2019) 123105.
[808] Liudmila Tumash, Simona Olmi, Eckehard Schöll, Influence of disorder and noise in controlling the dynamics of power grids, IFAC-PapersOnLine 51 (33) (2018) 44–49.
[809] Liudmila Tumash, Simona Olmi, Eckehard Schöll, Effect of disorder and noise in shaping the dynamics of power grids, Europhys. Lett. 123 (2) (2018) 20001.
[810] Lucia Valentina Gambuzza, Arturo Buscarino, Luigi Fortuna, Maurizio Porfiri, Mattia Frasca, Analysis of dynamical robustness to noise in power grids, IEEE J. Emerg. Sel. Top. Circuits Syst. 7 (3) (2017) 413–421.
[811] Benjamin Schäfer, Moritz Matthiae, Xiaozhu Zhang, Martin Rohden, Marc Timme, Dirk Witthaut, Escape routes, weak links, and desynchronization in fluctuation-driven networks, Phys. Rev. E 95 (6) (2017) 060203.
[812] Carl H. Totz, Simona Olmi, Eckehard Schöll, Control of synchronization in two-layer power grids, Phys. Rev. E 102 (2) (2020) 022311.
[813] Simona Olmi, Carl H. Totz, Eckehard Schöll, Dynamic control of intermittent renewable energy fluctuations in two-layer power grids, 2021, arXiv preprint arXiv:2111.14483.
[814] Martin Andreasson, Dimos V. Dimarogonas, Henrik Sandberg, Karl Henrik Johansson, Distributed control of networked dynamical systems: Static feedback, integral action and consensus, IEEE Trans. Automat. Control 59 (7) (2014) 1750–1764.
[815] Changhong Zhao, Enrique Mallada, Florian Dörfler, Distributed frequency control for stability and economic dispatch in power networks, in: 2015 American Control Conference, ACC, IEEE, 2015, pp. 2359–2364.
[816] Erik Weitenberg, Yan Jiang, Changhong Zhao, Enrique Mallada, Claudio De Persis, Florian Dörfler, Robust decentralized secondary frequency control in power systems: Merits and tradeoffs, IEEE Trans. Automat. Control 64 (10) (2018) 3967–3982.
[817] Pouyan Pourbeik, Prabha S. Kundur, Carson W. Taylor, The anatomy of a power grid blackout-root causes and dynamics of recent major blackouts, IEEE Power Energy Mag. 4 (5) (2006) 22–29.
[818] Paul Hines, Karthikeyan Balasubramaniam, Eduardo Cotilla Sanchez, Cascading failures in power grids, Ieee Potentials 28 (5) (2009) 24–30.
[819] Marianna Vaiman, Keith Bell, Yousu Chen, Badrul Chowdhury, Ian Dobson, Paul Hines, Milorad Papic, Stephen Miller, Pei Zhang, Risk assessment of cascading outages: Methodologies and challenges, IEEE Trans. Power Syst. 27 (2) (2012) 631.
[820] Guidong Zhang, Zhong Li, Bo Zhang, Wolfgang A. Halang, Understanding the cascading failures in Indian power grids with complex networks theory, Phys. A 392 (15) (2013) 3273–3280.
[821] Martin Rohden, Daniel Jung, Samyak Tamrakar, Stefan Kettemann, Cascading failures in ac electricity grids, Phys. Rev. E 94 (3) (2016) 032209.
[822] Géza Ódor, Bálint Hartmann, Power-law distributions of dynamic cascade failures in power-grid models, Entropy 22 (6) (2020) 666.
[823] Benjamin Schäfer, G. Cigdem Yalcin, Dynamical modeling of cascading failures in the Turkish power grid, Chaos 29 (9) (2019) 093134.
[824] Anton Plietzsch, Paul Schultz, Jobst Heitzig, Jürgen Kurths, Local vs. global redundancy–trade-offs between resilience against cascading failures and frequency stability, Eur. Phys. J. Spec. Top. 225 (3) (2016) 551–568.
[825] Dirk Witthaut, Martin Rohden, Xiaozhu Zhang, Sarah Hallerberg, Marc Timme, Critical links and nonlocal rerouting in complex supply networks, Phys. Rev. Lett. 116 (13) (2016) 138701.
[826] István Z. Kiss, Craig G. Rusin, Hiroshi Kori, John L. Hudson, Engineering complex dynamical structures: Sequential patterns and desynchronization, Science 316 (5833) (2007) 1886–1889.
[827] Dirk Witthaut, Marc Timme, Nonlocal failures in complex supply networks by single link additions, Eur. Phys. J. B 86 (9) (2013) 1–12.
[828] Michael J.B. Krieger, Jean-Bernard Billeter, Laurent Keller, Ant-like task allocation and recruitment in cooperative robots, Nature 406 (6799) (2000) 992–995.
[829] Silke Steingrube, Marc Timme, Florentin Wörgötter, Poramate Manoonpong, Self-organized adaptation of a simple neural circuit enables complex robot behaviour, Nat. Phys. 6 (3) (2010) 224–230.
[830] Imane Hafnaoui, Gabriela Nicolescu, Giovanni Beltrame, Timing information propagation in interactive networks, Sci. Rep. 9 (1) (2019) 1–14.
[831] Enrica Soria, Fabrizio Schiano, Dario Floreano, Predictive control of aerial swarms in cluttered environments, Nat. Mach. Intell. 3 (6) (2021) 545–554.
[832] Ivica Slavkov, Daniel Carrillo-Zapata, Noemi Carranza, Xavier Diego, Fredrik Jansson, J. Kaandorp, Sabine Hauert, James Sharpe, Morphogenesis in robot swarms, Science Robotics 3 (25) (2018) eaau9178.
[833] Michael Rubenstein, Alejandro Cornejo, Radhika Nagpal, Programmable self-assembly in a thousand-robot swarm, Science 345 (6198) (2014) 795–799.
[834] Dhruv Shah, Leena Vachhani, Swarm aggregation without communication and global positioning, IEEE Robot. Autom. Lett. 4 (2) (2019) 886–893.
[835] Miguel Duarte, Vasco Costa, Jorge Gomes, Tiago Rodrigues, Fernando Silva, Sancho Moura Oliveira, Anders Lyhne Christensen, Evolution of collective behaviors for a real swarm of aquatic surface robots, PLoS One 11 (3) (2016) e0151834.
[836] Wei Ren, Randal W. Beard, Consensus seeking in multiagent systems under dynamically changing interaction topologies, IEEE Trans. Automat. Control 50 (5) (2005) 655–661.
[837] Lorenzo Garattoni, Mauro Birattari, Autonomous task sequencing in a robot swarm, Science Robotics 3 (20) (2018) eaat0430.
[838] Frank Bonnet, Rob Mills, Martina Szopek, Sarah Schönwetter-Fuchs, José Halloy, Stjepan Bogdan, Luís Correia, Francesco Mondada, Thomas Schmickl, Robots mediating interactions between animals for interspecies collective behaviors, Science Robotics 4 (28) (2019) eaau7897.
[839] Gábor Vásárhelyi, Csaba Virágh, Gergő Somorjai, Tamás Nepusz, Agoston E. Eiben, Tamás Vicsek, Optimized flocking of autonomous drones in confined environments, Science Robotics 3 (20) (2018) eaat3536.

[840] K.N. McGuire, Christophe De Wagter, Karl Tuyls, H.J. Kappen, Guido C.H.E. de Croon, Minimal navigation solution for a swarm of tiny flying robots to explore an unknown environment, Science Robotics 4 (35) (2019) eaaw9710.
[841] Mohamed S. Talamali, Arindam Saha, James A.R. Marshall, Andreagiovanni Reina, When less is more: Robot swarms adapt better to changes with constrained communication, Science Robotics 6 (56) (2021) eabf1416.
[842] Xian-Ming Zhang, Qing-Long Han, Bao-Lin Zhang, An overview and deep investigation on sampled-data-based event-triggered control and filtering for networked systems, IEEE Trans. Ind. Inform. 13 (1) (2017) 4–16.
[843] Cameron Nowzari, Eloy Garcia, Jorge Cortés, Event-triggered communication and control of networked systems for multi-agent consensus, Automatica 105 (2019) 1–27.
[844] Eloy Garcia, Panos J. Antsaklis, Model-based event-triggered control for systems with quantization and time-varying network delays, IEEE Trans. Automat. Control 58 (2) (2013) 422–434.
[845] Yang Tang, Xin Jin, Yang Shi, Wenli Du, Event-triggered attitude synchronization of multiple rigid body systems with velocity-free measurements, Automatica 143 (2022) 110460.
[846] Xin Jin, Yang Shi, Yang Tang, Herbert Werner, Jürgen Kurths, Event-triggered fixed-time attitude consensus with fixed and switching topologies, IEEE Trans. Automat. Control 67 (8) (2022) 4138–4145.
[847] Florian Berlinger, Melvin Gauci, Radhika Nagpal, Implicit coordination for 3D underwater collective behaviors in a fish-inspired robot swarm, Science Robotics 6 (50) (2021) eabd8668.
[848] Hui Xie, Mengmeng Sun, Xinjian Fan, Zhihua Lin, Weinan Chen, Lei Wang, Lixin Dong, Qiang He, Reconfigurable magnetic microrobot swarm: Multimode transformation, locomotion, and manipulation, Science Robotics 4 (28) (2019) eaav8006.
[849] Jean-François Boudet, J. Lintuvuori, Claire Lacouture, T Barois, Antoine Deblais, Kaili Xie, Sébastien Cassagnere, Bernard Tregon, D.B. Brückner, Jean-Christophe Baret, et al., From collections of independent, mindless robots to flexible, mobile, and directional superstructures, Science Robotics 6 (56) (2021) eabd0272.
[850] Gaurav Gardi, Steven Ceron, Wendong Wang, Kirstin Petersen, Metin Sitti, Microrobot collectives with reconfigurable morphologies, behaviors, and functions, Nature Commun. 13 (1) (2022) 1–14.
[851] Artur Wolek, Derek A. Paley, A 3D underwater robotic collective called Blueswarm, Science Robotics 6 (50) (2021) eabf4315.
[852] Jiapeng Xu, Guoxiang Gu, Yang Tang, Feng Qian, Channel modeling and LQG control in the presence of random delays and packet drops, Automatica 135 (2022) 109967.
[853] Remy Wehbe, Ryan K. Williams, Probabilistic security for multirobot systems, IEEE Trans. Robot. 37 (1) (2020) 146–165.
[854] Thomas Wheeler, Ezhil Bharathi, Stephanie Gil, Switching topology for resilient consensus using Wi-Fi signals, in: 2019 International Conference on Robotics and Automation, ICRA, IEEE, 2019, pp. 2018–2024.
[855] Gunasekaran Raja, Sudha Anbalagan, Aishwarya Ganapathisubramaniyan, Madhumitha Sri Selvakumar, Ali Kashif Bashir, Shahid Mumtaz, Efficient and secured swarm pattern multi-UAV communication, IEEE Trans. Veh. Technol. 70 (7) (2021) 7050–7058.
[856] Brent Schlotfeldt, Vasileios Tzoumas, Dinesh Thakur, George J. Pappas, Resilient active information gathering with mobile robots, in: 2018 IEEE/RSJ International Conference on Intelligent Robots and Systems, IROS, IEEE, 2018, pp. 4309–4316.
[857] Paul J. Bonczek, Rahul Peddi, Shijie Gao, Nicola Bezzo, Detection of nonrandom sign-based behavior for resilient coordination of robotic swarms, IEEE Trans. Robot. (2022).
[858] Yang Tang, Dandan Zhang, Peng Shi, Wenbing Zhang, Feng Qian, Event-based formation control for nonlinear multiagent systems under DoS attacks, IEEE Trans. Automat. Control 66 (1) (2020) 452–459.
[859] Celine Irvene, David Formby, Samuel Litchfield, Raheem Beyah, HoneyBot: A honeypot for robotic systems, Proc. IEEE 106 (1) (2017) 61–70.
[860] Eduardo Castelló Ferrer, Thomas Hardjono, Alex Pentland, Marco Dorigo, Secure and secret cooperation in robot swarms, Science Robotics 6 (56) (2021) eabf1538.
[861] Venkatraman Renganathan, Kaveh Fathian, Sleiman Safaoui, Tyler Summers, Spoof resilient coordination in distributed and robust robotic networks, IEEE Trans. Control Syst. Technol. (2021).
[862] Weiming Fu, Jiahu Qin, Wei Xing Zheng, Yuhang Chen, Yu Kang, Resilient cooperative source seeking of double-integrator multi-robot systems under deception attacks, IEEE Trans. Ind. Electron. 68 (5) (2020) 4218–4227.
[863] Lifeng Zhou, Vasileios Tzoumas, George J. Pappas, Pratap Tokekar, Distributed attack-robust submodular maximization for multi-robot planning, in: 2020 IEEE International Conference on Robotics and Automation, ICRA, IEEE, 2020, pp. 2479–2485.
[864] Md Ishat-E-Rabban, Pratap Tokekar, Failure-resilient coverage maximization with multiple robots, IEEE Robot. Autom. Lett. 6 (2) (2021) 3894–3901.
[865] Kelsey Saulnier, David Saldana, Amanda Prorok, George J. Pappas, Vijay Kumar, Resilient flocking for mobile robot teams, IEEE Robot. Autom. Lett. 2 (2) (2017) 1039–1046.